NOVEL POLYMERIC MATERIALS VIA REACTIVE POLYMERS

by

NERGİZ CENGİZ

M.S., Chemistry, Ege University

B.S., Chemistry, Ege University

Submitted to the Institute for Graduate Studies in
Science and Engineering in partial fulfillment of
the requirements for the degree of
Doctor of Philosophy

Graduate Program in Chemistry

Boğaziçi University

NOVEL POLYMERIC MATERIALS VIA REACTIVE POLYMERS

APPROVED BY:

Assoc. Prof. Amitav Sanyal ...……
(Thesis Supervisor)

Assoc. Prof. Rana Sanyal …..……..…
(Thesis Co-supervisor)

Assist. Prof. Bülent Akgün …..…….

Prof. Viktorya Aviyente ...……..

Prof. İlknur Doğan …….

Prof. Ümit Tunca ...…….....

DATE OF APPROVAL: 09.06.2014

To My Dear Family,

ACKNOWLEDGEMENTS

I would like to express my most sincere gratitudes to my PhD advisors, Assoc. Prof. Amitav SANYAL and Assoc Prof. Rana SANYAL for their endless attention and scientific guidance throughout the study. I appreciate their support and helpful discussions and useful comments regarding all my research.

I would like to thank my collaborator, Anzar Khan in Department of Materials at ETH-Zurich for his support and advice. Anzar has given me the freedom to pursue the project without objection. I would also like to thank Prof. Dieter Schlüter and many nice people in Department of Materials at ETH-Zurich for their hospitality.

I would also thank Prof. Vincent Rotello and his group in Department of Chemistry University of Massachusetts Amherst for the collaborative work in the project.

I wish to express my thanks to Prof. Ümit Tunca, Prof. İlknur Doğan, Assist. Prof. Bülent Akgün and Prof. Viktorya Aviyente for their careful and constructive review of the final manuscript and for their care and help during my PhD program.

I would like to extend my thanks to Burcu Selen Çağlayan, Ayla Türkekul, Bilge Gedik Uluocak and Begüm Alaybeyoğlu for technique support and helpful discussion.

I want to thank Tuğçe Nihal Gevrek, Murat Tonga, Fırat Özdemir and Halil Kabadayıoğlu for their contribution to my research and their friendship.

I would like to express my thanks to present labmates Burcu Sümer Bolu, Filiz Emlik Çalık, Özgül Gök, Sadık Kaga, Mehmet Arslan, Harun Utku Aksoy, Janset Yener, Yavuz Öz, Duygu Aydın, Sesil Genç, Yasemin Üzüm, Özlem Kalaoğlu Altan, Hasan Can Helvacı, Laura Chambre and Merve Karaçivi, Hazal İpek for their companion, help and friendship.

I also thank my former labmates, Sezin Yiğit, Sebla Onbulak, Oyuntuya Munkhbat, Ece Geçici, Merve Turksoy, Serap Yapar, Gülen Yeşilbağ Tonga, Nazlı Böke, Merve Coşar, Melike Eceoğlu, Pelin Ertürk, Aslı Erdoğ, and Rabia Kolat Arslan for their enjoyable company, friendship and support.

I would like to thank Şule Erol, Sevgi Sarıgül, Selda Erkoç, Zeynep Bilgici, Jesmi Çavuşoğlu for their kind support and companion during my PhD.

I would like to extend my thanks to Seda Ata and Elif Zengin for their invaluable friendship.

I would like to thank all the members of the faculty in the Chemistry Department.

I want to thank to Boğaziçi University Research Foundation, TÜBİTAK BİDEB 2214 and TÜBİTAK 110T068 for financial assistance for the work reported in this thesis.

Finally my deepest thanks go to my large family, my little niece Asel and all my friends for their endless love, support and encouragement throughout these years.

ABSTRACT

NOVEL POLYMERIC MATERIALS VIA REACTIVE POLYMERS

Novel synthetic strategies for fabrication of reactive polymers, multifunctional hydrogels and bio-functionalizable micro-patterned hydrogels are described. A set of highly efficient chemical reactions referred as ‘click’ reactions are utilized. In conjunction with novel crosslinking strategies, various lithographic techniques during the fabrication enable the creation of micro-patterned hydrogels. In the first study, a novel N-hydroxy succinimide based carbonate monomer is designed to yield amine-reactive polymers that provide stable, yet hydrolysable carbamate-based conjugations. As the second study, novel functionalizable crosslinked hydrogels are obtained utilizing thiol-epoxy chemistry. Gelation of epoxide terminated telechelic polymers via thiol-epoxy reaction yields nearly well-defined functionalizable hydrogels. As an alternative, hydrogels were fabricated via photo-polymerization using PEG-based triblock copolymers containing glycidyl and PEG-methacrylate side chains in their outer blocks. These hydrogels can be further functionalized using epoxide ring-opening reactions. In the third project, thiol-reactive patterned polymeric platforms are obtained via nanoimprint lithography. Sub-micron patterned reactive materials that are stable through non-covalent crosslinking are fabricated. The thiol-reactive micro-patterned surfaces enable successful immobilization of dyes, peptides as well as cells. The fourth project describes fabrication of thiol-reactive maleimide-containing hydrogels using thiol-ene crosslinking. Furan-protected maleimide-containing triblock copolymers along with dithiol-based crosslinkers provide hydrogels via the radical thiol-ene reaction. Thermal activation of residual masked maleimides provides hydrogels that are functionalized with thiol-containing dyes and ligands that enable protein immobilization. In the last study, photo-dimerization of maleimide units in the side chains of copolymers is utilized for the synthesis of hydrogels without employing cross-linkers and photo-initiators. Residual maleimides are efficiently functionalized using the Michael conjugation or Diels-Alder. In summary, multifunctional polymeric platforms in soluble forms, as well as bulk and micro-patterned crosslinked hydrogels are designed. Efficient multi-funtionalization of these materials could be achieved using the reactive handles installed during the fabrication of polymeric materials.

ÖZET

REAKTİF POLİMERLERDEN YENİ POLİMERİK MALZEMELER

Reaktif polimerler, çoklu-işlevselleştirilebilir hidrojeller ve biyo-işlevselleştirilebilir mikro-desenli hidrojeller hazırlanması için yeni sentez stratejileri açıklandı. 'Klik' reaksiyonları olarak adlandırılan yüksek verimli kimyasal tepkimeler grubu kullanıldı. Yeni çapraz bağlama stratejileri ile birlikte hazırlanma sırasında çeşitli litografik teknikler kullanılması mikro desenli hidrojellerin oluşturulmasını sağlar. İlk çalışmada, N-hidroksi süksinimid tabanlı yeni bir karbonat monomer, kararlı ancak hidroliz edilebilen karbamat bağlantısını oluşturan amin reaktif polimerlerin eldesinde kullanıldı. İkinci çalışmada, işlevselleştirilebilir çapraz bağlanmış yeni hidrojeller, tiyol-epoksi kimyası kullanılarak elde edildi. Epoksi sonlu telekelik polimerlerin tiyol-epoksi reaksiyonu ile jelleştirilmesi sonradan işlev kazandırılabilen hemen hemen iyi tanımlanmış hidrojeller oluşturdu. Diğer seçenekte, dış bloklarında hem glisidil hem metakrilat grubu içeren, PEG tabanlı triblok kopolimerler kullanılarak hidrojeller hazırlandı. Hidrojeller, daha sonra epoksit halka açma reaksiyonları kullanılarak işlevselleştirilebilir. Üçüncü projede, tiyol-reaktif desenli hidrojel malzemeler nano baskı litografi yolu ile elde edildi. Kovalent olmayan çapraz bağlanma sayesinde kararlı hale gelen, mikron boyutundan daha küçük desenli reaktif malzemeler hazırlandı. Tiyol reaktif mikro desenli yüzeyler, boyalar, peptitler ve hücrelerin başarılı olarak sabitlenmesini sağladı. Dördüncü proje, tiyol-en çapraz bağlanması kullanılarak tiyol reaktif maleimid grubu içeren hidrojellerin hazırlanmasını anlatır. Ditiyol tabanlı çapraz bağlayıcı grupla furan korumalı maleimid birimi taşıyan kopolimerlerin arasındaki radikalik tiyol-en reaksiyonu ile hidrojeller oluşmaktadır. Kalan korunmuş maleimidlerin termal aktivasyonu, tiyol içeren boya ve protein bağlanmasına olanak sağlayan ligandlar ile işlevselleştirilebilen hidrojeller oluşturmaktadır. Son çalışmada, ek çapraz bağlayıcılar ve foto-başlatıcılar kullanılmadan, kopolimerin yan zincirlerindeki maleimid birimlerinin foto-dimerizasyonu ile yeni hidrojel sentezi yapıldı. Kalan maleimidler Michael katılma veya Diels-Alder ile yüksek verimle işlevselleştirildi. Özet olarak, kütle halinde veya mikro desenli çapraz bağlanmış çeşitli hidrojeller ya da çözünür formda çok işlevli polimerik malzemeler tasarlandı. Bu malzemelerin çoklu-işlevselleştirilmesi hazırlanma sırasında oluşan reaktif kollarla sağlandı.

TABLE OF CONTENTS

ACKNOWLEDGEMENTS…… .. iv

ABSTRACT…… vi

ÖZET…….. vii

LIST OF TABLES……. xxiii

LIST OF FIGURES…… xv

LIST OF ACRONYMS/ABBREVIATIONS……...…… xxiv

1. INTRODUCTION…….. 1

1.1. Functional Polymeric Materials…… 1

1.2. Functional Polymers……. 2

1.3. Versatile Tools in Functional Material Design……..... 3

1.4. Synthesis of Polymeric Materials and Post Polymerization Modification Using Amide Bond Formation…….. 5

1.4.1. Activated Esters…… 6

1.4.2. Carbonates……. 10

1.4.3. Amine-Epoxy Reaction……. 12

1.4.4. Isocyanate-Amine Reaction…….. 14

1.5. Synthesis of Polymeric Materials and Post Polymerization Modification Using Thiol Conjugation……... 16

1.5.1. Thiol Epoxy Reaction……... 17

1.5.2. Thiol-ene Addition…… 20

1.5.2.1. Radical Mediated Thiol-ene Addition…… 21

1.5.2.2. Nucleophilic Thiol-Ene Addition…… 25

1.5.3. Radical Mediated Thiol-yne Addition……. 27

1.6. Cycloaddition Reactions……. 29

1.6.1. [3+2] Huisgen Type 1,3-Dipolar Cycloaddition…….. 30

1.6.2. Diels-Alder Cycloaddition…… 34

1.6.3. Photochemical [2+2] Cycloaddition……. 40

1.7. Orthogonally Functionalizable Polymers……... 42

2. RESEARCH OVERVIEW……. 47

3. ORTHOGONALLY FUNCTIONALIZABLE COPOLYMERS WITH……...
HYDROLYZABLE AND NONHYDROLYZABLE LINKERS…….. 48

3.1. Introduction…… 48

3.2. Experimental……... 52

3.2.1. Materials…… 52

3.2.2. Synthesis of 2-(N-succinimidylcarboxyoxy)ethyl methacrylate……...
(SCEMA)…….. 53

3.2.3. Synthesis of 6-azidohexyl methacrylate (AHMA)…… 53

3.2.4. General Polymerization Procedure with SCEMA and MMA monomers. 54

3.2.5. Synthesis of Copolymer P4…….. 54

3.2.6. Synthesis of Copolymer P5…….. 55

3.2.7. Synthesis of Copolymer P6 ……..… 55

3.2.8. General Procedure for Amine Conjugation…….. 55

3.2.9. Fuctionalization of Copolymer P6 with Amine……..... 56

3.2.10. Modification Using 1,3-dipolar Cycloaddition……... 56

3.2.11. Functionalization Procedure with Propargylamine…… 56

3.3. Results and Discussion……... 57

3.3.1. Synthesis and Characterisation of the Carbonate Monomer……. 57

3.3.2. Synthesis of SCEMA and MMA Containing Copolymers…….. 59

3.3.3. Synthesis of SCEMA and PEGMA Containing Copolymer P4…… 60

3.3.4. Functionalization of Activated Carbonate Containing Copolymer…….. 61

3.3.5. Synthesis and Functionalization of Orthogonally Functionalizable…….
Copolymers …… 62

3.6. Conclusions…….. 69

4. MULTIFUNCTIONAL HYDROGELS THROUGH "THIOL –EPOXY" CLICK. CHEMISTRY…… 70

4.1. Introduction…… 70

4.2. Experimental…….. 73

4.2.1. Materials …….. 73

4.2.2. Mechanical Tests ……. 74

4.2.3. Swelling Studies …….. 75

4.2.4. Synthesis of Hydrogels via Gelation Procedure 1…… 75

4.2.5. Synthesis of Hydrogels via Gelation Procedure 2…… 75

4.2.5.1. PEG (1kDa) Hydrogel…… 75

4.2.5.2. PEG/PDMS (1/0.25 mol%) Hydrogel…… 75

4.2.5.3. PEG (2kDa) Hydrogel…… 76

4.2.6. Functionalization of Hydrogel 1 (H1)…….. 76

4.2.7. Synthesis of Peg ATRP Macroinitiator (6 kDa)……... 76

4.2.8. General Polymerization Procedure for the Synthesis of ABA Type…… Triblock Copolymers (P1)……... 77

4.2.9. Activation of ABA Triblock Copolymers through Converting Hydroxyl Groups into Methacrylate Group (P2)…….. 77

4.2.10. Gelation of Activated Triblock Copolymer P2…….. 78

4.3. Results and Discussion…….. 78

4.3.1. Gelation Procedure 1…… 78

4.3.2. Gelation Procedure 2…… 79

4.3.3. Gelation Procedure 3…… 82

4.3.4. Epoxy Bearing Hydrogels through Crosslinking of ABA Type…….. Polymers……... 91

4.4. CONCLUSION…….. 96

5. FABRICATION OF POLYMERIC MICROPATTERNS STABILIZED VIA NON-COVALENT CROSSLINKING…… 97

5.1. Introduction…… 97

5.2. EXPERIMENTAL……. 100

5.2.1. Materials……... 100

5.2.2. Characterization……..... 101

5.2.3. Synthesis of Copolymer 1…… 101

5.2.4. Synthesis of Copolymer 2…… 101

5.2.5. Synthesis of Copolymer 3…… 102

5.2.6. Film Preparation……... 102

5.2.7. Nanoimprint Lithography (NIL)……..… 102

5.3. Results and Discussion……. 102

5.3.1. Synthesis and Characterization of Polymer…….. 102

5.3.2. Dye Immobilization on Thiol-Reactive Micropatterns…… 105

5.3.3. Cellular Immobilization on Micro-Patterned Reactive Surface…….. 106

5.4. Conclusion……. 107

6. FABRICATION OF PATTERNED HYDROGELS VIA THIOL-ENE…….. CROSSLINKING……. 108

6.1. Introduction…… 108

6.2. Experimental……. 110

6.2.1. Materials……...…… 110

6.2.2. Characterization……..….. 111

6.2.3. Synthesis of PEG ATRP Macroinitiator…….…… 112

6.2.4. Polymerization of Triblock Copolymer (P1)……..……. 112

6.2.5. Partial Activation of A–B–A Triblock Copolymer (P2)…….. 113

6.2.6. Functionalization of Deprotected Maleimide Side Chains (P3)…….….. 113

6.2.7. Functionalization of Protected Maleimide Side Chains (P4)……..…. 113

6.2.8. Modification of Glass and Silicon Wafer for Hydrogel Adhesion…….. 114

6.2.9. Fabrication of Hydrogel Pattern 1 (H1)…… 114

6.2.10. Fabrication of Hydrogel Pattern 2 (H2)……..... 114

6.2.11. Fabrication of Hydrogel Pattern 3 (H3)……. 115

6.2.12. Activation of Hydrogel Patterns…… 115

6.2.13. Dye Immobilization of Hydrogel Patterns……..……..... 115

6.2.14. Bioimmobilization of Hydrogel Patterns…… 115

6.3. Results and Discussion……..... 116

6.3.1. Synthesis Activation and Functionalization of ABA Type Polymer……. 116

6.3.2. Preparation of Patterned Hydrogels……. 119

6.3.3. Functionalization of Reactive Hydrogel Micropatterns……... 121

6.3.3.1. Dye Immobilization onto Hydrogel Pattern…….. 121

6.3.3.2. Biomolecular Immobilization on…… Micro-patterned Hydrogels…….. 122

6.4. Conclusion……. 124

7. PATTERNED HYDROGELS VIA PHOTODIMERIZATION OF MALEIMIDE CONTAINING COPOLYMERS……...… 125

7.1. Introduction…… 125

7.2. Experimental…… 127

7.2.1. Materials……. 127

7.2.2. Characterization……. 127

7.2.3. Synthesis of PEG ATRP Macroinitiator…….. 128

7.2.4. Synthesis of ABA Triblock Copolymers (P1)……. 128

7.2.5. Synthesis of ABA Triblock Copolymers (P2)……..… 129

7.2.6. Synthesis of ABATriblock Copolymers (P3)…….. 129

7.2.7. Deprotection of the ABATriblock Copolymer P1 (P4)…… 130

7.2.8. Deprotection of the ABA Triblock Copolymer P2 (P5)……... 130

7.2.9. Deprotection of the ABA Triblock Copolymer P3 (P6)…….. 130

7.2.10. General Synthesis of Bulk-Hydrogel via Photo-crosslinking……. 131

7.2.11. Modification of Glass Surface and Silicon Wafer Substrate……..... with TMSMA…… 131

7.2.12. Preparation of Hydrogel Patterns……... …. 132

7.2.12.1. Micro Molding in Capillaries (MIMIC)……. 132

7.2.12.2. Photolithography…… 132

7.2.12.3. Synthesis of BODIPY-Furan…… 132

7.2.12.4. Functionalization of Patterned Hydrogel with ……. BODIPYC10SH……... 133

7.2.12.5. Functionalization of Patterned Hydrogel with…….. Furan-BODIPY…… 133

7.2.12.6. Biofunctionalization of Patterned Hydrogel…… 133

7.2.12.7. Control Experiment……..... 133

7.2.12.8. Swelling Studies of Bulk-Hydrogels…… 133

7.2.12.9. Scanning Electron Microscopy Analysis (SEM)…….. 134

7.2.12.10. Fluorescence Microscopy…….. 134

7.3. Results and Discussion……..... 134

7.3.1. Synthesis and Characterization of Copolymers……..... 134

7.3.2. Synthesis and Characterization of Bulk Hydrogels…….. 139

7.3.3. Gelation Studies on Surfaces……..... 141

7.3.3.1. Surface Modification for Good Adhesion…….. 141

7.3.3.2. Patterning via Micro Molding in Capillaries (MIMIC)……. 141

7.3.3.3. Fabrication of Hydrogel Micro-patterns via Photolithograpy.... 142

7.3.4. Functionalization of Hydrogels Micro-patterns with Small…… Molecules…….. 142

7.3.4.1. Synthesis and Functionalization of Hydrogels with Varying….. Group Content via Micromolding in Capillaries…… 144

7.3.4.2. Synthesis and Functionalization of Hydrogels via…… Photolithography…….. 144

7.3.4.3. Reversible Immobilization on the Micropatterned Hydrogels via Diels-Alder/ retro Diels-Alder Reactions…… 146

7.3.5. Ligand-mediated Biomolecular Immobilization on Hydrogel Micro-….. patterns…….. 147

7.4. Conclusion……..... 148

8. CONCLUSIONS…… 149

APPENDIX A: SPECTROSCOPY DATA…… 152

REFERENCES…….. 157

LIST OF FIGURES

Figure 1.1. Fabrication and functionalization of functional polymeric materials via click reactions. ……. 2

Figure 1.2. Functional monomers with specified properties. ……. 2

Figure 1.3. Synthesis of functional polymers by post-polymerization modification. 3

Figure 1.4. Reactions used in this thesis to obtain and/or functionalize polymeric materials. ……..…….. 5

Figure 1.5. Amine reactive polymers with various functional groups. …….. 6

Figure 1.6. Examples of commonly employed active esters groups. ……. 7

Figure 1.7 Synthesis of amine reactive end-group containing polymer and its….. modification. …… 7

Figure 1.8. Synthesis of photo-cross-linkable ferrocene redox polymer by using... NHS-amine reaction. ……... 8

Figure 1.9. Single molecule immobilization via AFM tip. ……... 9

Figure 1.10. Synthesis of pentafluorophenylacrylate and methacylate polymer and functionalization with amine containing molecules. …….. 10

Figure 1.11. Activation and functionalization of amine reactive thin film. ……... 11

Figure 1.12. Amine-epoxy reaction. …….. 12

Figure 1.13. Synthesis of epoxy bearing polymer and its amine modification. …. 13

Figure 1.14. Synthesis of amine-epoxy hydrogel……. 14

Figure 1.15. Reaction of a primary amine with an isocyanate…….. 14

Figure 1.16. Isocyanate containing copolymer synthesis, functionalization and….. crosslinking of the copolymer via amine. …… 15

Figure 1.17. Thiol conjugated polymer synthesis with various functional groups. 16

Figure 1.18. Thiol-epoxy reaction. …… 17

Figure 1.19. Mechanism of thiol-epoxy reaction. ……. 17

Figure 1.20. Reactive polymer sythesis via thiol-epoxy “click chemistry” and…… functionalization of the polymer. …… 18

Figure 1.21. Main-chain and end-chain functionalization. …….. 19

Figure 1.22. Chain-end functional polymer synthesis and functionalization. …… 20

Figure 1.23. Radical mediated thiol-ene addition. ……. 21

Figure 1.24. Mechanism of radical mediated thiol-ene addition. …… 21

Figure 1.25. Dendrimer synthesis via thiol-ene click reaction. ……... 22

Figure 1.26. Functional hydrogel microarrays via thiol-ene chemistry. ……. 23

Figure 1.27. Fabrication of catechol functionalized polymer networks. ……. 24

Figure 1.28. Modification of microspheres via thiol-ene chemistry. …… 25

Figure 1.29. Base- and nucleophile-catalyzed mechanism of thiol-ene addition. ... 26

Figure 1.30. Synthesis and functionalization of biodegradable polymer. …… 26

Figure 1.31. Synthesis of glucose functionalized scaffold. ……..... 27

Figure 1.32. Mechanism of thiol-yne reaction. …… 28

Figure 1.33. RAFT polymerization of N-isopropylacrylamide and end-group……. modification via thiol-yne reaction. …… 29

Figure 1.34. Cycloaddition reactions used in this thesis. ……. 30

Figure 1.35. [3+2] Huisgen type 1,3-dipolar cycloaddition. …… 30

Figure 1.36. Copper catalyzed [3+2] Huisgen type 1,3-dipolar cycloaddition ….. 31

Figure 1.37. Copper-free cycloaddition. ……... 31

Figure 1.38. The surface functionalization of a dendron via Huisgen…….. type cycloaddition. …….. 32

Figure 1.39. Step-growth networks via Huisgen click reaction and functionalization of pendant alkene units. ……... 33

Figure 1.40. Fabrication of functional block copolymer nanoparticles. ……... 34

Figure 1.41. Diels-Alder reaction mechanism. ……. 34

Figure 1.42. Some dienes appropriate for Diels-Alder reaction. …….. 35

Figure 1.43. Some dienophiles appropriate for Diels-Alder reaction. ……. 35

Figure 1.44. Block copolymer synthesis via Diels-Alder “click” reaction. ……. 36

Figure 1.45. Segment block dendrimers via Diels-Alder cycloaddition. ……. 36

Figure 1.46. Synthesis of HA based PEG hydrogels. …….. 37

Figure 1.47. Reversible patterning on reactive polymeric thin films by micro……
contact printing of maleimide-containing dye. …….. 38

Figure 1.48. Synthesis of anthracene-appended styrene polymer and dendron……
polymer cycloaddition. …….. 39

Figure 1.49. Contact angle of water on films of dendronized polymers. …… 40

Figure 1.50. Photodimerization of maleimide. …… 40

Figure 1.51. Copolymerization of acrylamide (AAm) with……..
N-(N'-acryloyl-2-aminoethyl)-dimethylmaleimide (DMMIAAm)…..
and photocrosslinking of the copolymer. ……... 41

Figure 1.52. Photo-crosslinking of the polymer. ……. 42

Figure 1.53. Orthogonal functionalization of reactive multi-functional polymers. 43

Figure 1.54. Synthesis and orthogonal functionalization of terpolymer. ……..…… 44

Figure 1.55. Synthetic method for the synthesis of brush copolymers. …….. 45

Figure 1.56. One-step preparation of heterograft polymers via Diels-Alder and....
Huisgen type 1,3-dipolar cycloadditions. …….. 46

Figure 3.1. Illustration of a typical polymeric construct for targeted drug delivery. 49

Figure 3.2. Commonly used linkages employed for attachment of therapeutic….
agents to polymers. …….. 50

Figure 3.3. Stability order of the linkers towards hydrolysis. …… 50

Figure 3.4. Different routes to synthesize carbonate-based reactive polymers:
Route A and B. Route B: methodology explored in this thesis. ……. 51

Figure 3.5. Functionalization of polymers containing reactive carbonate side…
chains. …….. 51

Figure 3.6. Orthogonally functionalizable polymers a) Polymer containing……...
amine reactive and alkyne reactive side chains, b) Polymer containing
two different amine reactive side chains. …….……... 52

Figure 3.7. Synthesis of HEMA based reactive monomer SCEMA. …… 57

Figure 3.8. ^{1}H-NMR and 13C NMR spectrum of the SCEMA monomer. …….. 58

Figure 3.9. IR spectrum of SCEMA monomer. ……..... 58

Figure 3.10. Synthesis of MMA containing copolymers containing reactive……. carbonate side chains. …… 59

Figure 3.11. ^{1}H NMR spectra of MMA containing copolymer P1, P2 and P3. ….. 60

Figure 3.12. Synthesis of MMA containing copolymers containing reactive…… carbonate side chains. …….. 61

Figure 3.13. Reaction of P4 with amine. ……. 61

Figure 3.14. ^{1}H-NMR spectra of P4 and after functionalization P11. …… 62

Figure 3.15. Monomers employed in this study. ……..... 63

Figure 3.16. Synthesis of 6-azidohexyl methacrylate (AHMA) monomer. …… 63

Figure 3.17. ^{1}H-NMR spectrum of AHMA monomer. ……... 64

Figure 3.18. Copolymerization of SCEMA monomer with AHMA monomer. ….. 65

Figure 3.19. Orthogonal functionalization of copolymer P5 with amine and..… alkyne containing molecules. .……..... 65

Figure 3.20. ^{1}H NMR spectra of the copolymer P5, before and after…… functionalization. ……. 66

Figure 3.21. Copolymerization of SCEMA monomer with NHSMA monomer. …. 67

Figure 3.22. Orthogonal functionalization of copolymer P6 with two different amines. ……. 68

Figure 3.23. ^{1}H NMR of copolymer P7 before and after functionalization. ……. 68

Figure 4.1. Illustrative reactions involving epoxide-ring opening. …….. 71

Figure 4.2. Hydroxyl (A) and epoxy (B) functional hydrogel formations. …….. 73

Figure 4.3. Stress-Strain measurements using rheometer. ……. 74

Figure 4.4. General gelation procedure 1. ……... 78

Figure 4.5. General gelation in presence of additional epoxide-containing……. crosslinker. ……... 79

Figure 4.6. FT-IR Spectra of hydrogel precusrsors. …….. 80

Figure 4.7. FT-IR spectra of hydrogels. …….. 81

Figure 4.8. Morphology of hydrogels G1, G2 and G3 observed using SEM. …… 82

Figure 4.9. a) Schematic illustration of hydrogel synthesis and b) photograph.....

of a typical thiol-epoxy hydrogel. …….. 83

Figure 4.10. Structure of diglycidyl ether-terminated poly(dimethylsiloxane)…….
(PDMS). …….. 83

Figure 4.11. Gel formulations before and after the gelling reaction……
H1 (a), H2 (b), H3 (c), and H 4 (d). ……... 84

Figure 4.12. IR spectra of H1, H2, H3 and H4. ……. 85

Figure 4.13. Water uptake by the hydrogels containing 0 (solid line),……...
20 (dash line), 33 (dash-dot) line, and 50 mole% (dash-dot-dot line)
of PDMS. PEG wt % 27. ……. 86

Figure 4.14. SEM images of the freeze-dried hybrid hydrogels varying…….
in hydrophilic/hydrophobic balance. …… 87

Figure 4.15. Diglycidyl ether-terminated poly(ethylene glycol) (PEG) 4. …….. 88

Figure 4.16. Water uptake by the hydrogels containing PEG 2 (solid line) and…
PEG 4. …… 88

Figure 4.17. Functionalization of hydrogels via esterification. …… 89

Figure 4.18. FT-IR spectra of the gel precursors PEG 2 (a) and PETMP 1……
(b), PEG-hydrogel (c), and pyrene-functionalized hydrogel (d). …… 90

Figure 4.19. Optical fluorescence microscopy image of (a), functionalized ……..
hydrogel (bright field, (b) upon excitation at 365 nm, and…….
(c) control experiment upon excitation at 365 nm. ……. 91

Figure 4.20. General outline for the synthesis of epoxy bearing hydrogels and….

their functionalization. …… 91

Figure 4.21. Synthesis of ABA triblock copolymer using a PEG macroinitiator,..
and its post-polymerization modification. …… 92

Figure 4.22. Hydrogel synthesis using P2. ……... 93

Figure 4.23. ^{1}H-NMR spectra of copolymers P1 and P2. …….. 94

Figure 4.24. FT-IR spectra of the copolymers P1 and P2. ……. 94

Figure 4.25. Image before(a) and (b) after photopolymerizationof polymer. …... 95

Figure 4.26. Water uptake profiles of hydrogels at different temperatures……..
(0 ^{o}C and 37 ^{o}C). … …… 96

Figure 5.1. Non-covalent stabilization of polymers. …… . 98

Figure 5.2. Basic work flow of the nanoimprint lithography process. …… 99

Figure 5.3. Schematic illustration of fabrication and functionalization of…… micro-patterned polymeric structures using thermal imprinting. 100

Figure 5.4. Copolymerization of monomers. …….. 103

Figure 5.5. ^{1}H-NMR spectra of (a) MMA containing copolymer P1 and……. (b) PEGMA-MMA containing copolymer P2 in CDCl3. ……... 104

Figure 5.6. a) ^{1}H-NMR spectra and b) thermogravimetric analysis of P3. …… 105

Figure 5.7. a) Schematic representation of BODIPY–SH attachment to the…… surface b) Bright field image. Inset in (b) shows the fluorescence… image of the imprinted pattern before BODIPY–SH conjugation…. c) Fluorescence image after BODIPY–SH conjugation……. 106

Figure 5.8. a) Schematic representation of RGD–SH attachment and cell…….. alignment to the surface, a, b and c shows the Fluorescence……. microscopy images of cell cultured surfaces a) the unpatterned….. maleimide surface b) the RGD immobilized unpatterned surface, .. c) the RGD immobilized patterned surface. ..…… 107

Figure 6.1. Fabrication and functionalization of micro-patterned hydrogels using... radical thiol-ene and nucleophilic thiol-ene reactions. …… 110

Figure 6.2. Overall reaction scheme for the synthesis of orthogonally……. reactive copolymer. ……. 116

Figure 6.3. ^{1}H-NMR spectra (400 MHz, $CDCI_3$) of furan-protected……... maleimide containing t_0, maleimide functionalized at different ….. temperature intervals (t_i) after 30 min, 1 h, 2h partial retro…… Diels-Alder deprotection of the maleimide……. groups and completion of retro Diels-Alder. ……..……. 117

Figure 6.4. a) Enlarged FT-IR spectra of C=C-H stretching: P1 (t_0) after 1 hour and 8 hours at 100 ^{o}C. b) GPC Spectra of copolymer P1 at before… and after heating for 1 hour and 8 hour. ……. 118

Figure 6.5. ^{1}H-NMR spectra (400 MHz, CD_2CI_2) of the product after partial…. retro Diels-Alder reaction (P2), the product after the…… Michael-Addition reaction of benzyl mercaptan to deprotected….. maleimide groups (P3), and the product after thiol-ene coupling…. with thioglycerol (P4). ……... 119

Figure 6.6. Schematic illustration of preparation of patterned hydrogel surface (a) Optical microscopy image of patterned surface. (b) Scanning…

Electron Microscopy image for the patterned surface H1. ……. 120

Figure 6.7. Fluorescence images of patterned PEG hydrogel (H2)…… (a) postfunctionalized by BODIPY-SH. (b) control:…….. functionalization without heating. ……. 121

Figure 6.8. Conceptual scheme showing the attachment of streptavidin…….. conjugate QDs to the biotinylated pattern (H3). (a) Fluorescence… micrograph of a mixture of CdSe/ZnS QD-tagged……. streptavidin-biotin surface. (b) Control experiment:…….. Fluorescence micrograph of a mixture of CdSe/ZnS QD-tagged….. streptavidin surface without biotinylation. ……. 123

Figure 6.9. XPS Spectra of pattern H3 (a) Binding energy of Cd and N of……. biotinylated surface and after attachment of streptavidin conjugated QDS. (b) Binding energy of Zn of biotinylated surface and after…. attachment of streptavidin conjugated QDS. …….. 124

Figure 7.1. [2+2] photodimerization of maleimide groups. …… 125

Figure 7.2. Schematic illustration of fabrication and functionalization of…… hydrogels. …….. 126

Figure 7.3. Synthesis of maleimide group containing ABA type triblock…… copolymers. ..…….. 135

Figure 7.4. ^{1}H-NMR spectra of copolymers P1-P3. …….. 136

Figure 7.5. ^{1}H-NMR spectra of copolymers (P4-P6) obtained after the retro….. Diels-Alder reaction. …… 137

Figure 7.6. Gel Permeation Chromatographs for copolymers before and after… retro Diels-Alder reaction. …… 138

Figure 7.7. Water uptake measurements of hydrogels H1, H2 and H3. …… 140

Figure 7.8. SEM microphotographs of bulk hydrogels a) H1 b) H2, c) H3. ….. 141

Figure 7.9. a) General scheme for patterning via MIMIC and functionalization of the patterned surface with BODIPYC10SH. b) Fluorescence….. microscopy image after BODIPYC10SH attachment to P2 at…….. 500 ms and c) Fluorescence microscopy image before…….. BODIPYC10SH attachment d) SEM image of patterned hydrogel.. surface at 5000 X magnification, e) SEM image of patterned…… hydrogel surface at 750 X magnification. …… 143

Figure 7.10. Fluorescence intensity of BODIPY-SH attached patterned hydrogel surface from different polymers a) patterned hydrogel using……

P4 polymer, b) patterned hydrogel using P5 polymer c) patterned.. hydrogel using P6 polymer, d) Relative fluorescence intensity of the surface a, b and c. ……. 144

Figure 7.11. Patterning of P5 through photolithography and fluorescence……. microscope images of BODIPYC10SH immobilized patterns…… a) 5 min b) 10 min UV irradiation time. ……. 145

Figure 7.12. Attachment of furan containing dye molecule to the hydrogel…….. pattern a) after dye attachment b) after removal of dye molecule….. c) SEM micrograph of the hydrogel pattern.d) Fluorescence intensity of the surface before and after attachment of the dye molecule. … 146

Figure 7.13. a) General schema for the immobilization of fluorescently……. labeled Extravidin to biotinylated surface. Fluorescence microscopy images of b) hydrogel pattern c) after attachment of ExtraAvidin… to the biotinylated surface d) Control experiment:……. Extravidin immobilization without biotinylation. …….. 147

Figure A.1. HPLC spectrum of SCEMA (Chapter 3). ……. 152

Figure A.2. FT-IR spectra of P1, P2, P3 and P4 (Chapter 6). …… 153

Figure A.3. XPS spectrum of pattern H3, after QD attachment to biotinylated.. surface (Chapter 6). ……... 154

Figure A.4. XPS spectrum of pattern H3, after biotinylation (Chapter 6). ….. 155

Figure A.5. ^{1}H-NMR spectrum of BODIPY-Furan (Chapter 7). …….. 156

LIST OF TABLES

Table 3.1.	Synthesis of reactive monomer containing random copolymers. ……	64
Table 4.1.	Chemical composition, water uptake and yield of hydrogels. …….	80
Table 4.2.	Effect of PDMS amount and % PEG to Stress…… Strain Measurements and water uptake capacity of the hydrogels. …	85
Table 7.1.	Synthesis of ABA type triblock polymers and activated polymers…… via retro Diels-Alder reaction. …….....	138

LIST OF ACRONYMS/ABBREVIATIONS

ATRP	Atom transfer radical polymerization
$CDCl_3$	Deuterated chloroform
CD_2Cl2	Deuterated dichloromethane
CH_2Cl_2	Dichloromethane
D_2O	Deuterated water
DA	Diels-Alder
rDA	Retro Diels-Alder
DMAP	4-Dimethylaminopyridine
EDCI	1-Ethyl-3-(3-dimethylaminopropyl) carbodiimide
EtOAc	Ethyl Acetate
FT-IR	Fourier Transform Infrared
G	Generation
GPC	Gel Permeation Chromotography
MeOH	Methanol
MHz	Mega hertz
MMA	Methylmetacrylate
NMR	Nuclear Magnetic Resonance
PEG	Poly(ethylene glycol)
PEGMEMA	Poly(ethylene glycol) monomethyl ether methacrylate
P*t*BA	Tertiary Butylacrylate
SEC	Size-Exclusion Chromatography
TEA	Triethylamine
THF	Tetrahydrofuran
TLC	Thin Layer Chromatography
UV	Ultraviolet

1. INTRODUCTION

1.1. Functional Polymeric Materials

The design, synthesis and modification of functional polymeric scaffolds has become focus of intense research in recent years due to their potential applications in areas such as cell and tissue engineering, drug delivery and platforms for biochip technology [1-2]. Depending on the application, different forms of soft polymeric materials such as soluble polymeric, uni-molecular or multi-component micelles, nanoparticles, nanorods, dendrimers, hydrogels, polymeric thin films and patterned surfaces are employed in different research fields [3-4]. These functional materials can be derived from well-defined polymers or created *in situ* during polymerization. Depending upon the desired macromolecular architecture and chemical composition, one can select among various available polymerization techniques. Bulk, micro and nanomaterials can be derived using covalent or noncovalent interactions between appropriately designed polymers.

Incorporation of various complex molecular fragments such as peptides, oligo-nucleotides, organic dyes and ligands are usually necessary in designing multifunctional materials. For example, a simple theranostic construct made of polymers contains drug molecules, targeting biomolecules or ligands and imaging agents. However, it is a challenge to address the incompatibility of all these functional groups at the same time with any polymerization technique. Since the advent of “click” chemistry utilization of “clickable attachment of functional moieties onto polymeric materials have gained popularity compared to direct polymerization of functional monomers for functional material design. In this research we are proposing fabrication and functionalization of functional materials by using various types of click reactions (Figure 1.1).

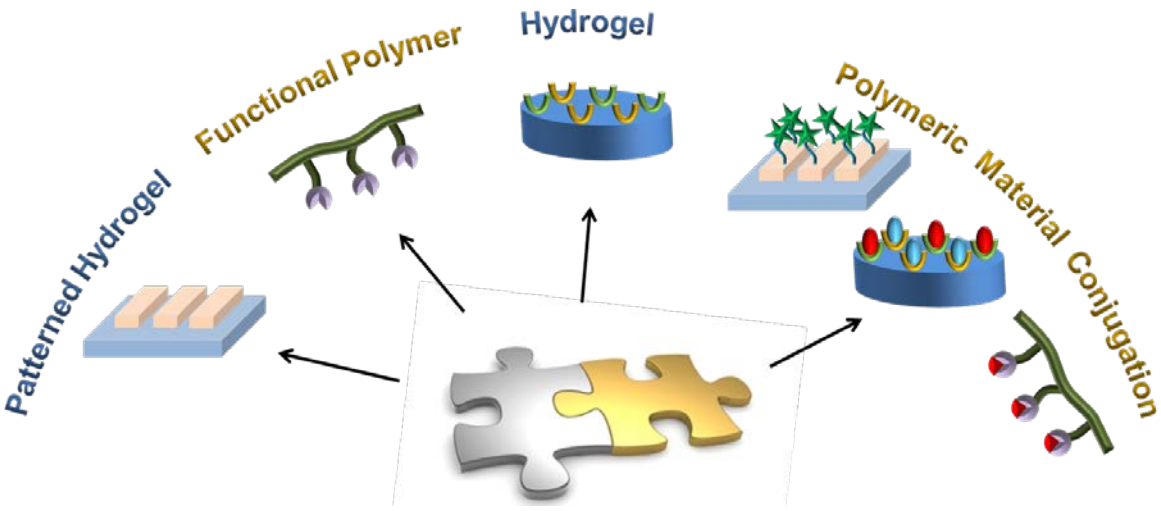

Figure 1.1. Fabrication and functionalization of functional polymeric materials via click reactions.

1.2. Functional Polymers

During the synthesis of reactive polymers, it is important that polymers retain the reactivity after the polymerization steps since the functionality on the monomer unit determines the functionalizability of the desired product (Figure 1.2). For example, hydrophilicity, hydrophobicity, polarity and the elasticity of a polymer can be controlled by selecting appropriate monomers [5-6]. In addition, functionality can bring properties like photosensitivity or conductivity to polymers [7]. Functional monomers are also responsible for both the binding interactions, for covalent and non-covalent imprinting protocols. It is indispensable to match the functionality of the polymeric materials with the functionality of the monomer in a complementary fashion.

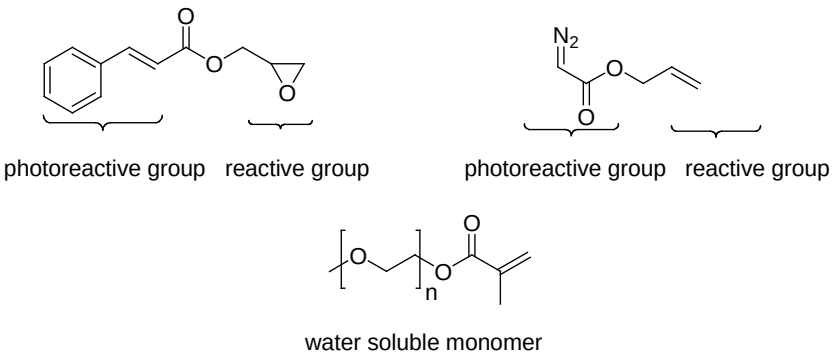

Figure 1.2. Functional monomers with specified properties.

For designing multifunctional polymers, incorporation of different types of functional groups on the polymer is required. This can be achieved through the copolymerization of various types of functionalized monomers. Monomer reactivity ratio is one of the factors that affects feasibility of homogenous copolymerization [8]. For example in a radicalic polymerization a styrene radical is more likely to react with itself instead of a methacrylate monomer, since electron donating tendency renders the styrene less electrophilic [9-12]. In addition, some other properties like polar groups or steric hindrance can affect the reactivity ratio. For instance, glycidyl (meth)acrylate or 2-hydroxyethyl (meth)acrylate are more electrophilic due to the electron withdrawing nature of oxygen compared to alkyl methacrylates [13]. Such considerations should be taken into account while designing multifunctional copolymers. Nowadays, simple techniques for post-polymerization functionalization using robust and efficient "click" chemistry have become important for the preparation of functional polymers since various functionalities can be introduced to the polymer backbone via post-polymerization modification of side chains (Figure 1.3).

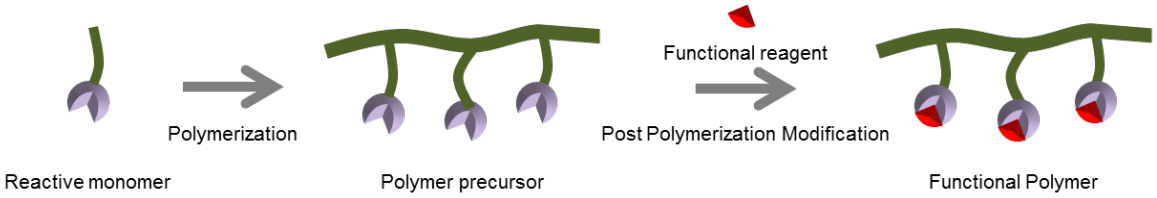

Figure 1.3. Synthesis of functional polymers by post-polymerization modification.

1.3. Versatile Tools in Functional Material Design

Design of well-defined functional polymeric material requires a suitable choice of polymerization technique accompanied by appropriate reactions [14]. Easy and high yielding modular reactions without by products or with trace amount of by products are preferably chosen for the fabrication of multifunctional materials. In 2001, the term "click" chemistry was first introduced by Sharpless [15] and Fokin [16] to describe the junction of small modular units to generate a new structure using simple, efficient and high yielding

chemistries. Nowadays “click” chemistry has widespread applications such as dendrimer synthesis [17], hydrogel design [18-19], bioconjugation [20], modification of natural [21] and synthetic [19] materials in nanotechnology and material science. In this research we focused on design of novel functionalizable biomaterials using various click reactions such as:

- Thiol-ene addition reaction;
- Amidation reaction with activated carbonate esters;
- Michael addition reaction;
- Thiol-epoxide opening reaction;
- [3+2] Huisgen cycloaddition;
- Diels-Alder cycloaddition;
- [2+2] cycloaddition;

The complementary chemical functional groups utilized to bring about desired conjugations are outlined in Figure 1.4.

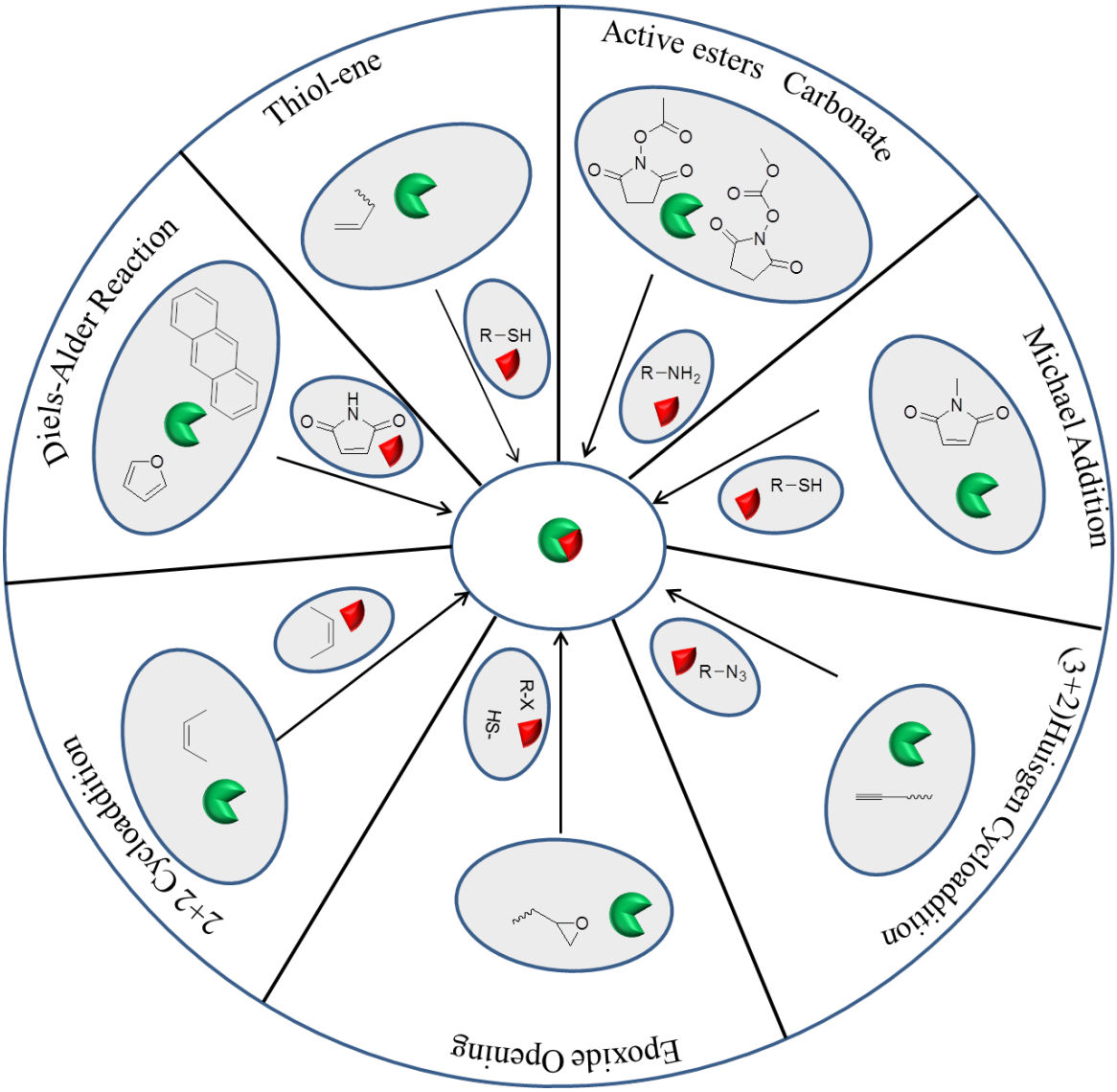

Figure 1.4. Reactions used in this thesis to obtain and/or functionalize polymeric materials.

1.4. Synthesis of Polymeric Materials and Post Polymerization Modification Using Amide Bond Formation

Amine moieties are common in proteins due to the frequent presence of lysines [22]. Amine-reactive polymeric materials are widely used to modify biomolecules for the preparation of bioconjugates [21]. The kinetics of this reaction largely depends on the reactivity of the functional group. Several types of click reactions have been described to covalently attach amines. Among the amine reactive group containing polymers, activated

esters such as N-hydroxysuccinimide esters and pentafluorophenol esters have played a role [21]. In addition, epoxide or isothiocyanate group containing polymers have been widely studied for amine conjugation (Figure 1.5).

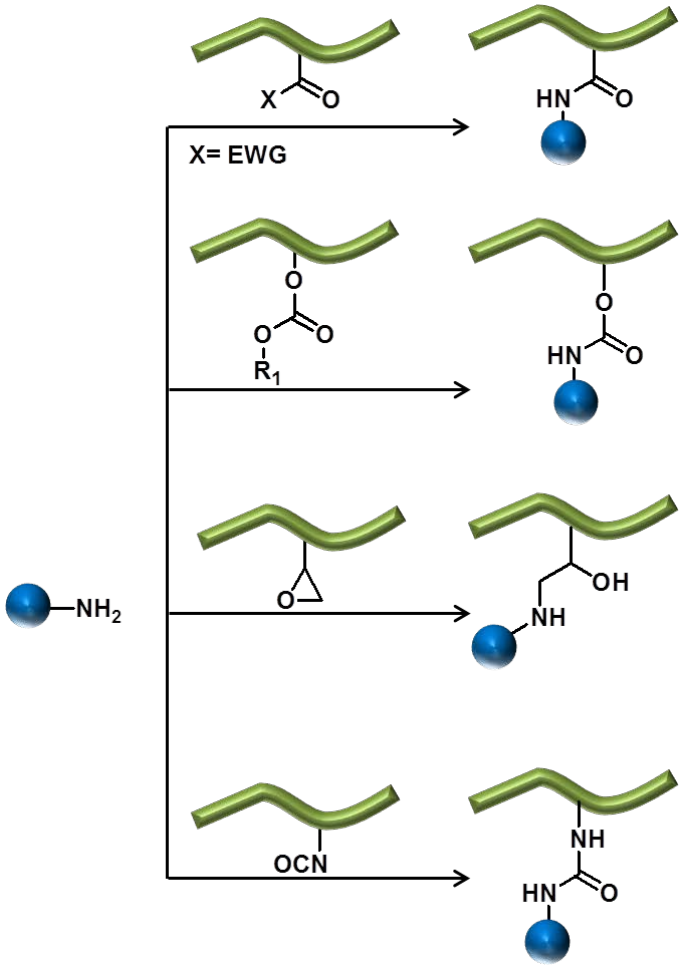

Figure 1.5. Amine reactive polymers with various functional groups.

1.4.1. Activated Esters

Polymers modified with active esters i.e. esters with high reactivity, are prone to reaction with amine groups on biomolecules. Multifunctional polymeric materials can be obtained by combining the versatility of the active ester chemistry with post-polymerization modification method. Ferruti and Ringsdorf pioneered in the post-polymerization modification of active ester containing polymers as early as the 1970s [23-24]. To date, a variety of active ester containing monomers and polymers have been

synthesized with different polymerization techniques for various applications. Activated esters containing electron withdrawing groups exhibit enhanced reactivity towards the amine functional group (Figure 1.6).

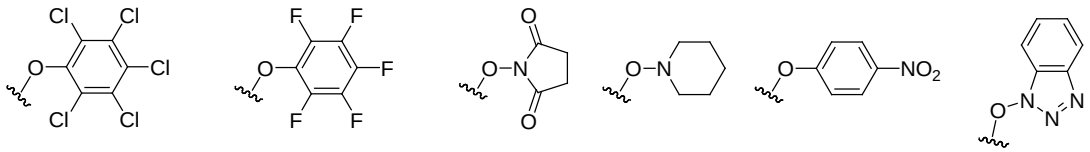

Figure 1.6. Examples of commonly employed active esters groups.

Among various activated esters, *N*-Hydroxysuccinimidyl (NHS) esters have been most widely studied [25-31]. NHS-modified polymers can be readily obtained using various polymerizations such as Atom Transfer Radical Polymerization (ATRP) and Reversible Addition-Fragmentation Chain Transfer (RAFT) [32]. For example, Sumerlin and coworkers recently synthesized an end-chain amine reactive polymer using a RAFT agent containing an activated-ester moiety (Figure 1.7) [33]. They used RAFT polymerization of *N*-isopropylacrylamide with an active ester containing RAFT agent to prepare thermoresponsive polymers for conjugation to amine-containing proteins. Conjugation efficiency of NHS termini polymers was demonstrated with lysozyme.

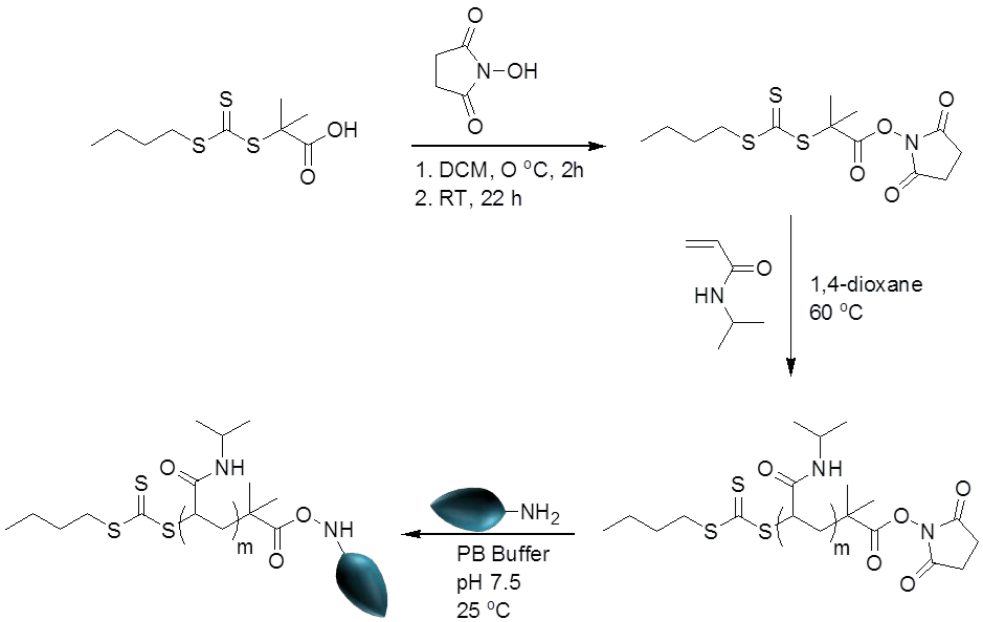

Figure 1.7. Synthesis of amine reactive end-group containing polymer and its modification.

In another study, Rühe and coworkers synthesized pendant NHS-active ester containing polymers by using a photoreactive benzophenone monomer along with a dimethylacrylamide comonomer (Figure 1.8) [34]. Side chain NHS groups were functionalized with an amino linker modified electroactive ferrocene. Functionalized photoreactive redox polymer was deposited on a surface and mixed with an enzyme. UV irradiation of the functional polymer-enzyme mixture resulted in a redox-active hydrogel which can find potential applications in biosensor and biofuel cell design.

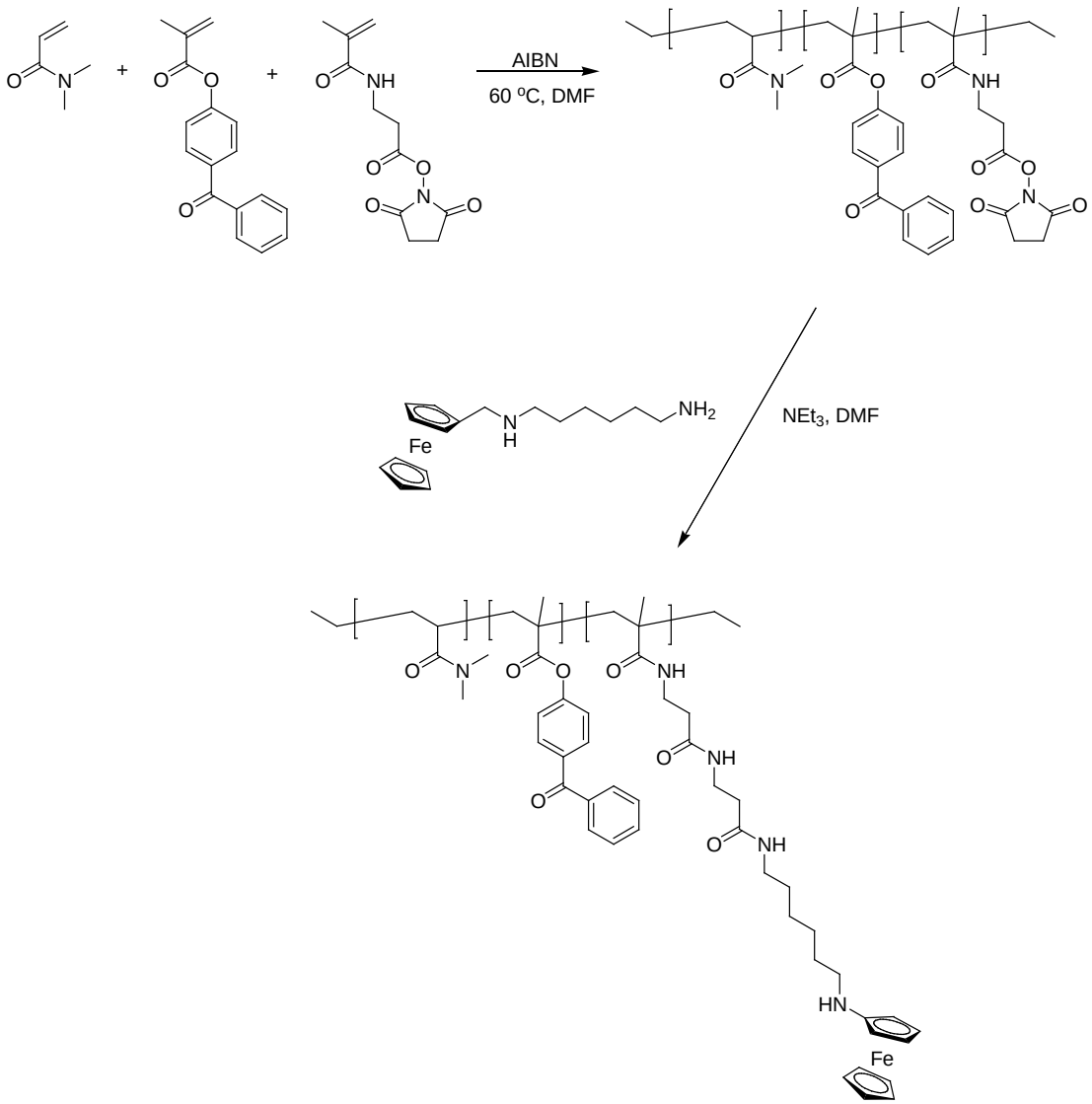

Figure 1.8. Synthesis of photo-cross-linkable ferrocene redox polymer by using NHS-amine reaction.

In another example, the NHS active ester was utilized for single molecule immobilization via an AFM tip by Duwez *et al* (Figure 1.9) [35]. Gold-coated AFM tips were functionalized with poly-N-succinimidyl acrylate based polymers and silicon surfaces were modified with aminopropyltrimethoxysilane. When the AFM tip is brought in contact with the surface, a chemical reaction occurred between the succinimide group on the polymer and the amine group on the surface. Hence, poly-N-succinimide is transferred to the amine functionalized surface. The left over free succinimide groups on the surface immobilized polymers are accessible for further bioimmobilization.

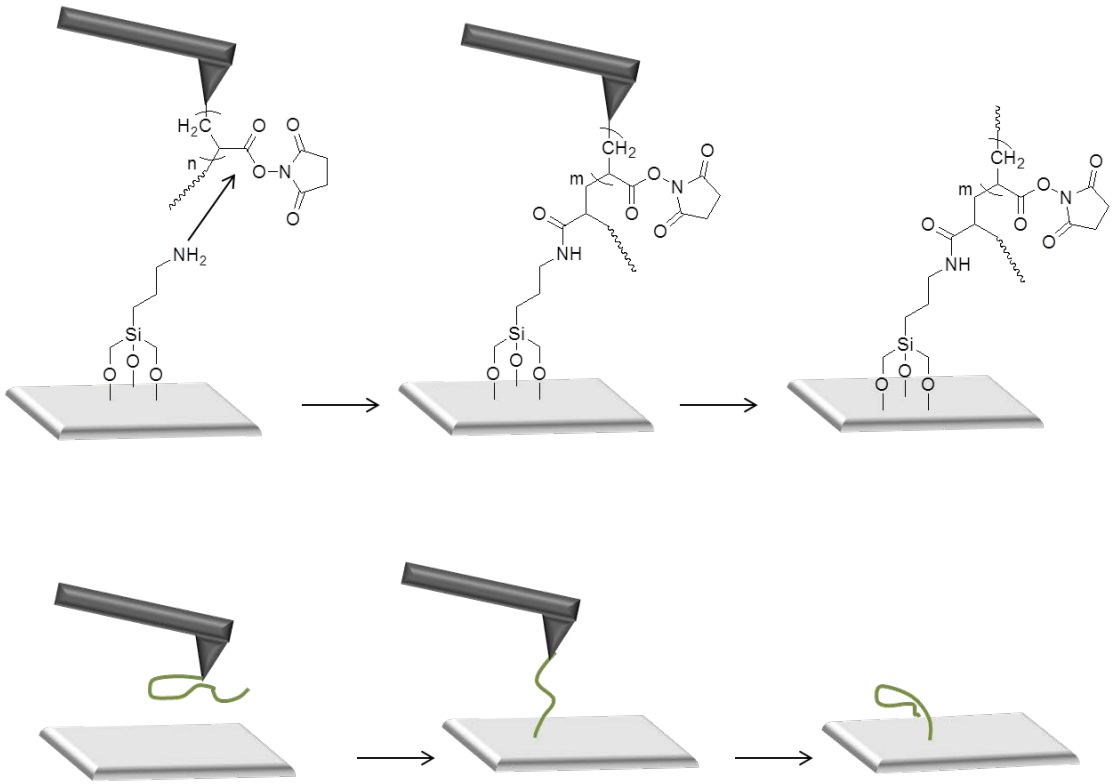

Figure 1.9. Single molecule immobilization via AFM tip.

In another study, Theato and coworkers utilized a pentafluorophenyl activated ester for designing multifunctional polymers (Figure 1.10) [36]. Pentafluorophenyl acrylate and methacrylate monomers were polymerized via free radical polymerization in the presence of AIBN as radical source. The reactivity of synthesized polymers of pentafluorophenylacrylate and pentafluorophenylmethacrylate was compared with secondary and primary amines using IR spectroscopy. It was observed that the reactivity of secondary amines was lower than primary amines.

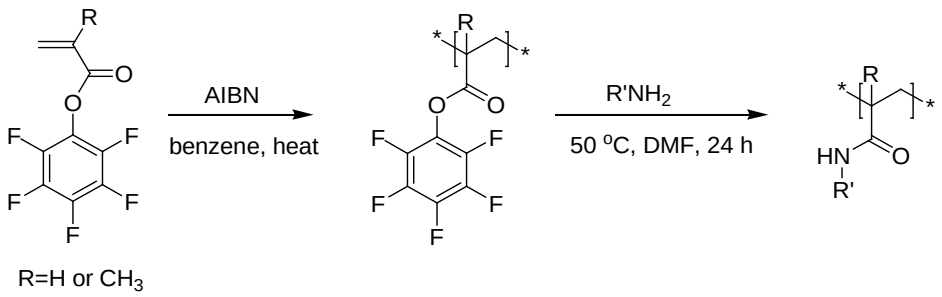

Figure 1.10. Synthesis of pentafluorophenylacrylate and methacylate polymer and functionalization with amine containing molecules.

1.4.2. Carbonates

Carbonate functional groups are transformed into a carbamate group after covalent binding of an amine group. This hydrolyzable linker has been utilized in design of prodrugs but has not been studied extensively in polymeric materials [37-38]. In the literature, one extensively finds cyclic carbonates which were used to synthesize polycarbonates [39]. However, there are very few examples that utilize carbonates for the synthesis of amine reactive multifunctional polymeric materials [40]. Carbamate linkage which is formed from the reaction of an amine with a carbonate group can undergo fragmentation. Therefore, polymeric materials that utilize conjugation of drug molecules with this chemistry can release the parent drug, whereas amide linkages cannot be cleaved easily while the widely used ester linkages are not stable enough in *in vivo* studies [41].

Recently, functional polymeric materials with pendant carbonate moiety have also been shown. For example, Vaia and coworkers formed carbonate groups via postpolymerization functionalization and utilized them to prepare multifunctional polymer brushes [42]. In another study, Choi and coworkers designed poly(oligo(ethylene glycol) based polymeric thin films to play a role as a bioconjugation platform with the specific binding of biomolecules [43]. After modifying silicon or gold surface by ATRP initiator, they grafted OEGMA on the surface and terminal hydroxyl groups were reacted with N,N′-Disuccinimidyl Carbonate to obtain NHS carbonate ester which can be easily coupled with amine containing biomolecules. The amine containing ligand, biotin-amine, was attached

to the NHS carbonate groups while the remaining NHS carbonate groups were deactivated using an amine containing hydrophilic small molecule (Figure 1.11).

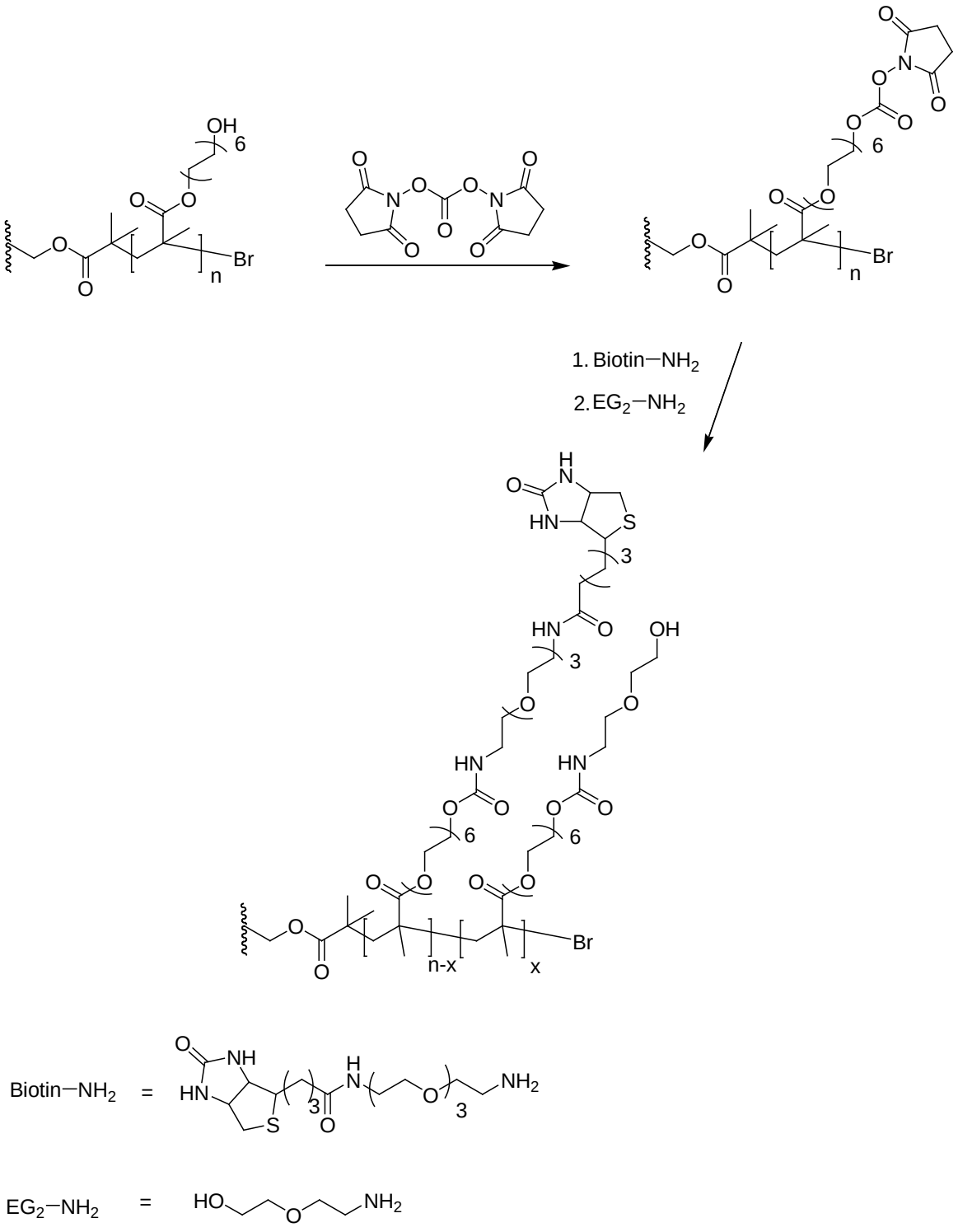

Figure 1.11. Activation and functionalization of amine reactive thin film.

1.4.3. Amine-Epoxy Reaction

Epoxy-amine chemistry is very well-known and especially used in industry for the adhesive property of the outcome of the reaction. This reaction is a nucleophilic substitution reaction and it proceeds via the attack of the lone pair of the nitrogen to the carbon atom of the epoxy group generating a sigma bond which is the rate determining step [44]. In the first addition step, a secondary amine is formed bearing an alcohol group. Later, the second lone pair of the nitrogen can attack another epoxy group to form a tertiary amine. Since the epoxy-amine reaction is fast and easy, it is considered as a "click" reaction and has been used for synthesizing polymers, dendrimers [45], hydrogels [46], thin films [47] and for post polymerization modification of polymeric structures [48]. Moreover, the hydroxyl group which is formed after the addition of amine group to the epoxy carbon can be utilized to attach additional functionalities (Figure 1.12).

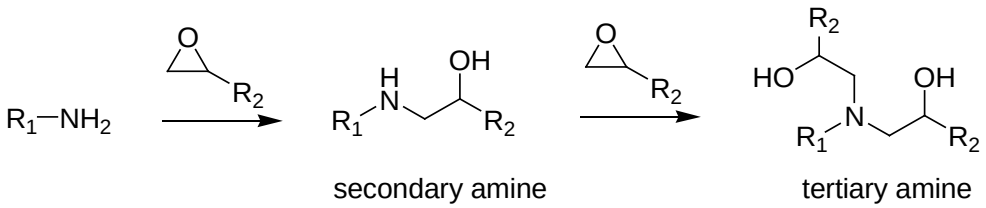

Figure 1.12. Amine-epoxy reaction.

Siegwart and coworkers reported the synthesis of epoxy bearing functional polymers and the post polymerization modification of the pendant epoxy groups of the polymer with amine containing molecules (Figure 1.13) [49]. First, they synthesized -ene group containing polymer with step growth polymerization of trimethylolpropane allyl ether and diacid chloride. Then -ene groups on the polymer chain was converted to epoxy groups via epoxidation reaction using *m*-CPBA. Amine modification was performed using various secondary or primary amine containing model molecules.

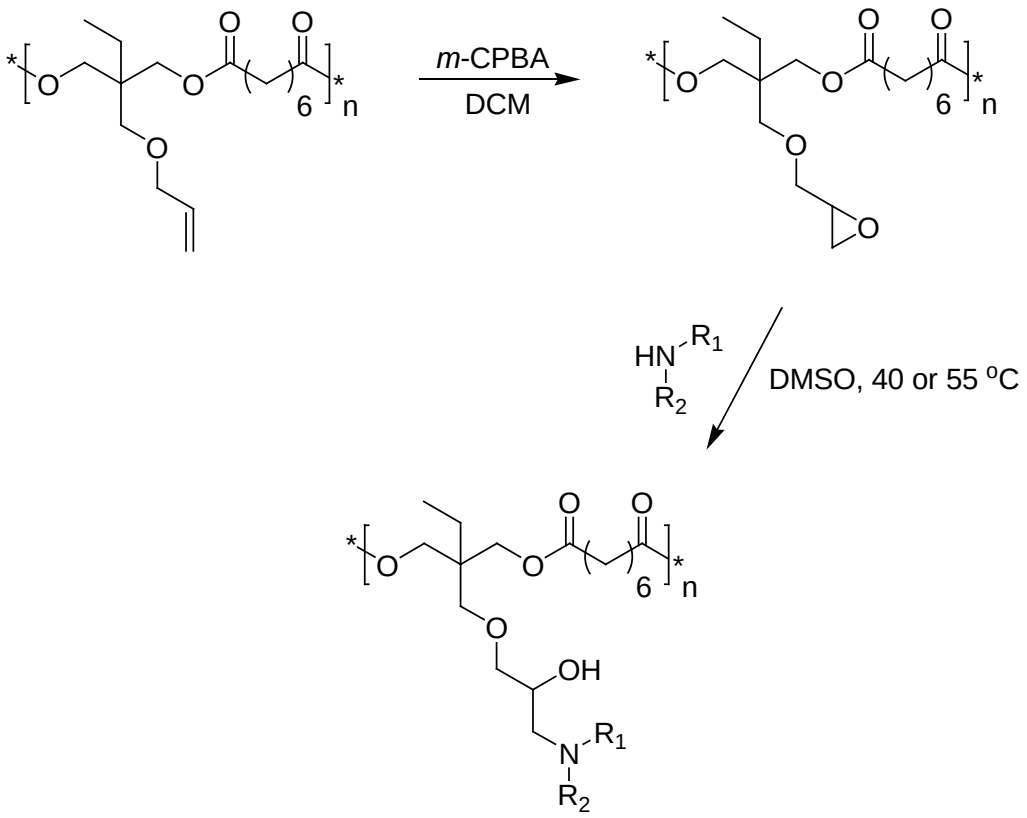

Figure 1.13. Synthesis of epoxy bearing polymer and its amine modification.

Amine-epoxy chemistry was also used to design polymeric cross-linked materials for biological applications. Qiao and coworkers produced hydrogel scaffolds for soft-tissue engineering via covalent crosslinking of amine and epoxy containing materials [46]. For this purpose terminal diepoxy containing PEGDGE and terminal diamine containing cystamine were mixed with α,ω-diamino functionalized poly(Є-caprolactone) (PCL) crosslinker in the presence of salt templates to get porous hydrogels (Figure 1.14). *In vitro* and *in vivo* studies were also performed to show their non-cytotoxic and degradable properties. The resulting hydroxyl functionalities from the amine-epoxy crosslinking reaction were available for further reaction.

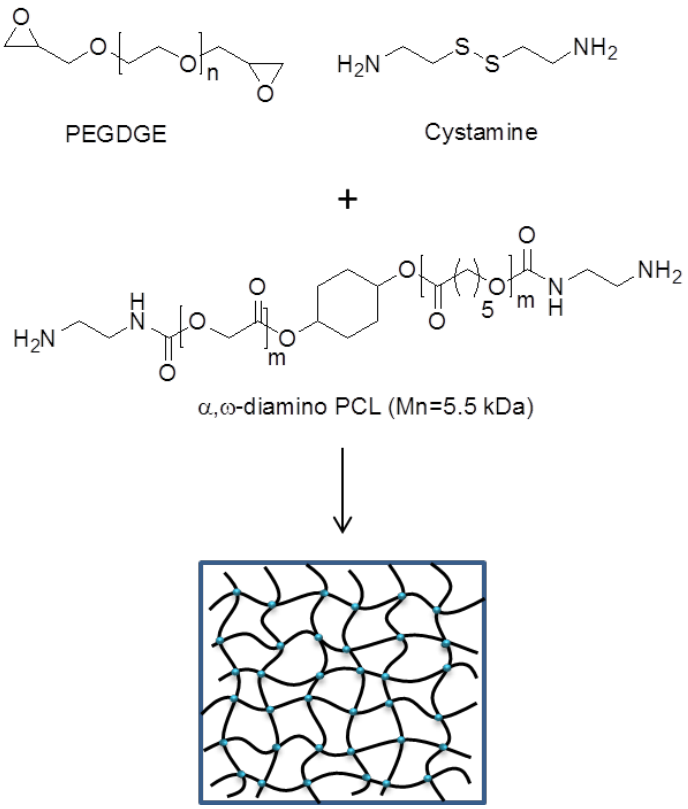

Figure 1.14. Synthesis of amine-epoxy hydrogel.

1.4.4. Isocyanate-Amine Reaction

The isocyanate group, which was first discovered by Wurtz in 1849 is one of the popular starting materials to synthesize numerous biologically active compounds that contain urea [50]. Isocyanates react with amines to form ureas forming a stable covalent bond (Figure 1.15) [51].

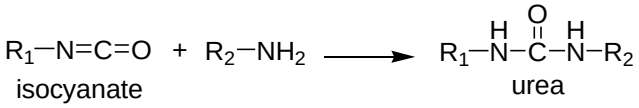

Figure 1.15. Reaction of a primary amine with an isocyanate.

This reaction takes place rapidly in high yields under mild conditions with the addition of triethylamine. Isocyanate-amine reaction makes post polymerization modification of isocyanate bearing polymers possible with amine containing compounds as well as thiol compounds. Urea which is the outcome of amine-isocyanate reaction is a very important functional group [52]. Especially substituted ureas have many applications in

biomedical science due to the good biocompatibility and physical properties and they are found in many natural products and supramolecules. In addition, it is known that urea forms stronger hydrogen bonding compared to the corresponding urethane [53-55].

Hawker and coworkers used this reaction for demonstrating functionalization and crosslinking of pendant isocyanate bearing polymers [56]. For utilizing amine recativity of isocyanate group, they synthesized isocyanate containing linear copolymers from commercially available monomers via RAFT polymerization (Figure 1.16). Isocyanate groups of the linear polimer were reacted with monoamine or diamine molecules, to yield functionalized polymer and functionalized nanoparticle with bisurea crosslinks, respectively.

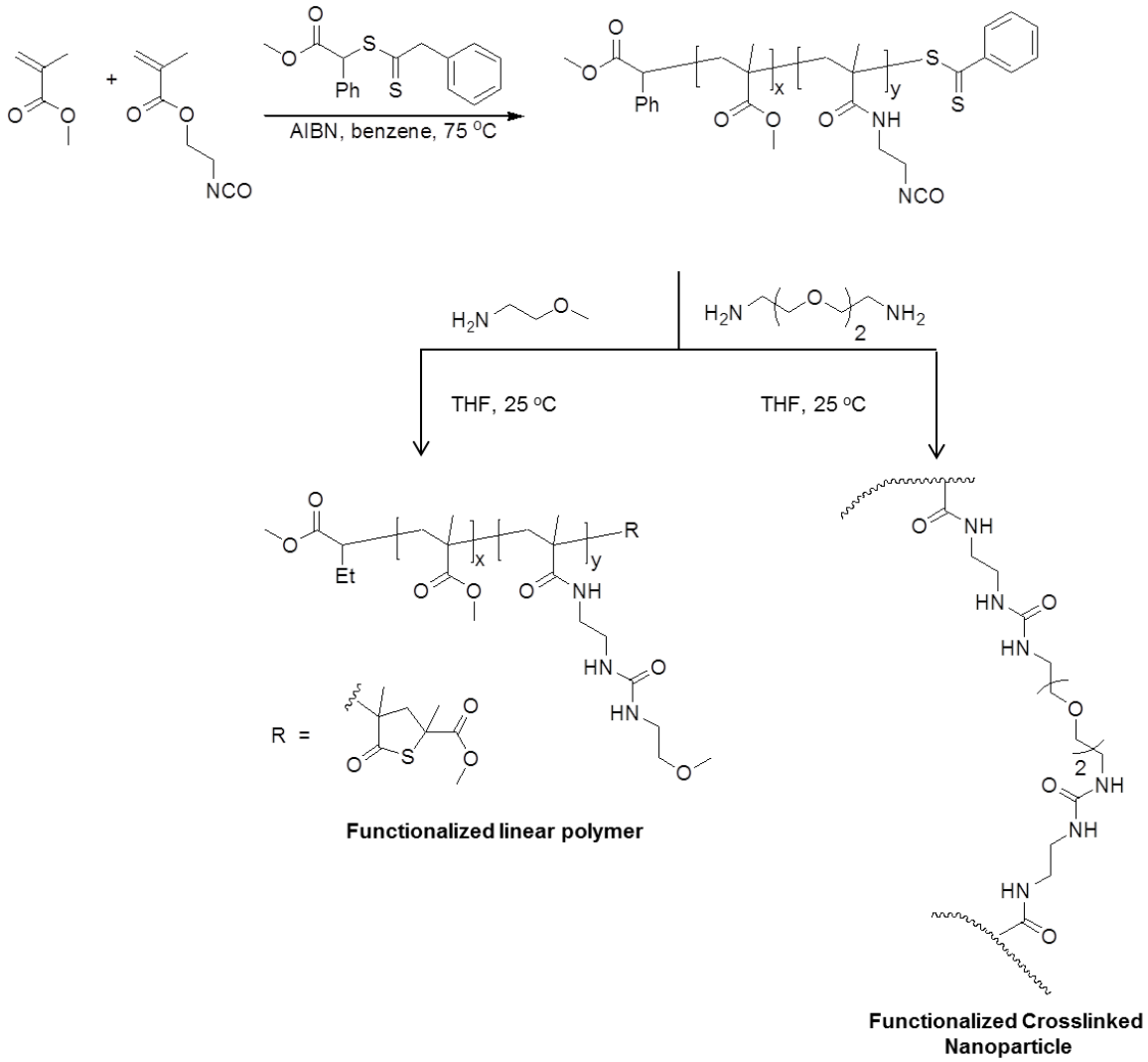

Figure 1.16. Isocyanate containing copolymer synthesis, functionalization and crosslinking of the copolymer via amine.

1.5. Synthesis of Polymeric Materials and Post Polymerization Modification Using Thiol Conjugation

Numerous post-polymerization modifications have been described to install thiol-reactive end-groups into polymers such as maleimide, alkene, alkyne, and epoxy groups (Figure 1.17) [57]. These functional groups have been demonstrated to be effective for direct modification of cysteines in proteins [21]. Building blocks of many biological structures contain thiol groups and this property make thiol groups very important especially in the application related to polymer therapeutics. Hence the synthesis of thiol reactive polymers or modification of polymers with thiol reactive functional groups is an actively pursued research area of the research. For example, the amino acid cysteine which is one of the protein building blocks in human body contains thiol group. So, the thiol part of cysteine serves as a nucleophile and participates in bioconjugation. The pKa of cysteine is around 8.2 that is more nucleophilic compared to an amino group (NH_3^+) on cysteine which has the pKa of 10.3. Especially below pH = 9 the amino group is protonated so thiol group becomes more nucleophilic. Free cysteines are important in immobilization studies as they are less in abundance and less prone to react with random orientation [58].

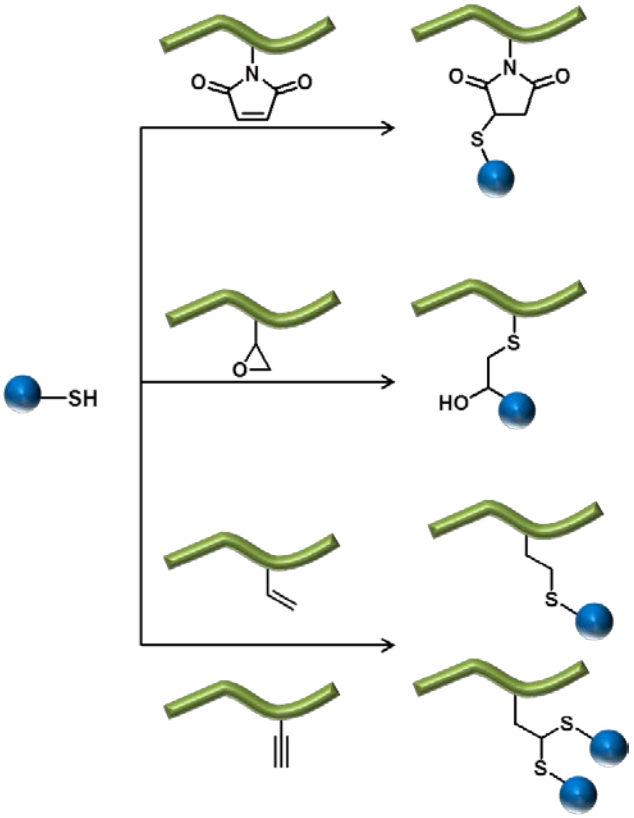

Figure 1.17. Thiol conjugated polymer synthesis with various functional groups.

1.5.1. Thiol Epoxy Reaction

The basic thiol–epoxy reaction mechanism is a simple nucleophilic ring-opening reaction by the thiolate anion followed by protonation of the alcolate anion via the quaternary ammonium (Figure 1.18) [59].

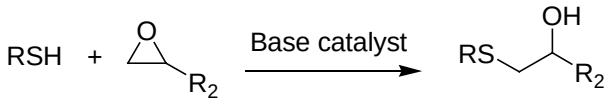

Figure 1.18. Thiol-epoxy reaction.

A thiol anion is formed via the reaction of a tertiary amine and a thiol functional group. The thiol anion attacks an epoxide group via an anionic addition. In the meantime, an epoxide anion can also be formed with the reaction of the epoxide group with a tertiary amine (Figure 1.19). Although both the thiol anion and the epoxide anion can proceed the polymerization in a nucleophilic displacement, the relative rate of nucleophilic displacement of a thiol anion is over 3 orders of magnitude faster than a similar alcohol anion which was explained by Streitweiser [60-61]. The reaction can be catalyzed by a variety of strong bases through deprotonation of the thiol. Catalysts, like Lewis acids, which weaken the carbon oxygen bond and stabilize the alcolate anion upon direct attack by the nucleophilic thiol, are also effective for carrying out thiol–epoxy reactions in bulk.

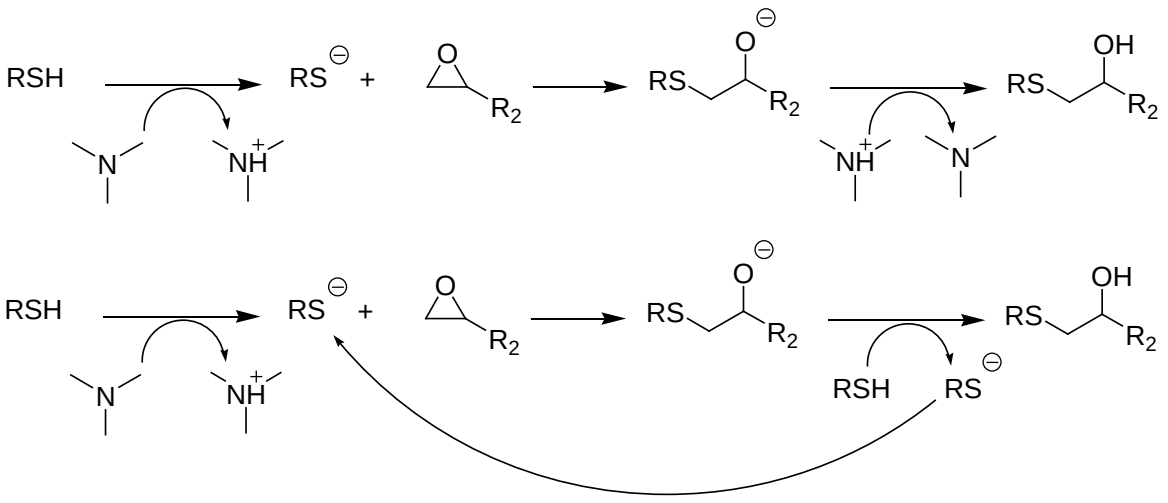

Figure 1.19. Mechanism of thiol-epoxy reaction.

Recently, thiol–epoxy reaction is employed by Khan to obtain linear polymer chains bearing hydroxyl groups. Just a simple reaction of commercially available monomers, polymerization of 1,2-ethanedithiol and 1,4-butanediol diglycidyl ether, proceeds efficiently in the presence of LiOH as catalyst [62]. Then, hydroxyl groups are functionalized with p-toluoyl chloride and 2-naphthoyl chloride which resulted toluoyl-functionalized or naphthyl-functionalized polymers respectively (Figure 1.20).

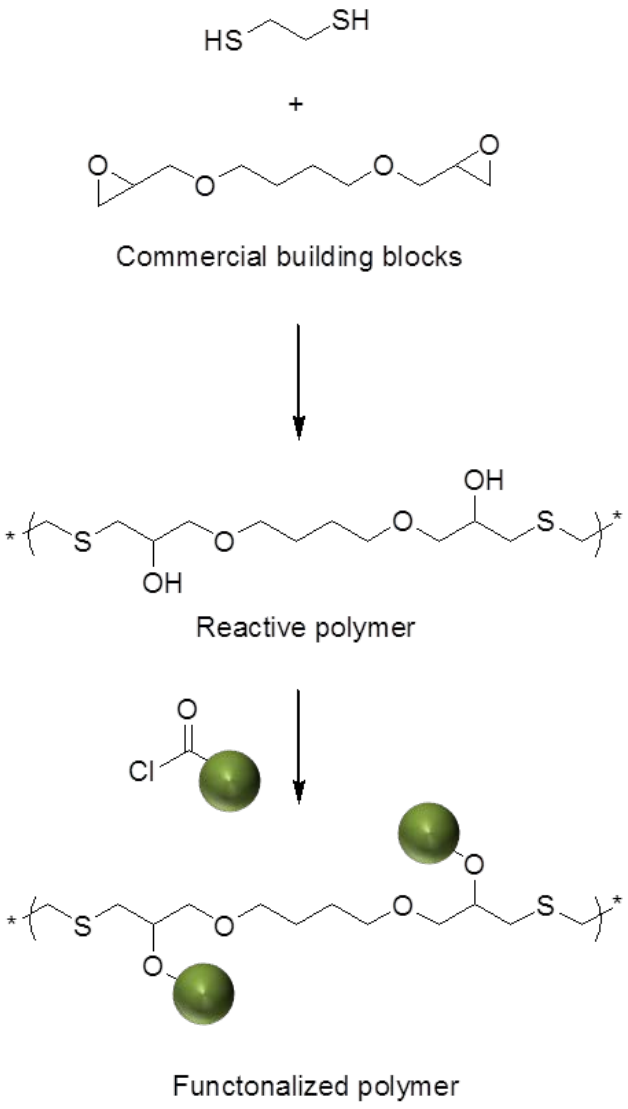

Figure 1.20. Reactive polymer sythesis via thiol-epoxy “click chemistry” and functionalization of the polymer.

Khan and coworkers also described the preparation of a variety of high molecular weight dual functional homopolymers as well as chain-end bifunctional oligomers through thiol-epoxy chemistry [63]. To obtain the functional homopolymer, glycidyl methacrylate was polymerized to yield poly(glycidyl methacrylate) using free radical polymerization to get pendant epoxy groups on the main chain (Figure 1.21). Later, epoxy groups were functionalized with thiol containing molecules. Secondary hydroxyl group which formed after thiol-epoxy reaction was postfunctionalized. To obtain the chain-end functional polymer, commercially available poly(ethylene glycol) diglycidyl ether was employed. Further functionalization with thiol bearing molecules was achieved effectively (Figure 1.21).

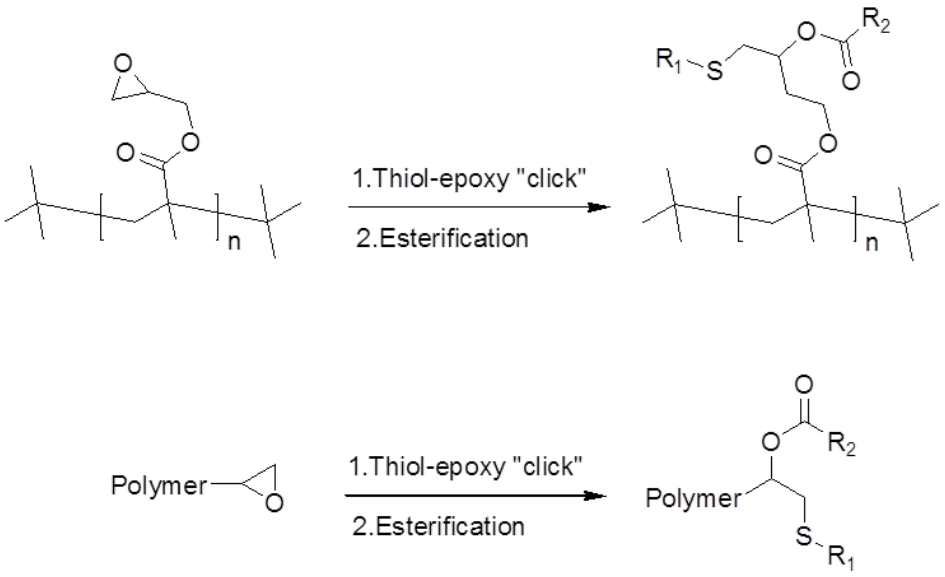

Figure 1.21. Main-chain and end-chain functionalization.

In another study, Khan and coworkers demonstrated another functional end chain polymerization using ATRP with initiators carrying one, two, or three epoxide units and methyl methacylate monomer [64]. Functionalization of epoxy group was performed through thiol-epoxy click reaction, and final esterification of the hydroxyl unit with toluoyl chloride resulted targeted chain-end functional polymer (Figure 1.22).

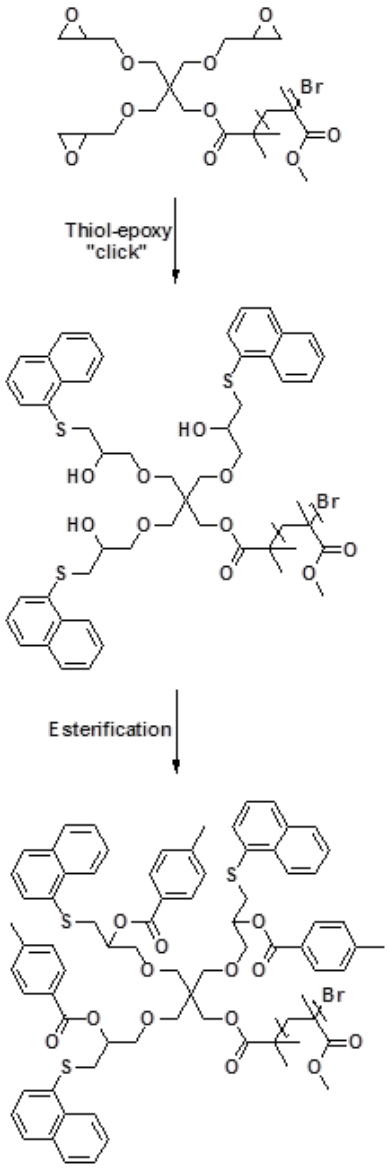

Figure 1.22. Chain-end functional polymer synthesis and functionalization.

1.5.2. Thiol-ene Addition

The reaction of thiols with alkenes is also considered as a “click” reaction[17] showing the simplicity and high efficiency as expected for this category of reactions. Therefore, the thiol-ene click reaction has been utilized for the synthesis of dendrimers, copolymers, biofunctionalization, as well as modification of thin films and polymers [65]. There are two types of thiol-ene reaction: Radical mediated thiol-ene reaction and Michael type nucleophilic thiol-ene reaction depending on the addition mechanism of the thiol

across the double bond. Since sulfur-hydrogen bond is weak, thiols act as strong hydrogen donors, and they can be added to double bonds easily. The reactions are efficient, high yielding, and can tolerate various solvents and functional groups.

1.5.2.1. Radical Mediated Thiol-ene Addition. Free radical mediated thiol-ene reaction is the thiol addition to carbon–carbon double bond via free radical mechanism (Figure 1.23) [66-67].

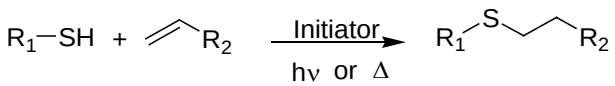

Figure 1.23. Radical mediated thiol-ene addition.

Thiol-ene reaction can be conducted under radicalic conditions and it proceeds like a typical radical chain growth process with initiation, propagation and termination steps. Treatment of a thiol with photoinitiator can be done under UV irradiation or heat. As a result thiyl radical is formed. Propagation involves the direct addition of the radical across the C=C bond via anti-Markovnikov rule, resulting a radical intermediate followed by chain transfer to a second molecule of thiol to give the thiol-ene addition product, with the generation of a new thiyl radical. Termination reactions consist of usual radical–radical coupling processes (Figure 1.24).

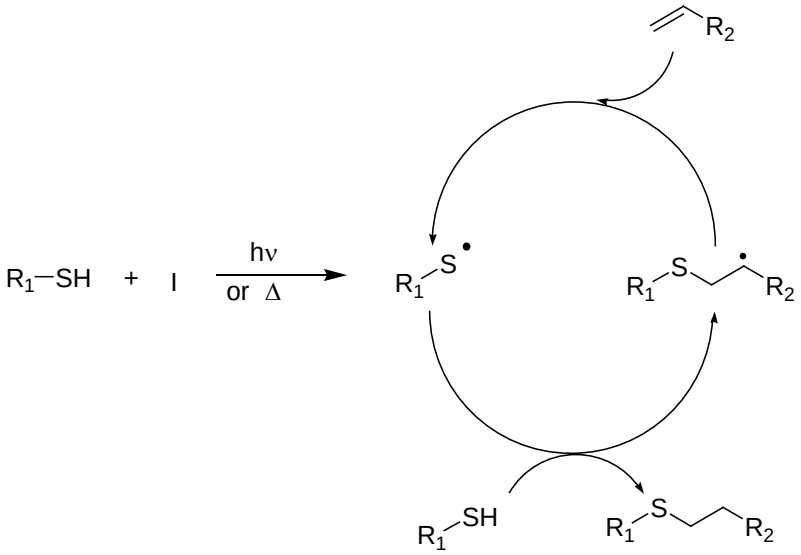

Figure 1.24. Mechanism of radical mediated thiol-ene addition.

Synthesis of dendritic macromolecules and their end-group functionalization was demonstrated using thiol-ene chemistry [17]. Divergent approach was used to synthesize the dendritic structures in order to demonstrate the adequacy of the reaction. For this purpose, tris-alkene 2,4,6-triallyloxy-1,3,5-triazine and 1-thioglycerol were reacted to give the thiol-ene product (Figure 1.24). Then, esterification of the resultant alcohol with 4-pentenoic anhydride gave the first generation product. After repetition of the two-step procedure to increase generations, the periphery of the dendrimer was functionalized with different functional thiols again via thiol-ene chemistry (Figure 1.25).

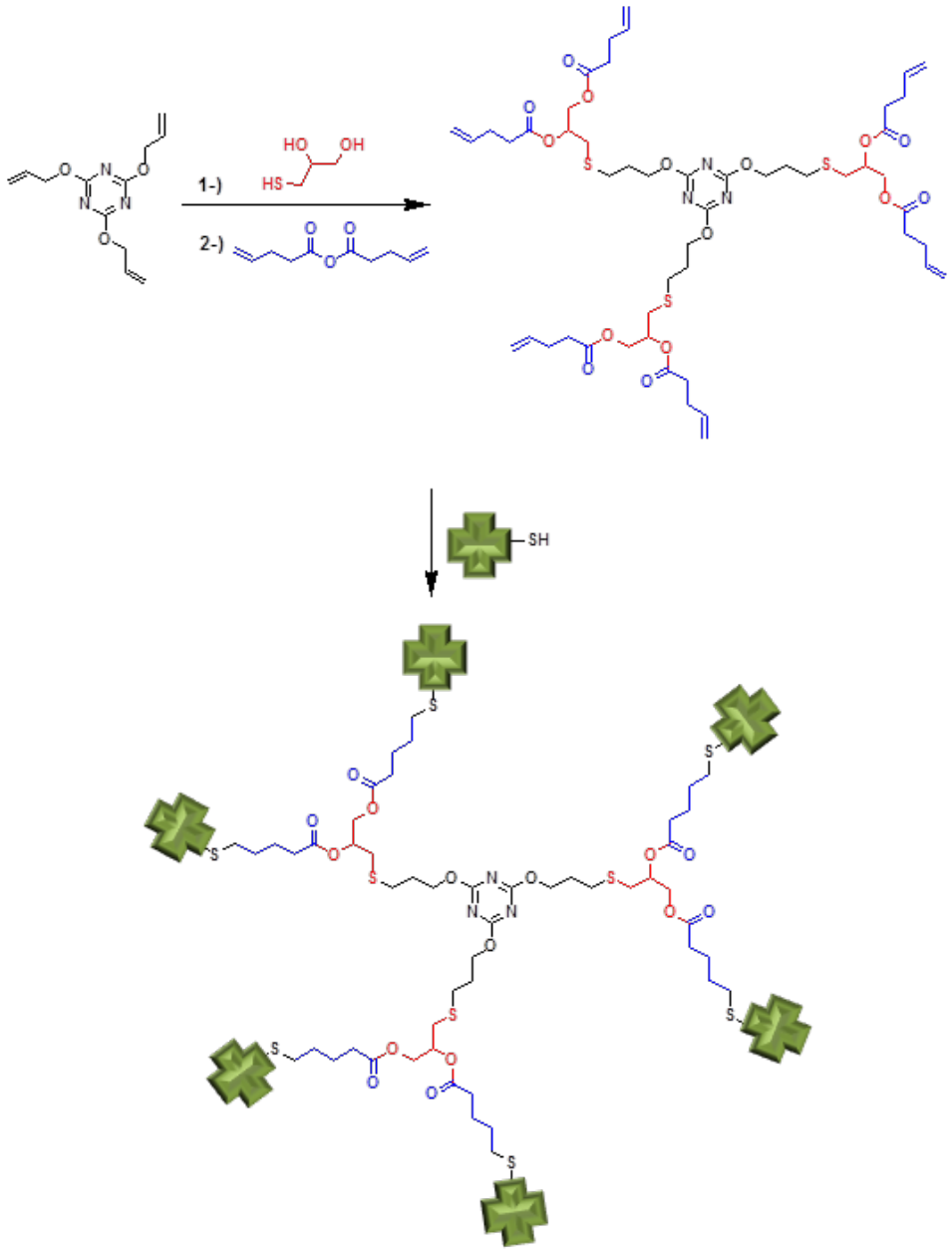

Figure 1.25. Dendrimer synthesis via thiol-ene click reaction.

A strategy developed by Hawker and colleagues was to design multifunctional microarrays using thiol-ene chemistry (Figure 1.26) [68]. Two strategies were applied to reveal the applicability of different functionalities to the hydrogel microarray.

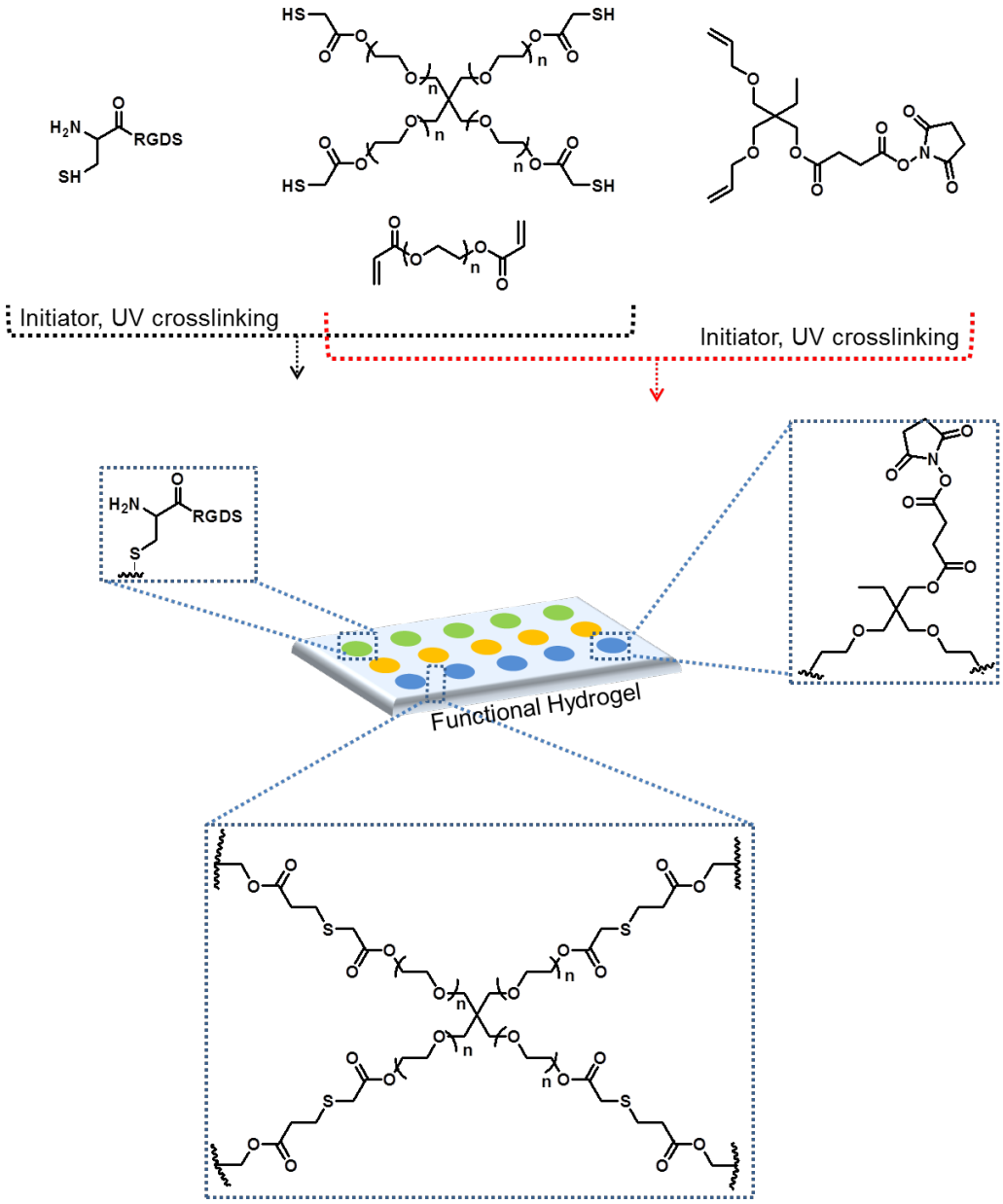

Figure 1.26. Functional hydrogel microarrays via thiol-ene chemistry.

In the first strategy, dye molecules or peptides were attached to the obtained poly(ethylene glycol) based hydrogels. For this purpose, thiol containing peptide molecules were mixed into pre-polymer mixture and then covalently attached to the hydrogel matrix

via thiol-ene click reaction successfully (Figure 1.26). As an alternative strategy, heterobifunctional crosslinker bearing alkene units and one other functionality like NHS, azide, thioester or aldehyde was used to have hydrogels that can be further functionalized, through different chemistries (Figure 1.26).

Patton and coworkers demonstrated the synthesis of a cross-linked thiol–ene network incorporating a dopamine acrylamide to investigate the biomimetic adhesion and hydrogen bonding capability of dopamine-functionalized polymer network to a variety of substrate surfaces [69]. Dopamine is a catecholamine that serves a dual function in natural adhesives as cross-linking agents and as “sticky” group. They synthesized polymer networks based on tri-arm alkene and four-arm thiol with incorporation of dopamine (Figure 1.27). The effect of dopamine acrylamide in the catechol form was studied. Hydrogen bonding interactions among the catechol and several hydrogen bond acceptors (ethers, amides, esters) in the network, resulted in considerable increase on the glass transition temperature of the network after the incorporation of catechol.

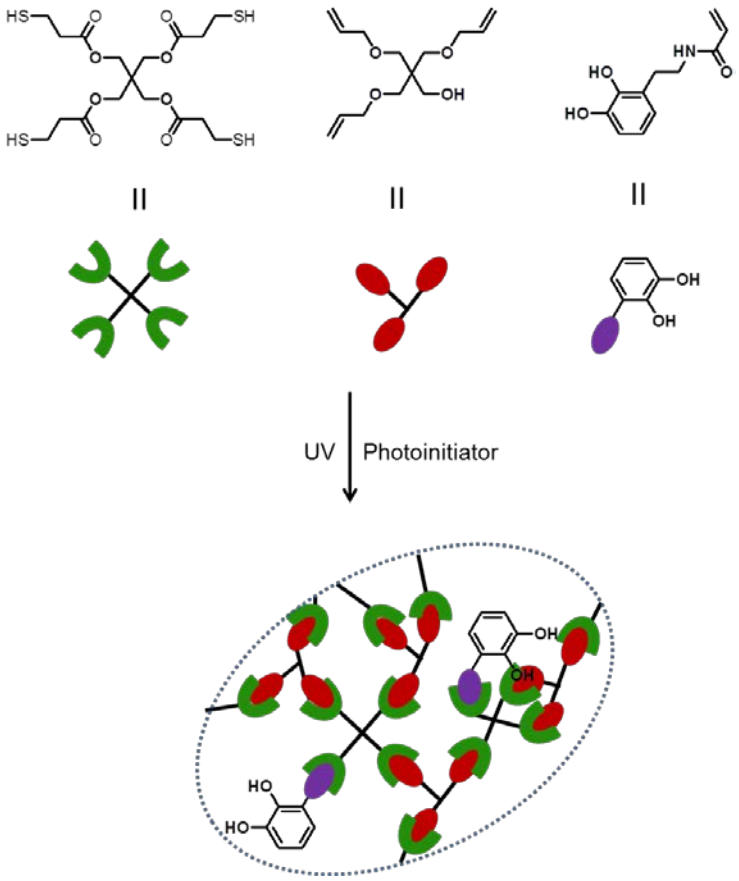

Figure 1.27. Fabrication of catechol functionalized polymer networks.

Goldmann *et al*. established the surface modification of micron-sized polydivinylbenzene (PDVB) particles utilizing both thiol-ene and alkyne-azide ‘‘click’’ chemistries [70]. Microspheres were prepared using divinyl benzene and 3- and 4-(ethylvinyl) styrene [71]. Subsequently, homopolymer of N-isopropylacrylamide was prepared by RAFT polymerization and end-modified to obtain thiol polymer. Finally, thiol-terminated pNIPAAm polymer was reacted with residual alkene units on the surface of the PDVB microspheres in the presence of AIBN, yielding grafted-to $PNIPAAm_{45}$-PDVB nanoparticles (Figure 1.28).

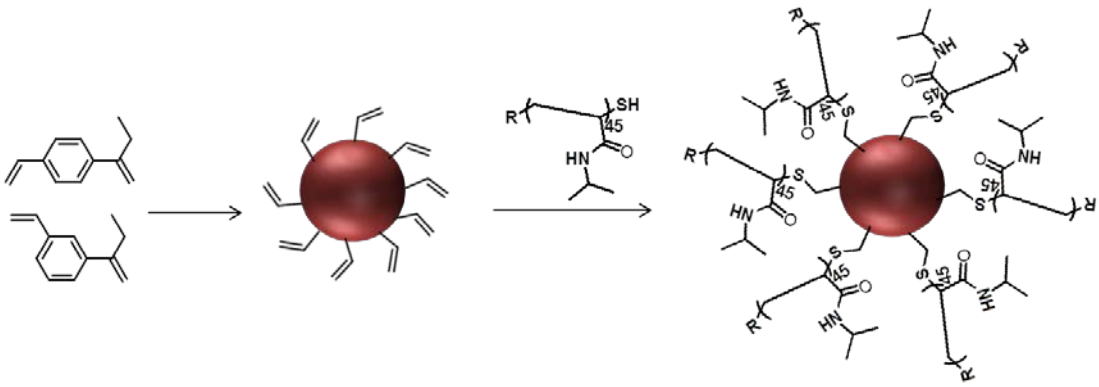

Figure 1.28. Modification of microspheres via thiol-ene chemistry.

1.5.2.2. Nucleophilic Thiol-Ene Addition. The nucleophilic thiol-ene addition to electron poor alkenes is one of the most widely implemented click reactions in polymer science, to fabricate a variety of macromolecular architectures including step-growth polymers, dendrimers, and cross-linked networks, as well as polymer bioconjugation and polymer functionalization. The nucleophilic thiol-ene reaction can be catalyzed through a base [72]. Since the sulfhydryl group is a strong nucleophile, it can easily react with electrophiles such as Michael acceptors forming a carbon-sulfur bond which has significant importance in bioapplications. Therefore, scientists have paid considerable attention to the addition of thiols to electron deficient alkenes.

For a base-catalyzed reaction, the thiolate anion is formed by the direct deprotonation of a thiol by a base catalyst. However, for the nucleophile-catalyzed system the thiol acts efficiently as the sole proton source and the initial step is an attack of the nucleophile on an

electron deficient α,β-unsaturated carbonyl which then produces an extremely basic enolate zwitterion that behaves as a base for the deprotonation of the thiol (Figure 1.29).

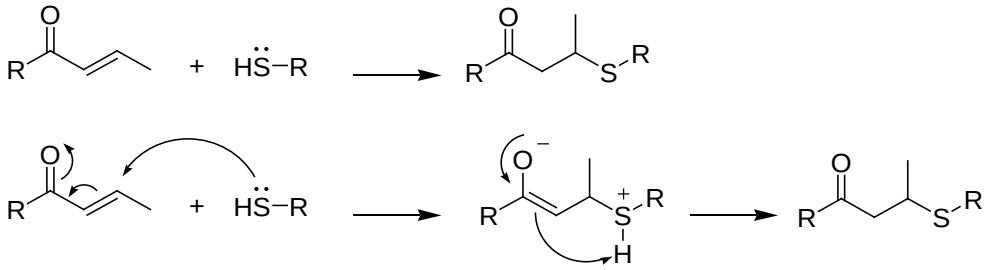

Figure 1.29. Base- and nucleophile-catalyzed mechanism of thiol-ene addition.

Recently, Sanyal and coworkers utilized thiol maleimide chemistry to functionalize maleimide containing biodegradable polymers (Figure 1.30) [73]. They first synthesized furan-protected maleimide containing cyclic carbonate monomer and achieved the copolymerization via ring-opening polymerization (ROP) to obtain furan-protected maleimide containing biodegradable polymer. Pendant furan protected maleimide side chains were reactivated via retro-DA reaction and generated maleimides were functionalized with thiol containing molecules via Michael addition reaction.

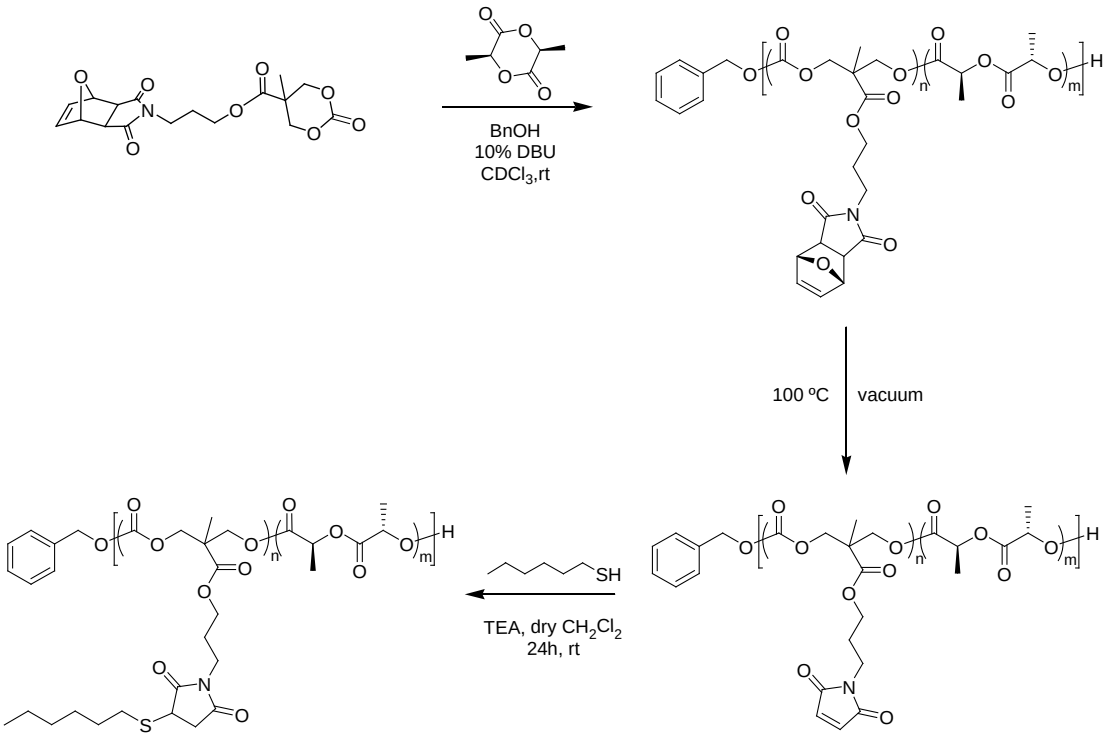

Figure 1.30. Synthesis and functionalization of biodegradable polymer.

Stenzel and coworkers used Michael reaction to decorate microspheres, as surface modification via Michael addition is an efficient tool for tuning the properties of microspheres [74]. Microspheres were successfully synthesized using EGDMA via suspension polymerization. Then, glucothiose was attached to the vinyl groups of microspheres to furnish bioactive property to the structure. The bioactivity of resins was tested with a lectin, Con A, which binds specifically to mannose or glucose sugars. In addition, Wang resin which is used for peptide synthesis was also studied as a scaffold for making microspheres with bioactive properties (Figure 1.31)

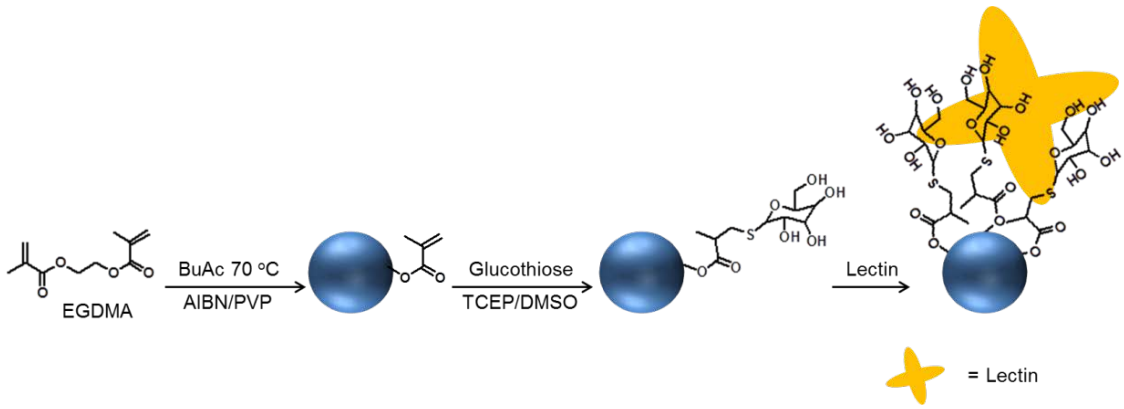

Figure 1.31. Synthesis of glucose functionalized scaffold.

1.5.3. Radical Mediated Thiol-yne Addition

Thiol-yne reaction is the addition of a thiol to the alkyne group which was first reported in 1949 by Bader *et al.* However, Anseth and Bowman recently made the reaction popular as thiol-yne "click" reaction and it was shown that the reaction can be used for network construction and functionalization of the surfaces in an efficient manner. It is differentiated from the thiol-ene free radical addition with the addition of two thiol groups to the alkyne unit while thiol-ene raction occurs between one thiol and one alkene unit (Figure 1.32). In the course of the reaction, first addition of the thiol group generates alkenyl sulfide and then another thiol radical is added to this alkenyl sulphide which results in a denser network structure. Thiol-yne reaction also adds increased functionality to the material compared to thiol-ene reaction.

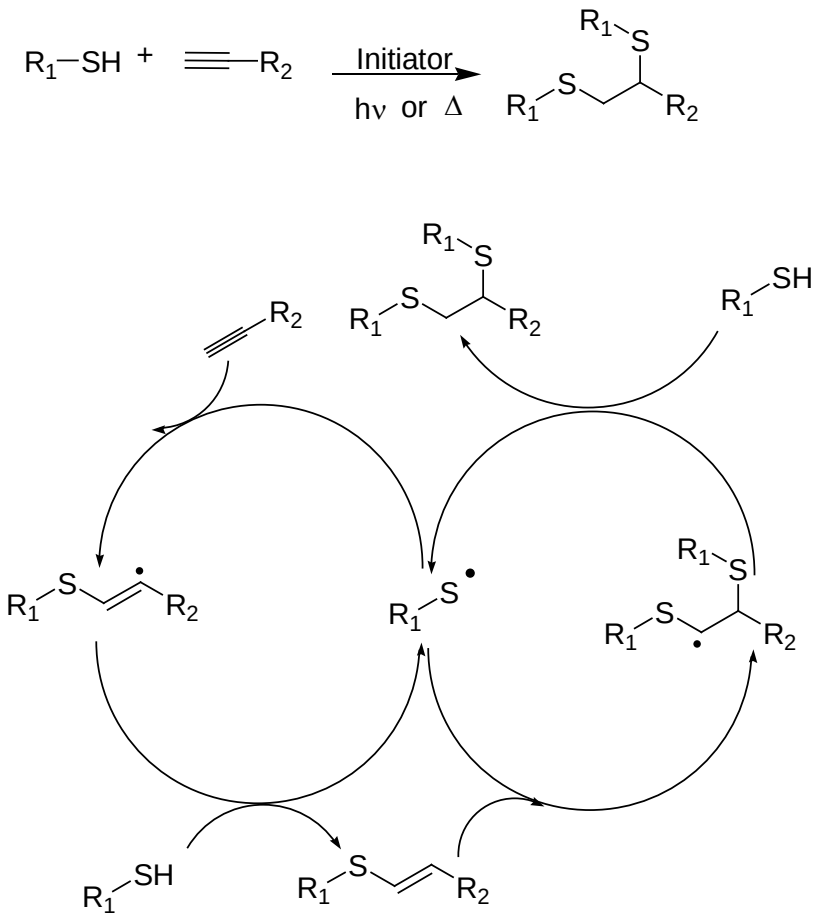

Figure 1.32. Mechanism of thiol-yne reaction.

Lately thiol-yne reaction was utilized by Lowe and coworkers for end group modification of N-isopropylacrylamide homopolymer (Figure 1.33) [75]. PolyNIPAm homopolymer was prepared using RAFT polymerization. Then, dithiobenzoate end groups of the homopolymer were converted to alkyne units via modification with propargyl acrylate by amine/phosphine-mediated nucleophilic thiol-ene “click” reaction. Alkyne functional terminal groups were functionalized with thiol containing molecules resulting end functional polymer with the free radical mediated addition of two thiol molecules to one alkyne unit.

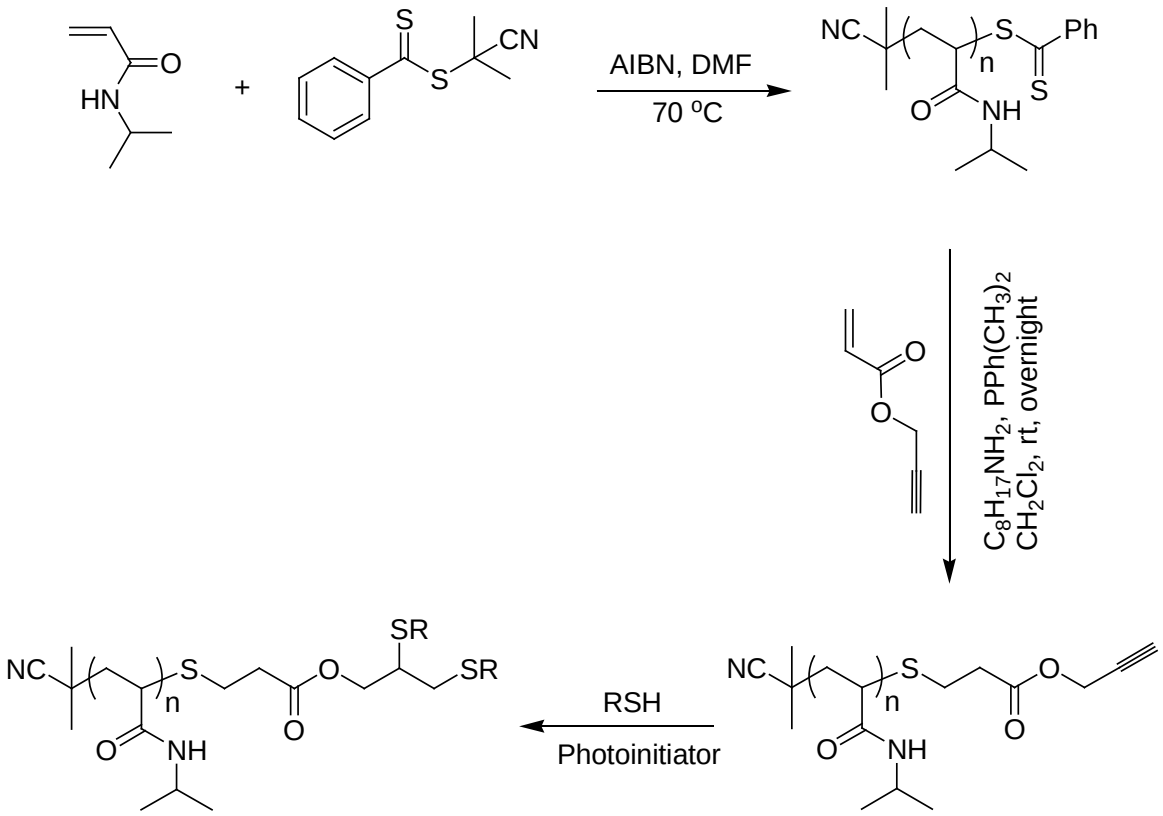

Figure 1.33. RAFT polymerization of N-isopropylacrylamide and end-group modification via thiol-yne reaction.

1.6. Cycloaddition Reactions

In cycloaddition reactions two or more unsaturated molecules combine together to form a cyclic adduct along with the reduction of the bond multiplicity. They can be initiated by thermal or photochemical conditions. Cycloaddition reactions are widely used in post-polymerization modification of polymers, surface modification or fabricating crosslinked materials [76]. In this thesis, three cycloaddition reaction are described including [3+2] Huisgen type 1,3-dipolar cycloaddition [4+2] Diels-Alder reaction and [2+2] dimerization reaction (Figure 1.34).

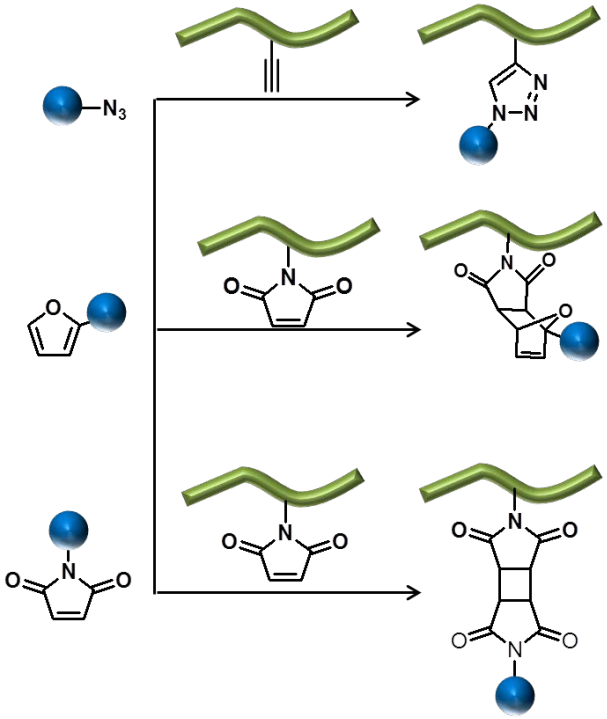

Figure 1.34. Cycloaddition reactions used in this thesis.

1.6.1. [3+2] Huisgen Type 1,3-Dipolar Cycloaddition

[3+2] Huisgen type 1,3-dipolar cycloaddition is a cycloaddition between an azide and a terminal or internal alkyne to give a 1,2,3-triazole. Rolf Huisgen was the first to understand the scope of this organic reaction in 1961 [77] without using a catalyst. Azide and alkyne groups react at high temperature to produce a mixture of 1,4 and 1,5-disubstituted triazoles (Figure 1.35).

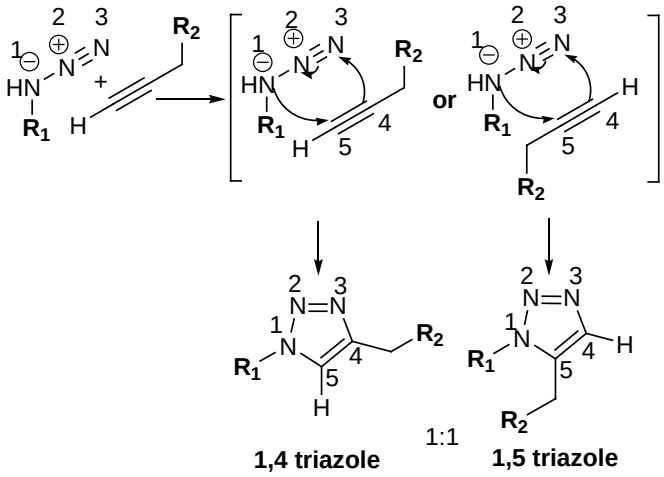

Figure 1.35. [3+2] Huisgen type 1,3-dipolar cycloaddition.

In 2001, Sharpless and Fokin introduced a Cu (I) catalyst [78-79] to the azide-alkyne cycloaddition reaction. Through Cu (I) catalyst regiospecific reaction results only in formation of the 1,4-disubstituted triazole (Figure 1.36).

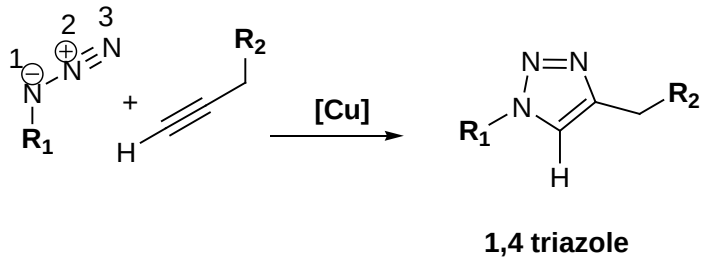

Figure 1.36. Copper catalyzed [3+2] Huisgen type 1,3-dipolar cycloaddition.

Copper catalyst allows the synthesis of physiologically stable product in aqueous or organic solvents in high yields. The catalyst can be introduced as Cu (I) salt (CuI or CuBr) or generated in situ by reduction of Cu (II) salts and amine containing base such as 2,6-lutidine, triethylamine, pyridine and PMDETA. Commonly used Cu-systems are $CuSO_4$/ NaAsc and CuBr/PMDETA due to exclusive regiospecificity, mild reaction conditions, easy purification, high yield and functional group tolerance.

Since leftover copper catalyst can be toxic for biological systems, copper-free click chemistry is developed by Bertozzi [80], based on the work by Fokin and Sharpless. This reaction is based on the cycloaddition of cyclooctynes instead of terminal alkyne without the benefit of copper catalyst (Figure 1.37). Due to the exclusion of Cu catalyst this reaction can be easily used for biological applications.

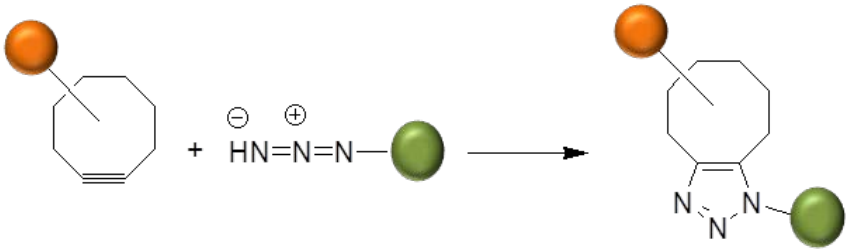

Figure 1.37. Copper-free cycloaddition.

Since [3+2] Huisgen type 1,3-dipolar cycloaddition offers highly selective and an orthogonal reaction under a variety of mild conditions [81], it has been widely used in the synthesis of well-defined macromolecules such as dendrimers, dendronized polymers and hydrogels [19].

As an example of this strategy was demonstrated by Sanyal and coworkers, tosynthesize orthogonally functionalizable and biodegradable bis-MPA based dendrons [82]. The periphery of the dendrons was decorated with alkyne moieties and the focal point was furnished with a maleimide group. Later to show the orthogonality of the functional groups, alkyne units were reacted with benzyl azide via Huisgen type “click” cycloaddition while the focal point maleimide was reacted with undecene thiol via Michael addition in a one pot synthesis. In addition, to show the multifunctionality of dendrons the alkyne units at the periphery were functionalized with PEG chains via copper catalyzed Huisgen click reaction while maleimide containing focal point was employed to attach BODIPY thiol, a hydrophobic dye via efficient Michael addition. Thus, with the addition of PEG unit via Huisgen type cycloaddition reaction hydrophobic dye molecule became water soluble. (Figure 1.38).

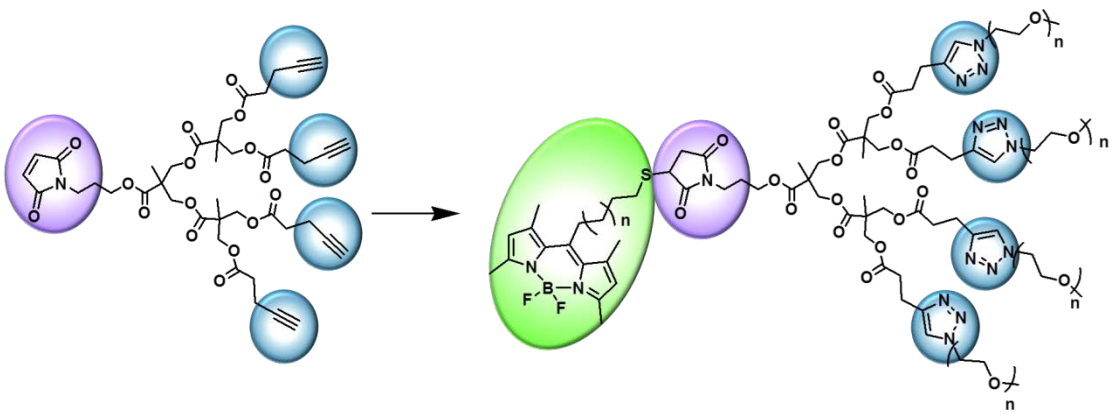

Figure 1.38. The surface functionalization of a dendron via Huisgen type cycloaddition.

Anseth and coworkers developed a strategy which was a copper-free, azide-alkyne click chemistry between tetrafunctional PEG azide molecules and dialkyne functionalized synthetic polypeptides [18]. They showed that with step-growth polymerization of azide and alkyne units, an idealized network formed with minimum defects. Changing crosslink

density and PEG molecular weight, mechanical properties could also be tuned. Pendant alkene functionality on hydrogel network was used for further functionalization via thiol-ene click chemistry for the attachment of cysteine-containing peptides (Figure 1.39).

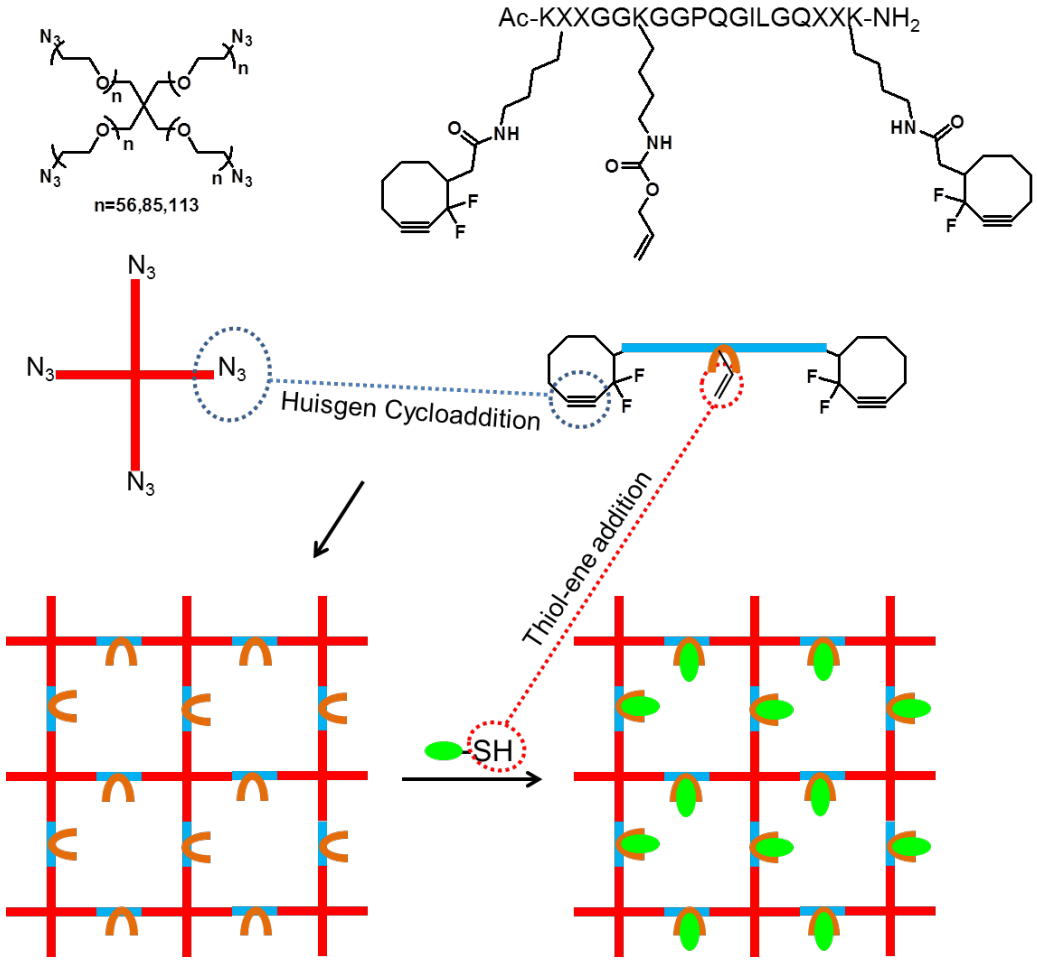

Figure 1.39. Step-growth networks via Huisgen click reaction and functionalization of pendant alkene units

Hawker and collegues used Huisgen type cycloaddition to demonstrate the orthogonal functionalization of block copolymer nanoparticles [83]. For this purpose, a block copolymer with a polylactide block which contains alkyne functionality and polyether with alkene functionality was synthesized. Subsequently, self-assembly of the material was achieved in THF and block copolymer nanoparticles containing pendant alkyne groups reacted with azide-functional coumarin dyes via copper catalyzed 1,3 dipolar cycloaddition to show the feasibility of the reaction (Figure 1.40).

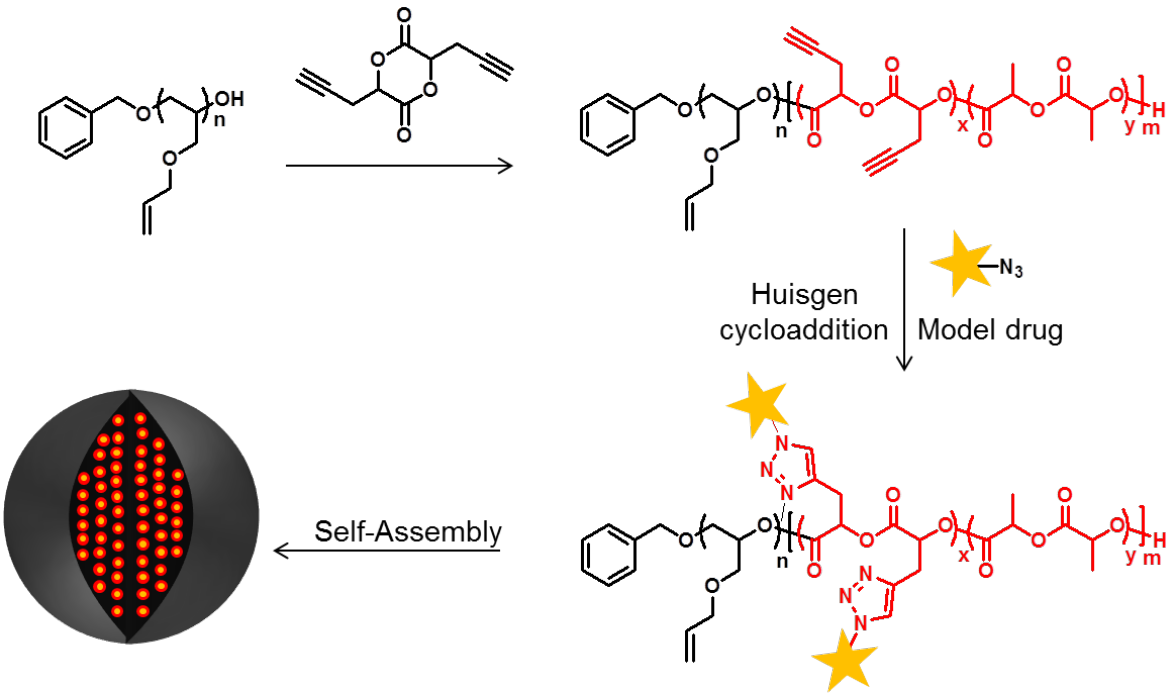

Figure 1.40. Fabrication of functional block copolymer nanoparticles.

1.6.2. Diels-Alder Cycloaddition

The Diels-Alder reaction is one of the most versatile reactions in chemistry [84-85]. This reaction was named after scientists who discovered this reaction, Otto Diels and Kurt Alder. They received the Nobel Prize in Chemistry in 1950 for this discovery. The reaction involves a [4π+2π] cycloaddition reaction among a conjugated diene and a substituted alkene (generally regarded as dienophile) to produce a cyclohexene (Figure 1.41) [86-87]. The reaction shown below requires tough reaction conditions, but electron withdrawing groups on the electrophilic dienophile and electron donating groups on the nucleophilic diene makes the reaction favourable.

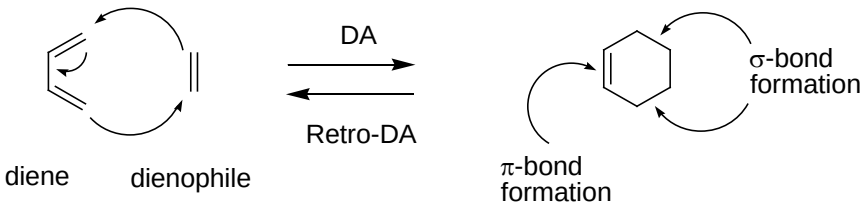

Figure 1.41. Diels-Alder reaction mechanism.

Diene of the Diels–Alder reaction may be considered as an open-chain or cyclic compound with different kinds of substituents (Figure 1.42), and should be in s-cis conformation in order to carry out the reaction. S-trans conformation does not undergo Diels-Alder reaction.

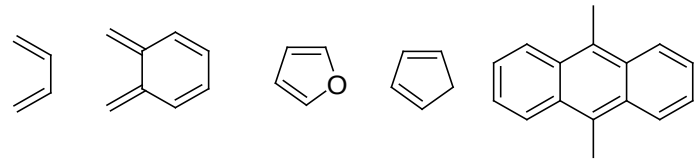

Figure 1.42. Some dienes appropriate for Diels-Alder reaction.

Although it is not a characteristic feature of Diels–Alder, dienophiles may have an electron-withdrawing group conjugated to the alkene (Figure 1.43). Therefore, they can have some extra conjugation with different groups in order to increase the rate of reaction by many folds.

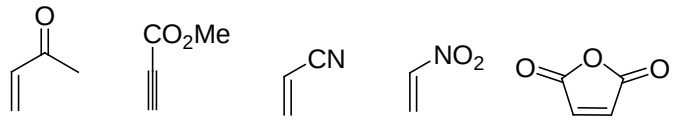

Figure 1.43. Some dienophiles appropriate for Diels-Alder reaction.

Using Diels-Alder chemistry a number of complex molecular and macromolecular architectures and a variety of cross-linked systems have been synthesized. In addition, it has also been used for functionalization steps. Thermoreversible nature of this chemistry is another advantage to design stimuli responsive materials by utilization of cycloreversion reaction. This reaction can be affected from temperature depending on the the diene–dienophile selection. Electron-rich dienes and electron-deficient dienophiles make the reaction easier so lower temperatures are required for both forward and the reverse reaction.

Recently Tunca and coworkers used Diels-Alder click chemistry to prepare well-defined block copolymer structures using anthracene end-functionalized polycarbonate and furan-protected maleimide end-functionalized PEG (Figure 1.44) [88].

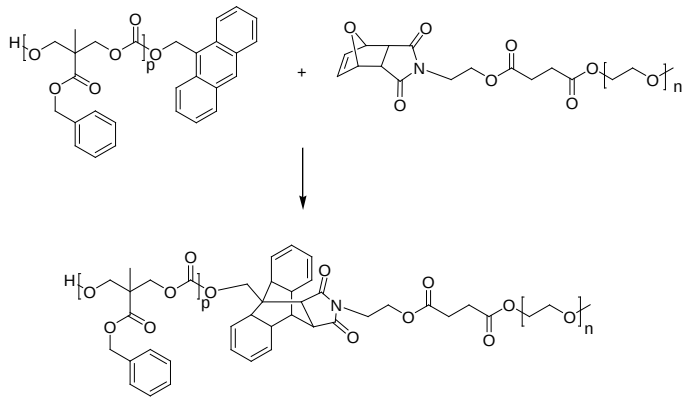

Figure 1.44. Block copolymer synthesis via Diels-Alder “click” reaction.

Many type of macromolecular scaffolds with various topologies such as block, graft, star, and cyclic copolymers have been synthesized using Diels-Alder click reaction. For instance, Diels−Alder reaction has been utilized for the synthesis of unsymmetrical dendrimers with the combination of discrete dendrons [89]. Initially, maleimide containing third generation polyester dendron and furan containing third generation polyaryl dendron was synthesized divergently and focal points of dendrons were combined via Diels-Alder reaction to get unsymmetrical dendrimers. This was an early example for the production of AB type dendrimers with Diels−Alder cycloaddition. Thermoreversibility of the reaction was also demonstrated through heating in the presence of anthracene to capture the released maleimide containing polyester dendron (Figure 1.45). Since the reaction works with catalyst free conditions, it is more applicable for biological systems.

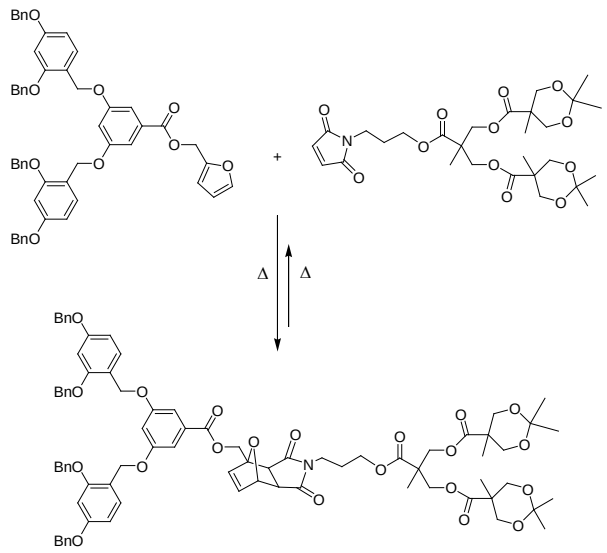

Figure 1.45. Segment block dendrimers via Diels-Alder cycloaddition.

The Diels-Alder methodology also permits the production of a large number of cross-linked systems exhibiting thermoreversible behaviour. For example, Shoichet and co-workers focused on the synthesis of hyaluronic acid (HA) based hydrogel scaffolds using Diels-Alder click chemistry [90]. Furan modified HA derivatives were synthesized, and reacted with bismaleimide functionalized PEG to give crosslinked hydrogel network in one step procedure (Figure 1.46).

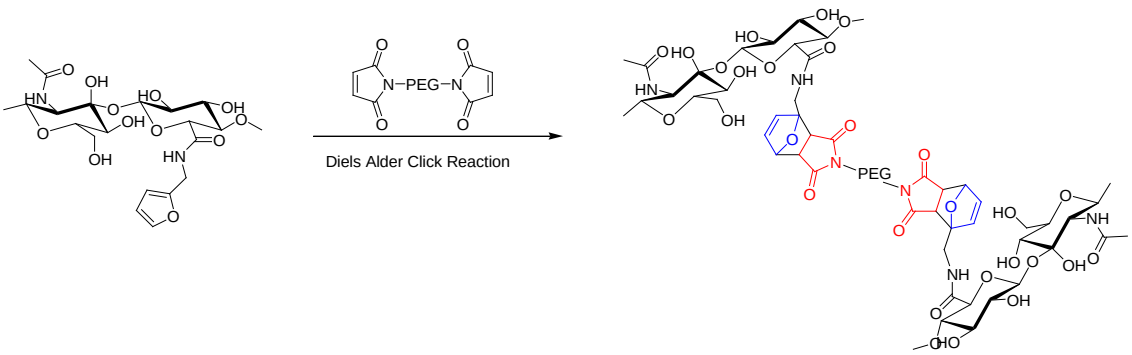

Figure 1.46. Synthesis of HA based PEG hydrogels.

Sanyal and coworkers reported the fabrication of polymeric thin films that are decorated with a diene which can be functionalizable with dienophile containing dye molecules via micro contact printing using the Diels–Alder reaction [91]. At first, PEGMA-based reactive copolymer which contains furan as a pendant group was synthesized. Subsequently, thin films were prepared and functionalized with maleimide-appended dye molecules via Diels–Alder reaction. Since Diels-Alder reaction is thermoreversible, these surfaces were used as rewritable platforms. After micro contact printing of fluorescent dye molecules, they were erased from the surface utilizing retro-Diels-Alder reaction, and refunctionalization of the maleimide appended dye molecule was achieved via Diels-Alder reaction (Figure 1.47). Immobilization of biomolecules to this reactive surface also accomplished using Diels-Alder chemistry.

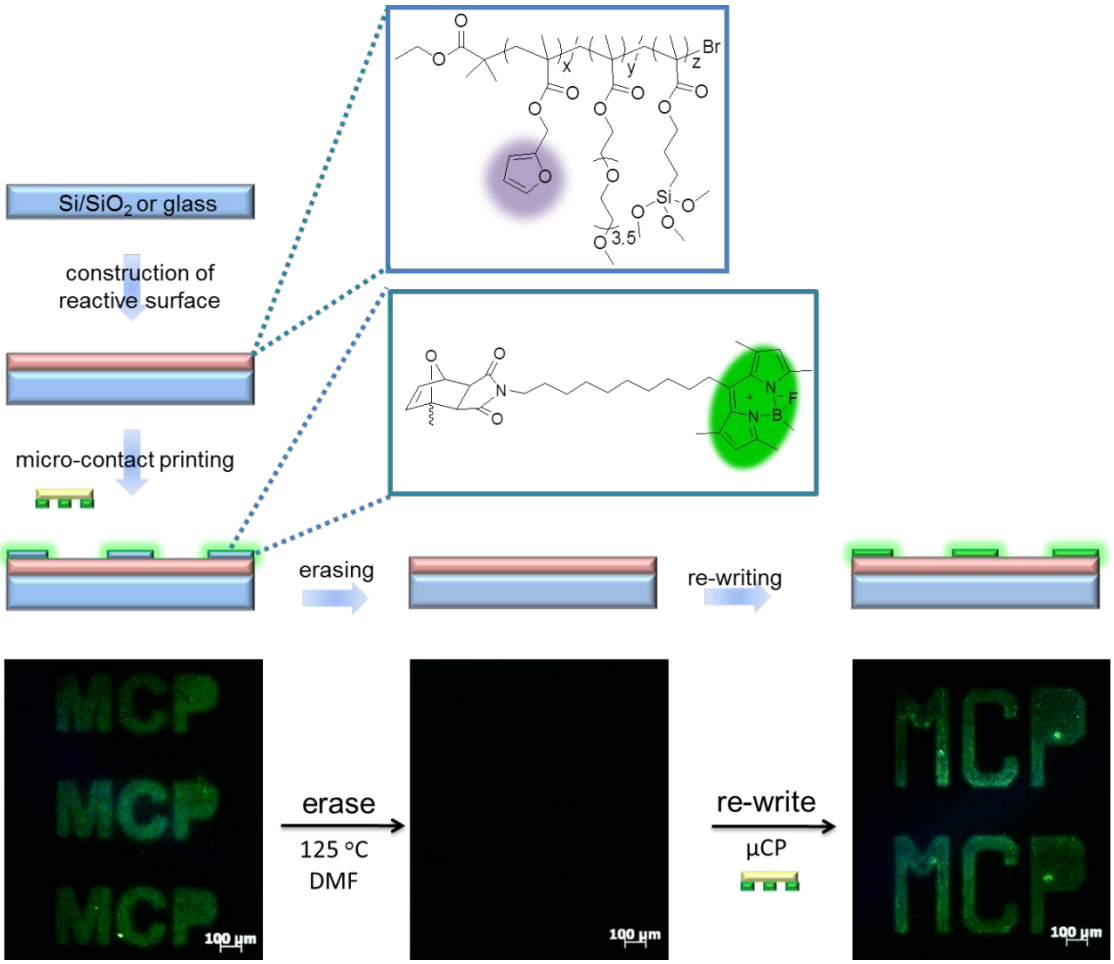

Figure 1.47. Reversible patterning on reactive polymeric thin films by micro contact printing of maleimide-containing dye.

A novel approach for the synthesis of polymers containing dendron groups as side chains is developed using the Diels–Alder "click" reaction as well [92]. Styrene-chloromethyl styrene polymer was synthesized viaRAFT polymerization technique. Subsequently, anthracene groups were incorporated from the chloromethyl styrene points via simple nucleophilic displacement reaction (Figure 1.48). Latent reactive polyester dendrons containing furan-protected maleimide on their focal points were prepared divergently. Thermal deprotection of the focal points of polyester dendrons uncovered the reactive maleimide groups which ignite Diels–Alder cycloaddition between the anthracene-containing polymer and latent-reactive dendrons to afford dendronized polymers.

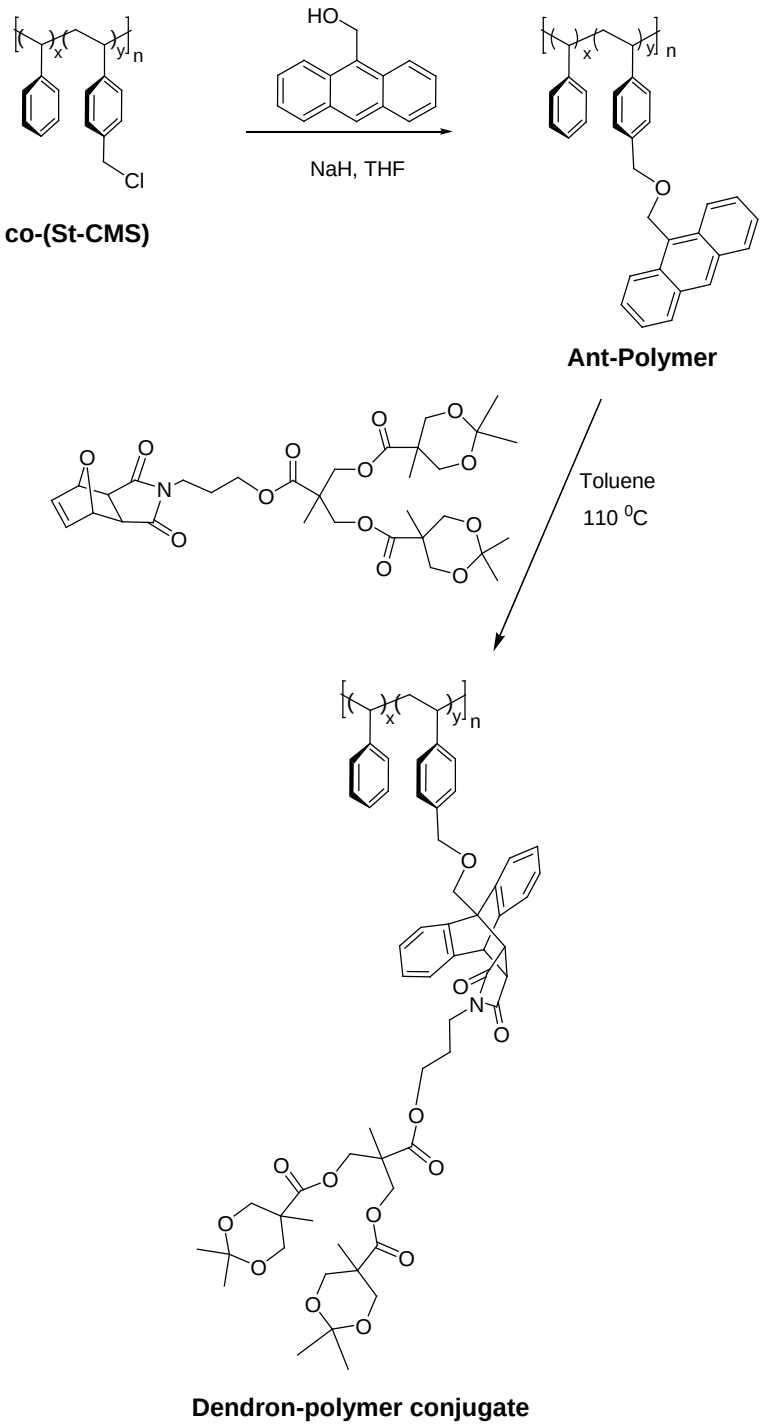

Figure 1.48. Synthesis of anthracene-appended styrene polymer and dendron polymer cycloaddition.

Attached dendrons were deprotected to yield hydroxyl group containing polymers to demonstrate the feasibility of the scaffolds as hydrophilic films, in which the water contact angle (WCA) drops considerably. The hydroxyl groups on these films can also be used for further functionalization studies (Figure 1.49).

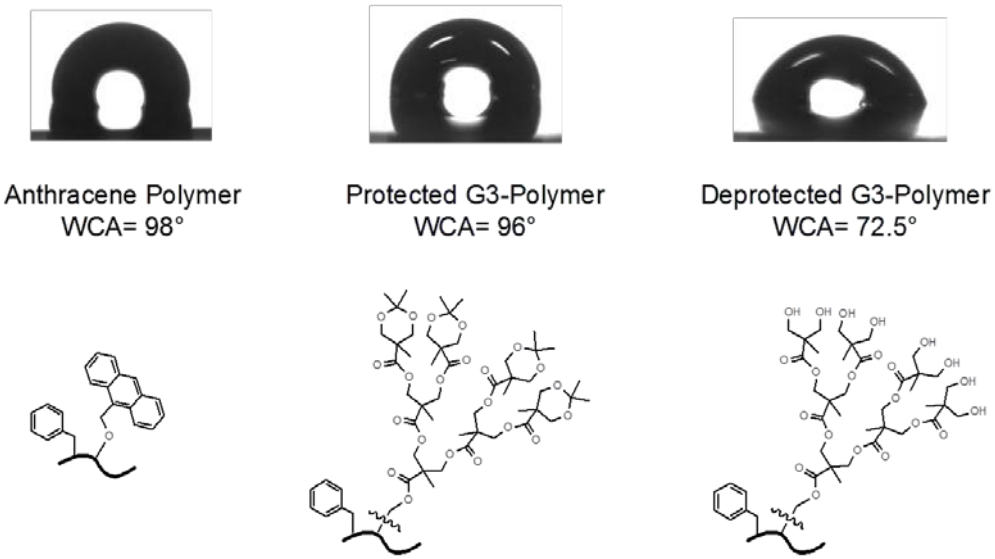

Figure 1.49. Contact angle of water on films of dendronized polymers.

1.6.3. Photochemical [2+2] Cycloaddition

Different approaches are possible for designing cross-linked networks. Especially, the development of smart polymeric materials in the form of external stimuli like light is one of the growing research areas suitable for bioappplications. As a result of photochemical activation, cycloaddition reactions occur between two double bonds in which 4n π electrons participate to form a ring. When appropriate functional groups are available, crosslinking can be performed via UV photocrosslinking (Figure 1.50)

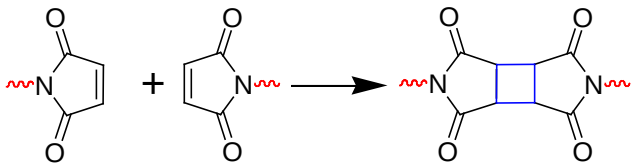

Figure 1.50. Photodimerization of maleimide.

Saalwaechter and coworkers demonstrated the synthesis of polyacrylamide hydrogels from linear polyacrylamide chains with pendant dimethylmaleimide groups through 2+2 cycloaddition reaction. (Figure 1.51) [93]. Thioxanthone disulfonate was used

as a triplet sensitizer. Rate of dimerization was shown to be related to the concentration of sensitizer and the intensity of irradiation. Crosslinking rate was monitored by UV spectroscopy.

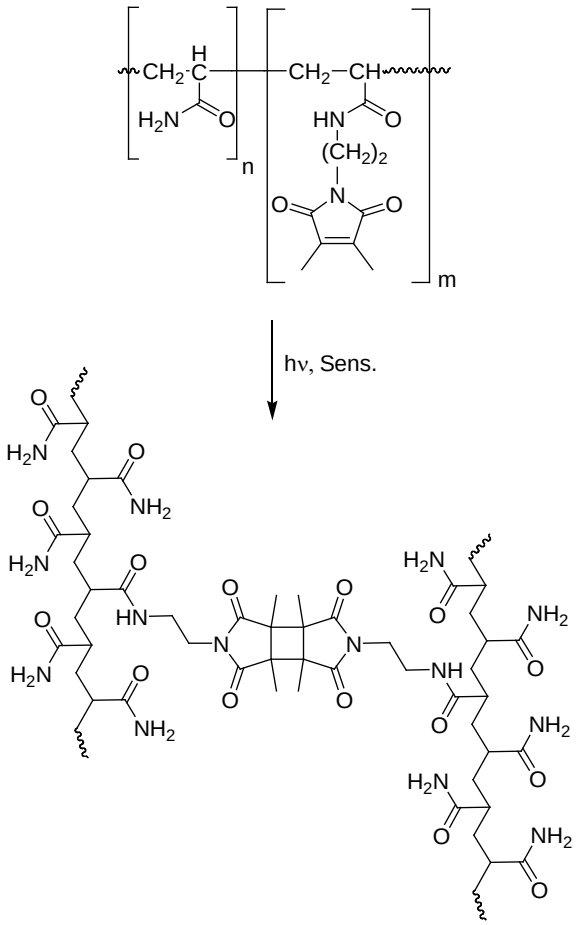

Figure 1.51. Copolymerization of acrylamide (AAm) with N-(N'-acryloyl-2-aminoethyl)-dimethylmaleimide (DMMIAAm) and photocrosslinking of the copolymer.

Photo-crosslinkable materials carrying maleimide groups on the side chains have been designed for the preparation of membranes for separation processes by Kleinermanns group [94]. They exhibit some advantages in membrane fabrication over conventional crosslinked polymer materials. Poly [ethene-*stat*-(methacrylic acid)], which is a potential membrane polymer, was functionalized with photo-crosslinkable maleimide units. Later, crosslinking experiments carried out both in the liquid phase and solid phase yielding crosslinked materials (Figure 1.52).

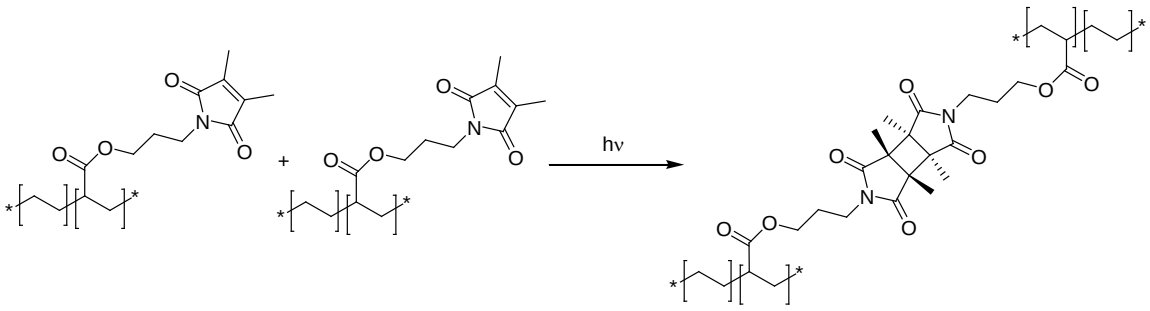

Figure 1.52. Photo-crosslinking of the polymer.

1.7. Orthogonally Functionalizable Polymers

Recently, scientists started to investigate unique chemoselective reactions which can take place without interference with other functional groups in the medium. This property is described as the orthogonal nature of the reactions. In biological systems chemical reactions occur in an orthogonal fashion, for instance an enzyme can bind to a substrate selectively in the presence of many other functional groups. Thus, these studies in the field of chemoselective orthogonal reactions became the center of the research [95]. Functional polymeric materials have many applications as they can mimic biological systems. For instance, they can be used in targeted drug delivery systems providing the possibility to attach both drug molecule and a targeting moiety. In that respect, instead of time consuming ligation strategies with side reactions, novel orthogonal ligation strategies have been discovered with high yield and without side reactions under mild reaction conditions.

Recently, Sanyal and coworkers showed the synthesis of orthogonally functionalizable styrene-based copolymers via AIBN initiated free radical polymerization and RAFT polymerization [96]. They synthesized two sets of orthogonally functionalizable polymers. The first set involved multifunctional polymers reactive towards both amines and thiols. NHS-based active ester groups on the copolymer were functionalized with amines and maleimide groups were functionalized with thiol containing molecules. The second set contained two different alkenes: first thiol containing molecule was attached via free radical based thiol-ene addition to the ene-based side chain of the reactive polymer

whereas the second thiol moiety was attached via nucleophilic thiol-eneto maleimide-based side chain of the reactive polymer. (Figure 1.53)

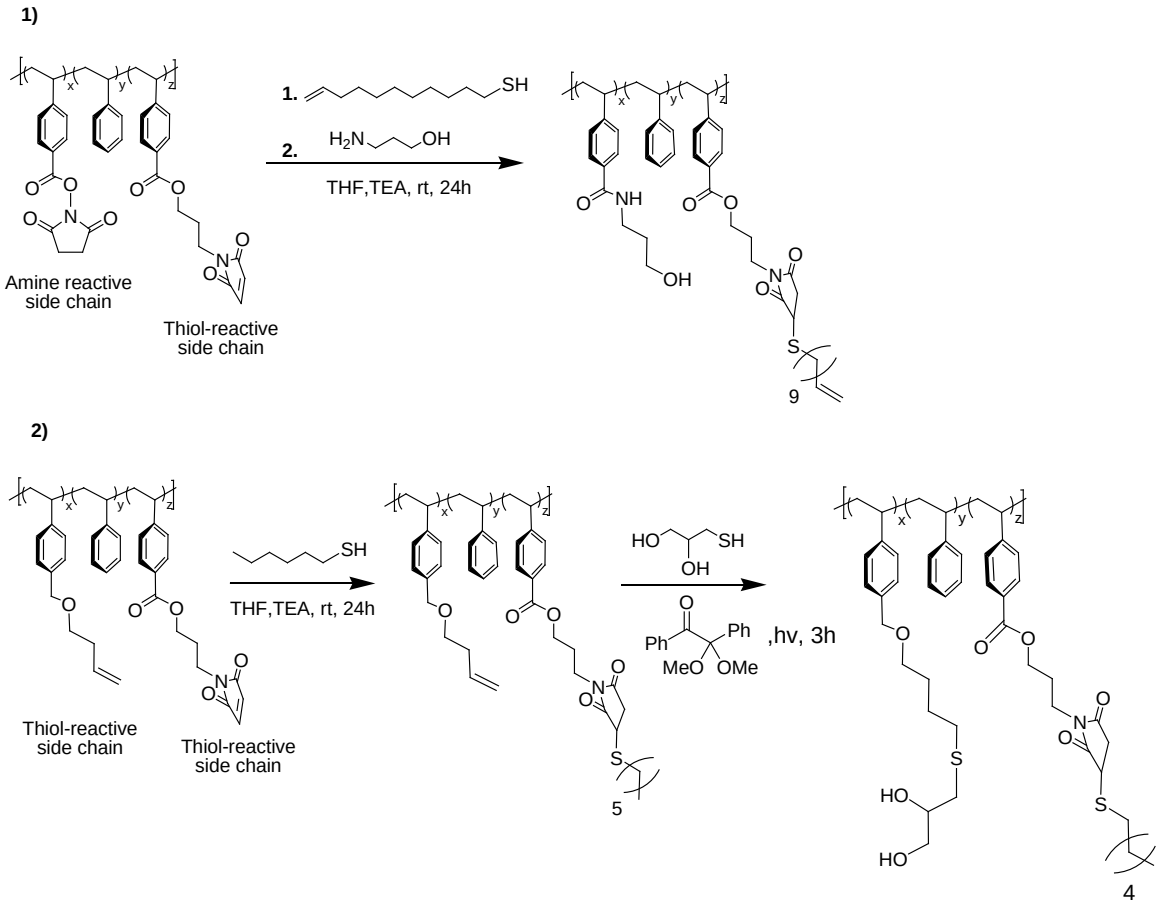

Figure 1.53. Orthogonal functionalization of reactive multi-functional polymers.

Weck and coworkers synthesized orthogonally functionalizable random polymers for biological applications such as targeted drug delivery or biosensors using three different norbornene monomers (Figure 1.54) [97]. The functional side chains of the polymer were functionalizable with three different ligation strategies: 1,3-dipolar cycloaddition, nucleophilic thiol-ene reaction and hydrozone formation. For this purpose, norbornene containing monomers were prepared and polymerized via ring-opening metathesis polymerization (ROMP). Later, reactive groups were functionalized at three separate steps via nucleophilic thiol-ene addition to the maleimide side chain, [3+2] Huisgen type functionalization of bromo side chain after converting the bromo to azido group, and finally hydrozone formation via the reaction of the ketonealdehyde side chains with benzylhydrazide.

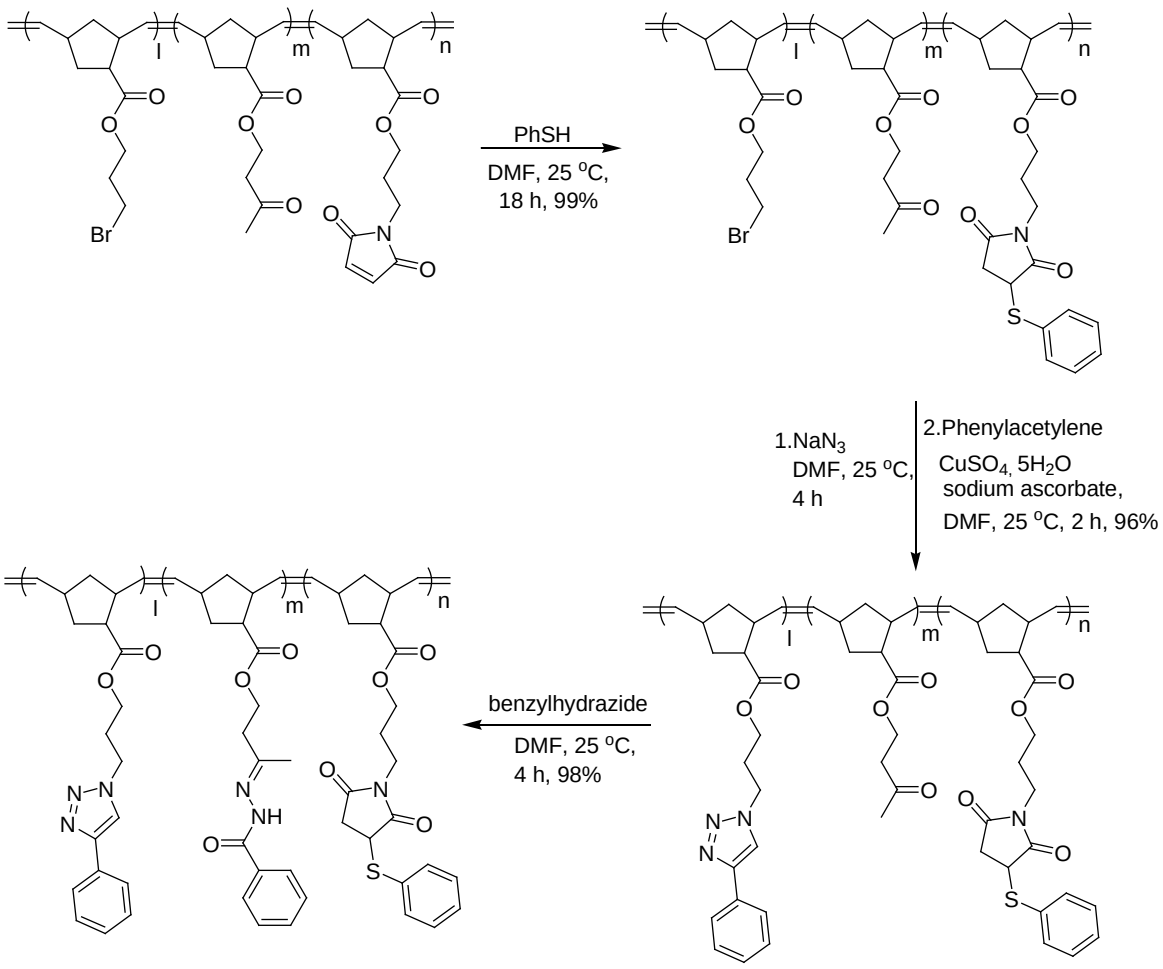

Figure 1.54. Synthesis and orthogonal functionalization of terpolymer.

Tunca and coworkers reported the synthesis of orthogonally functionalizable brush copolymers carrying anthryl and azido functionalities via ROMP [98]. Bromo bearing monomer was utilized for the copolymer synthesis, which thenwas converted to the azide functionality. Post-polymerization modification of azide pendant chains were done with alkyne end-functionalized PCL via Huisgen type 1,3-dipolar cycloaddition and anthryl side chains were reacted with maleimide end-functionalized PMMA via Diels-Alder "click" reaction (Figure 1.55).

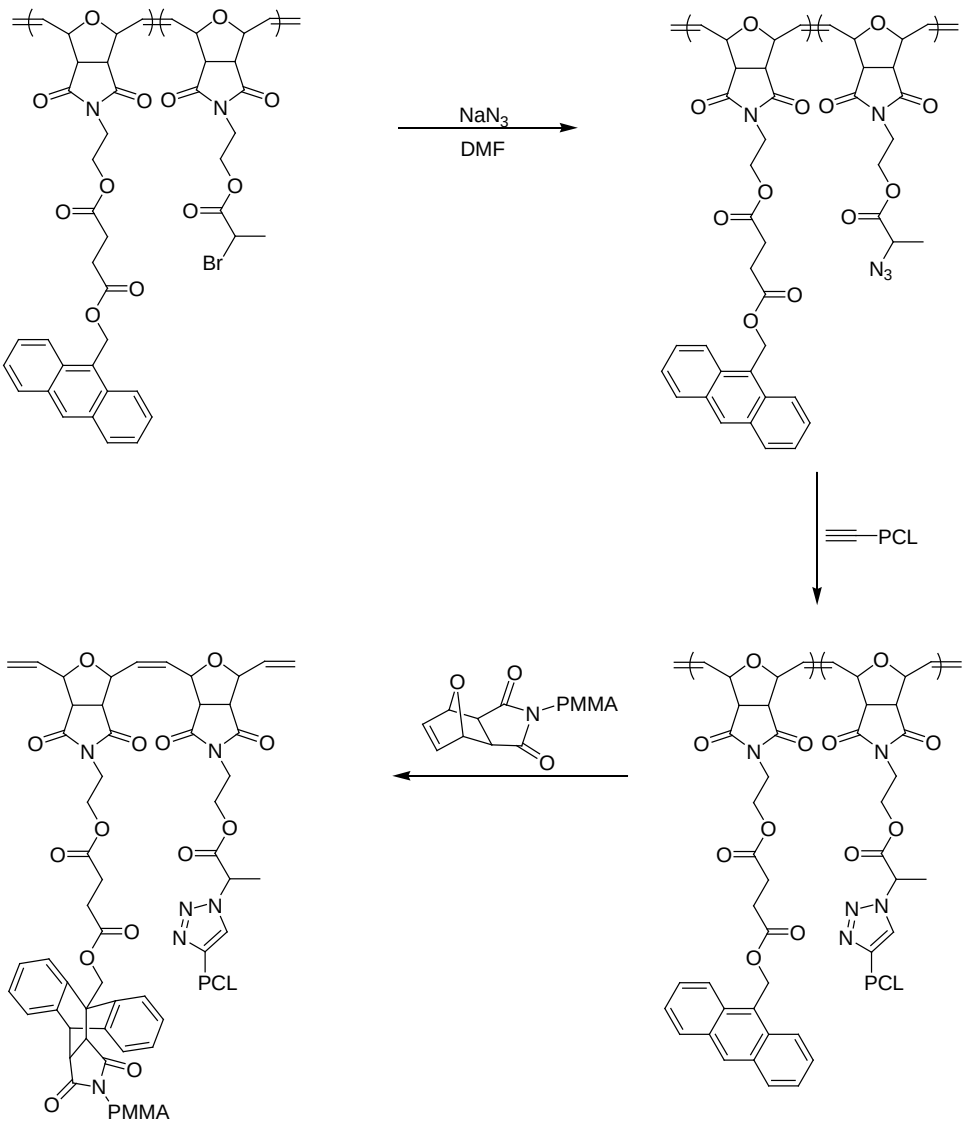

Figure 1.55. Synthetic method for the synthesis of brush copolymers.

In another study, Tunca and coworkers used a single step method to prepare well-defined orthogonally functional polymeric structures from reactive polymers via Huisgen type 1,3-dipolar cycloaddition and Diels–Alder cycloaddition (Figure 1.56) [99]. For this purpose, they synthesized random copolymer from styrene and p-chloromethylstyrene. Then p-chloromethylstyrene was partially converted to anthracene functionality via nucleophilic substitution reaction. Remaining p-chloromethylstyrene was converted to azido group. Finally, the copolymer was functionalized with PMMA-maleimide on the anthracene side chain via Diels-Alder reaction and PEG-alkyne on the azido side chain via Huisgen type 1,3-dipolar cycloaddition in a single step.

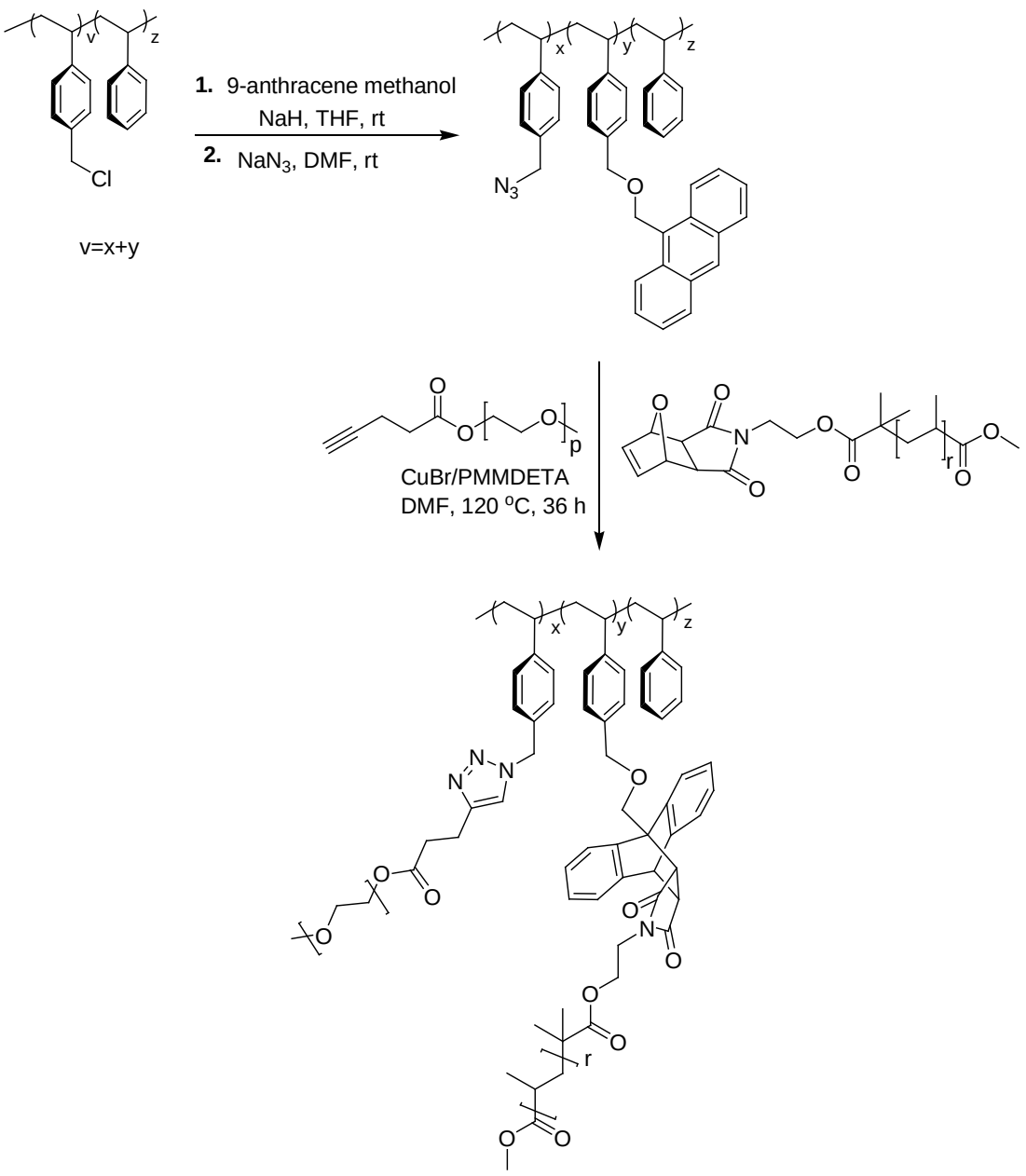

Figure 1.56. One-step preparation of heterograft polymers via Diels-Alder and Huisgen type 1,3-dipolar cycloadditions.

In summary, a brief survey of recent synthesis and functionalization of polymeric materials highlight the important role of efficient reactions like “click” chemistry in this area. These reactions can be employed in combination to synthesize multifunctional polymeric materials that would be difficult to obtain using traditional polymer synthesis.

2. RESEARCH OVERVIEW

This thesis ties five major research projects under one objective which is to design novel reactive polymeric materials suitable for biomedical and biotechnology applications. This goal has been achieved by the synthesis of functional polymers, hydrogels and the fabrication of functional hydrogel surfaces with polymeric materials that can be orthogonally functionalized with different molecules. Top-down approaches like nano-imprint lithography, photolithography and soft lithography were used to obtain micro-patterned reactive surfaces.

Initial efforts were directed towards synthesis of novel reactive polymers that can be efficiently functionalized with amine and thiol group containing molecules and ligands. These polymers were incorporated with different reactive groups to enable their functionalization in an orthogonal fashion. The functional groups on these polymers were used for attachment of various molecules of interest. Additionally, the reactivity of these functional groups was used as a tool to fabricate functionalizable cross-linked materials such as hydrogels. In an alternative approach, thiol-based chemistry was utilized using commercially available monomers or polymers to obtain reactive hydrogels. Lastly, maleimide containing reactive polymers were used to fabricate micro-patterned reactive surfaces using photo-crosslinking based approach.

In recent years, a number of efficient chemical ligation strategies such as Huisgen-type 1,3-dipolar cycloaddition, thiol-epoxy chemistry, Diels-Alder cycloaddition, [2+2] photo-dimerization, thiol-ene reactions, nucleophilic reactions between activated esters or carbonates and Michael-type addition reactions have been utilized in synthesis and functionalization of polymers. In this research, all of these strategies were employed either alone or in combination for the development of novel functional polymeric materials.

3. ORTHOGONALLY FUNCTIONALIZABLE COPOLYMERS WITH HYDROLYZABLE AND NONHYDROLYZABLE LINKERS

The materials in this chapter have been adapted with modifications from the following article: Cengiz N., H. Kabadayıoğlu, R. Sanyal, *Journal of Polymer Science Part A: Polymer Chemistry,* Vol. 48, No. 21, pp. 4737-4746, 2010.

3.1. Introduction

Functional polymers serve as promising scaffolds for various applications such as polymer conjugated drug delivery, micellar assemblies for drug delivery, functional coatings for *in vivo* implants and *in vitro* sensing platforms. To obtain functional polymeric materials, parent polymers containing reactive functional groups are utilized since they can be modified post-fabrication for the intended application. When functionalization is targeted with amine group containing (bio)molecules or ligands, polymers bearing activated esters are widely employed, as discussed in Chapter 1. The nucleophilic substitution of active esters is an attractive post-polymerization modification since the reaction proceeds under mild conditions, oftentimes without need of additional catalysts. Well-defined polymers containing activated esters can be obtained using various free radical polymerization techniques. The comonomer ratios in the polymerization feed can be adjusted to obtain specific amount of reactive units. Moreover, it is also possible to use combination of different monomers that can be efficiently derivatized as desired to obtain orthogonally functionalizable polymers. For applications of polymers in biomedical sciences, especially in drug delivery, orthogonal functionalization of polymers is very important because it provides an opportunity to selectively attach targeting groups along with drug molecules for targeted therapies (Figure 3.1).

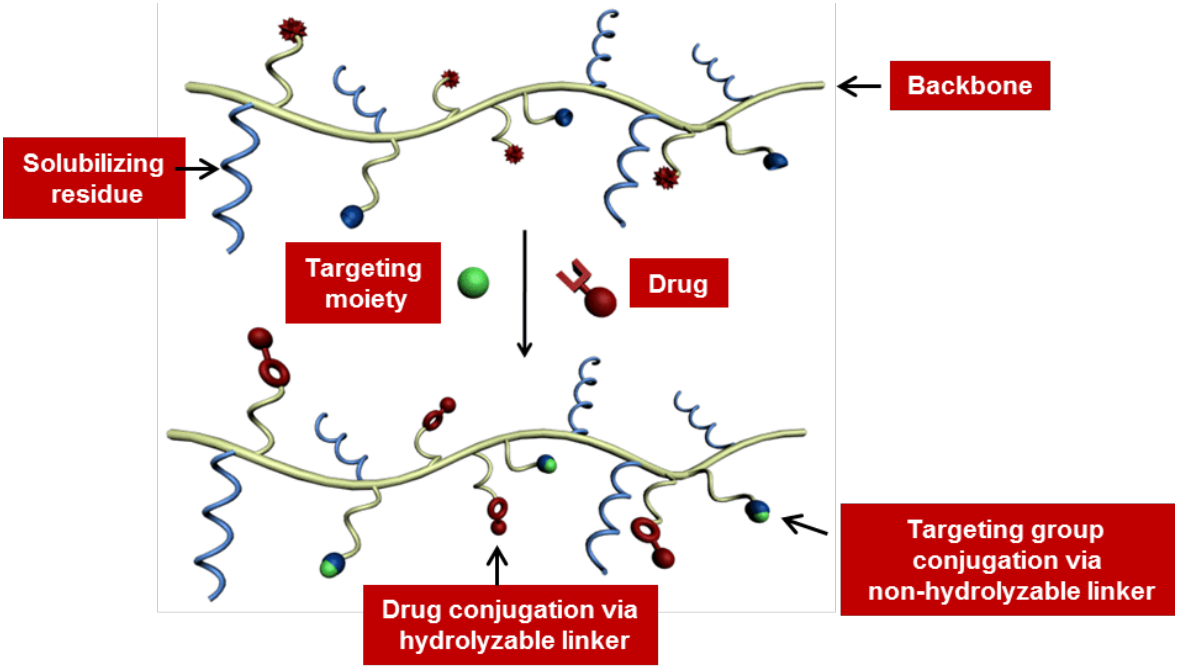

Figure 3.1. Illustration of a typical polymeric construct for targeted drug delivery.

The choice of the linkers is crucial for polymer–drug conjugates because the targeting group should remain on the polymer, therefore should be attached with a non-metabolizable linker, and the drug should be released as desired, requiring cleavable attachment [100]. Hence, the drug linker can be designed to degrade in different conditions such as in acidic media or by specific enzymes. In addition, hydrophilicity and biocompatibility of these polymeric constructs is a primary requirement.

Therapeutic agents can be conjugated to polymers using a variety of chemical linkages including carbamate, carbonate, amide, ether and ester (Figure 3.2). Due to the stability and cleavage conditions carbamate linkage is important for polymer conjugated drug delivery [101-103]. Linkers connecting the drug molecule to the polymeric macromolecule require being stable in the plasma while possessing the inherent biodegradability property to release the payload. Carbamate-based linkers are well suited for this purpose [104-108]. The hydrolyzable nature of these carbamate side chains are known to allow slow release of covalently attached molecules, providing different release profiles for drugs than more common ester or amide linkages.

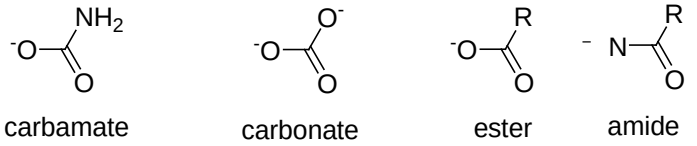

Figure 3.2. Commonly used linkages employed for attachment of therapeutic agents to polymers.

It was revealed for model prodrugs that ester linkages are hydrolysed fast in plasma whereas carbamates are relatively stable [109-110]. Paclitaxel prodrugs which contain an ester or carbamate linkage also showed stability in a similar fashion [111]. The order of stability towards plasma esterases was found to be as shown in Figure 3.3. Sproat and Brown also demonstrated that a carbamate linker is significantly more stable towards the standart concentrated ammonia deprotection when compared compared to a succinate linkage [112]. However, interestingly, a brief survey of literature disclosed that the carbamate linker is not widely utilised for polymer drug conjugates. We realized that there is no readily available reactive functional monomer bearing a reactive group to obtain attachment of amine group containing molecules of interest through a carbamate linkage. The aim of this chapter is to develop novel functional polymers bearing activated carbonyl compounds to yield conjugation via carbamate linkages.

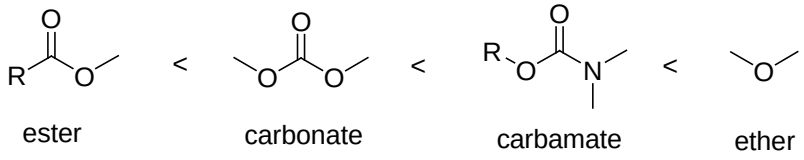

Figure 3.3. Stability order of the linkers towards hydrolysis.

It must be noted that one can choose among two possible pathways for preparing NHS-carbonate reactive group attached polymers (Figure 3.4). Route A is based on post-polymerization modification of the polymer via activation of the hydroxyl-group with disuccinimidyl-carbonate, whereas Route B is the direct polymerization of the monomer as presented in this thesis. The variety of drawbacks in Route A such as the incomplete activation of all hydroxyl functional groups as well as inter- and intra-chain coupling resulting from further addition of hydroxyl group to the newly formed carbonate units,

makes this approach less desirable. An attractive and versatile approach as sown in Route B is to employ a NHS-activated carbonate group containing monomer to have direct access to well-defined polymers.

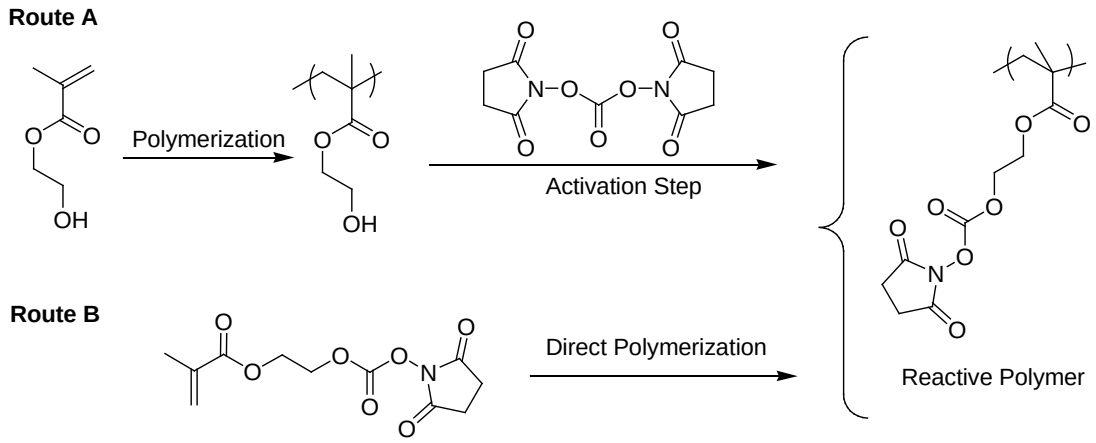

Figure 3.4. Different routes to synthesize carbonate-based reactive polymers: Route A and B. Route B: methodology explored in this thesis.

The primary objective of this research was to obtain a reactive monomer that can be easily functionalized with amine-containing molecules but can release the molecule of choice as required. We envisioned achieving this goal via a carbonate monomer, where the carbonate polymer will be functionalized with amines producing carbamate linkages which are known to hydrolyze under physiological conditions (Figure 3.5).

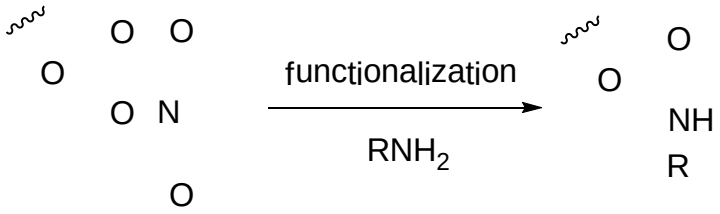

Figure 3.5. Functionalization of polymers containing reactive carbonate side chains.

After the synthesis of novel carbonate monomer orthogonally functionalizable copolymers based on the novel carbonate monomer were aimed to prepare for the application of conjugated drug delivery systems. Copolymers bearing the NHS-carbonate based side chains were obtained by copolymerization with other monomers such as PEG

methacrylates. PEG-based monomers were chosen since they provide soluble supports for applications in drug delivery that are nonimmunogenic [19, 113-114]. Additionally, orthogonally reactive polymeric constructs were synthesized to obtain attachment via hydrolysable as well as non-hydrolyzable linkages. Polymer ***a*** was designed to contain both amine reactive and alkyne reactive side chains (Figure 3.6). In such a copolymer, amine reactive side chains can be utilized to attach amine containing drug molecules while the pendant azide groups can be used to attach alkyne containing targeting moiety via the Huisgen-type cycloaddition reaction. Polymer ***b*** was designed to contain two different amine reactive groups, a carbonate group and the other one as an active ester. Here our aim is to demonstrate that two different amine containing drug molecule can be attached to the polymer in an orthogonal fashion (Figure 3.6).

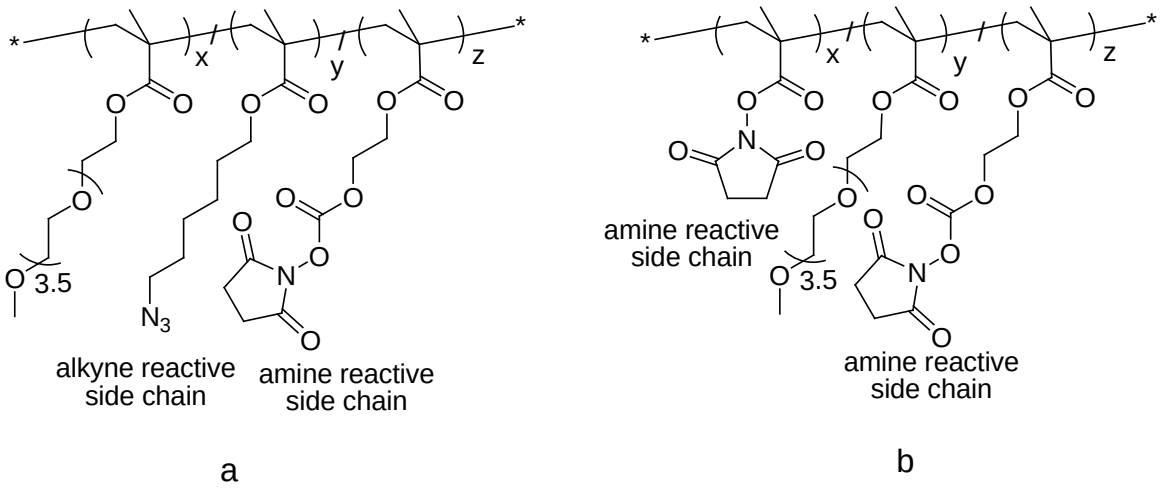

Figure 3.6. Orthogonally functionalizable polymers a) Polymer containing amine reactive and alkyne reactive side chains, b) Polymer containing two different amine reactive side chains.

3.2. Experimental

3.2.1. Materials

All reagents were obtained from commercial sources and were used as received unless otherwise stated. Methyl methacrylate (MMA, 99%, Aldrich), poly(ethylene glycol) methylether methacrylate (M_n = 300 gmol^{-1}) (PEGMA, 99%, Aldrich), 2-hydroxyethyl

methacrylate (HEMA, 98%, Aldrich), *N,N,N',N'',N''*-pentamethyldiethylenetriamine (PMDETA, 99%) were passed through basic alumina column to remove inhibitor and then distilled over CaH_2 in vacuum prior to use. CuBr (99.9%) and N,N'-disuccinimidyl carbonate (DSC) were obtained from Aldrich and allylamine (98%) was obtained from Alfa Aesar. 1-((Prop-2-ynyloxy)methyl)benzene and N-hydroxysuccinimide methacrylate (NHSMA) were synthesized according to the literature [115-116]. The monomer and copolymer characterizations involved ^{1}H NMR spectroscopy (Varian 400 MHz) and Fourier transform infrared (ATR - FTIR) spectroscopy (Thermo Fisher Scientific Inc. Nicolet 380). The molecular weights were estimated by gel permeation chromatography (GPC) analysis using a Viscotek GPCmax VE-2001 analysis system. PLgel (length/ID 300 mm x 7.5 mm, 5 μm particle size) Mixed-C column was calibrated with polystyrene standards (1K - 150K), using refractive index detector. THF was used as eluent at a flow rate of 1 mL/min at 30 ^{o}C. High Pressure Liquid Chromatography (HPLC) was performed with Shimadzu LC-20 AT with ACN:Water (50:50) solvent system.

3.2.2. Synthesis of 2-(N-succinimidylcarboxyoxy)ethyl methacrylate (SCEMA)

To a solution of N,N'-disuccinimidyl carbonate (0.31 g, 1.21 mmol) in dry dichloromethane (10 mL) under N_2 atmosphere, a solution of hydroxyethylmethacrylate (0.08 g, 0.80 mmol) and the triethylamine (0.11 mL, 0.80 mmol) was added. The solution was stirred for 2.5 h at room temperature. The reaction mixture was diluted and purified by suction filtration on SiO_2 (150 mL, 1:1 EtOAc: Hexane) affording 0.19 g (91 % yield) as a clear waxy liquid. Purity has been determined by HPLC (95 %). ^{1}H NMR ($CDCl_3$, δ, ppm) 6.15 (s, 1H, CH_2=C), 5.61 (s, 1H, CH_2=C), 4.56 (t, 2H, *J* = 4.4 Hz, OCH_2), 4.41 (t, 2H, *J* = 4.4 Hz, OCH_2), 2.82 (s, 4H, succinimide *H*), 1.93 (s, 3H, CH_3-);^{13}C NMR ($CDCl_3$, δ, ppm) 168.3, 166.5, 151.6, 135.1, 126.3, 68.2, 61.2, 25.2, 17.6; IR: ν = 1807.7, 1782.3, 1733.2, 1707.4, 1631.3 cm^{-1}.

3.2.3. Synthesis of 6-azidohexyl methacrylate (AHMA)

To a solution of 6-chloro-1-hexanol (4.0 mL, 30 mmol) in distilled water (40 mL) NaN_3 (3.9 g, 60 mmol) was added and heated to 50 ^{o}C for 24 h. The reaction mixture was cooled to room temperature and extracted with CH_2Cl_2 (3 x 25 mL) to obtain pure 6-azidohexan-1-ol (4.6 g, 95% yield). Then, 6-azidohexan-1-ol (1.0 g, 7.7 mmol) was reacted with methacrylolyl chloride (1.05 g, 10.0 mmol) in dry CH_2Cl_2 (100 mL) at 0 ^{o}C in the

presence of triethylamine (1.24 mL, 9.0 mmol) for 2.5 h. The reaction mixture was extracted with saturated $NaHCO_3$ (3 x 15 mL) and H_2O (3 x 15 mL). The combined organic layers were dried over anhydrous Na_2SO_4 and evaporated under *vacuo*. The liquid was purified with column chromatography, using 1:99 EtOAc: Hexanes (75 % yield). ^{1}H NMR ($CDCl_3$, δ, ppm) 6.08 (s, 1H, C*H*$_2$=C), 5.53 (s, 1H, C*H*$_2$=C), 4.13 (t, 2H, *J* = 6.8 Hz, OC*H*$_2$), 3.25 (t, 2H, *J* = 6.8 Hz, N_3C*H*$_2$), 1.92 (s, 3H, C-C*H*$_3$), 1.67 – 1.40 (m, 8H, C*H*$_2$-C*H*$_2$-C*H*$_2$-C*H*$_2$); IR: ν = 2095.1, 1715.3, 1637.6 cm^{-1}

3.2.4. General Polymerization Procedure with SCEMA and MMA Monomers

In a typical experiment, to a solution of methyl methacrylate (0.062 g, 0.62 mmol) and SCEMA (0.167 g, 0.62 mmol, 1 eq) in dry THF (6 mL), was added 2,2'-azobisisobutyronitrile (AIBN, 6.8 mg, 0.041 mmol). The mixture was degassed and then heated to 65 ^{o}C. At the end of the reaction, volatiles were evaporated under *vacuo*. The polymer was washed with cold ether to obtain **P1** (53% yield). ^{1}H NMR ($CDCl_3$, δ, ppm) 4.52 (br s, 2H, C*H*$_2$-O-COO-), 4.23 (br s, 2H, COO-C*H*$_2$), 3.55 (br s, 3H, COO-C*H*$_3$), 2.84 (br s, 4H succinimide *H*), 1.83 – 0.84 (m, C*H*$_2$ and C*H*$_3$ along polymer backbone); IR: ν = 1813.2, 1790.4, 1718.4 cm^{-1}. Synthesis of **P2** (using 2 eq SCEMA) and **P3** (using 4 eq SCEMA) were carried out according to the general procedure.

3.2.5. Synthesis of Copolymer P4

To a solution of PEGMA (0.394 g, 1.31 mmol) and SCEMA (0.089 g, 0.328 mmol) in dry THF (9.0 mL), was added AIBN (8.95 mg, 0.054 mmol). The mixture was degassed and then heated to 65 ^{o}C for 12 h. The volatiles were evaporated under *vacuo* and the residue was washed with cold ether to obtain copolymer **P4** (59% yield). ^{1}H NMR ($CDCl_3$, δ, ppm) 4.53 (br s, 2H, C*H*$_2$OCOO), 4.22 – 3.79 (m, 4H, COO-C*H*$_2$) 3.63 (br s, 14H, (-C*H*$_2$C*H*$_2$O-)$_{3.5}$), 3.52 (br s, 2H, -C*H*$_2$CH$_2$O-), 3.34 (s, 3H, O-C*H*$_3$), 2.84 (br s, succinimide *H*), 1.89 – 0.82 (m, C*H*$_2$ and C*H*$_3$ along polymer backbone); ^{13}C NMR ($CDCl_3$, δ, ppm) 177.7, 177.1, 168.8, 151.7, 71.9, 70.6, 68.6, 68.4, 63.7, 61.7, 58.9, 45.0, 44.7, 25.5, 18.0, 16.4; IR: ν = 1813.5, 1790.5, 1730.7 cm^{-1}.

3.2.6. Synthesis of Copolymer P5

To a solution of PEGMA (0.416 g, 1.38 mmol) and SCEMA (0.062 g, 0.23 mmol) and AHMA (0.048 g, 0.23 mmol) in dry THF (10.0 mL), was added AIBN (12.0 mg, 0.06 mmol). The mixture was degassed and then heated to 65 ^{o}C for 12 h. The reaction mixture was cooled to room temperature and the volatiles were evaporated under *vacuo*. The residue was washed with cold ether to obtain **P5** (50% yield). ^{1}H NMR ($CDCl_3$, δ, ppm) 4.52 (br s, 2H, C*H*$_2$-O-COO-), 4.21 – 3.89 (m, 6H, COO-C*H*$_2$), 3.63 (br s, 14H, (-C*H*$_2$C*H*$_2$O-)$_{3.5}$), 3.53 (br s, 2H, -CH_2CH_2O-), 3.35 (s, 3H, O-C*H*$_3$), 3.28 (br s, 2H, C*H*$_2$-N_3), 2.85 (br s, 4H, succinimide *H*) 1.73 – 0.84 (m, 8H, COO-CH_2-C*H*$_2$-C*H*$_2$-C*H*$_2$-C*H*$_2$-CH_2-N_3 and C*H*$_2$ and C*H*$_3$ along polymer backbone) IR: ν = 2094.8, 1729.5, cm^{-1}.

3.2.7. Synthesis of Copolymer P6

To a solution of PEGMA (0.385 g, 1.28 mmol) and SCEMA (0.087 g, 0.32 mmol) and NHSMA (0.059 g, 0.32 mmol) in dry THF (9.0 mL), was added AIBN (12.5 mg, 0.08 mmol). The mixture was degassed and then heated to 65 ^{o}C for 12 h. The residue was washed with cold ether to obtain **P6** (40 % yield). ^{1}H NMR ($CDCl_3$, δ, ppm) 4.54 (br s, 2H, C*H*$_2$OCOO), 4.21 – 4.06 (br s, 4H, COO-C*H*$_2$) 3.63 (br s, 14H, (-C*H*$_2$C*H*$_2$O-)$_{3.5}$), 3.52 (br s, 2H, C*H*$_2$$CH_2$O), 3.35 (s, 3H, O-C*H*$_3$), 2.84 (br s, 4H succinimide *H* at SCEMA), 2.78(br s, 4H, succinimide *H* at NHSMA) 1.74 – 0.82 (m, C*H*$_2$ and C*H*$_3$ along polymer backbone); IR: ν = 1811.8, 1788.8, 1735.9, cm^{-1}.

3.2.8. General Procedure for Amine Conjugation

To a solution of polymer **P5** (0.050 g, 0,006 mmol) in THF (2.0 mL), and was added allylamine (0.002 g, 0.030 mmol) in the presence of the triethylamine (4.0 µL, 0.030 mmol) at room temperature for 18 h. The residue was washed with cold ether to obtain **P7** (% 92 yield). ^{1}H NMR ($CDCl_3$, δ, ppm) 5.85 (br s, 1H, *H*C=CH_2), 5.21-5.09 (m, 2H, C*H*$_2$=CH), 4.26 – 3.90 (m, 6H, COO-C*H*$_2$), 3.79 (br s,4H, NH-C*H*$_2$ and NH-COO-C*H*$_2$), 3.63 (br s, 14H, (-C*H*$_2$C*H*$_2$O-)$_{3.5}$), 3.53 (br s, 2H, -C*H*$_2$$CH_2$O-), 3.35 (s, 3H, O-C*H*$_3$), 3.28 (br s, 2H, C*H*$_2$-$N_3$), 1.78 – 0.84 (m, 8H, COO-CH_2-C*H*$_2$-C*H*$_2$-C*H*$_2$-C*H*$_2$-CH_2-N_3 and C*H*$_2$ and C*H*$_3$ along polymer backbone) IR: ν = 2093.4, 1728.5 cm^{-1}.

3.2.9. Fuctionalization of Copolymer P6 with Amine

P6 was functionalized with allylamine according to general amination procedure to obtain **P9** (89% yield). ^{1}H NMR ($CDCl_3$, δ, ppm) 5.85 (br s, 1H, *H*C=CH_2), 5.20-5.10 (m, 2H, C*H*$_2$=CH), 4.28 – 4.09 (br s, 4H, COO-C*H*$_2$), 3.79 (br s, 4H, NH-C*H*$_2$ and NH-COO-C*H*$_2$) 3.63 (br s, 14H, (-C*H*$_2$C*H*$_2$O-)$_{3.5}$), 3.52 (br s, 2H, C*H*$_2$CH$_2$O), 3.35 (s, 3H, O-C*H*$_3$), 2.78 (br s, 4H, succinimide *H* at NHSMA) 1.73 – 0.82 (m, C*H*$_2$ and C*H*$_3$ along polymer backbone); IR: 1806.7, 1779.6, 1724.8 cm^{-1}.

3.2.10. Modification Using 1,3-dipolar Cycloaddition

To a solution of **P7** (50.0 mg, 0.0063 mmol) in THF (0.8 mL) was PMDETA (0.380 mg, 0.0022 mmol) under N_2 atmosphere. Then, the mixture of 1-((prop-2-ynyloxy)methyl)benzene (6.0 mg, 0.0438 mmol) and Cu(I)Br (0.31 mg, 0.0022 mmol) in THF (0.2 mL) was added to the polymer/PMDETA containing solution. It was stirred at room temperature for 24 h and washed with ether to remove excess monomer to obtain **P8** (90 % yield). ^{1}H NMR ($CDCl_3$, δ, ppm) 7.60 (br s, 1H, triazole *H*), 7.33-7.32 (m, 5H, Ar-*H*), 5.85 (br s, 1H, *H*C=CH_2), 5.21-5.09 (m, 2H, C*H*$_2$=CH), 4.66 (s, 2H, C*H*$_2$-Ar), 4.59 (s, 2H, C*H*$_2$O-CH_2-Ar), 4.35 (s, 2H, C*H*$_2$-triazole), 4.26 – 3.88 (m, 6H, COO-C*H*$_2$), 3.80 (br s,4H, NH-C*H*$_2$ and NH-COO-C*H*$_2$), 3.63 (br s, 14H, -C*H*$_2$C*H*$_2$O-), 3.53 (br s, 2H, -C*H*$_2$C*H*$_2$O-), 3.36 (s, 3H, O-C*H*$_3$) 1.78 – 0.85 (m, 8H, COO-CH_2-C*H*$_2$-C*H*$_2$-C*H*$_2$-C*H*$_2$-CH_2-N_3 and C*H*$_2$ and C*H*$_3$ along polymer backbone); IR: ν = 1727.4 cm^{-1}.

3.2.11. Functionalization Procedure with Propargylamine

Polymer **P9** (0.010 g, 0.001 mmol) was dissolved in THF (2 mL) and reacted with propargylamine (1.0 mg, 0.018 mmol) in the presence of the triethylamine (1.5 µL, 0.01 mmol) at 50 ^{o}C for 12 h. The residue was washed with cold ether to obtain **P10** (86% yield). ^{1}H NMR ($CDCl_3$, δ, ppm) 5.85 (br s, 1H, *H*C=CH_2), 5.20-5.10 (m, 2H, C*H*$_2$=CH), 4.27 –4.07 (br s, 4H, COO-C*H*$_2$), 3.79 (br s, 4H, NH-C*H*$_2$ and NH-COO-C*H*$_2$) 3.64 (br s, 14H, (-C*H*$_2$C*H*$_2$O-)$_{3.5}$), 3.53 (br s, 2H, C*H*$_2$CH$_2$O), 3.36 (s, 3H, O-C*H*$_3$), 2.55 (br s, 1H, NH), 2.28 (br s, 1H, C≡C*H*) 1.73-0.82 (m, C*H*$_2$ and C*H*$_3$ along polymer backbone); IR: 1727.5 cm^{-1}.

3.3. Results and Discussion

3.3.1. Synthesis and Characterisation of the Carbonate Monomer

The desired carbonate monomer **SCEMA** was synthesized by the reaction of 2-hydroxyethyl methacrylate (**1**) with commercially available N,N'-disuccinimidyl carbonate (**2**) in the presence of triethylamine at room temperature (Figure 3.7). The **SCEMA** monomer was obtained as white waxy solid after passing through a short silica gel column. Purity of thus obtained monomer was also confirmed via HPLC.

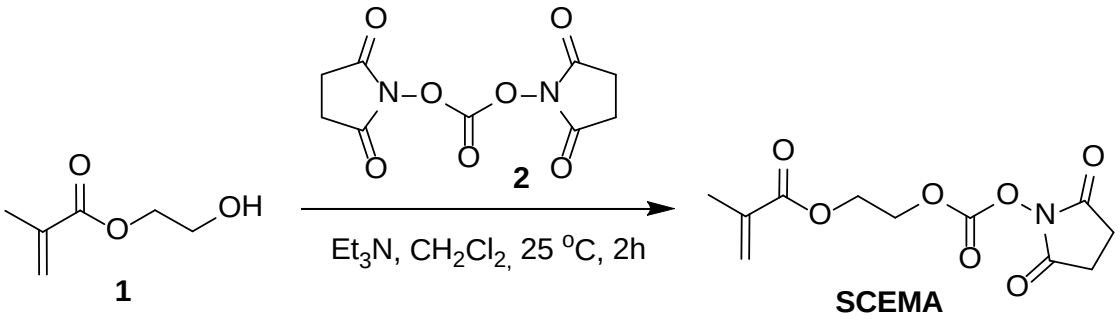

Figure 3.7. Synthesis of HEMA based reactive monomer SCEMA.

Satisfactory NMR (^{1}H and ^{13}C) characterizations were obtained to confirm the monomer structure. In the ^{1}H NMR spectrum of the monomer, vinylic protons are readily distinguishable (Figure 3.8). The resonances of the vinylic protons on the acrylic group appear at 5.6 and 6.1 ppm. The methylene protons of the succinimide moiety appear at 2.82 ppm and 25.2 ppm in ^{1}H and ^{13}C NMR, respectively. Additionally, the resonances of the carbon atoms of the acrylate bond appear at 126.3 and 135.1 ppm and the newly formed carbonate resonance show up at 151.6 ppm. IR spectrum of the monomer was also proved the formation of carbonate band at 1733 cm^{-1}, and succinimide bands at 1807 and 1782 cm^{-1} (Figure 3.9).

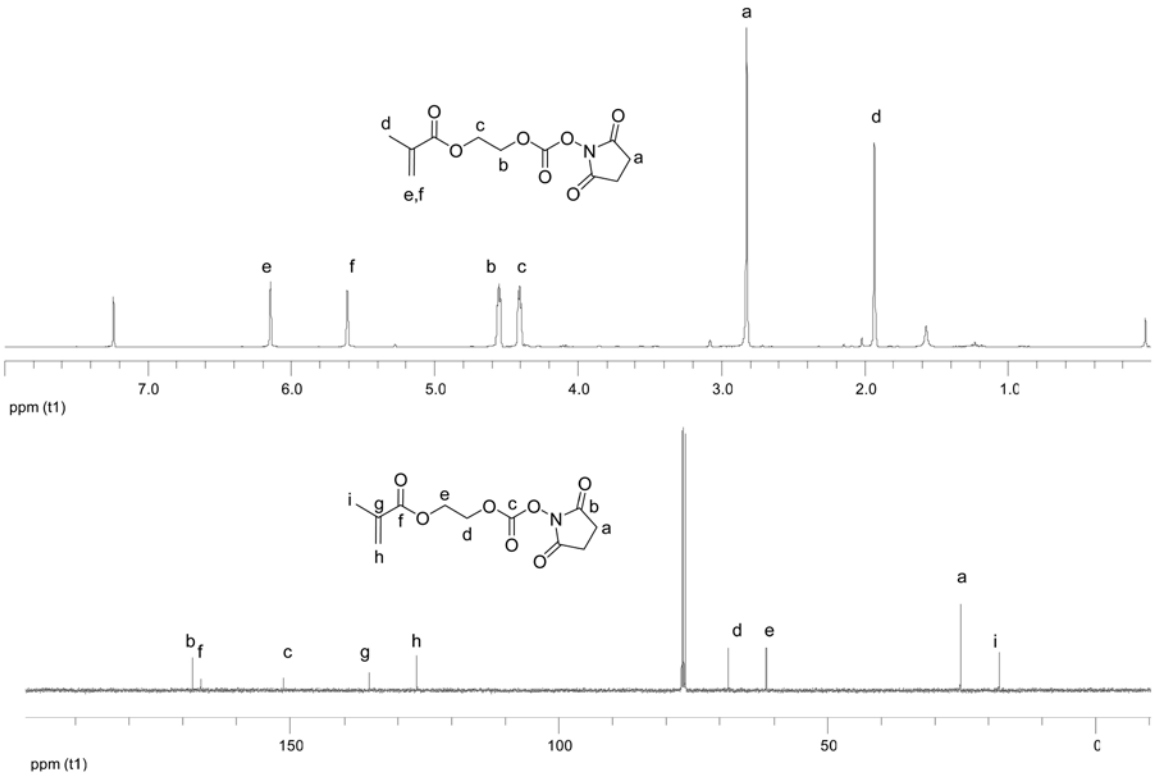

Figure 3.8. ^{1}H-NMR and 13C NMR spectrum of the SCEMA monomer.

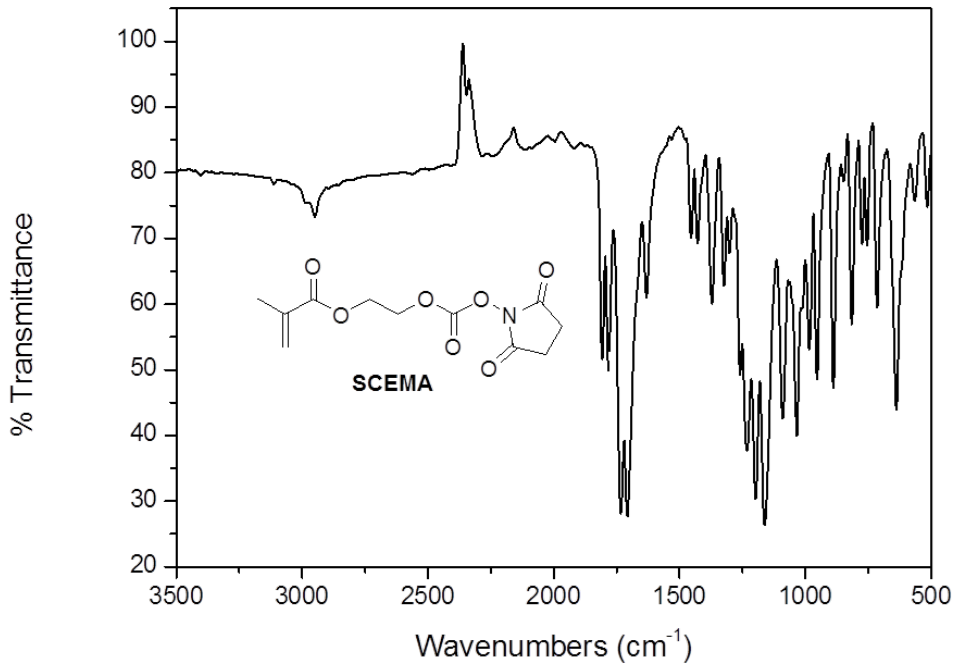

Figure 3.9. IR spectrum of SCEMA monomer.

3.3.2. Synthesis of SCEMA and MMA Containing Copolymers

With the novel carbonate monomer **SCEMA** at hand, free radical polymerizations with **MMA** were investigated using AIBN as the initiator (Figure 3.10).

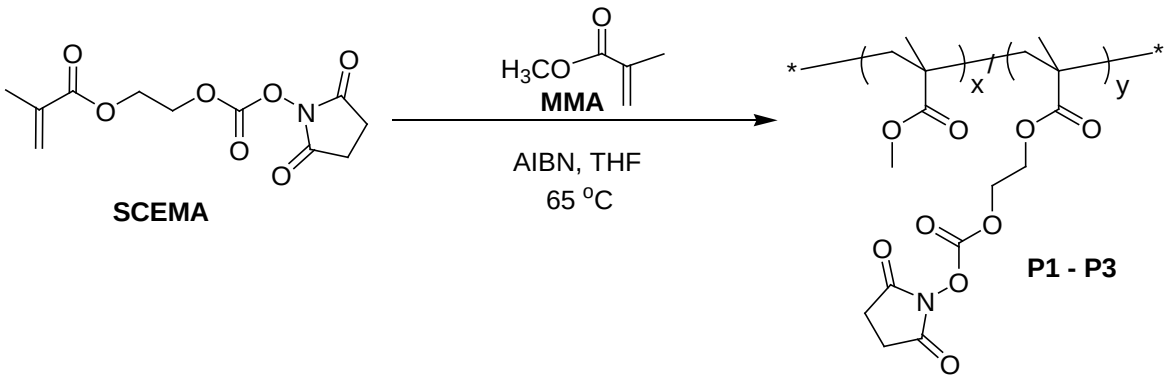

Figure 3.10. Synthesis of MMA containing copolymers containing reactive carbonate side chains.

Table 3.1 shows the polymerization conditions that were investigated and the results obtained. The ratio of the monomers incorporated in the polymer closely correlated with the feed ratio of the monomers. Copolymers **P1** – **P3** are polymers obtained from polymerization of **MMA** with the **SCEMA** monomer with different feed ratios (**MMA**:**SCEMA** 1:1, 2:1, 4:1, items 1, 2 and 3). The composition of the copolymers could be easily determined from the integration of the ^{1}H NMR spectra.

The incorporation ratio of the monomers onto the polymer backbone was estimated by the relative integration of the peaks at 2.84 and 3.56 ppm, corresponding to the succinimide protons of **SCEMA** and methoxy protons of **MMA**, respectively (Figure 3.11).

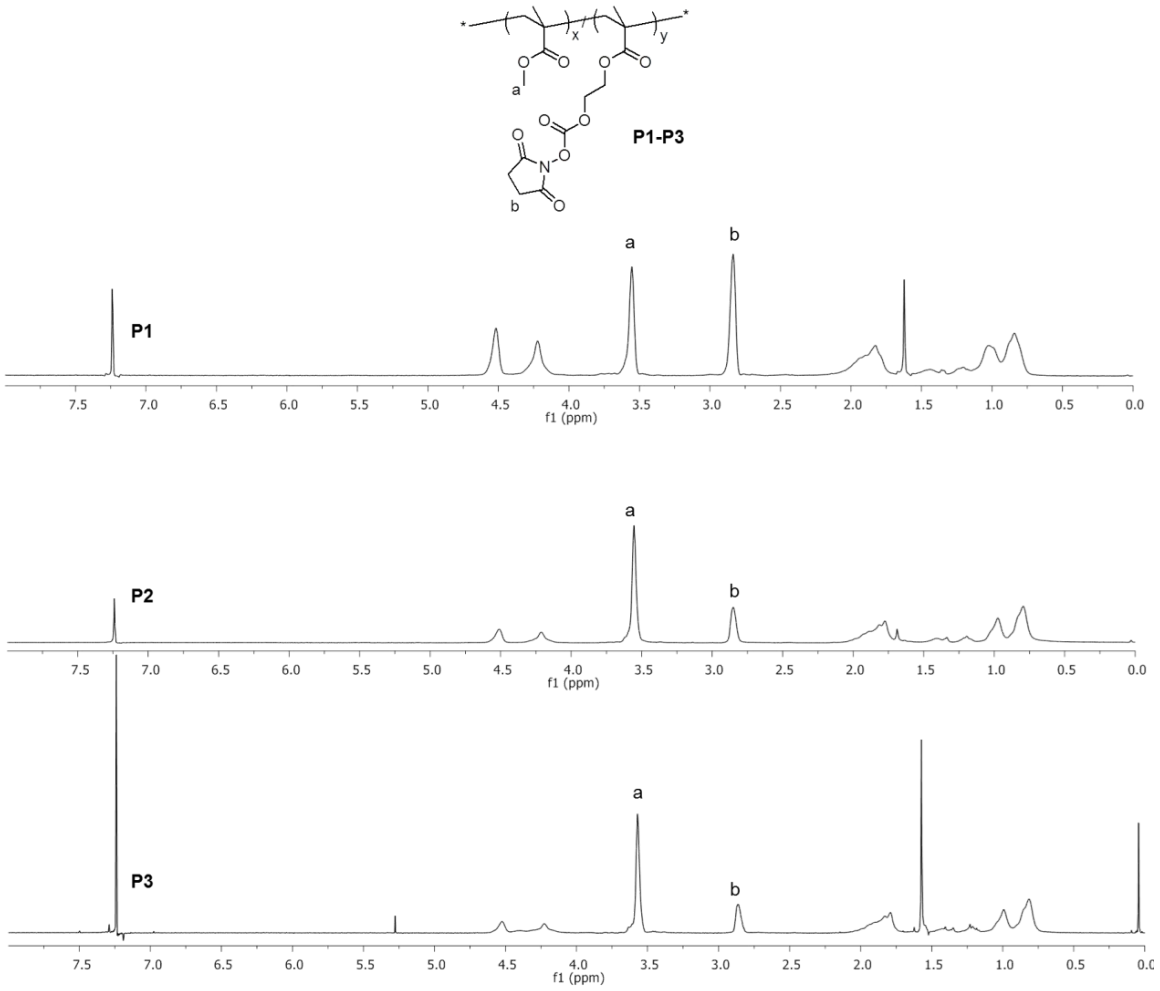

Figure 3.11. 1H NMR spectra of MMA containing copolymer P1, P2 and P3.

3.3.3. Synthesis of SCEMA and PEGMA Containing Copolymer P4

Polymer **P4**, a macromolecule with potential drug delivery applications, was synthesized via polymerization of **PEGMA** with the **SCEMA** monomer (Figure 3.12). The incorporation ratio of the **SCEMA** monomer onto the polymer backbone in polymer **P4** was estimated by the relative integration of the peaks at 2.84 and 3.34 ppm, corresponding to the succinimide protons on **SCEMA** and methoxy protons of **PEGMA**, respectively.

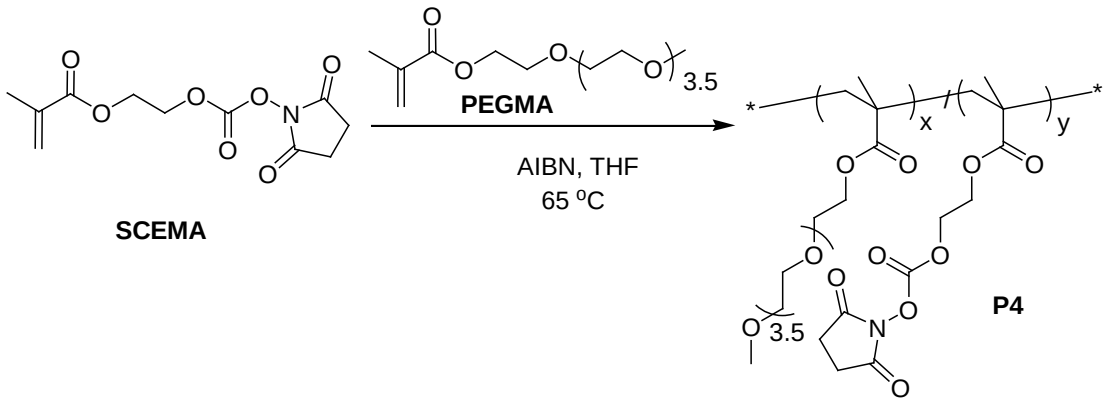

Figure 3.12. Synthesis of MMA containing copolymers containing reactive carbonate side chains.

3.3.4 Functionalization of Activated Carbonate Containing Copolymer

Carbonate group containing copolymer was expected to be amenable to functionalization by amines. Allyl amine was chosen as a model amine substrate since it adds double bonds to the polymer side chains, which can be further, derivatized using the thiol-ene click reaction using thiol containing molecules. To evaluate the efficiency of functionalization with amine, polymer **P4** was reacted with allylamine in the presence of catalytic amounts of triethylamine in THF at room temperature for 12 h to obtain polymer **P11** (Figure 3.13). Upon using two fold excess amine per carbonate unit, quantitative functionalization of the polymer was evident from the disappearance of proton resonances at 2.84 ppm from the succinimide peak from the polymer (Figure 3.14).

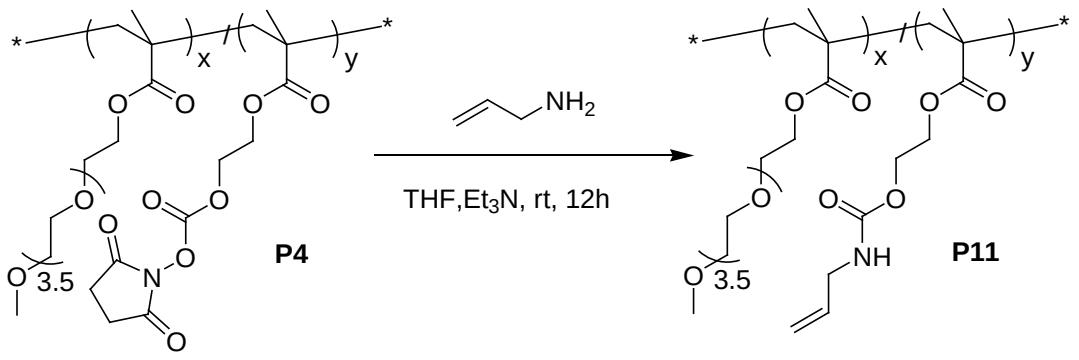

Figure 3.13. Reaction of P4 with amine.

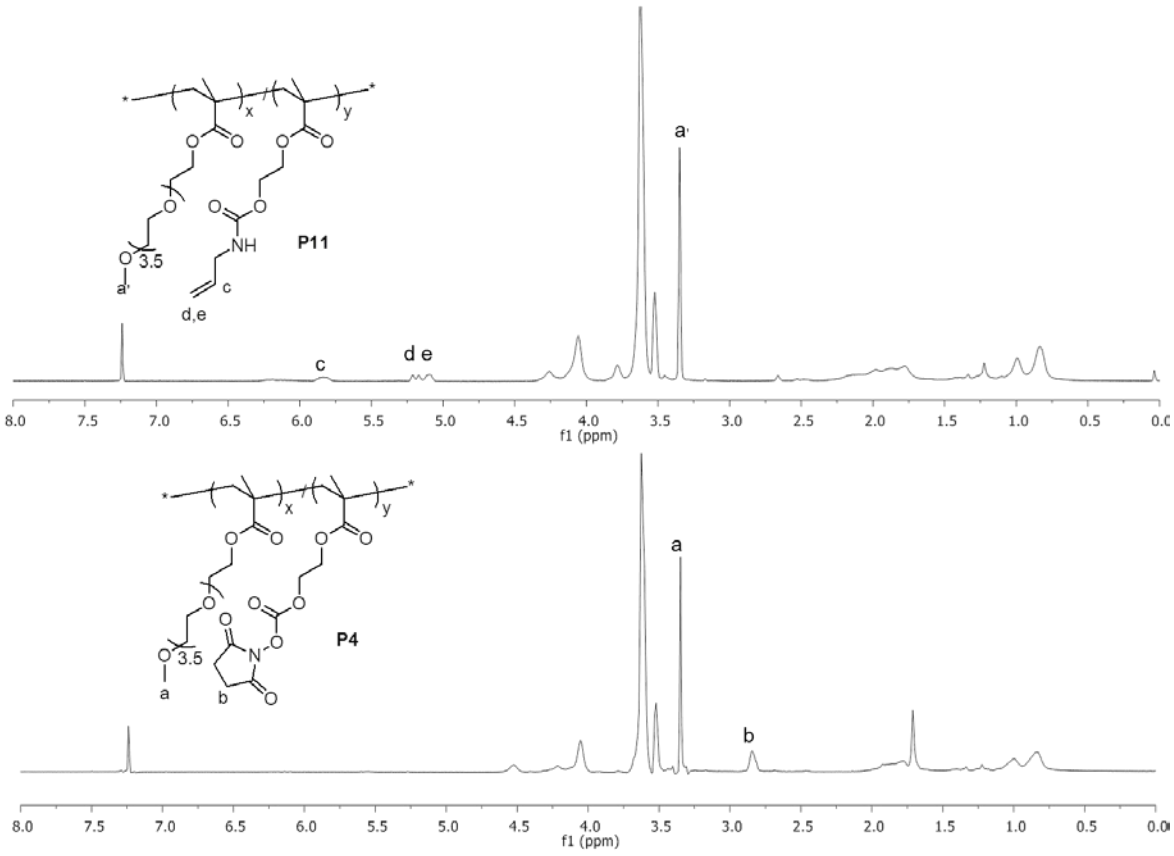

Figure 3.14. ^{1}H-NMR spectra of P4 and after functionalization P11.

3.3.5. Synthesis and Functionalization of Orthogonally Functionalizable Copolymers

To demonstrate the orthogonality of this carbonate monomer 2-(N-succinimidylcarboxyoxy)ethyl methacrylate (SCEMA), it was copolymerized with four other monomers: 6-azidohexyl methacrylate (AHMA), a reactive monomer for 1,3-dipolar cycloaddition; *N*-acryloxysuccinimide (NAS), a reactive monomer for amine conjugation; methyl methacrylate (MMA), a general monomer for investigating the properties of the copolymers and poly(ethylene glycol) methylether methacrylate (PEGMA), a monomer bringing in the biocompatibility to the system (Figure 3.15).

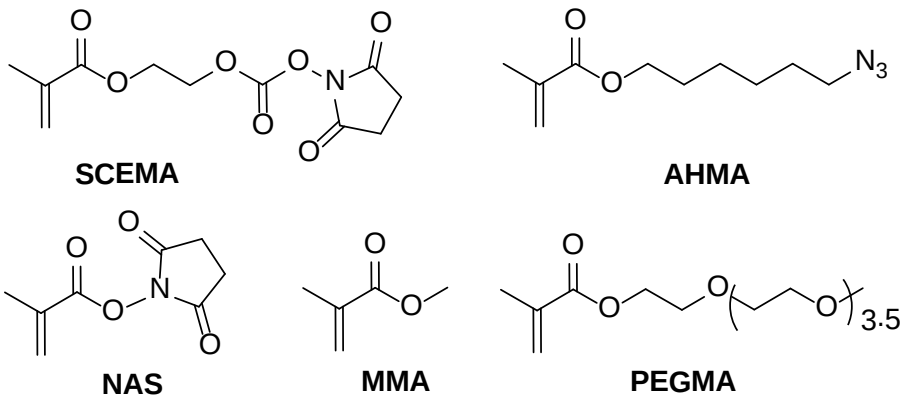

Figure 3.15. Monomers employed in this study.

The other reactive monomer AHMA was synthesized similar to the literature procedure (Figure 3.16) [117]. It was aimed to use in copper-catalyzed 1,3-dipolar cycloaddition reaction to obtain functionalizable polymers.

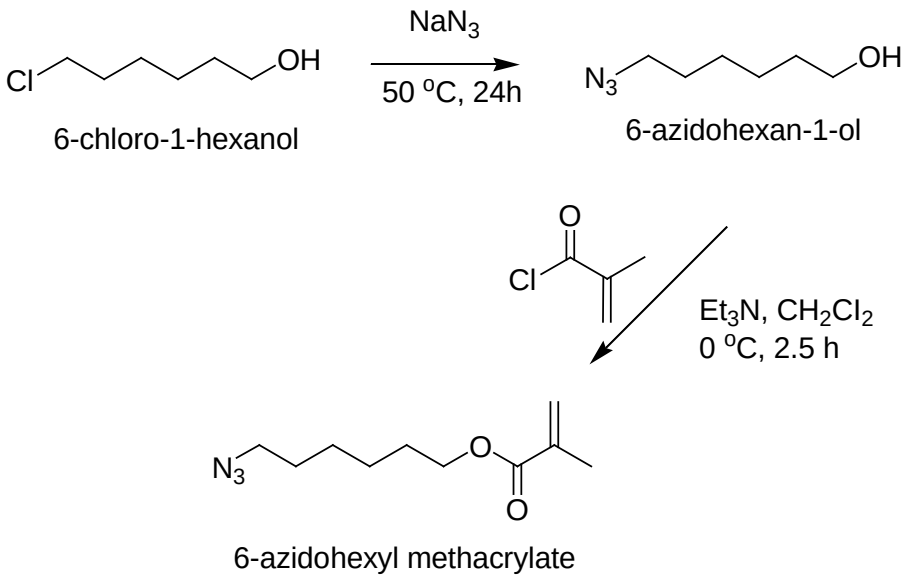

Figure 3.16. Synthesis of 6-azidohexyl methacrylate (AHMA) monomer.

^{1}H NMR spectrum was used to confirm the monomer structure. The resonances of the vinylic protons on the acrylic group appear at 5.5 ppm and 6.1 ppm (Figure 3.17). IR spectrum of the monomer also proved the formation of ester band at 1715 cm^{-1}, and azide band at 2095 cm^{-1} and alkene band at 1638 cm^{-1}.

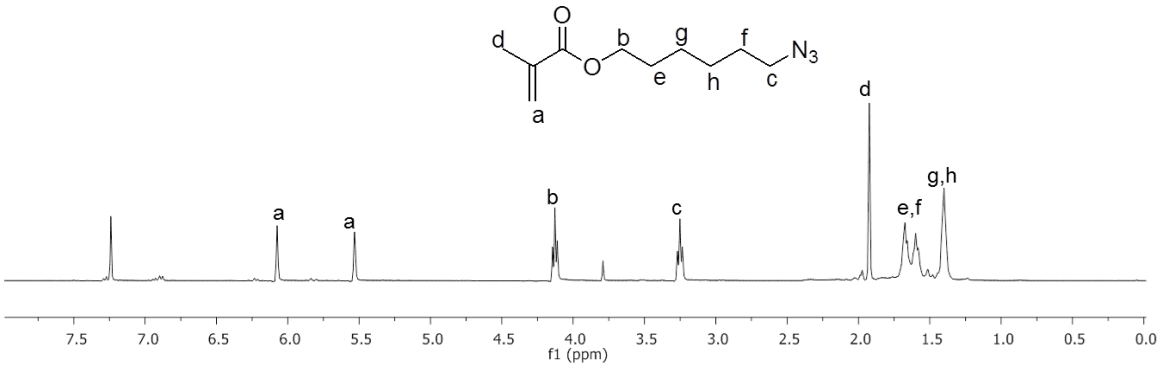

Figure 3.17. ^{1}H-NMR spectrum of AHMA monomer.

Table 3.1. Synthesis of Reactive Monomer Containing Random Copolymers.

Poly	Monomers			$F_{theoretical}$(%)[b]			$F_{observed}$(%)[c]			Yield	M_n[d]	M_w/M_n[d]
	M1	M2	M3	M1	M2	M3	M1	M2	M3	(%)		
P1	SCEMA	MMA	-	50	50	-	45	55	-	53	4900	1.42
P2	SCEMA	MMA	-	33.3	66.7	-	32	68	-	57	5000	1.67
P3	SCEMA	MMA	-	20	80	-	18	82	-	32	5900	1.41
P4	SCEMA	PEGMA	-	20	80	-	20	80	-	59	5500	1.98
P5	SCEMA	AHMA	PEGMA	12.5	12.5	75	14	20	65	50	8000	1.81
P6	SCEMA	NHSMA	PEGMA	16.7	16.7	66.6	15	17	68	40	7600	1.83

a Initiator, AIBN; solvent, THF; temperature, 65 ^{o}C; time: 12 h
b Feed ratio of monomers
c % Incorporation of monomers in the copolymer as determined by ^{1}H NMR.
d Estimated by SEC eluted with THF, using polystyrene calibrations.

AHMA monomer was copolymerized with **SCEMA** and **PEGMA** to obtain the orthogonally functionalizable copolymer (Figure 3.18). Analysis of chemical composition

of the copolymer using 1HNMR spectroscopy revealed that the feed ratio was preserved after copolymerization (Table 3.1).

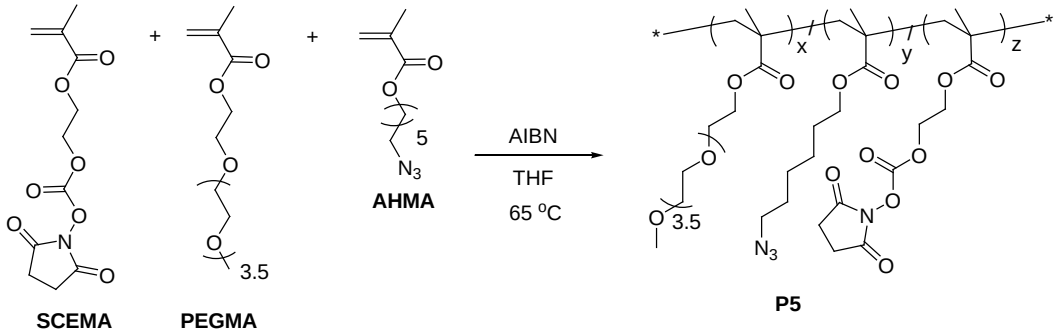

Figure 3.18. Copolymerization of SCEMA monomer with AHMA monomer.

With the random copolymer P5 at hand, we investigated the stepwise orthogonal functionalization strategies of these polymers via amine conjugation and 1,3-dipolar cycloaddition. Allylamine was used as a model amine substrate again, which can be further derivatized using the thiol-ene click reaction using thiol containing molecules. Copolymer P5 was reacted with allylamine in the presence of small amount of triethylamine in THF at room temperature for 12 h to obtain polymer P7 (Figure 3.19). Using two fold excess of amine per carbonate unit, quantitative functionalization of the polymer was evident from the disappearance of proton resonance at 2.85 ppm from the succinimide peak of polymer P5 (Figure 2.20, peak b).

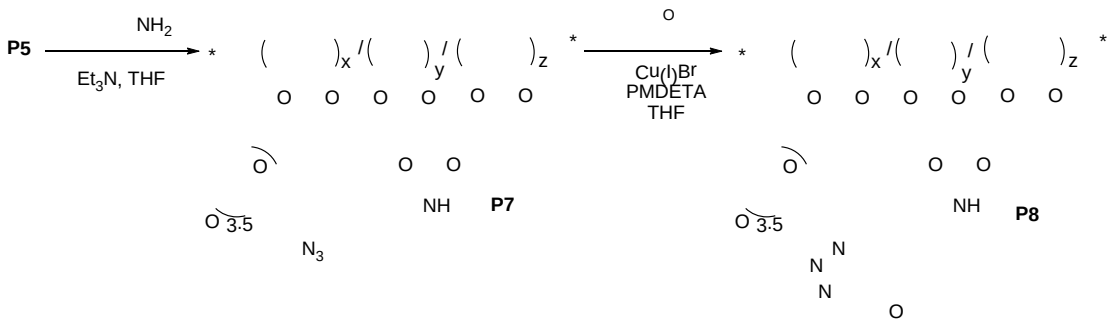

Figure 3.19. Orthogonal functionalization of copolymer P5 with amine and alkyne containing molecules.

Subsequently, copolymer **P7** was reacted with 1-((prop-2-ynyloxy)methyl)benzene under typical 1,3-dipolar cycloaddition conditions using Cu(I)Br and PMDETA in THF to obtain copolymer **P8**. The quatitative conversion of the azide to the corresponding triazole product **P8** was observed via the emergence of the triazole proton at 7.60 ppm (Figure 3.20, peak i) and the diagnostic downfield shift of the azidomethyl signal from 3.28 ppm (Figure 3.20, peak c') to 4.35 ppm (Figure 3.20, peak c").

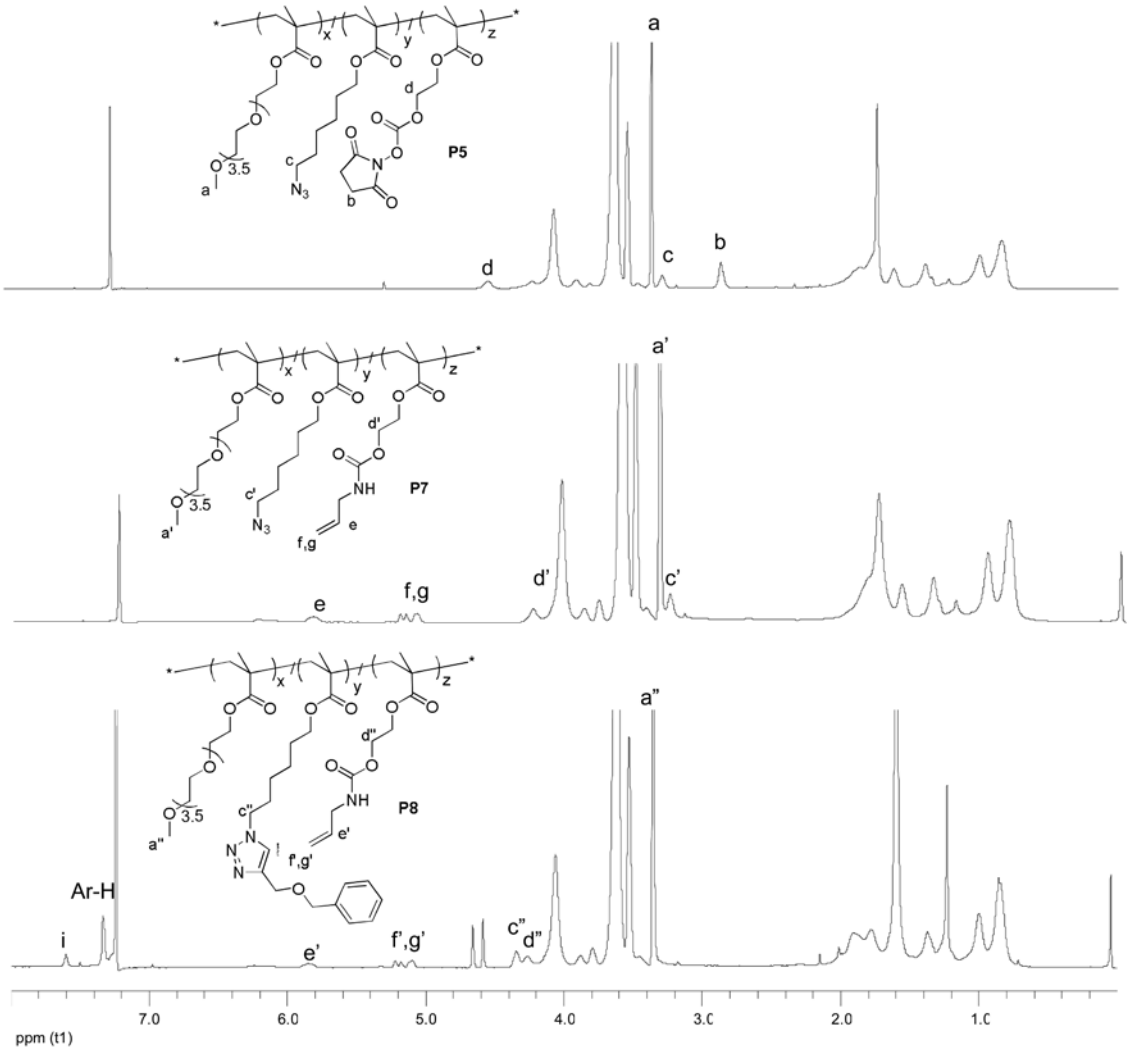

Figure 3.20. 1H NMR spectra of the copolymer P5, before and after functionalization.

The second copolymer was prepared using the **NHSMA** monomer, **SCEMA** and **PEGMA** (Figure 3.21). In this copolymer both the reactive groups are amenable for functionalization with amines but the resulting covalent bonding is different: amine conjugation with NHSMA affords amides, a hydrolytically stable linkage, whereas the

reaction of carbonate side chains with amines result in a carbamate linkage, a degradable linker therefore potentially releasing the amine. The feed ratio of the monomers were preserved in the copolymer as deduced from the ^{1}H NMR spectrum (Table 3.1).

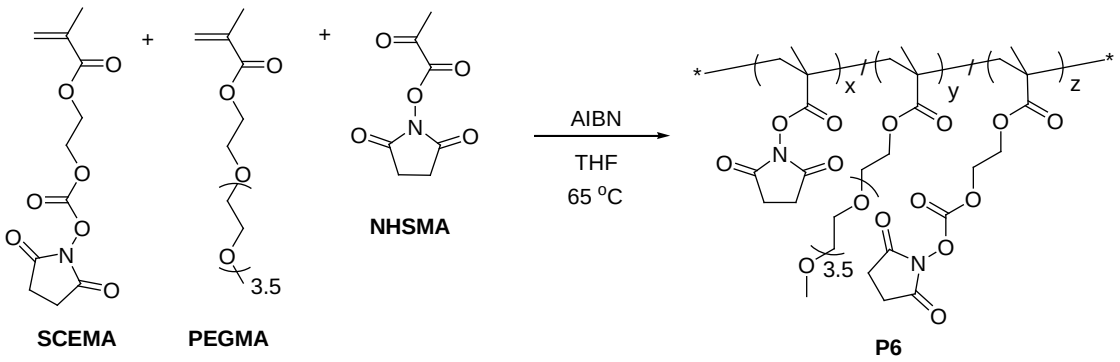

Figure 3.21. Copolymerization of SCEMA monomer with NHSMA monomer.

The functionalization of copolymer **P6** was investigated with two different amines (Figure 3.22). The copolymer **P6** was treated with the first reactant of choice, allylamine, at room temperature for only 18 h. The ^{1}H NMR spectrum showed the complete consumption of the carbonate with disappearance of the succinimide peak at 2.84 ppm (Figure 3.23, peak b) and upfield shift of the ethereal peak (-CH_2O) at 4.54 ppm (Figure 3.23, peak d). The integration of the newly appearing alkene protons e, f and g with respect to the already existing methyl peak of the PEG side chain (Figure 3.23, peak a') fit well with the integration of the ethereal peak d with respect to the PEG side chain (Figure 3.23, peak a). Interestingly, even in the presence of excess allylamine, selective formation of carbamate was observed. Near quantitative preservation of N-hydroxysuccinimide based activated ester was evident from ^{1}H NMR spectrum analysis: integration of proton resonances at 3.35 ppm (peak a') belonging to the PEG side chain methyl (-OCH_3) and succinimide protons at 2.78 ppm (peak c', Figure 3.23). The consecutive functionalization was accomplished with another amine containing molecule: propargylamine. Copolymer **P9** was treated with excess propargylamine in THF at 50 ^{o}C and the resulting copolymer **P10** was characterized with ^{1}H NMR analysis (Figure 3.23). The succinimide peak at 2.78 ppm disappeared in the fully functionalized copolymer spectrum. The appearance of the alkyne proton at 2.28 ppm (peak i, Figure 3.23) confirmed the amide formation.

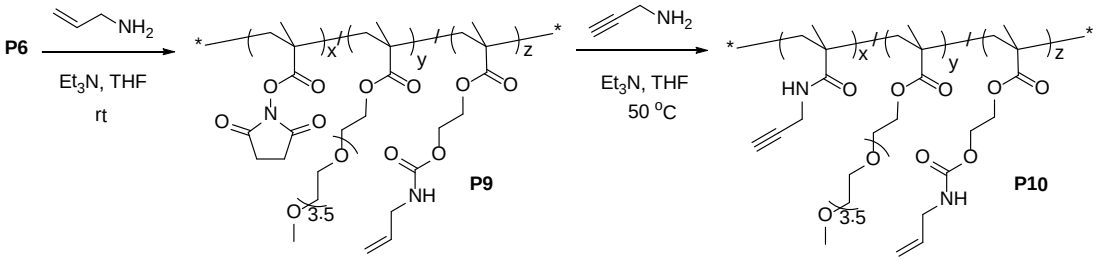

Figure 3.22. Orthogonal functionalization of copolymer P6 with two different amines.

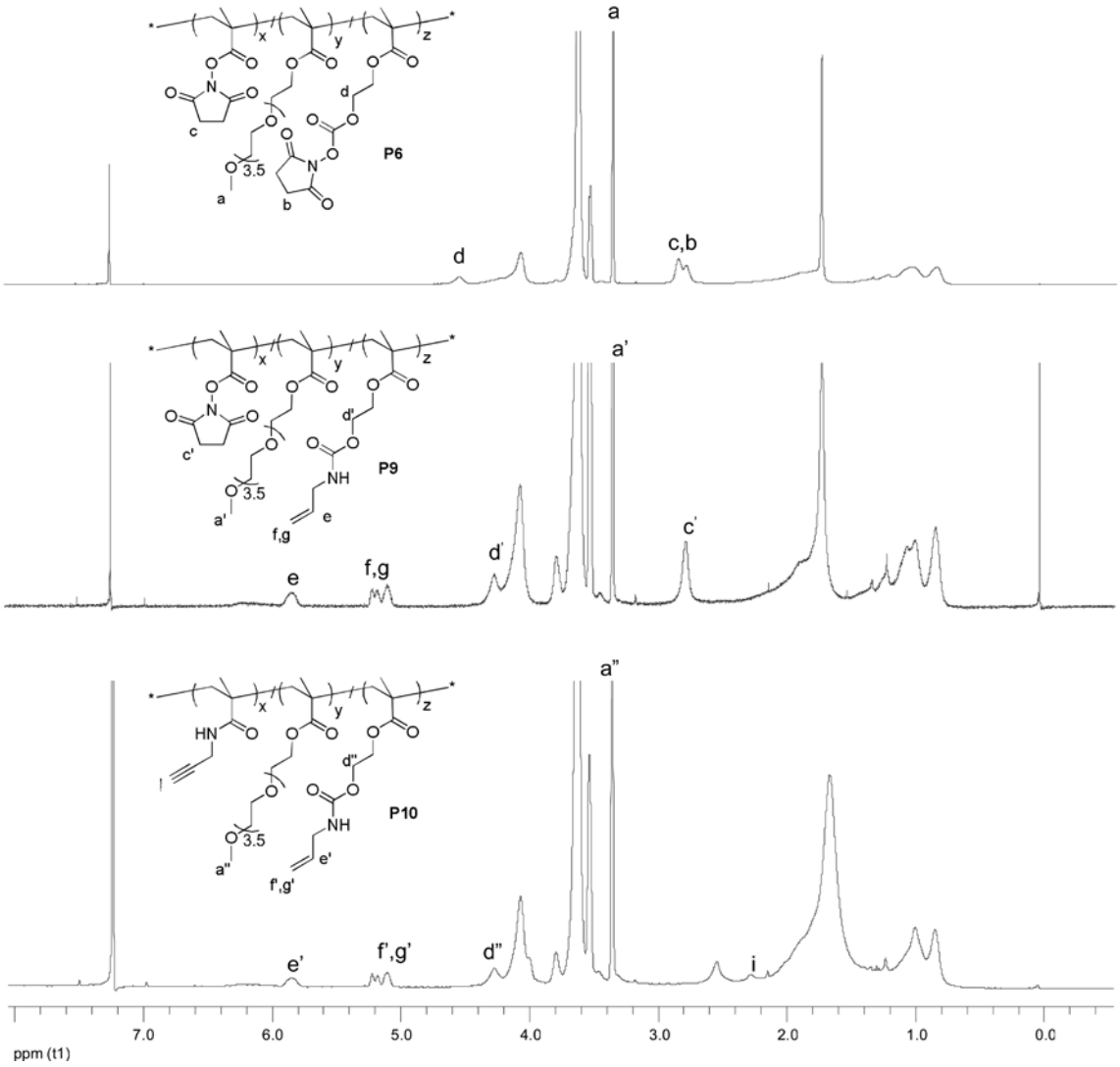

Figure 3.23. 1H NMR of copolymer P7 before and after functionalization.

As revealed by the NMR studies, stepwise functionalizations of the reactive copolymers were achieved without affecting the copolymer backbone and other functional groups. In both the cases, carbonate-azide or carbonate-NHS couple, the two functional groups act independently of each other and can be functionalized in an orthogonal and stepwise manner. Notably, the later combination allows for the first time a step-wise selective orthogonal functionalization with two different amine containing molecules. Furthermore, owing to the high efficiency of the reactions used for small molecule conjugation, quantitative functionalizations were achieved under mild conditions.

3.6. Conclusions

A novel N-hydroxy succinimide carbonate functional group containing monomer was designed to enable direct synthesis of polymers incorporating a amine reactive carbonate group as pendant side-chains. This monomer was copolymerized with MMA and PEGMA using free radical polymerization. Additionally, the carbonate monomer was also copolymerized with reactive monomers containing an azide group and a N-hydroxysuccinimide containing active ester group to yield orthogonally functionalizable copolymers. The pendant reactive carbonate groups were easily functionalized with amines containing molecules via carbamate linkages. The highly efficient second functionalization involved, mild and versatile synthetic reactions such as 1,3-dipolar cycloaddition and amidation. Orthogonal functionalizations proceeded in a highly selective and efficient manner as confirmed using ^{1}H NMR spectroscopy of modified copolymers. The NHS-containing carbonate monomer is currently investigated for fabrication of reactive polymeric materials such as hydrogels and is tested for developing polymer-drug conjugates.

4. MULTIFUNCTIONAL HYDROGELS THROUGH "THIOL – EPOXY" CLICK CHEMISTRY

The materials in this chapter have been adapted with modifications from the following article: Cengiz, N., J. Rao, A. Sanyal and A. Khan, *Chemical Communications*, Vol. 49, pp. 11191-11193, 2013.

4.1. Introduction

Fabrication of crosslinked polymeric networks with properties like biocompatibility, elasticity, swelling ability in water, and diffusion of small moleculas are of high interest in many areas of biomedical sciences, particularly in tissue engineering [118-121]. Due to an ever-increasing interest in these materials, development of novel synthetic methods to obtain such functionalizable using simple and straightforward methods are required [122-130].

As noted in the first chapter, the ligation strategies that has been used to fabricate reactive hydrogels generally employ the 1,3-dipolar azide-alkyne cycloaddition, [4+2] Diels-Alder reaction, [2+2] cycloaddition chemistry, thiol-ene reactions, Michael-type addition reactions and epoxy-amine reactions. The last combination i.e. reaction of an epoxide functional group with an amine has been widely used since the epoxide ring can be readily incorporated into polymeric materials by use of monomers like glycidyl methacrylate. Epoxy unit provides a handle for facile post-fabrication modification of polymeric materials since it can be converted to many useful functionalities including hydroxides, thiols, amines, acids, chlorides, and also azides (Figure 4.1) [131-132]. Hence, the epoxy functional group is very versatile and useful in both designing polymeric scaffolds and post-fabrication modification of scaffolds.

To the best of our knowledge thiol-epoxy click chemistry has not been used to synthesize hydrogels though there are some examples to make polymer composites and

there are some hydrogels utilizing amine-epoxy chemistry [133]. Nevertheless, S-H bond energy is 339 kJ/mol, while N-H bond energy is 391 kJ/mol which means the energy required to break the S-H bond is less than the energy to break N-H bond. In addition, thiolate anion is a better nucleophile than amine. As thiolate (RS^-) is chemically more reactive than the protonated thiol form (RSH) it is preferable to use as a base catalyst for thiol-epoxide ring opening.

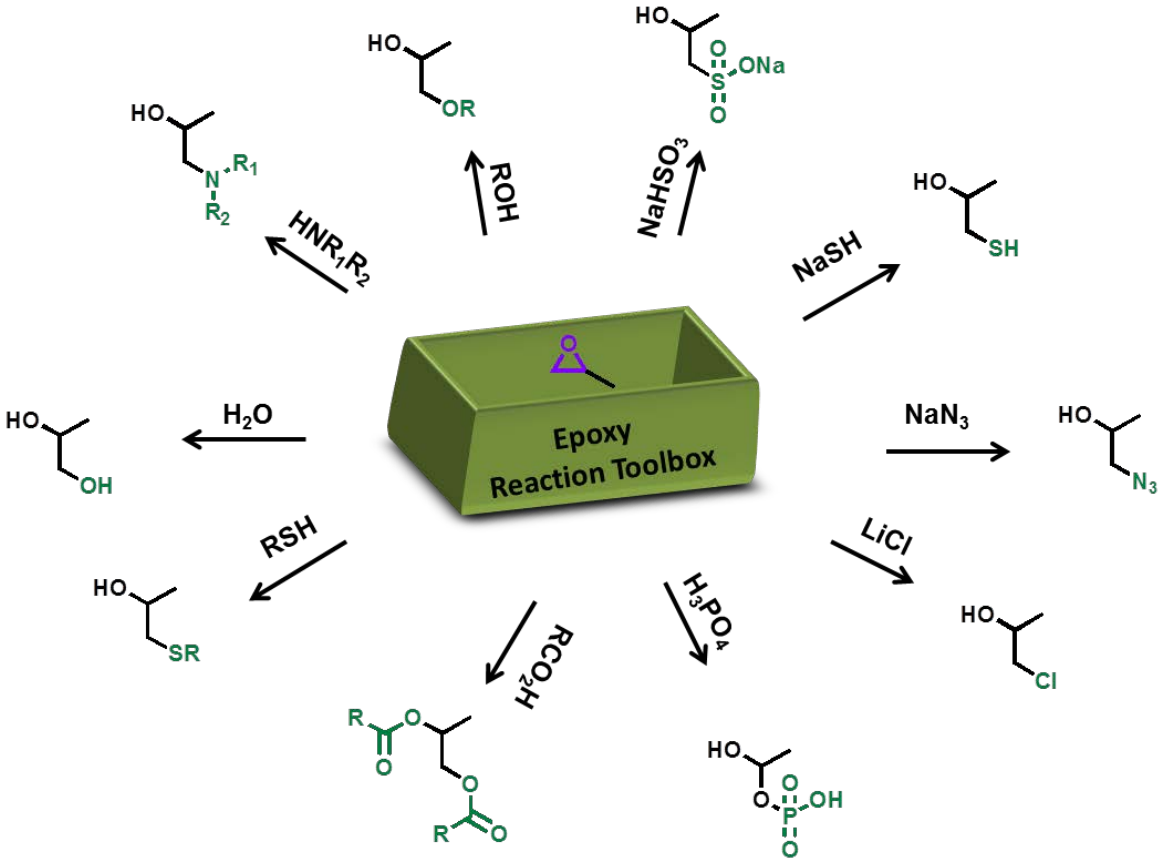

Figure 4.1. Illustrative reactions involving epoxide-ring opening.

An added advantage of the thiol-epoxy reaction is that a reactive hydroxyl group is produced as a result of the coupling reaction (Figure 4.2). This secondary hydroxyl group, although less reactive than a primary hydroxyl group, can be converted into an ester moiety upon reaction with an acid group [62-64, 134-136].

This chapter outlines fabrication and functionalization of hydrogels using the thiol-epoxy chemistry. The abovementioned sequence of epoxide ring opening followed by derivatization of the new hydroxyl group can be utilized to obtain functional hydrogel scaffolds in two simple steps. In particular, the thiol-epoxy coupling chemistry between commercially available and appropriately chosen precursors would give rise to a hydrophilic network carrying the hydroxyl groups. Transformation of the hydroxyl units into ester functionalities would furnish the targeted functionalized hydrogel.

In this study, poly(ethylene glycol) (PEG) was used as a major component of the hydrogels since it is a common hydrophilic and biocompatible polymer. Importantly, it is suitable for in vivo applications since it does not cause an immune response [137]. PEG is non-toxic and has been used to modify proteins and peptides to prolongs their half-life in the body [138]. Due to high degree of flexibility and swelling in water, in some instances PEG does not provide the desired mechanical stiffness required for some applications. It is known that polydimethylsiloxane (PDMS) can be used for hydrogel synthesis to develop mechanical properties due to its high gas permeability, optical transparency, high flexibility, nontoxicity, biocompatibility, stability towards heat and chemicals, low curing temperature, mold-ability, and ease of mixing with other materials [139-144]. So, we hypothesized that the incorporation of PDMS and PEG into polymer network will provide both hydrophilicity and enhanced mechanical properties. To this end, since our goal is to design hydrogels through thiol-epoxy coupling reaction, we decided to use epoxy terminated PDMS with epoxy terminated poly(ethylene glycol) in the thiol-epoxy crosslinking procedure in order to prove the mechanical properties of hydrogels while retaining good water uptake capacity.

In addition, both acrylate and epoxy group incorporated polymers can be used to synthesize epoxy functional hydrogels. Hence, thiol-epoxy chemistry can be directly utilized for the conjugation of molecules to the hydrogel network and the secondary hydroxyl group formed after the first functionalization can be further derivatized.

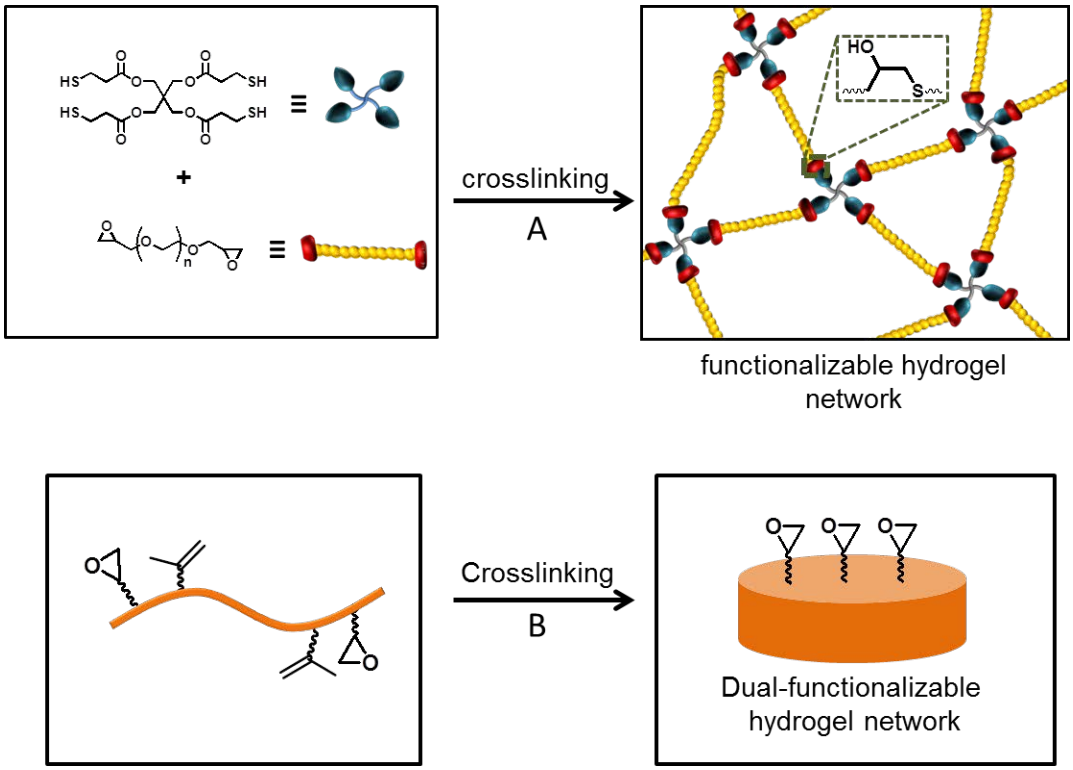

Figure 4.2. Hydroxyl (A) and epoxy (B) functional hydrogel formations.

4.2. Experimental

4.2.1. Materials

Poly(ethylene glycol)diglycidyl ether (M_n~1kDa) was purchased from Polysciences, Inc. Tetra-n-butylammonium fluoride-Trihydrate was purchased from ABCR. Lithium Hydroxide Monohydrate was purchased from Fluka. All other reagents Poly(ethylene glycol)diglycidyl ether (M_n~526 Da and ~2 kDa), Poly(dimethylsiloxane), diglycidyl ether terminated (M_n ~800 Da), Pentaerythritol tetrakis(3-mercaptopropionate) and Trimethylolpropane triglycidyl ether were purchased from Sigma Aldrich and utilized as received unless otherwise indicated. Diethylene Glycol Methacrylate, Glycidyl Methacrylate and 2-Hydroxyethyl Methacrylate were purchased from Sigma Aldrich. Polyethylene Glycol with molecular weight of M_n~6 kDA was purchased from Fluka. Cu(I)Br, 4,4 dimethyl 2,2 dipyridiyl and triethylamine (TEA) were purchased from Acros

and used without further purification. Methacryloyl chloride was obtained from Sigma Aldrich. 2-Bromo-2-methylpropionyl bromide was purchased from Acros Organics. Other chemical reagents were obtained from commercial resources and were used as received. The dry solvents such as dichloromethane (DCM), tetrahydrofuran (THF) were obtained from SciMatCo purification system. Column chromatography was performed using silica gel 60 A^o. Thin layer chromatography was performed using silica gel plates (Kieselgel 60 F254, 0.2 mm, Merck). The plates were viewed under 254 nm UV lamp otherwise plates were developed either by $KMnO_4$ stain.

4.2.2. Mechanical Tests

The mechanical properties of the prepared hydrogels were measured by unconfined uniaxial compression tests using an Instron 5864 mechanical tester (Figure 4.3). Cylindrical-shaped hydrogel samples were prepared and immersed in distilled water until they reached equilibrium. They were compressed at a rate of 2 mm/min^{-1}. The compressive modulus was determined as the slope of the linear region in the strain range of the stress-strain curve.

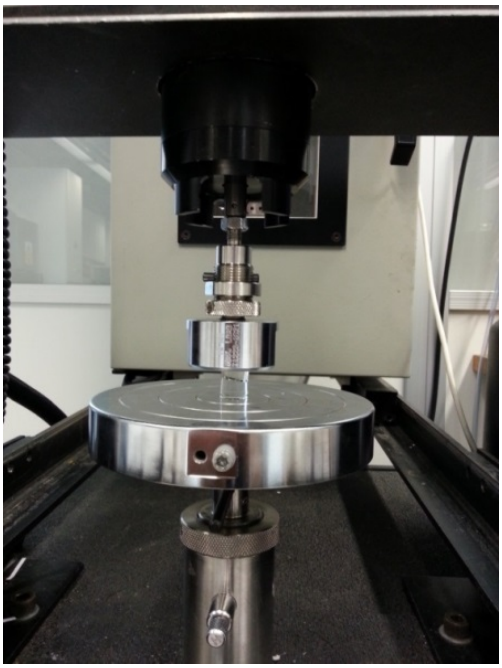

Figure 4.3. Stress-Strain measurements using rheometer.

4.2.3. Swelling Studies

Cylindrical-shaped hydrogel samples were immersed into distilled water and then freeze-dried. The initial mass of the samples was measured and then they were immersed in distilled water. Swollen hydrogels were weighed (after removal of surface water using filter paper) at designed time intervals. Swelling was calculated according to the equation, $Q\ (\%) = [(W_s - W_d)/W_d] \times 100$, where, W_s is the mass of the hydrogel in the swollen state, W_d is the mass of the hydrogel in the dried state, and Q is the equilibrium-swelling ratio.

4.2.4. Synthesis of Hydrogels via Gelation Procedure 1

In a typical experiment, poly(ethylene glycol)diglycidyl ether (M_n~526 Da, M_n~1kDa, or ~2 kDa) and trimethylolpropane triglycidyl ether were dissolved in DMF and mixed with pentaerythritol tetrakis(3-mercaptopropionate) crosslinker at 25 ^oC (Scheme 2). The molar ratio between the epoxy and the thiol group was fixed at 1:1 in all the experiments. 25 wt% aqueous solution of LiOH was used as a catalyst. This constituted 20 mol% of the catalyst related to the thiol/crosslinker ratio.

4.2.5. Synthesis of Hydrogels via Gelation Procedure 2

4.2.5.1. PEG (1kDa) Hydrogel. PETMP (**1**) (58.83 mg, 0.12 mmol) and TBAF.$3H_2O$ (97%) (39.16 mg, 0.12 mmol) were dissolved in 225 mg of DMF, stirred for 5 minutes, and then added to an already prepared solution of PEG **2** (240.80 mg, 0.24 mmol) in 550 mg of DMF. This formulation was subjected to a vigorous stirring process to obtain a clear solution. This solution was heated to 70 ºC for 30 minutes. After cooling to the room temperature, the crosslinked material was washed thoroughly with ethanol and then water for several times and then used for further studies (yield = ~90%).

4.2.5.2. PEG/PDMS (1/0.25 mol%) Hydrogel. PETMP (**1**) (73.54 mg, 0.15 mmol) and TBAF.$3H_2O$ (97%) (48.96 mg, 0.15 mmol) were dissolved in 225 mg of DMF, stirred for 5 minutes, and then added to an already prepared mixture of PEG (**2**) (240.8 mg, 0.24 mmol) and PDMS (**3**) (48.16 mg, 0.06 mmol) in 550 mg DMF. This formulation was subjected to a vigorous stirring process to give a fine dispersion. This dispersion was heated to 70 ºC for 30 minutes. After cooling to the room temperature, the crosslinked material was

washed thoroughly with ethanol and then water for several times and then used for further studies (yield = 88-91%).

4.2.5.3. PEG (2kDa) Hydrogel. PETMP (**1**) (12.22 mg, 0.025 mmol) and TBAF.$3H_2O$ (99%) (7.97 mg, 0.025 mmol) were dissolved in 150 mg of DMF, stirred for 5 minutes, and then added to an already prepared solution of PEG 2kDa (100 mg, 0.05 mmol) in 200 mg of DMF. This formulation was subjected to a vigorous stirring process to obtain a clear solution. This solution was heated to 70 ºC for 30 minutes. After cooling to the room temperature, the crosslinked material was washed thoroughly with ethanol and then water for several times and then used for further studies (yield = ~86%).

4.2.6. Functionalization of Hydrogel 1 (H1)

The hydrogel network was freeze-dried, soaked in THF, and freeze-dried again. This dry sample was then immersed in anhydrous DCM (0.5 mL) containing pyrene-carboxylic acid (0.008 g), DCC (0.050 g), and DMAP (0. 015 g). This reaction mixture was stirred at the room temperature for 12 hours. After this time, the hydrogel film was washed with DMSO, water, MeOH, and THF for several times, freeze-dried, and analysed for fluorescence under UV-irradiation.

4.2.7. Synthesis of Peg ATRP Macroinitiator (6 kDa)

In a typical experiment, PEG (1.5 g, 0.25 mmol) was dissolved in toluene and dried by removal of water-toluene by azeotropic rotary evaporation, followed by drying under high vacuum for 24 hours. Thus obtained anhydrous PEG was dissolved in anhydrous THF (30 mL). TEA (0.15 mL, 1.06 mmol) was added to the PEG solution under nitrogen. The solution of temperature was cooled to 0 °C and 2-bromo-2-methylpropionyl bromide (0.23 g, 1 mmol) was added dropwise and the reaction was left stirring overnight. The organic solvent was removed under reduced pressure. The crude product was dissolved in methylene chloride (200 mL) and washed with saturated $NaHCO_3$ solution (200 mL) three times. The combined organic layers were dried over anhydrous Na_2SO_4 and concentrated in vacuum. The crude product was dissolved in minimum amount of DCM and precipitated in diethyl ether. Product is obtained as white powder (yield = 85 %). ^{1}H NMR (δ, ppm,

$CDCI_3$) 4.32-4.29 (4H, m, -COO-*CH_2*-), 3.81-3.78 (4H, m, -COO-CH_2-*CH_2*-), 3.73-3.71 (4H, m, -COO-CH_2CH_2O-*CH_2*), 3.66-3.59(530H, br s, -CH_2CH_2O-), 3.45-3.43 (4H, m, -CH_2CH_2O-), 1.92 (12H, s, -CH_3-C-COO-)

4.2.8. General Polymerization Procedure for the Synthesis of ABA Type Triblock Copolymers (P1)

In a typical bulk polymerization, the round bottomed flask was charged with polyethylene glycol bromo macroinitiator (0.40 g, 0.067 mmol), diethylene glycol methacrylate (0.75 g, 4.002 mmol), 2-hydroxyethyl methacrylate (0.17 g, 1.334 mmol), and glycidyl methacrylate (0.19 g, 1.334 mmol) in the solution of anisol (2.5 mL), and degassed under nitrogen. Then, a solution of 4,4 dimethyl 2,2 dipyridiyl (54.5 mg, 0.1334 mmol) and Cu(I)Br (9.56 mg, 0.067 mmol) in 0.7 ml anisol sonicated and added to the system under nitrogen and stirred with varying timescales at room temperature. After polymerization the reaction mixture was diluted with DCM and passed over a column of neutral alumina to remove the catalyst. The solution was concentrated and precipitated into excessive amount of diethyl ether. The resulting polymer was dried under vacuum at room temperature (yield: 35%). M_n=10 kDa, ^{1}H NMR (δ, ppm, $CDCI_3$) 4.32 (2H, br s, -COO-*CH_2*-), 4.11-3.82 (4H, m, -COO-*CH_2*-), 3.64-3.55(530+6 H, m, -*CH_2CH_2*O-), 3.40 (br s, 3H, OC*H_3*), 3.22 (2H, br s, epoxy-*CH_2*-), 2.85 and 2.64 (epoxy protons) , 1.96-0.98 (m, C*H_2* and C*H_3* along polymer backbone.

4.2.9. Activation of ABA Triblock Copolymers Through Converting Hydroxyl Groups into Methacrylate group (P2)

In a typical experiment copolymer 1 (150 mg, 0.01 mmol) was dissolved in dry DCM under N_2 atmosphere. Et_3N (0.55 mmol) was added to reaction mixture and stirred for 15 minutes. Methacryloyl chloride (0.154 mmol) was added drop by drop at 0° C and reaction was ended after 12 hours (yield = 91%). ^{1}H NMR (δ, ppm, $CDCI_3$) 6.14 and 5.63 (2H, br s, br s C*H_2*=C-), 4.32 (2H, br s, -COO-*CH_2*-), 4.11-3.82 (4H, m, -COO-*CH_2*-), 3.64-3.55(530+6 H, m, -*CH_2CH_2*O-), 3.40 (3H, br s, OC*H_3*), 3.22 (2H, br s, epoxy-*CH_2*-), 2.85 and 2.64 (2H, br s, br s, epoxy protons) , 1.96-0.98 (m, C*H_2* and C*H_3* along polymer backbone.

4.2.10. Gelation of Activated Triblock Copolymer P2

P2 (25 mg, 0.0016 mmol) was dissolved in 150 µL H_2O, 150 µL EtOH mixture. 2, 2-Dimethoxy-2-phenylacetophenone DMPA (0.3 mg, 0.001 mmol) was added to the polymer solution. The clear solution is irradiated by Ultraviolet light at 365 nm for 1 hour. Hydrogel is washed with EtOH and H_2O several times to remove unreacted materials (yield = 80%).

4.3. Results and Discussion

4.3.1. Gelation Procedure 1

We hypothesized that hydrogels could be synthesized using linear poly(ethylene glycol) diglycidyl ether polymers (PEG 2) and pentaerythritol tetrakis(3-mercaptopropionate) (PETMP 1) via thiol-epoxy "click" chemistry. Hence we evaluated gelation using PEG 2 and the PETMP 1 crosslinker in various organic solvent (EtOH, DMF or THF) using catalysts such as 2,4,6-tris(dimetylaminomethyl)phenol, triethyl amine and LiOH at temperatures ranging from 25° C to 100° as described in Figure 4.4. However, none of the reactions succeeded properly since the resulting gel-like structures were easily dispersed/solubilized in water or in an organic solvent.

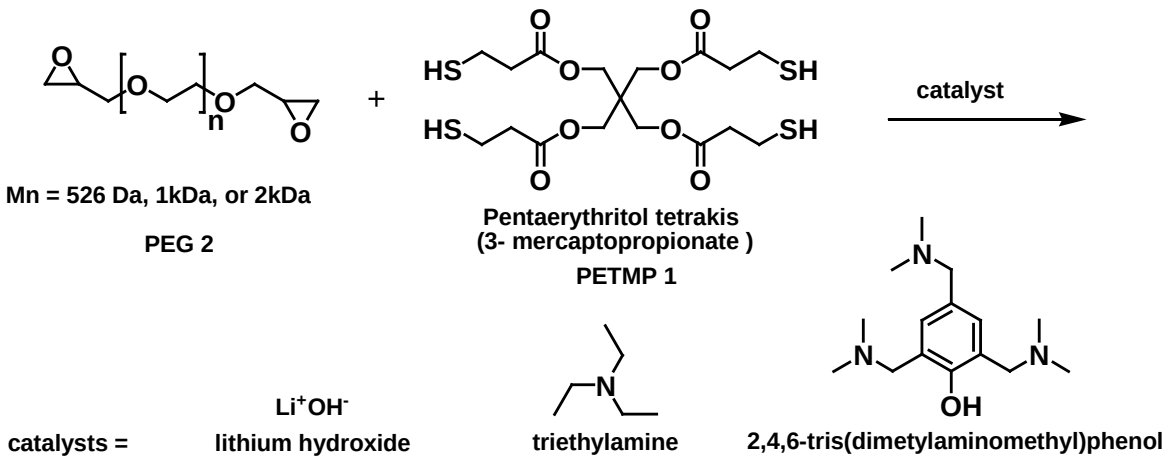

Figure 4.4. General gelation procedure 1.

4.3.2. Gelation Procedure 2

After the failed trials as described above, we decided to add trimethylolpropane triglycidyl ether (TGE), which has three branching sites, to enhance the gelation via increased crosslinking. This change was beneficial as it facilitated the gelation process and stable crosslinked networks could be obtained. We proposed that hydrogel properties can be tuned depending on the length of poly(ethylene glycol) unit. So we used different molecular weight of linear poly(ethylene glycol) diglycidyl ethers 536 Da, 1 kDa and 2 kDa respectively to compare the mechanical properties of hydrogels We hypothesized that adding a certain amount of 3-arm glycidyl creates more crosslinking needed to yield hydrogel as we did not observe gel structures in the absence of trimethylpropane triglycidyl ether (Figure 4.5).

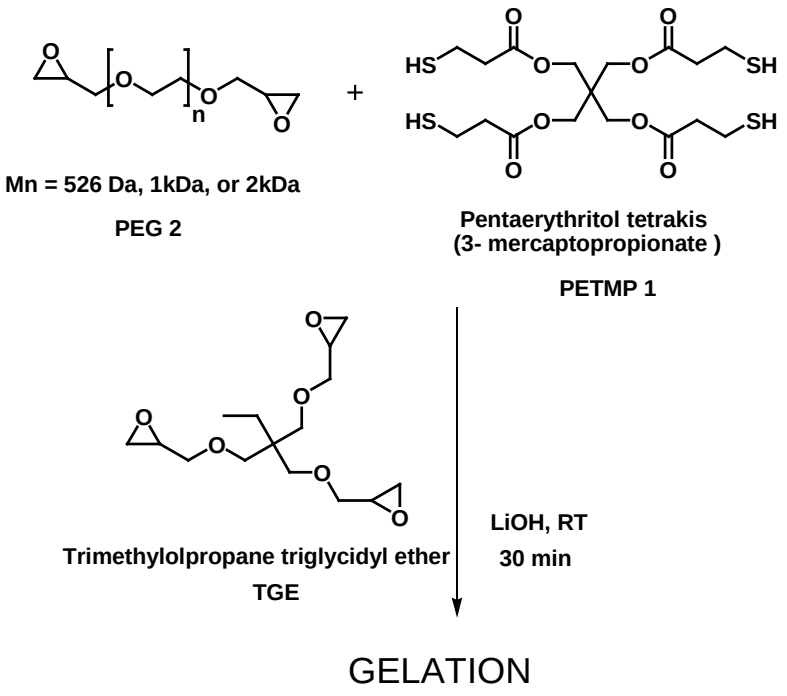

Figure 4.5. General gelation in presence of additional epoxide-containing crosslinker.

Swelling studies of the gels were consistent with the length of the poly(ethylene glycol) unit. Table 4.1 shows the water uptake tests for hydrogels G1, G2 and G3. When we increased the molecular weight of poly(ethylene glycol) polymer, from 526 to 1kDa, and 2 kDa, %water uptake increased from 140% to 317% and 441%, respectively.

Table 4.1. Chemical composition, water uptake and yield of hydrogels.

	PEG (mol eq)	TGE (mol eq)	PETMP 1 (mol eq)	Water Uptake (%)	Conversion (%)
G1[a]	13.7	6.1	11.4	140	76
G2[b]	13.7	6.1	11.4	317	62
G3[c]	13.7	6.1	11.4	441	76

[a] PEG (M_n=526 Da); [b] PEG (M_n=1 kDa); [c] PEG (M_n=2 kDa);

Total thiol:epoxy 1:1, 25 ^oC, solvent DMF, catalyst LiOH, % 25 weight percent aqueous solution of LiOH is used as a catalyst by 20% moles of total thiol crosslinker ratio.

FTIR spectra of the starting materials and the hydrogels were analysed to understand the gelation. We observed a band at 3056 cm^{-1} due to the C-H stretching, and at 909 cm^{-1} due to the C-O stretching of epoxy group in PEG (526 Da). Similar bands at 3056 cm^{-1} and 909 cm^{-1} were observed for the TGE monomer. However the intensity of the peaks was a bit higher due to the higher epoxy content. The band at 2569 cm^{-1} in IR spectrum of PETMP **1** corresponds to S-H stretching and the band at 1733 cm^{-1} corresponds to the C=O stretching of the molecule (Figure 4.6).

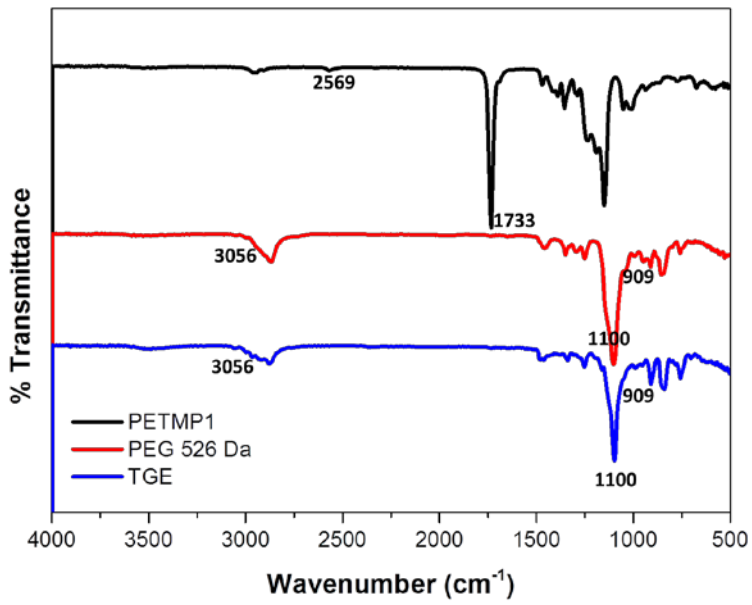

Figure 4.6. FT-IR Spectra of hydrogel precusrsors.

After the gelation step we characterized the cross-linked material with FTIR to confirm its composition and identify consumption of starting materials. It was difficult to observe the band at 909 cm^{-1} which corresponds to C-O stretching of epoxy group because of the overlap with other bands at this region. However, the adsorption peaks due to the epoxy groups of starting material at 3056 disappeared. In addition, S-H band at 2570 cm^{-1} also disappeared and new peak appeared at 1736 cm^{-1} due to the C=O stretching after gelation (Figure 4.7).

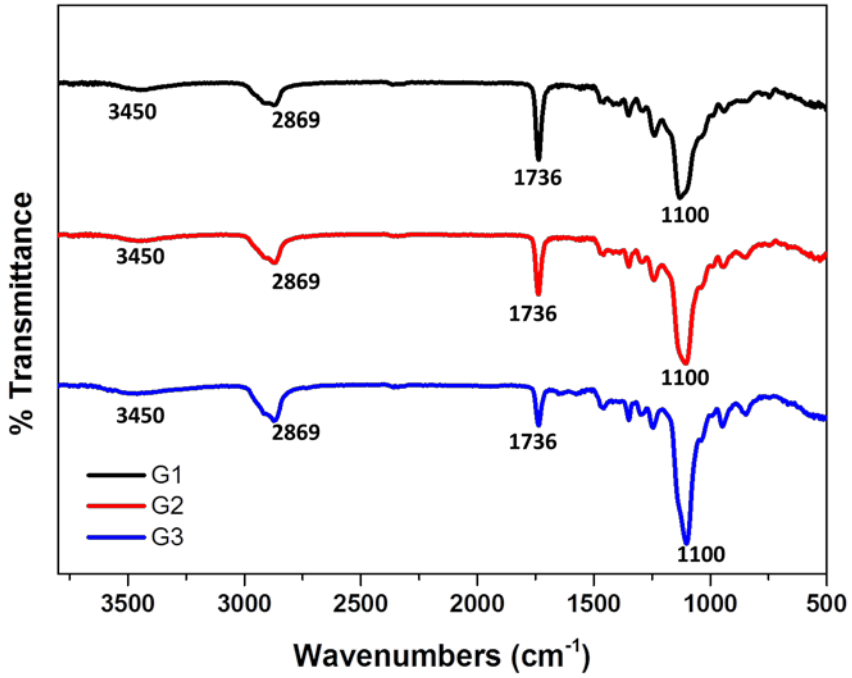

Figure 4.7. FT-IR spectra of hydrogels.

Morphology of gels G1, G2, and G3 were analysed using a scanning electron microscopy (Figure 4.8). Hydrogel G3, obtained using a 2 kDa PEG precursor showed higher degree of porosity than the rest of the materials. When we increase the molecular weight of poly(ethylene glycol) unit, the chain length between crosslinks increases, thus decreasing the overall crosslinking density. Further, the swelling also increases with increasing PEG content (Table 4.1).

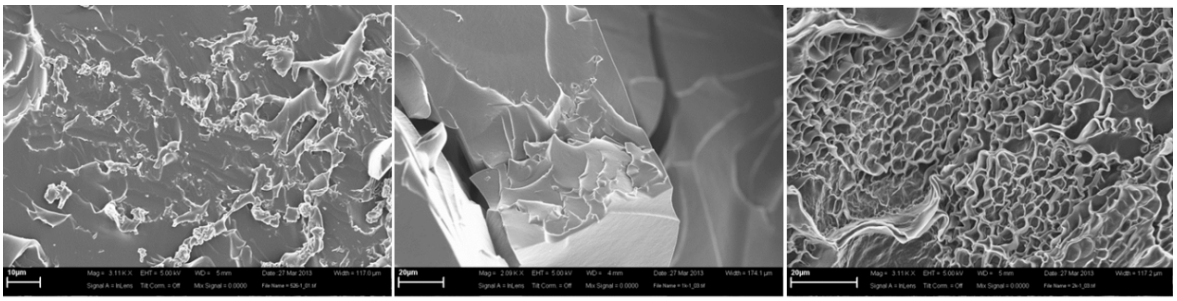

Figure 4.8. Morphology of hydrogels G1, G2 and G3 observed using SEM.

Although, hydrogels were successfully obtained after addition of the triepoxide based crosslinker TGE, obtained hydrogels were highly brittle possessed unsuitable mechanical properties for biomedical applications. However through these experiments we deduced that the thiol-epoxy chemistry is capable of inducing the gelation. We also noted that LiOH was not an appropriate catalyst for the gelation process since LiOH does not possess good solubility in organic solvent, whereas epoxy ring opening reactions requires the use of polar aprotic solvents like DMF and acetonitrile.

4.3.3. Gelation Procedure 3

A brief survey at the literature indicated that quaternary ammonium fluorides are soluble in many organic solvents and they are effective catalysts in thiol-epoxy reactions in organic synthesis [145-146]. These previous reports prompted us to use TBAF as a catalyst in gelation process as described in Gelation Process 2.

To test the feasibility of this concept, initially, crosslinking between PETMP (**1)** and diglycidyl ether terminated PEG (**2**) (M_n = 1 kDa), was carried out in the presence of tetrabutyl ammonium fluoride (TBAF) (Figure 4.9).

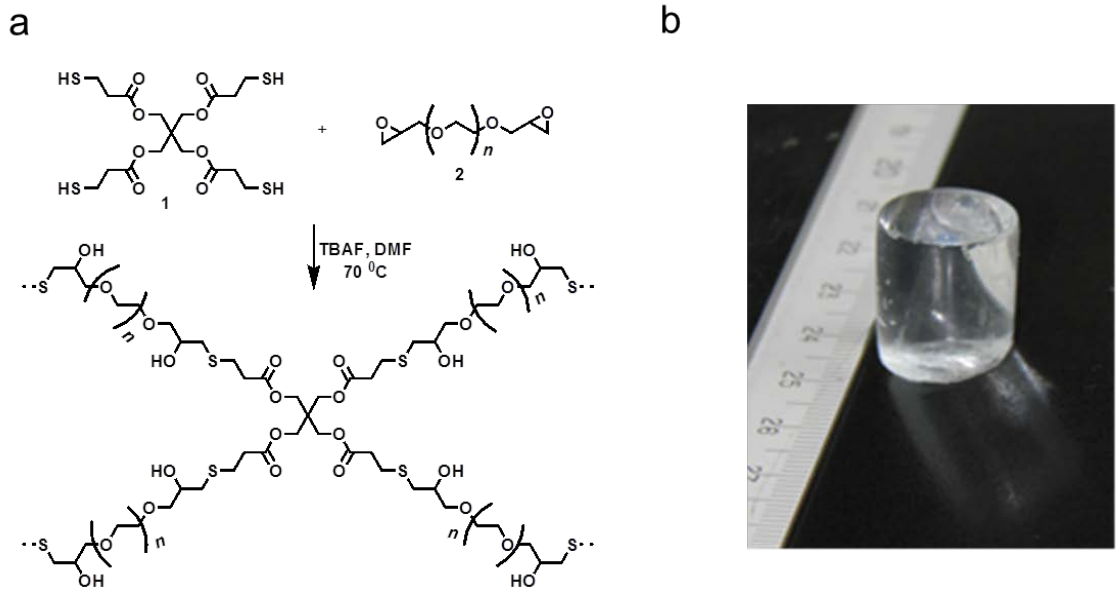

Figure 4.9. a) Schematic illustration of hydrogel synthesis and b) photograph of a typical thiol-epoxy hydrogel.

Gelation using TBAF as a catalyst could be carried out within 30-60 at 70 ºC with conversions ranging between 88-91%. At the end of the gelation period, the resulting solid materials were thoroughly washed with ethanol and water to remove all unreacted starting materials and reagents. The hydrogel containing PETMP **1** and PEG **2** exhibited a modulus of 47 kPa (Table 4.2). To improve the mechanical properties, commercially available diglycidyl ether-terminated poly(dimethylsiloxane) (PDMS) (M_n = 0.8 kDa), **3**, which can participate in crosslinking into the hydrogel structure due to its terminal epoxy groups (Figure 4.10) was introduced into the gel formulation. A variety of hydrogels with different feed of PDMS (3) were obtained and it was gratifying to note that the presence of PDMS did not affect the efficiency of gelation in any negative manner (Figure 4.11). The compositions studied are outlined in Table 4.2.

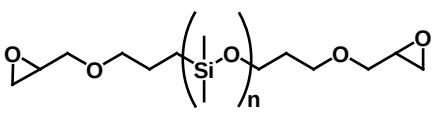

3
n = 8

Figure 4.10. Structure of diglycidyl ether-terminated poly(dimethylsiloxane) (PDMS).



Figure 4.11. Gel formulations before and after the gelling reaction. H1 (a), H2 (b), H3 (c), and H 4 (d).

IR spectroscopy demonstrated that the SH stretch present at 2570 cm^{-1} in the precursor **1** disappeared after the gelation reaction (Figure 4.12 and 4.18). Moreover, a broad signal, centered on 3470 cm^{-1}, could be observed due to the formation of the hydroxyl groups. The ester stretch at 1730 cm^{-1} remained unperturbed after the gelation process indicating stability of the ester functionalities towards the TBAF-catalyzed thiol-epoxy reaction.

FTIR spectra of the hydrogels are relevant with the PDMS ratio in the gelation feed as described in Table 4.2. Hydrogel H1 doesn't show signal at 805 cm^{-1}, since it does not contain PDMS, whereas H2, H3 and H4 have the characteristic peak for Si-O bending at 805 cm^{-1}. Increasing the PDMS ratio in H2 to H4 we observed an increase in the Si-O bending at 805 cm^{-1}. In addition, we found that the O-H stretch in the spectral range 3200 to 3600 cm^{-1} are due to the secondary hydroxyl groups which are formed through addition of thiols to the epoxy groups during the gelation process (Figure 4.12).

Addition of PDMS-diglycidyl ether **3** to the gelation mixture produced hydrogels with significantly enhanced mechanical properties (Table 4.2). Addition of 20, 33, and 50 mole% of **3**, relative to the PEG content, in the formulations resulted in gels with modulus of 72, 157, and 204 kPa, respectively.

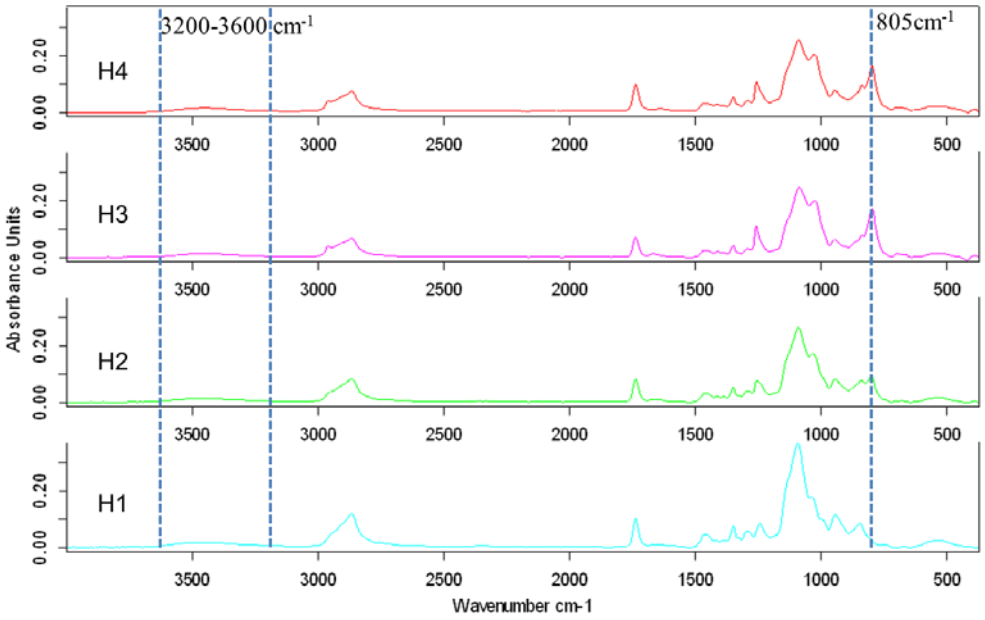

Figure 4.12. IR spectra of H1, H2, H3 and H4.

Table 4.2. Effect of PDMS amount and % PEG to Stress Strain measurements and water uptake capacity of the hydrogels.

Entry	PDMS (% mole epoxy)	Thiol-Epoxy (mol ratio)	Swelling (%)	Compressive modulus (kPa)
H1	0	1:1	400	47[a]
H2	20	1:1	275	72
H3	33	1:1	180	157
H4	50	1:1	110	204
H5	0	1:1	500	28
H6	20	1:1	235	150
H7	33	1:1	176	196
H8	50	1:1	118	367

Temp = 70 °C, time = 30 mins, For entry H1 to H4: 27 wt % PEG **2** in DMF, For entry H5 to H8: 31 wt % PEG **2** in DMF was used for gelation, [a]time of 60 minutes was required for sample solidification.

To study the swelling behaviour and the extent of water uptake by the hydrogels, the dried materials were swollen in water and studied by gravimetric analysis until they reached equilibrium. This study showed that the water uptake capacity of the gels without PDMS **3** was about 400% and exhibited a compressive modulus of about 47 kPa (Table 4.2). When we add PDMS **3** to the hydrogel formulations, the decrease in water uptake capacity of hydrogels were directly proportional to the amount of PDMS in the feed (Figure 4.13).

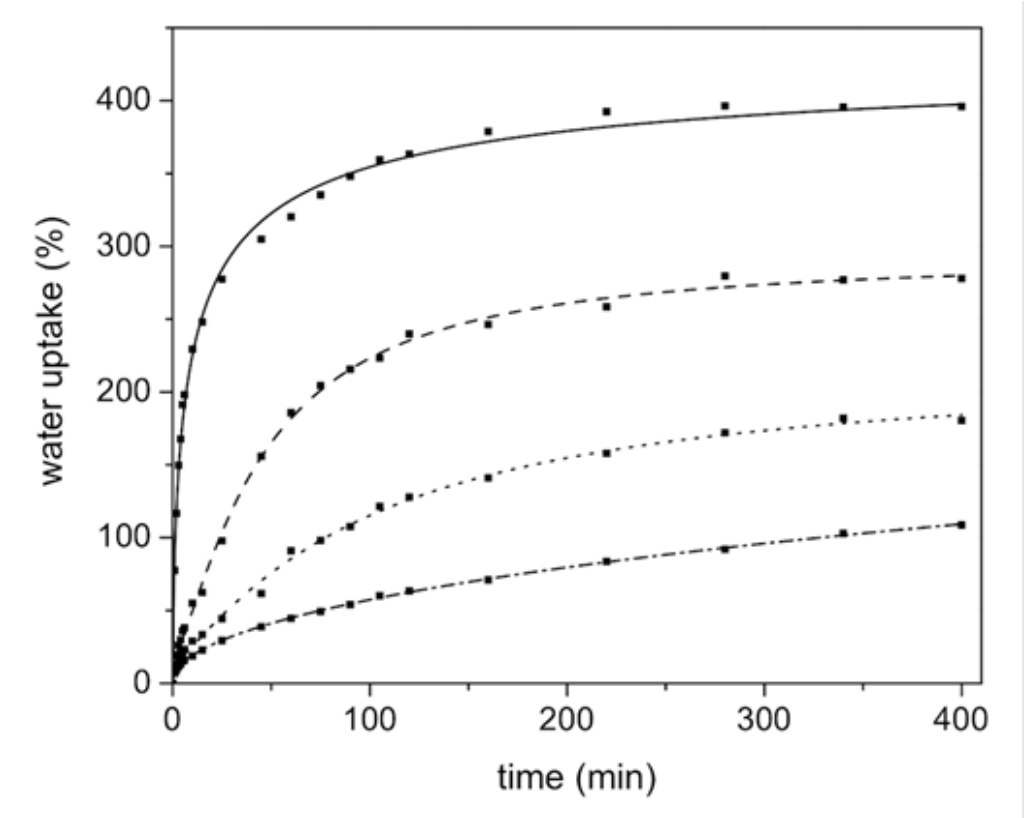

Figure 4.13. Water uptake by the hydrogels containing 0 (solid line), 20 (dash line), 33 (dash-dot) line, and 50 mole% (dash-dot-dot line) of PDMS. PEG wt % 27.

Morphologies of hydrogels were also investigated via scanning electron microscopy. We did not observe a porous structure probably because of the insufficient chain length of 1 kDa poly(ethylene glycol) unit. It is likely that the contrast in SEM micrographs are due to PEG and PDMS domains because of their hydrophilic and hydrophobic phases (Figure 4.14).

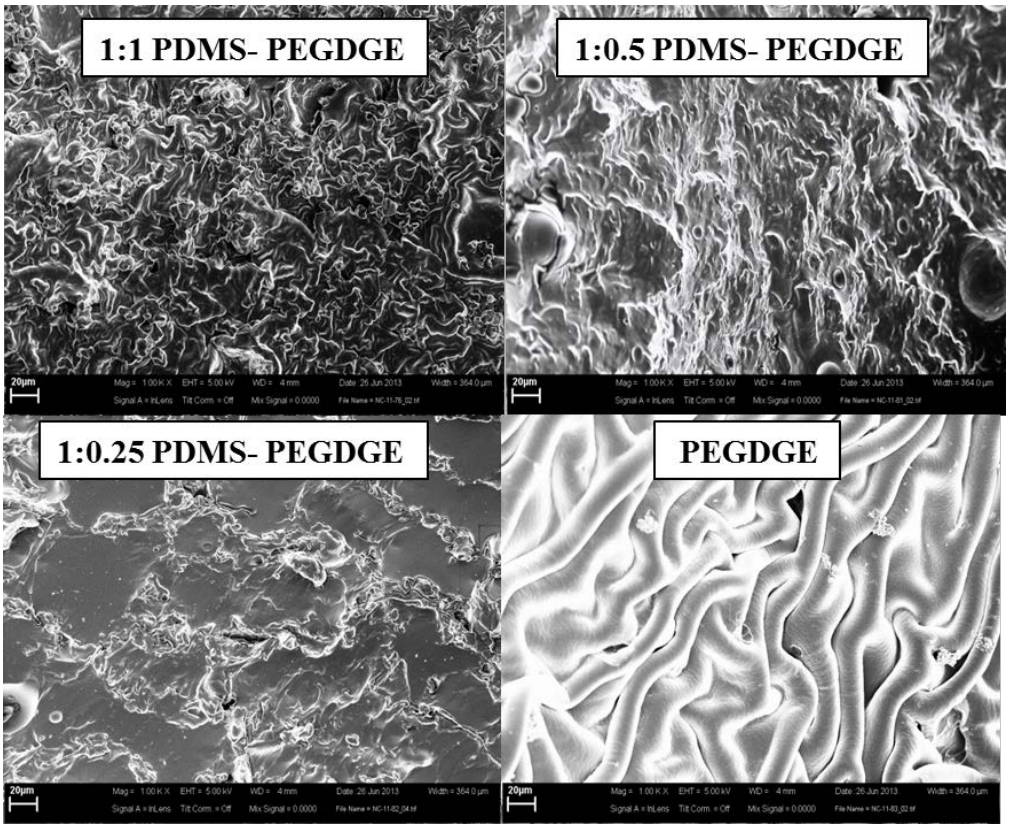

Figure 4.14. SEM images of the freeze-dried hybrid hydrogels varying in hydrophilic/hydrophobic balance.

An alternative strategy to improve the mechanical strength of the materials is by increasing the crosslinking density. This can be achieved by increasing the concentration of the precursors in the gel formulation [147]. Application of this strategy resulted in a significant increase in the compressive modulus of the hydrogels (Table 4.2). For example, increasing the PEG concentration from 27 to 31 wt% (corresponding increase in PETMP concentration from 7.6% to 8.6 wt%) could increase the modulus of the material at equilibrium swelling from 72 kPa to 150 kPa (Table 4.2).

Therefore, by combining the aforementioned two concepts – addition of PDMS and an increase in the PEG concentration – materials with a wide range of mechanical strengths (28-367 kPa) could be obtained. This is an important aspect considering that mechanical properties of a hydrogel can critically affect the cell-material interaction [148].

To further increase the water uptake capacity of the hydrogels, PEG **2** (1 kDa) was replaced with PEG **4** (2 kDa) (Figure 4.15). A longer reaction time (60 min) was required for obtaining a freestanding hydrogel. This increase in the chain length of the hydrophilic gel-component resulted in a sharp increase in the degree of material swelling (Figure 4.16). Gels from precursor **2** and **4** exhibited a water uptake capacity of 400% and 1500%, respectively. Additionally, these gels were fragile in comparison to ones obtained using shorter PEG chains. Gel from precursor **4** (H9) showed 4 kPa modulus.

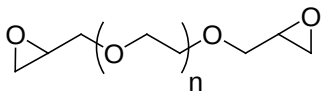

4
n = 45

Figure 4.15. Diglycidyl ether-terminated poly(ethylene glycol) (PEG) 4.

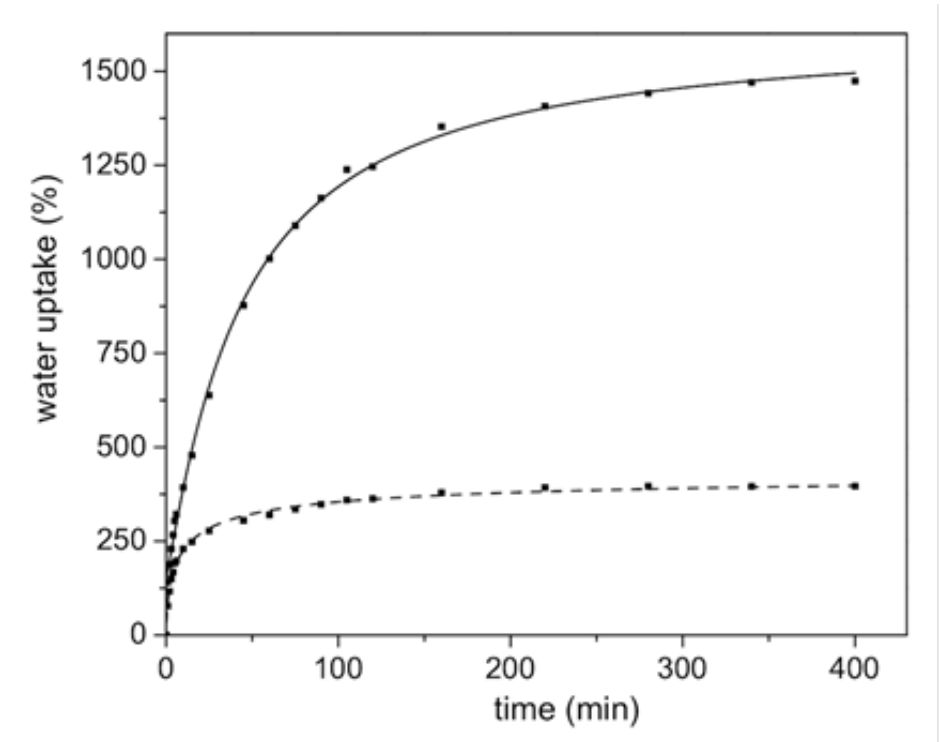

Figure 4.16. Water uptake by the hydrogels containing PEG 2 (solid line) and PEG 4 (dash line).

Finally, to probe the reactivity of the newly formed hydroxyl groups for functionalization of obtained hydrogels, esterification of gels swollen in THF with 1-pyrenecarboxylic acid was undertaken (Figure 4.17). Thereafter, the gels were thoroughly rinsed with organic solvents like dimethyl sulfoxide (DMSO), methanol, and THF as well as water to remove any physically absorbed materials and then analysed for fluorescence under UV-irradiation. As can be seen in Figure 4.19, pyrene functionalized gel exhibited blue fluorescence upon excitation at the wavelength of 365 nm. A control experiment performed using pyrene instead of 1-pyrenecarboxylic acid did not result in any considerable fluorescence which hints the covalent attachment of 1-pyrenecarboxylic acid to the gel.

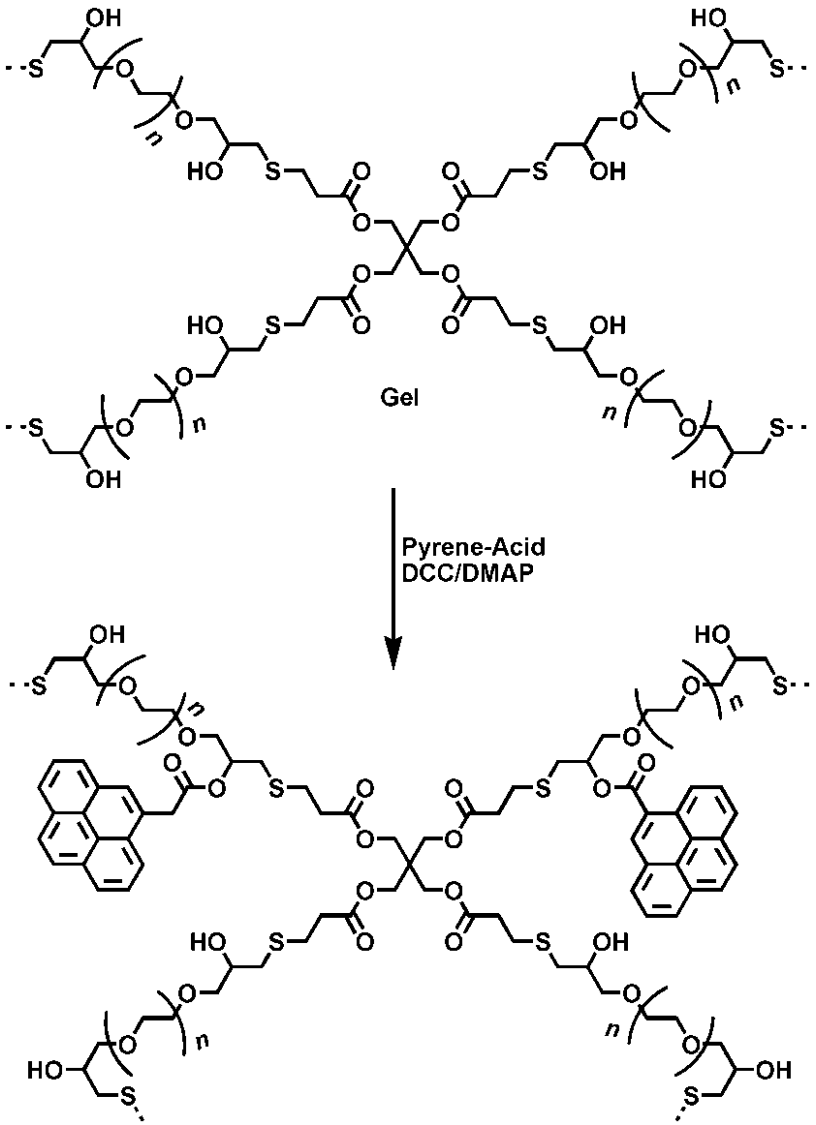

Figure 4.17. Functionalization of hydrogels via esterification.

Analysis of the functionalized hydrogels using FTIR spectroscopy indicated a significant reduction in the intensity of the OH band at 3470 cm^{-1} due to consumption of the hydroxyl groups because of their esterification. Apart from appearance of an ester band appeared at 1710 cm^{-1}, a band at 710 cm^{-1} due to the C=C aromatic stretches of the pyrene ring was present. Thus esterification reactions under mild conditions could be used to functionalize the hydrogels obtained using thiol-epoxy chemistry (Figure 4.18).

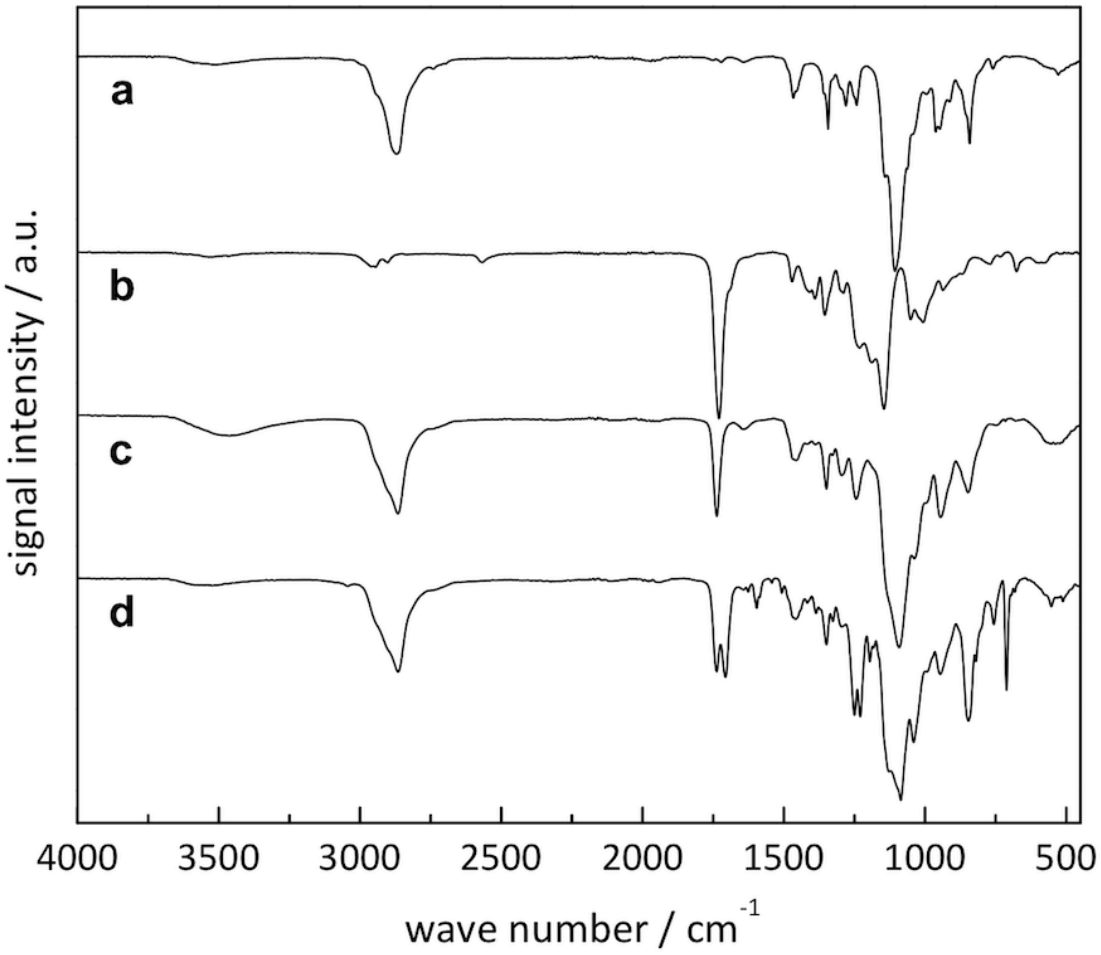

Figure 4.18. FT-IR spectra of the gel precursors PEG 2 (a) and PETMP 1 (b), PEG-hydrogel (c), and pyrene-functionalized hydrogel (d).



Figure 4.19. Optical fluorescence microscopy image of (a), functionalized hydrogel (bright field, (b) upon excitation at 365 nm, and (c) control experiment upon excitation at 365 nm.

4.3.4. Epoxy Bearing Hydrogels Through Crosslinking of ABA Type Polymers

In this part of the project, we aimed to design epoxy group bearing reactive hydrogels using ABA type block copolymers. As the characteristic importance of the epoxy bearing hydrogel is the formation of a reactive hydroxyl group after first functionalization of epoxy group, this feature can be used to prepare dual-functional hydrogels by introducing two chemically different reactive groups at the same hydrogel scaffold for various applications. By taking the advantage of orthogonal nature of epoxy chemistry functionalizable hydrogels were prepared as shown in Figure 4.20.

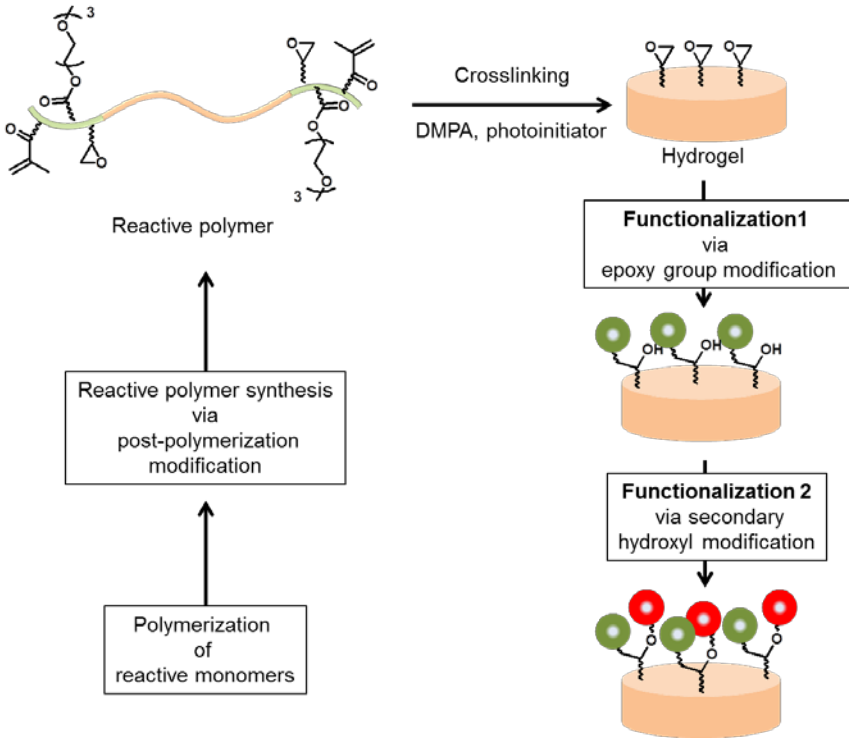

Figure 4.20. General outline for the synthesis of epoxy bearing hydrogels and their functionalization.

ABA type reactive polymers were synthesized for gelation reaction. For this aim we initially synthesized a telechelic PEG macroinitiator (Mn = 6 kDa) (Figure 4.21). Then triblock copolymers were synthesized using atom transfer radical polymerization using diethylene glycol methacrylate, glycidyl methacrylate and 2-hydroxyethyl methacrylate monomers with the PEG based macroinitiator. In the following step, post-polymerization modification was performed to convert the hydroxyl side chains into polymerizable double bonds. Polymer P1 which contains hydroxyl groups in the side chains was reacted with methacryloyl chloride to install methacrylate groups which can participate in free radical-initiated crosslinking reaction. These polymerizable double bonds were crosslinked in the presence of a photoinitiator, namely, DMPA, under UV irradiation (Figure 4.22).

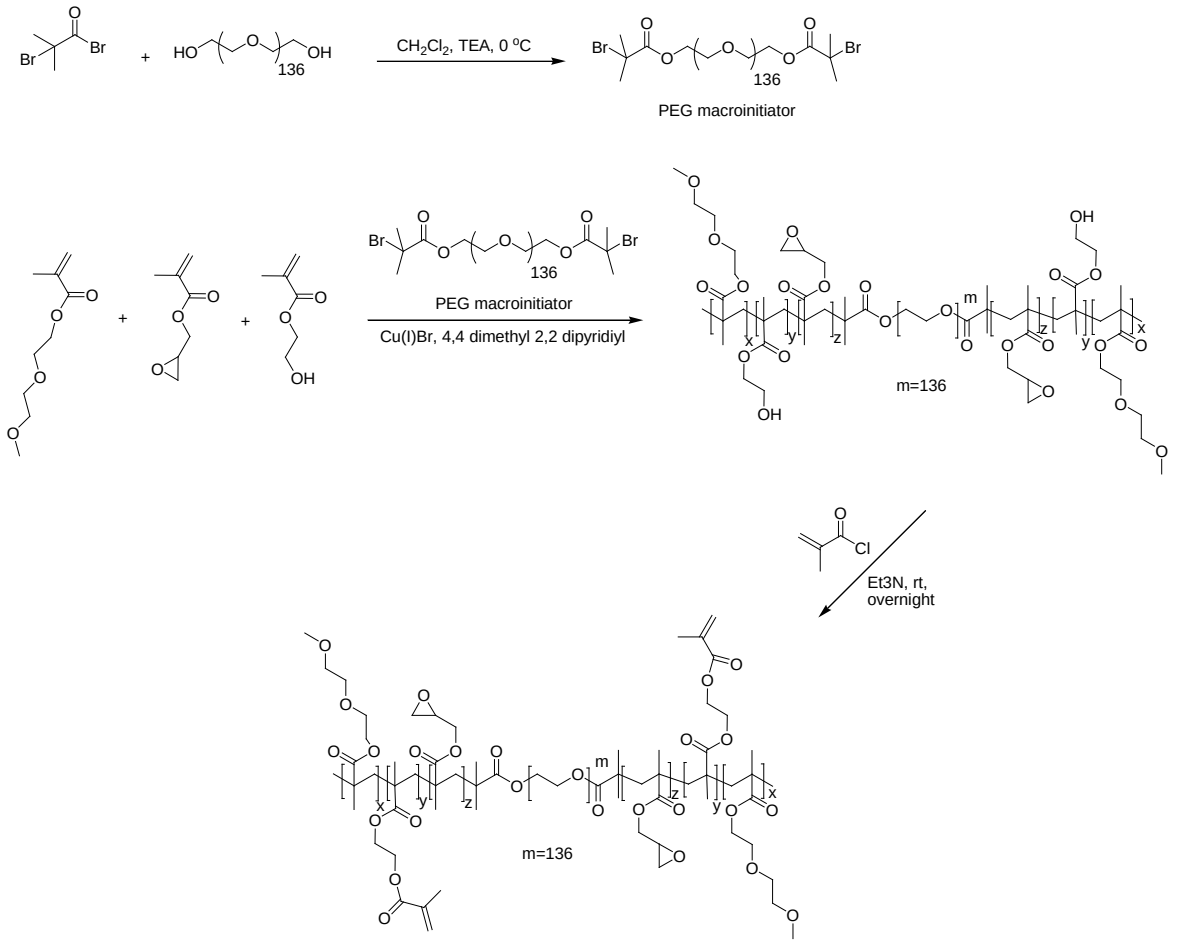

Figure 4.21. Synthesis of ABA triblock copolymer using a PEG macroinitiator, and its post-polymerization modification.

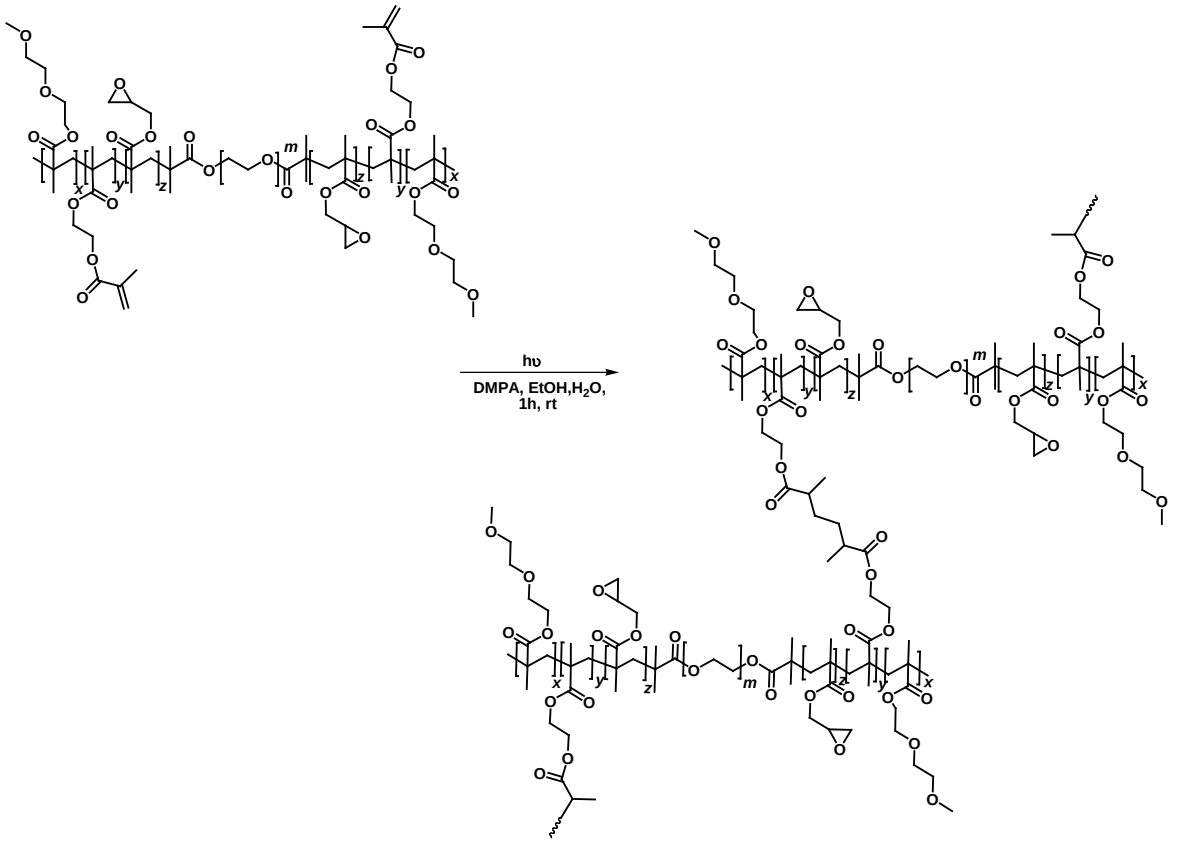

Figure 4.22. Hydrogel synthesis using P2.

Figure 4.22 shows the ^{1}H-NMR spectra of the triblock copolymer P1 and the functionalized copolymer P2. The proton resonances at 2.6 ppm, 2.8 ppm and 3.2 ppm in both spectra arise from the protons on the epoxide rings. ^{1}H-NMR spectrum of copolymer after functionalization with methacryloyl chloride also confirms the attachment of the methacrylate group to the polymer chain since we observe the appearance of new peaks at 6.1 ppm and 5.6 ppm. Additionally, the FTIR spectra of the polymers before activation (P1) and after activation (P2) also confirm the attachment of methacrylate groups to the hydroxyl side chains (Figure 4.23). We observed a band at 3470 cm^{-1} due to the OH stretching resulting from hydroxyl side chains for P1. After the attachment of methacrylate groups, the band at 3470 cm^{-1} disappears and new peaks due to the C=C stretch can be seen for copolymer P2 at 1636 and 1677 cm^{-1}.

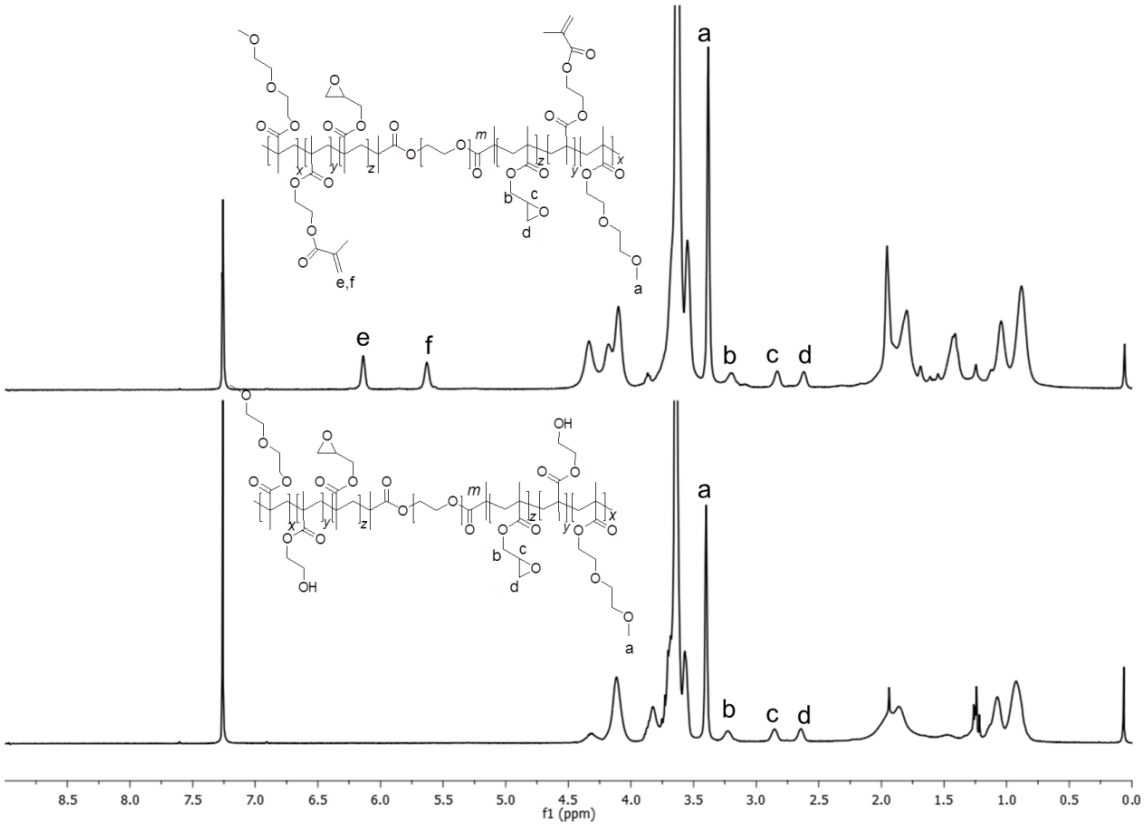

Figure 4.23. ^{1}H-NMR spectra of copolymers P1 and P2.

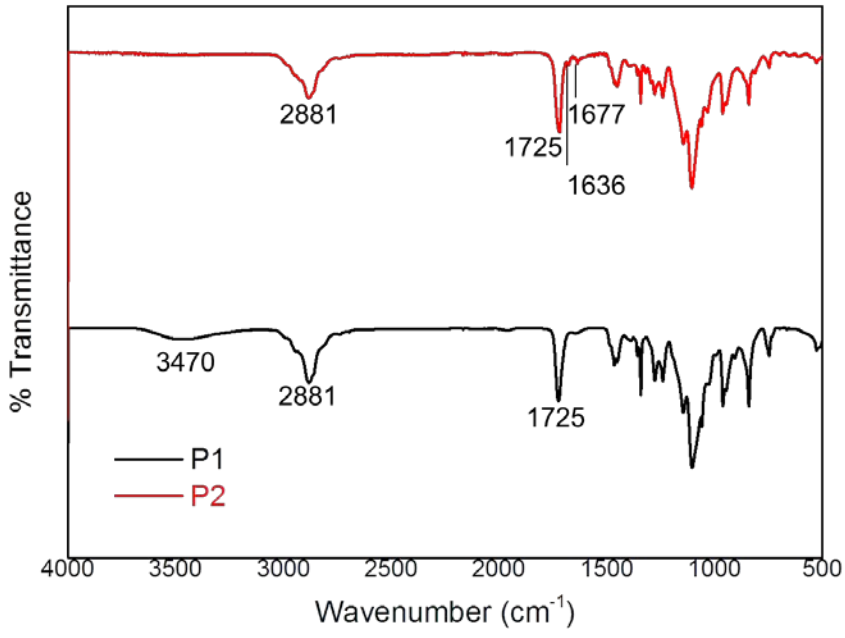

Figure 4.24. FT-IR spectra of the copolymers P1 and P2.

After the post-polymerization step P2 was dissolved in H_2O:EtOH (1:1) and double bonds on the polymer chain were crosslinked in the presence of photoinitiator dimethoxy-2-phenylacetophenone (DMPA), under UV irradiation at 365 nm 1 hour Resulting hydrogel was washed with EtOH and H_2O several times to remove the unreacted materials. Figure 4.24 shows the digital image of the hydrogel formation after UV irradiation.

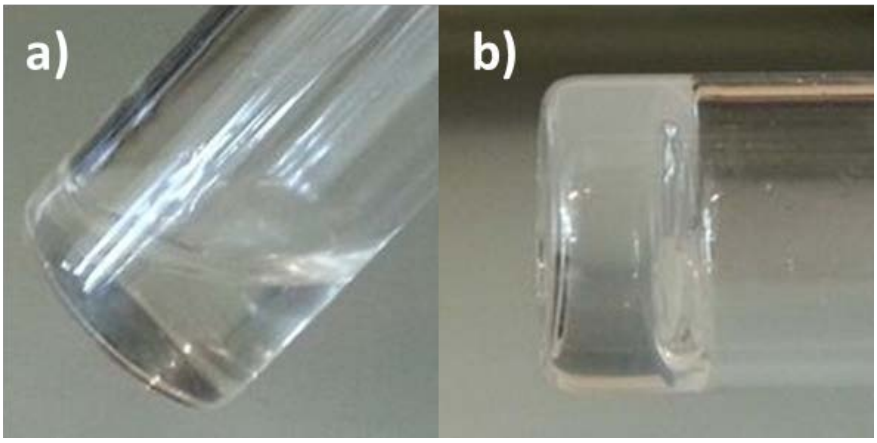

Figure 4.25.Image before(a) and (b) after photopolymerizationof polymer.

Environmentally responsive hydrogels have the ability to show different physical properties in different conditions. In polymerization step we used diethylene glycol methacrylate which brings thermoresponsive behaviour to the hydrogel. It is known that polymers containing diethylene glycol based side chains exhibit thermoresponsive behaviour and exhibit a lower critical solution temperature (LCST) around 35°C [149]. We also carried out the water upake test at different temperature to observe the presence of the thermoresponsive behavior in these gels. A decrease in the water uptake by the hydrogel was observed when the swelling experiment was carried out at 37° C instead of 0° C, as a result of collapse of diethylene glycol units in side chain at higher temperatures because of its thermoresponsive behaviour. The equilibrium water uptake of hydrogel at 0° C is % 800 while water uptake of the same hydrogel was % 600 at 37° C (Figure 4.25).

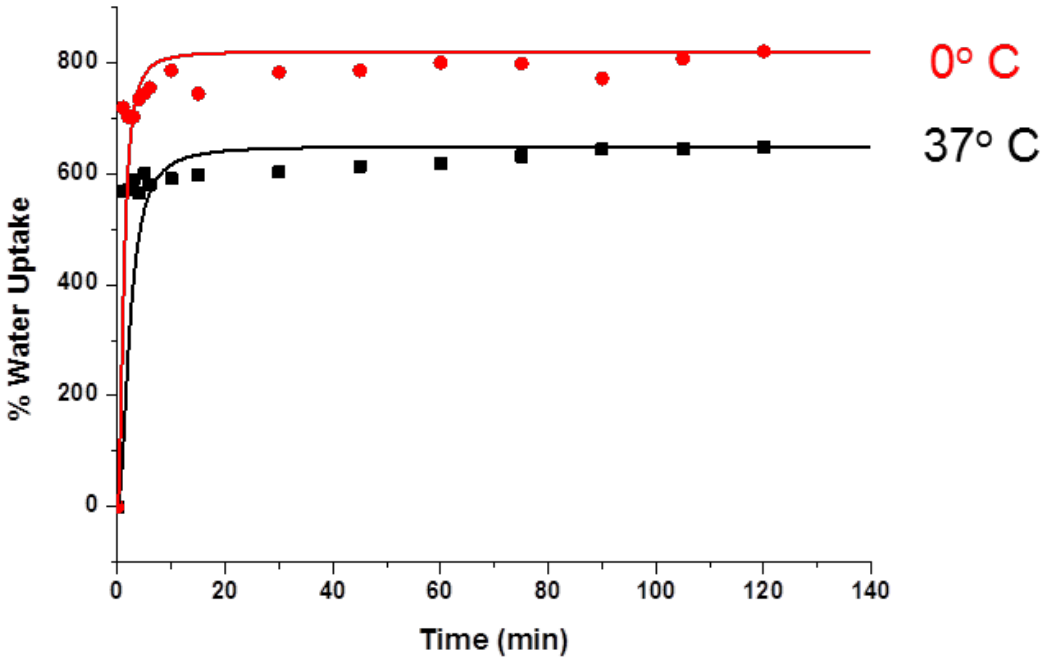

Figure 4.26. Water uptake profiles of hydrogels at different temperatures (0 ^{o}C and 37 ^{o}C).

4.4. CONCLUSION

In conclusion, thiol-epoxy coupling chemistry is an effective synthetic tool for the preparation of PEG-based hydrogel materials. An added benefit of this chemistry is that it produces a reactive hydroxyl group during the gelation process. This reactive group can be used as an anchoring site to install a desired functional group to the hydrogel scaffold through an esterification reaction. Therefore, functionalized hydrogels can be obtained in a simple two-step process starting from commercially available precursors. In addition, ABA type polymers containing thermoresponsive diethylene glycol units, reactive epoxy groups, and hydroxyl groups in their side chains were synthesized using ATRP. The hydroxyl side chains were modified with methacrylate units to enable photo-initiated gelation to furnish hydrogel networks which containing reactive epoxy groups that can be used for further functionalization.

5. FABRICATION OF POLYMERIC MICROPATTERNS STABILIZED VIA NON-COVALENT CROSSLINKING

The materials in this chapter have been adapted with modifications from the following article: Subramani, C., N. Cengiz, K. Saha, T. N. Gevrek, X. Yu, Y. Jeong, A. Bajaj, A. Sanyal, and V. M. Rotello**,** *Advanced Materials*, Vol. 23, pp. 3165-3169, 2011.

5.1. Introduction

Hydrogels are materials of high importance in biomaterial science since they can show similar properties to tissues such as water uptake and retention, softness and biocompatibility [150]. Patterning of soft polymeric materials is widely studied in biomaterial science especially in tissue engineering since it micropatterns modulate growth of cells and provides mimicking the tissue for regenerative purposes. The generation of complex structures like artificial organs is becoming possible via patterning [151]. Also for various biosensors applications based on the cells, positioning of the cells can be controlled through the use of patterns [152].

Depending on the application and polymeric materials of choice, the type of the patterning technique becomes very important when fabricating polymeric scaffolds. The patterning technique should allow obtaining microstructures without compromising the properties of the parent polymeric material. There are several lithography techniques available to design patterned surfaces such as photolithography, nanoimprinting lithography, soft lithography and scanning probe microscope lithography [153-155]. Depending on the desired application and type of the material one can utilize a suitable lithography technique to build a patterned scaffold.

Stable micropatterns can be fabricated through covalent or non-covalent crosslinking chemistries. Herein, we were focused on non-covalent crosslinking. Non-covalent crosslinking can be accomplished through assembly of polymeric materials via forces like

van der Waals, electrostatic, hydrogen bonding and hydrophilic-hydrophobic interactions. The type of the crosslinks makes difference on the mechanical stability of the crosslinked materials. In general, non-covalently crosslinked hydrogels have limited mechanical properties comparing to covalently crosslinked ones due to nature of crosslinks, whereas they have more flexible structures so recovery is better after shear.

In this part of the work, we utilized the hydrophilic hydrophobic balance of the polymeric materials via non-covalent interactions to obtain stable microstructures that were fabricated using nanoimprinting lithography technique (NIL) to create functional polymeric scaffolds (Figure 5.1).

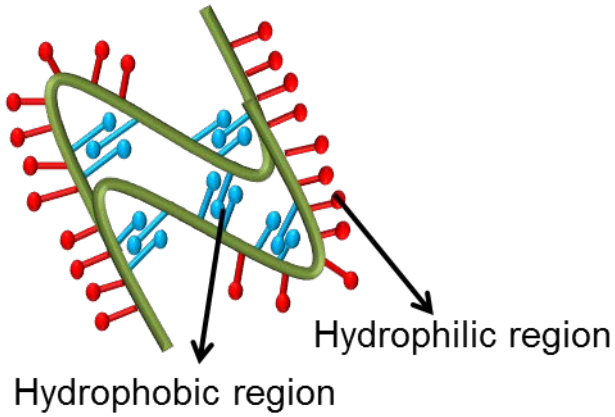

Figure 5.1. Non-covalent stabilization of polymers.

Nanoimprinting lithography is a simple developing high resolution nanolithography method for high-throughput patterning of polymer nanostructures at low costs. It provides resolution from several hundred microns down to 5 nm. This method mainly based on mechanical deformation of the material through hot embossing of the materials. Depending on the aim it can be applied thermal or UV based. The principle of the process is very simple. Figure 5.2 shows the basic NIL process [156-157]. The surface pattern was prepared replicating the mold into the resist material through hot embossing above the glass transition temperature of the resist. Generally, a thin layer of polymeric material is left below the mold on purpose to protect the direct contact of the hard mold with substrate. This also protects the features on the mold. Later the residual part can be removed through plasma-etching depending on the application [158].

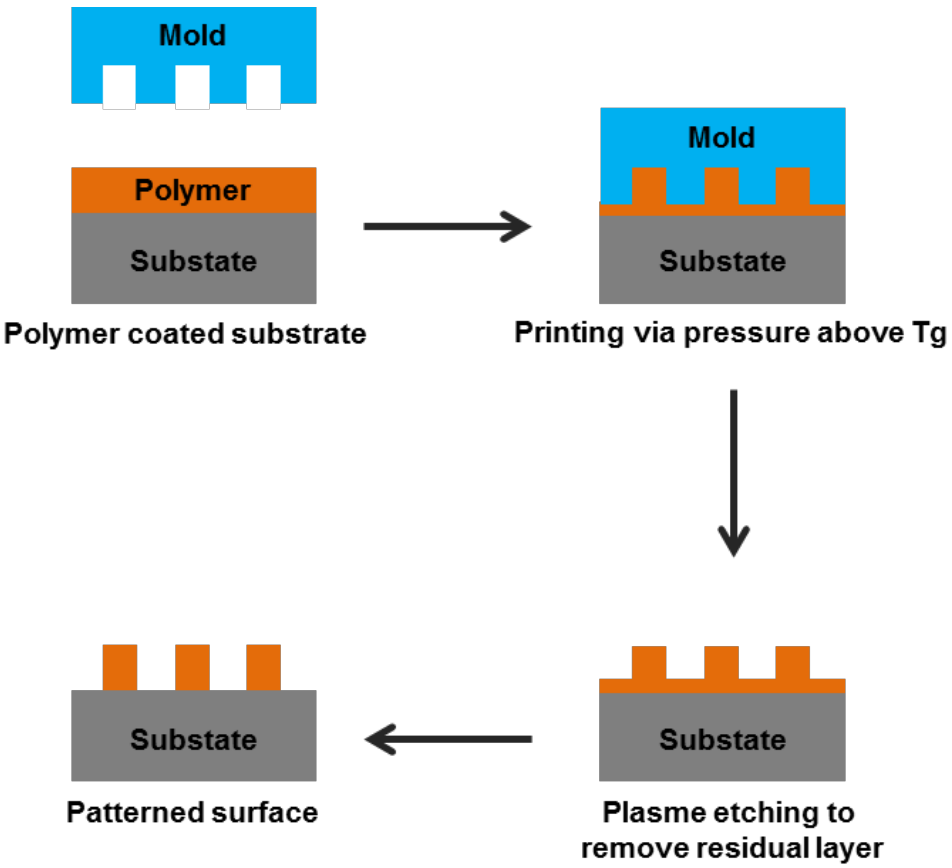

Figure 5.2. Basic work flow of the nanoimprint lithography process.

In this study, our goal was to design micropatterns containing the maleimide functional group to obtain functional surfaces via post-fabrication functionalization. Since the maleimide group is very reactive towards thiols it can be effectively derivatized with thiol containing (bio)molecules via Michael type “click” reaction under mild conditions. To achieve this goal, polymers were designed for successful utilization in thermal nanoimprinting process to create thiol-reactive polymeric platforms from furan protected maleimide containing polymers in one single step without any further need of the deprotection step (Figure 5.3).

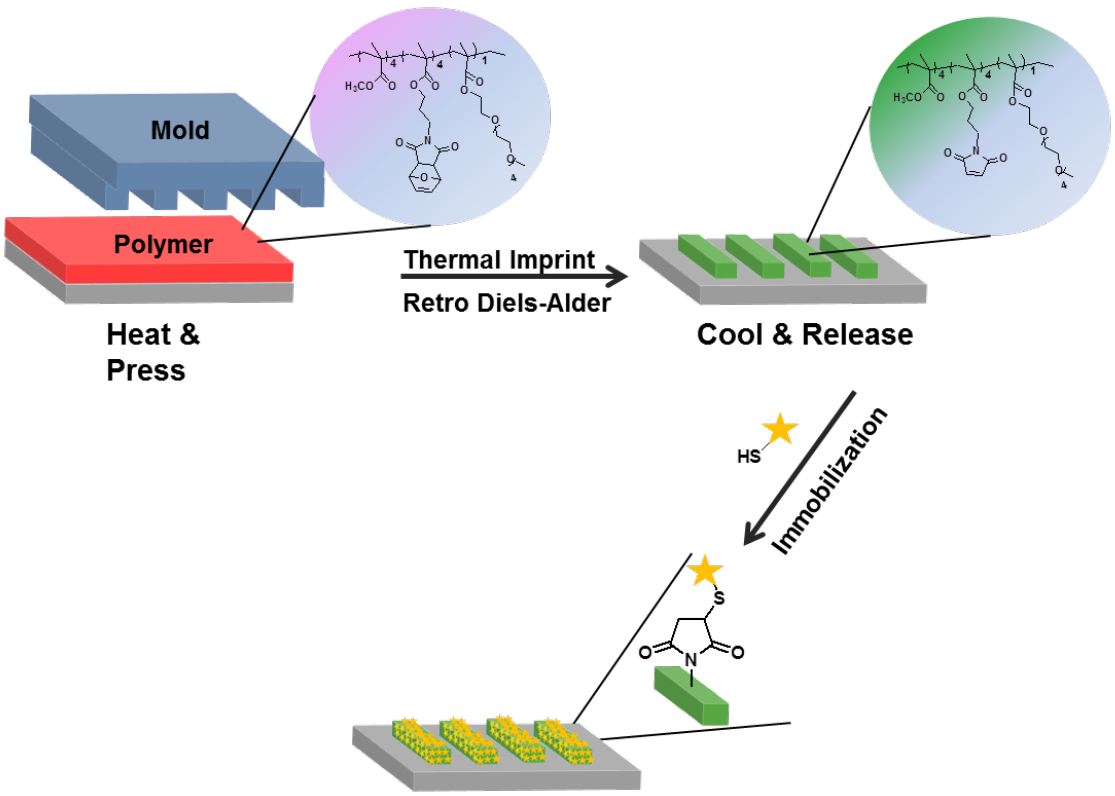

Figure 5.3. Schematic illustration of fabrication and functionalization of micro-patterned polymeric structures using thermal imprinting.

5.2. EXPERIMENTAL

5.2.1. Materials

All reagents were obtained from commercial sources and were used as received unless otherwise stated. Monomer furan-functionalized methyl methacrylate (FMMA) was prepared as reported previously. Methyl methacrylate Poly (ethylene glycol) methyl ether methacrylate (PEGMEMA, M_n = 300 Da) was purchased from Sigma Aldrich and purified by passing through the activated aluminum oxide column prior to use.

5.2.2. Characterization

The monomer and polymer characterizations involved ^{1}H and ^{13}C solution NMR spectroscopy (Varian 400 MHz) and Fourier transform infrared (FTIR) spectroscopy (Perkin Elmer 1600 Series). Differential scanning calorimetry (DSC) and thermogravimetric analysis (TGA) were done on Rheometric Scientific (Software V5.42) and TA instrument, respectively. The molecular weights were estimated by gel permeation chromatography (GPC) analysis using a Viscotek GPCmax VE-2001 analysis system. PLgel (length/ID 300 mm × 7.5 mm, 5 μm particle size) Mixed-C column was caliberated with polystyrene standards, using refractive index detector. THF was used as elutent at a flow rate of 1 mL/min at 30 °C. Bright field images and fluorescence were detected using an Olympus IX51 microscope with excitation wavelengths of 470 nm and 535 nm.

5.2.3. Synthesis of Copolymer 1

Azobisisobutyronitrile (AIBN) (0.009 g, 0.056 mmol) was added to a solution of FMMA (0.2 g, 0.68 mmol), MMA (0.068 g, 0.68 mmol), and polyethyleneglycol methacryalte (PEGMA) (0.102 g, 0.34 mmol) in anhydrous $CHCl_3$ (10 mL). The mixture was degassed and then heated to reflux for 16 h. At the end of the reaction, $CHCl_3$ was evaporated under vacuum and the residue was dissolved in minimum amount of dichloromethane and added to cold methanol to precipitate polymer **1** as a white solid (yield = 60%). M_n = 4380 Da, PDI = 1.38.

5.2.4. Synthesis of Copolymer 2

Azobisisobutyronitrile (AIBN) (0.033 g, 0.201 mmol) was added to a solution of FMMA (0.35 g, 1.202 mmol), and MMA (0.481 g, 4.808 mmol) in anhydrous $CHCl_3$ (10 mL). The mixture was degassed and then heated to reflux for 12 h. At the end of the reaction, $CHCl_3$ was evaporated under vacuum and the residue was dissolved in minimum amount of dichloromethane and added to cold methanol to precipitate polymer **2** as a white solid (yield = 62%). M_n = 4100 Da, PDI = 1.42.

5.2.5. Synthesis of Copolymer 3

Azobisisobutyronitrile (AIBN) (0.009 g, 0.056 mmol) was added to a solution of FMMA (0.2 g, 0.68 mmol), MMA (0.068 g, 0.68 mmol), and polyethyleneglycol methacryalte (PEGMA) (0.102 g, 0.34 mmol) in anhydrous $CHCl_3$ (10 mL). The mixture was degassed and then heated to reflux for 12 h. At the end of the reaction, $CHCl_3$ was evaporated under vacuum and the residue was dissolved in minimum amount of dichloromethane and added to cold methanol to precipitate polymer **3** as a white solid (yield = 52%). M_n = 3600 Da, PDI = 1.36.

5.2.6. Film Preparation

A solution consisting of 50 mg polymer **3** was dissolved in 10 mL chloroform. The solution was filtered and spin-coated at 3000 rpm for 60 s onto a silicon substrate, yielding a thin film of polymer **1** (≈65 nm).

5.2.7. Nanoimprint Lithography (NIL)

Nanoimprinting of polymer **3** was performed by Rotello and coworkers using a Nanonex NX-2000 nanoimprintor at UMASS-Amherst with a patterned silicon mold that contained test patterns of various feature sizes. Imprinting was performed at 175 °C and a pressure of 400 psi for 5 min. A silicon NIL mold (line width 303 nm, period 606 nm, and groove depth 190 nm) from Lightsmyth Technologies was used in the cell patterning. Molds were primed with heptadecafluoro-1,1,2,2-(tetrahydrodecyl)dimethyl- chlorosilane before use at 75 °C for 48 hours in a vacuum chamber.

5.3. Results and Discussion

5.3.1. Synthesis and Characterization of Polymer

A set of polymers P1-P3 were synthesized with different feed ratio of FMMA-MMA-PEGMA (FMMA:MMA:PEGMA 4:1:0, 2:2:1, 4:4:1) using free radical polymerization to reach the proper hydrophobic-hydrophilic balance since this balance is crucial to achieve the noncovalent crosslinking to provide stability to the microstructure

obtained using nanoimprinting lithography (NIL) during their functionalization under aqueous conditions (Figure 5.4). Figure 5.5 shows the evolution of the ^{1}H-NMR spectra of copolymers P1 and P2, and Figure 5.6.a shows the H-NMR spectrum of copolymer P3. In the ^{1}H-NMR spectra of copolymers two types of vinylic protons are readily distinguishable at 6.51 and 5.23 ppm, originating from the bicylic moiety of the furan-maleimide cycloadduct.

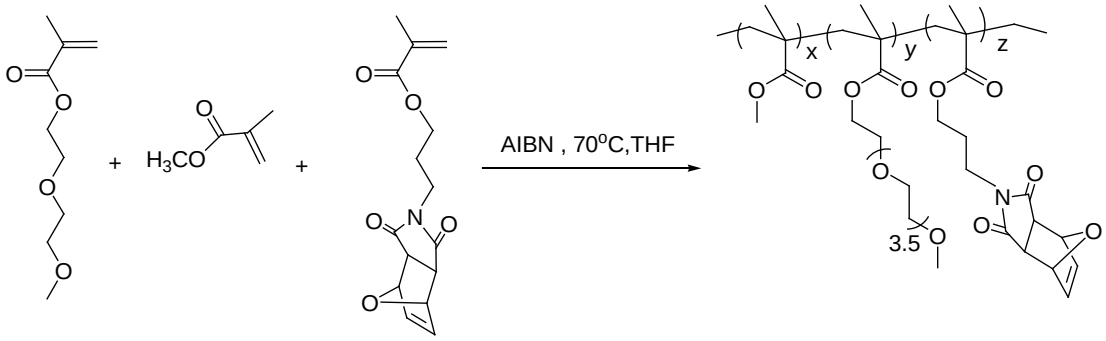

Figure 5.4. Copolymerization of monomers.

Some amount of PEG was desirable in the polymers to obtain proper wettability in aqueous media. Also polymers containing PEG produced better quality micropatterns. When the ratio between MMA and PEGMA was not suitable, the material became water soluble. Copolymer P3 possessed the most suitable composition (FMMA:MMA:PEGMA 4:4:1 feed ratio, M_n=3600, PDI=1.36) for obtaining good quality patterns that were stable due to non-covalent crosslinking. Since the NIL process is carried out at high temperature, we needed to be aware of the thermal stability of the polymer. Hence, we determined the furan loss temperature for furan-protected maleimide containing polymer **3** using thermogravimetric analysis to set the NIL conditions (Figure 5.6b). The first weight loss between 100 ^{o}C and 150 ^{o}C indicates loss of the furan protecting group due to the retro-Diels Alder reaction. In addition, we did not observe decomposition of the polymer below 200 ^{o}C. Hence it was decided that temperature below 200 ^{o}C would be appropriate to carry out the imprinting process with these copolymers. After establishing retro-DA conditions, thermal nanoimprinting lithography was performed at UMASS-Amherst by Rotello and co-worker at 175 ^{o}C under 400 PSI for 5 minutes onto a spin cast Polymer **3** film, resulting in a transfer of the mold pattern onto the Polymer **3** layer.

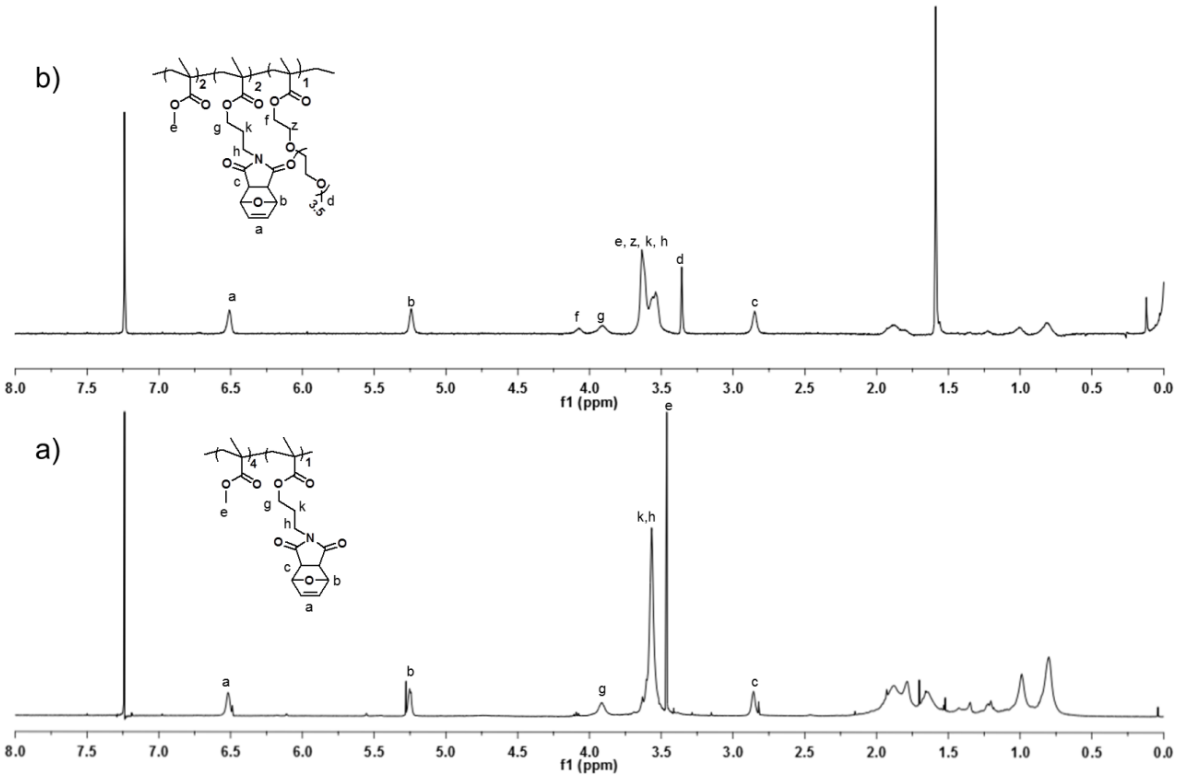

Figure 5.5. ^{1}H-NMR spectra of (a) MMA containing copolymer P1 and (b) PEGMA-MMA containing copolymer P2 in $CDCl_3$.

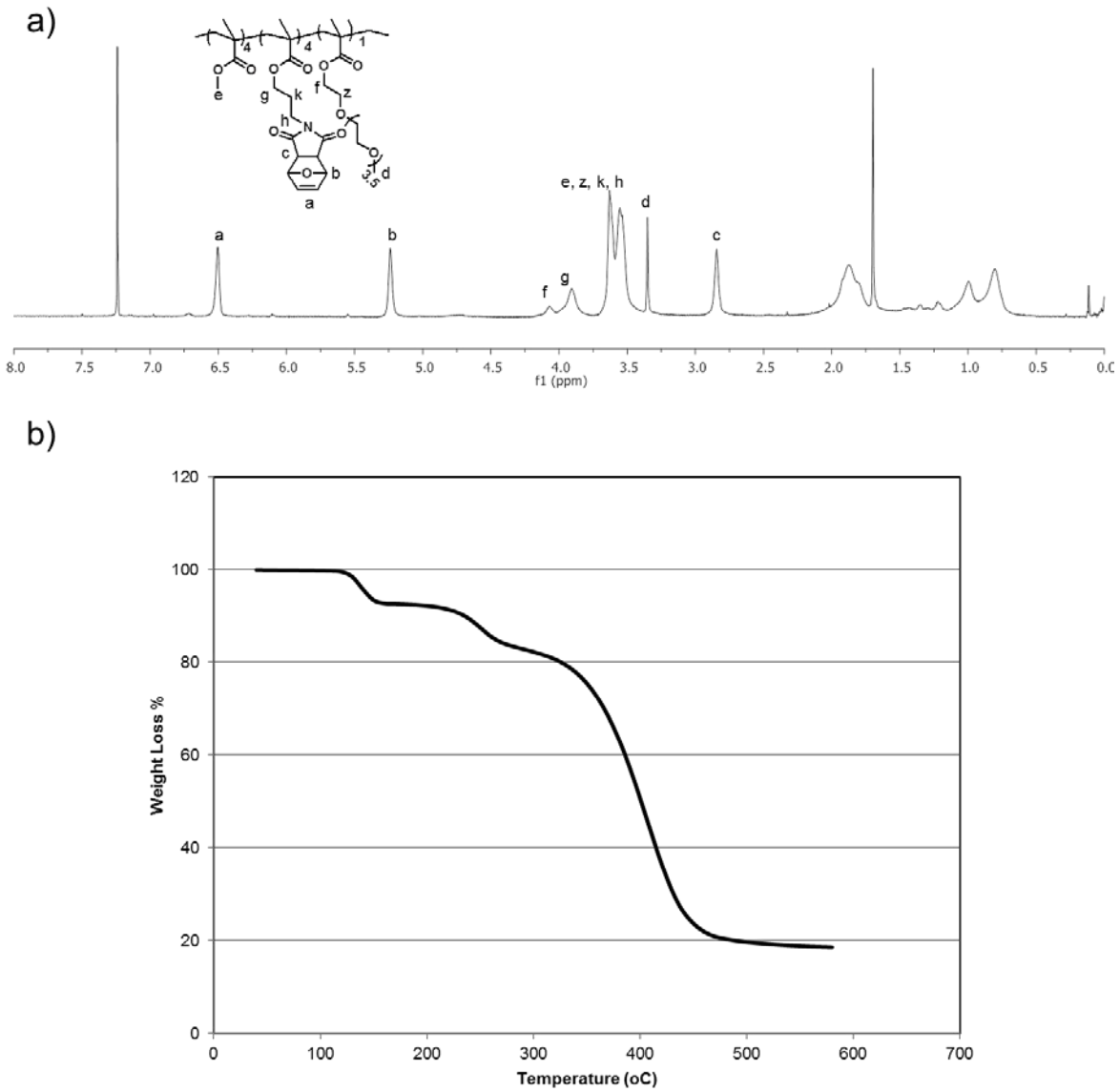

Figure 5.6. a) ^{1}H-NMR spectra and b) thermogravimetric analysis of P3.

5.3.2. Dye Immobilization on Thiol-Reactive Micropatterns

Surface functionalizations of thus obtained patterns were carried out by Rotello and co-workers to demonstrate the utility of these fabricated structures. To show the effectiveness in functionalization of the patterned surfaces containing maleimide functionality, the surfaces were reacted with a thiol containing fluorescent dye, BODIPY–SH via Michael type conjugation reaction (Figure 5.7a). Figure 5.7b shows the bright field

image of the imprinted surface, while Figure 5.7b (inset) and Figure 5.7c show the fluorescence images before and after conjugation of the green fluorescent dye BODIPY–SH, respectively. The bright green uniform fluorescence of the image proves the dye attachment on these micropatterns takes place in an efficient and homogenous manner (Figure 5.7c).

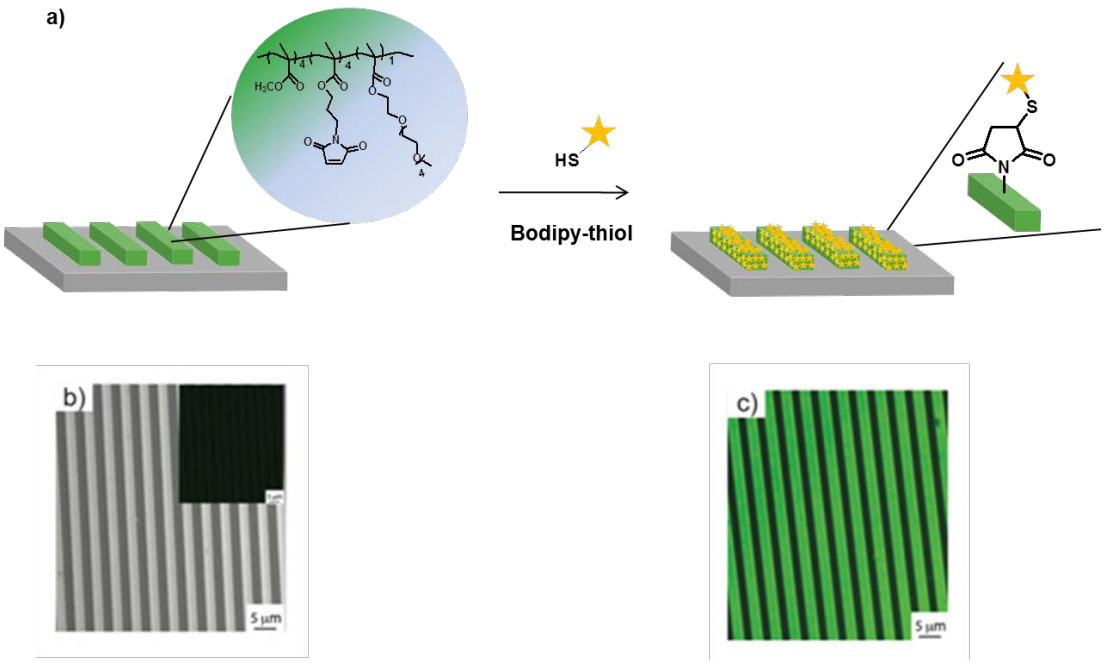

Figure 5.7. a) Schematic representation of BODIPY–SH attachment to the surface b) Bright field image. Inset in (b) shows the fluorescence image of the imprinted pattern before BODIPY–SH conjugation. c) Fluorescence image after BODIPY–SH conjugation.

5.3.3. Cellular Immobilization on Micro-Patterned Reactive Surface

Maleimide-functionalized patterns were also used to design materials to control interactions between cell and surface, which is an important requirement in tissue engineering since surface reliefs modulate cellular adhesion and their proliferation. It can be expected that adhesion of cells on a surface in a directional manner should be achievable by presenting biological cues like RGD containing peptides that have high binding affinity for the integrin receptors found on cell surface. Rotello and coworkers at

UMASS-Amherst utilized a surface coated with 300 nm micropatterns as template to obtain cell attachment. RGD containing peptide was attached onto the micropatterns via Michael addition (Figure 5.8). Cell culture experiments on this template showed that the attached cells were aligned along the direction of pattern (Figure 5.8c). Unpatterned surface with RGD immobilization did not show any preferred orientation in the attachment of cells (Figure 5.8b).

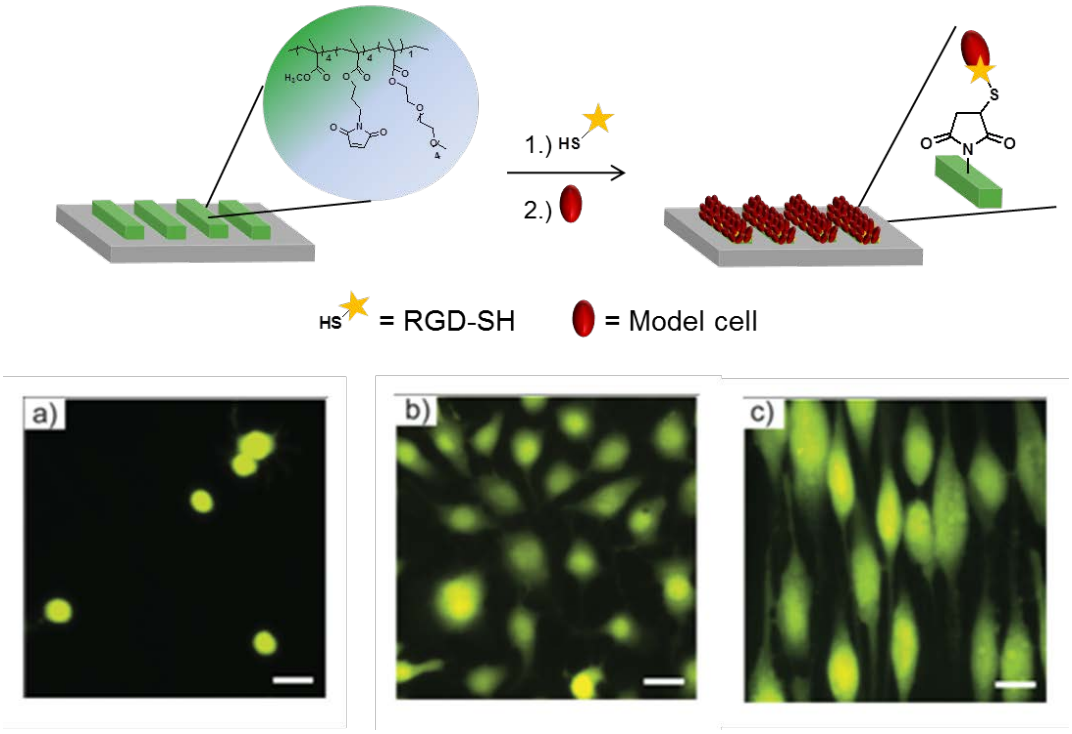

Figure 5.8. a) Schematic representation of RGD–SH attachment and cell alignment to the surface, a, b and c shows the Fluorescence microscopy images of cell cultured surfaces a) the unpatterned maleimide surface b) the RGD immobilized unpatterned surface, c) the RGD immobilized patterned surface.

5.4. Conclusion

A novel copolymer containing furan-protected maleimide side chains was synthesized using free radical polymerization. Comonomers like MMA and PEGMA were utilized to achieve the desired hydrophobic-hydrophilic balance. These copolymers were utilizing to obtain maleimide functional micropatterns using nano-imprinting lithography.

These microstructures were found useful for obtaining functional surfaces appended with fluorescent dyes, peptide ligands and cells.

6. FABRICATION OF PATTERNED HYDROGELS VIA THIOL-ENE CROSSLINKING

6.1 Introduction

Micro-patterned polymeric materials can be fabricated through either covalent or non-covalent crosslinking chemistries. In the aforementioned chapter we focused on fabrication of reactive polymeric micro-patterns that were stable in aqueous media by taking advantage of the non-covalent interactions between the predominantly hydrophobic domains of the parent polymers. However, achieving stable micro-patterns using non-covalent patterning method is not very versatile since a slight change in the hydrophobic-hydrophilic balance compromises the robustness of these structures due to the weaker physical interactions. Conversely, cross-linked structures obtained using covalent linkages are robust and can be used in harsh environments. Crosslinked polymeric materials can be obtained either by using a methodology that involves polymerization of monomers in the presence of a crosslinker, or through covalent crosslinking between polymers by addition of crosslinking agents. The later approach allows one to employ well-defined polymeric building blocks to obtain materials with superior homogeneity in their structure and chemical composition.

This chapter outlines a methodology to fabricate chemically crosslinked thiol-reactive hydrogels using the photochemical radical thiol-ene click reaction. The photochemically initiated radical reaction that enables the conjugation of thiols to alkenes allows one to take advantage of spatially controlled illumination to obtain crosslinking in desired locations. In other words, one can utilize photolithographic techniques to obtain microstructures from materials that can be crosslinked photochemically. Photolithography is a technique which utilizes light to create patterned structures from photosensitive materials on a substrate like glass, silicon, titanium [159]. In photolithography, first the substrate is spin-coated with a photosensitive polymer oftentimes referred to as a

photoresist. Then the photoresist is exposed to light through a photomask to promote photocrosslinking or degradation of the photoresist. The pattern is obtained after washing away the soluble part. Photolithography brings about the design of two-dimensional (2D) or three-dimensional (3D) substrates. Furthermore, encapsulation of biological materials such as cells can be done during the photolithographic process [160-161]. The feature size and resolution of the pattern depends on the diffraction of light which means smaller features can be obtained via shorter wavelengths like x-rays and electron beams [159, 162]. In recent years, creation of microstructures using photolithographic techniques has gained popularity since it has been observed that surface relief modulates biological interaction and this has been used to study and understand cellular adhesion and migration [163-164].

In particular, a furan-protected maleimide containing triblock copolymer is used to obtain an “orthogonally” functionalizable polymer that can be reacted with two different thiol-containing molecules. Subjecting the polymer containing the furan-protected maleimide side chains to varying duration of thermally promoted deprotection allows one to obtain copolymers containing a mixture of masked and unmasked maleimide functional groups. While the maleimide groups can be readily functionalized using Michael type conjugation reaction with thiol containing molecules, the furan-protected maleimide groups can be conjugated with thiols using a radical promoted thiol-ene reaction. Additionally, this orthogonal reactivity can be exploited to utilize one set of reactions for the fabrication of crosslinked material and employ the other reactive handle for intended functionalization of these materials. The thiol-ene reaction on the furan-protected maleimide containing side chain moiety locks these groups from participating in retro Diels-alder reaction. Subjecting a polymer to retro Diels-Alder reaction after the thiol-ene reaction, releases the residual masked maleimide groups that can be used for desired functionalization. A strategy based on sequential use of radical thiol-ene and nucleophilic thiol-ene was used for fabrication of functional micro-patterned surfaces (Figure 6.1).

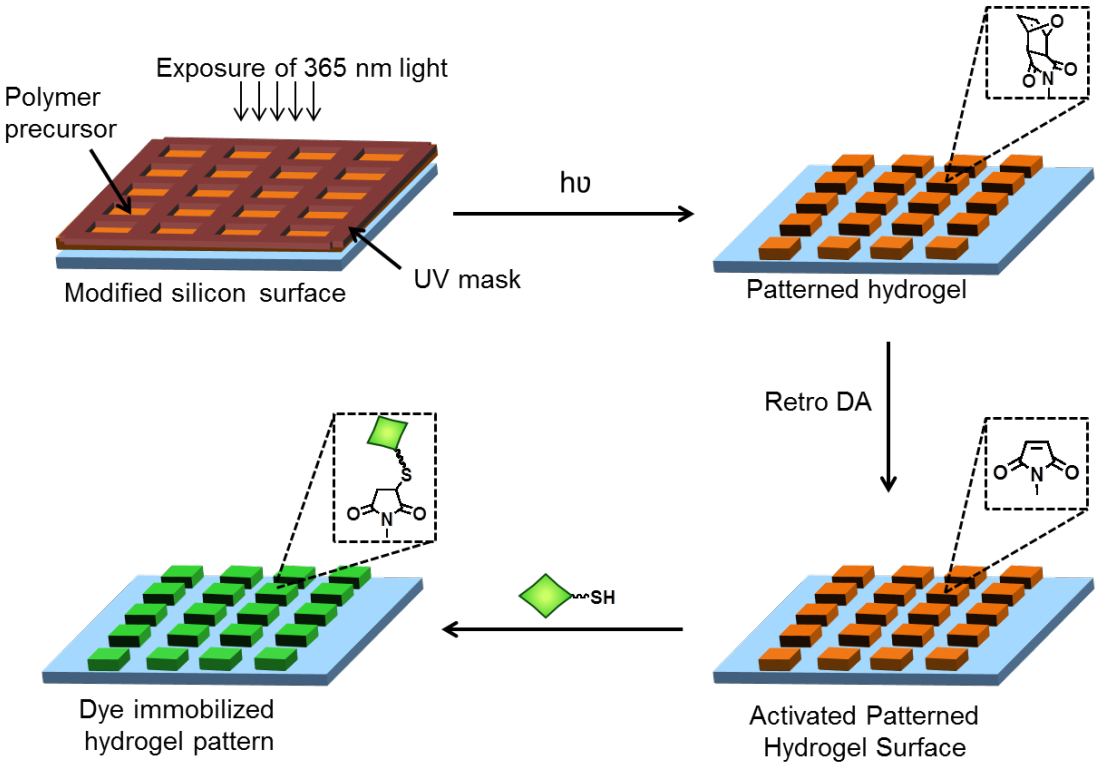

Figure 6.1. Fabrication and functionalization of micro-patterned hydrogels using radical thiol-ene and nucleophilic thiol-ene reactions.

6.2. Experimental

6.2.1. Materials

The furan-protected maleimidyl methacrylate (FMMA) monomer was synthesized according to a previous report [165]. Poly(ethylene glycol) methyl ether methacrylate (PEGMEMA, M_n = 300 Da) was purchased from Sigma Aldrich and purified by passing through activated aluminium oxide column prior to use. Poly(ethylene glycol) (PEG, M_n = 8 kDa), was purchased from Fluka. 3-(Trimethoxysilyl)propyl methacrylate (TMSMA), triethylamine (TEA), copper(I)bromide and 2,2'-bipyridyl were obtained from Sigma Aldrich, and 2-bromo-2-methylpropionyl bromide was obtained from Acros and used as received. Biotin-SH was obtained from Nanoscience Instruments. Qdot® 605 Streptavidin Conjugate was obtained from Sigma and used as received. 4,4-Difluoro-1,3,5,7-tetramethyl-8-[(10-mercapto)]-4-bora-3a,4a-diaza-*s*-indacene (BODIPY-SH) was synthesized according to the literature procedure[166]. Anhydrous solvents such as

dichloromethane (DCM), tetrahydrofuran (THF) and toluene were obtained from SciMatCo purification system and other solvents were dried over molecular sieves when necessary. Column chromatography was performed using silica gel 60 (43-60 nm, Merck). Thin layer chromatography was performed using silica gel plates (Kieselgel 60 F254, 0.2 mm, Merck). The plates were viewed under 254 nm UV lamp and/or developed by $KMnO_4$ stain. Blak-Ray® B-100 AP/R High Intensity 100 Watt/365 nm UV lamp is used for crosslinking process.

6.2.2. Characterization

^{1}H-NMR spectra were recorded with a Varian Mercury VX 400 MHz spectrometer, and referenced to $CDCl_3$ or $CDCl_2$. The weight and number average molecular weights (Mw and Mn) as well as the polydispersity index (PDI) were determined by gel permeation chromatography (GPC) using a Shimadzu GPC furnished with a PSS-SDV (length/ID 8×300 mm, 10 mm particle size) mixed-C column. Polystyrene standards (1-150 kDa) from Viscotek were used for calibration. Tetrahydrofuran (THF) was used as eluent at a flow rate of 1 m/min^{-1} at 30 ^{o}C. FT-IR spectra were recorded with a Thermo Fischer Scientific Inc. Nicolet 380 instrument (spectral range between 4000 and 450 cm^{-1}). The surfaces of films were studied with scanning electron microscopy (SEM). Scanning electron microscopy (SEM) micrographs were taken using Philips XL-30 instrument with an acceleration voltage of 10 kV. Chemical properties of patterned surfaces of quantum dot streptavidin biotin conjugates were also studied using X-ray electron spectroscopy (XPS). X-ray photoelectron spectra were obtained using Surface Science Instruments. The instrument was operated in a fixed analyzer transmission mode using a monochromatic Al *Kα* X-ray source. The pass energy of 150 Ev with a 400 μm spot size was used for survey spectra. Immobilization experiments to confirm the attachment of BODIPY-SH and Streptavidin conjugated quantum dot adsorption were determined using LD-A-Plan 20x/0.30 objective in Zeiss Axio Observer inverted microscope (ZEISS Fluorescence Microscopy, Carl Zeiss Canada Ltd, Canada). Zeiss Filter set 38 (Excitation BP 470/40, Emission BP 525/50) was used for imaging of BODIPY-SH attached hydrogel surface. For visualization of streptavidin conjugated quantum dot, filter set 43 (Excitation BP 545/25, Emission BP 605/70) was used. Images were processed using Zeiss AxioVision software.

6.2.3. Synthesis of PEG ATRP Macroinitiator

A solution of HO-PEG-OH (M_n=8000, 4 g, 0.502 mmol) was dissolved in toluene and dried azeotropically using toluene rotary evaporation, followed by drying under vacuum. The polymer HO-PEG-OH and triethylamine (0.15mL, 1.06 mmol) was dissolved in anhydrous methylene chloride (30 mL) and the flask was in an ice-water bath. Then, 2-bromoisobutyryl bromide (0.62 mL, 5.02 mmol) was slowly added to the reaction mixture. The solution was warmed to room temperature and stirred for 24 h. The organic solvent was removed under reduced pressure. The crude product was dissolved in methylene chloride (250 mL) and washed with saturated $NaHCO_3$ solution (250 mL) three times. The combined organic layers were dried over anhydrous Na_2SO_4 and concentrated in vacuum. The crude product was dissolved in a minimum amount of methylene chloride and then precipitated in cold diethyl ether. The precipitate was recovered by simple filtration to yield the desired polymer as a white powder (yield = 85%). ^{1}H NMR (δ, ppm, $CDCI_3$) 4.32-4.29 (4H, m, -COO-*CH_2*-), 3.81-3.78 (4H, m, -COO-CH_2-*CH_2*-), 3.73-3.71 (4H, m, -COO-CH_2CH_2O-*CH_2*), 3.66-3.59(712H, br s, -CH_2CH_2O-), 3.45-3.43 (4H, m, -CH_2CH_2O-), 1.92 (12H, s, -CH_3-C-COO-).

6.2.4. Polymerization of Triblock Copolymer (P1)

In a 10 mL flask, the PEG macroinitiator (Br−PEG−Br) [M_n=8300 Da] (0.100 g, 0.01 mmol), FuMa-MA monomer (0.075 g, 0.26 mmol) and PEGMEMA [M_n=300 Da] (0.231 g, 0.77 mmol) were dissolved in a mixture of MeOH (1.8 mL) and H_2O (0.2 mL). The flask was sealed with a rubber septum and thoroughly degassed under nitrogen purge. Polymerization was started after addition of a solution of 2, 2'-bipyridine (0.049 g, 0.31 mmol) and Cu(I)Br (0.022 g, 0.11 mmol) dissolved in MeOH (0.6 mL) and the polymerization was carried out at room temperature for 2 hours. After the polymerization, the reaction mixture was precipitated into cold diethyl ether (100 mL). The viscous liquid obtained after discarding the diethyl ether layer was diluted with DCM and passed over a column of basic alumina to remove the catalyst. After evaporating the organic solvent, the residue was dried under vacuum at room temperature (yield 50%). M_n=23 kDa, PDI=1.2, ^{1}H NMR (δ, ppm, $CDCl_3$) 6.51 (s, 2H, *CH=CH* protected), 5.23 (s, 2H, *CH* bridgehead protons), 4.32-4.01 (m, 6H, -COO-*CH_2*-), 3.91-3.78 (m, 6H, -COO-CH_2-*CH_2*-), 3.66-3.54, (712+14H, br s, -*CH_2CH_2*O-), 3.45-3.43 (4H, m, -CH_2C*H_2*O-), 3.35 (s, 3H,

O-*CH3*), 2.86 (s, 2H,*CH-CH*, bridge protons), 1.91–0.84 (m, 7H,$NCH_2CH_2CH_2O$, CH_2 and CH_3 along polymer backbone.

6.2.5. Partial Activation of A–B–A Triblock Copolymer (P2)

Triblock copolymer P1 (25 mg, 0.001 mmol) was partially activated at 100 °C for 50 min in toluene (10 mL) to give partially activated copolymer P2. Copolymer P2 was precipitated in cold diethyl ether (yield = 92%). ^{1}H NMR (δ, ppm, $CDCl_2$) 6.76 (s, 2H, *CH=CH* deprotected), 6.51 (s, 2H, *CH=CH* protected), 5.23 (s, 2H, CH bridgehead protons), 4.32-4.01 (m, 8H, -COO-CH_2-), 3.91-3.78 (m, 8H, -COO-CH_2-CH_2-), 3.66-3.54, (br s, 712+14H, -CH_2CH_2O-), 3.45-3.43 (m, 4H, -CH_2CH_2O-), 3.35 (s, 3H, O-CH_3), 2.86 (s, 2H, CH-CH, bridge protons), 1.91–0.84 (m, 7H,$NCH_2CH_2CH_2O$, CH_2 and CH_3 along polymer backbone.

6.2.6. Functionalization of Deprotected Maleimide Side Chains (P3)

Benzyl mercaptan **(**4.8 mg, 0.039 mmol) and copolymer P2 (23 mg, 0.001 mmol) was dissolved in THF (l mL) and stirred for 20 hours at room temperature. Copolymer P3 was precipitated in cold diethyl ether (yield = 94%). ^{1}H NMR (δ, ppm, $CDCl_2$) 7.32-7.14 (m, 5H, Ar-) 6.51 (s, 2H, CH=CH protected), 5.23 (s, 2H, CH bridgehead protons), 4.32-4.01 (8H, m, -COO-CH_2-), 3.91-3.78 (m, 8H, -COO-CH_2-CH_2-), 3.66-3.54, (br s, 712+14H, -CH_2CH_2O-), 3.45-3.43 (m, 4H, -CH_2CH_2O-), 3.35 (s, 3H, O-CH3), 3.00-2.89 (br s, 2H, Ar-*CH2*-S-) 2.86 (s, 2H,CH-CH, bridge protons), 1.91–0.84 (m, 7H,$NCH_2CH_2CH_2O$, CH_2 and CH_3 along polymer backbone.

6.2.7. Functionalization of Protected Maleimide Side Chains (P4)

Copolymer P3 (7.5 mg, 0.00036 mmol) and DMPA (1 mg, 0.0039 mmol) was dissolved in 0.3 mL THF. Thioglycerol (0.509 mg, 0.0047 mmol) was added to the solution. Finally, solution was subjected to 365 nm UV exposure for 7 hours. The resulting polymer was precipitated in cold diethyl ether. (yield: 85%). ^{1}H NMR (δ, ppm, $CDCl_2$) 7.32-7.14 (m, 5H, Ar-), 4.76 (br s, 1H, -OH), 4.70 (br s, 1H, -OH) 4.32-4.01 (8H, m, -COO-CH_2-), 3.91-3.78 (m, 8H, -COO-CH_2-CH_2-), 3.66-3.54, (br s, 712+14H, -CH_2CH_2O-), 3.45-3.43 (4H, m, -CH_2CH_2O-), 3.35 (s, 3H, O-CH_3), 3.00-2.89 (br s, 2H, Ar-

CH_2-S-), 2.89-2.81 (br s, 2H, *CH_2*-S-), 2.81-2.65 (br s, 2H,CH-CH, bridge protons), 1.91–0.84 (m, 7H,$NCH_2CH_2CH_2O$, CH_2 and CH_3 along polymer backbone.

6.2.8. Modification of Glass and Silicon Wafer for Hydrogel Adhesion

TMSMA was used for modification of silicon wafer to promote the covalent adhesion between the surface and the hydrogel. Silicon wafers were first treated with nonchromix acid solution (0.5 g / 20 mL nonchromix / H_2SO_4) for 1 hour to remove the native oxides, organic impurities and metallic contaminants, rinsed with deionized water, and then sonicated in acetone and isopropyl alcohol respectively and blown dry using stream of nitrogen. TMSMA was dissolved in anhydrous toluene (1 wt % solution) and clean surfaces were incubated in this solution under nitrogen atmosphere overnight. The modified wafer was washed several times in toluene and methanol and then dried under vacuum.

6.2.9. Fabrication of Hydrogel Pattern 1 (H1)

Copolymer P1 (11 mg, 0.00049 mmol) was mixed with 2,2′-(ethylenedioxy)diethanethiol (0.278 mg, 0.0033 mmol) and DMPA (0.846 mg, 0.0033 mmol) to prepare a 10 wt% polymer solution in EtOH/H_2O (10:1). Selective photo patterning was performed through a photomask. For this aim, dried glass substrate was coated with polymer solution by spin coating at 500 rpm for 10 s and 2000 rpm for 30 s. The prepared polymer films were lithographically patterned by selective 365 nm UV exposure through a photo mask for 10 minutes, then washed with THF and dried under nitrogen.

6.2.10. Fabrication of Hydrogel Pattern 2 (H2)

Copolymer P1 (3 mg, 0.00014 mmol) was mixed with 2,2′-(ethylenedioxy)diethanethiol (0.046 mg, $0.25x10^{-3}$ mmol) and DMPA (0.013 mg, $5x10^{-5}$ mmol) to prepare a 10 wt% polymer solution in EtOH/H_2O (10:1). Selective photo patterning was performed through a photomask. For this aim, dried glass substrates were coated with polymer solution by spin coating at 500 rpm for 10 s and 2000 rpm for 30 s.

The prepared polymer films were lithographically patterned by selective 365 nm UV exposure through a photo mask for 5 minutes, then washed with THF and dried under nitrogen.

6.2.11. Fabrication of Hydrogel Pattern 3 (H3)

Copolymer P1 (3 mg, $1.4x10^{-4}$ mmol) was mixed with 2,2′-(ethylenedioxy)diethanethiol (0.069 mg, 0.00038 mmol) and DMPA (0.019 mg, 0.00008 mmol) to prepare a 10 wt% polymer solution in EtOH/H_2O (10:1). Selective photo patterning was performed through a photomask. For this aim, dried silicon wafer substrates were coated with polymer solution by spin coating at 500 rpm for 10 s and 2000 rpm for 30 s. The prepared polymer films were lithographically patterned by selective 365 nm UV exposure through a photo mask for 5 minutes, then washed with THF and dried under nitrogen.

6.2.12. Activation of Hydrogel Patterns

To activate hydrogel pattern through retro Diels-Alder reaction, patterned hydrogel surfaces were put in a vacuum oven under 100 ^{o}C for 30 min. This furnished surfaces with micro-patterned hydrogels containing thiol reactive maleimide groups.

6.2.13. Dye Immobilization of Hydrogel Patterns

A solution of BODIPY-SH in THF (1 mg/mL) was prepared. Then, maleimide group containing hydrogel surfaces were incubated with the BODIPY-SH solution. After 18 hours, patterned surface was washed with THF to remove unbound dye molecules.

6.2.14. Bioimmobilization of Hydrogel Patterns

A solution of Biotin-SH in MeOH (1 mg/mL) was prepared and dropped onto a dried hydrogel pattern 1. After 45 min, the sample was washed with MeOH several times and dried. A solution of Qdot® 605 Streptavidin Conjugate (20 μL, 0.5 mM in H_2O) was dropped on the biotinylated patterned surface. The pattern was placed a dark place for 45 min, and then gently rinsed with copious amounts of water.

6.3. Results and Discussion

6.3.1. Synthesis Activation and Functionalization of ABA Type Polymer

ABA-type triblock copolymer containing a linear PEG-based polymer as the middle block was synthesized using ATRP. To obtain this copolymer, FMMA monomer (2) synthesized according the published procedure [165], was polymerized with PEGMEMA (1) using the PEG macroinitiator (3) using ATRP. After the polymerization step, partial activation of the maleimide groups through retro Diels-Alder reaction was used to obtain the orthogonally reactive copolymer P2 (Figure 6.2).

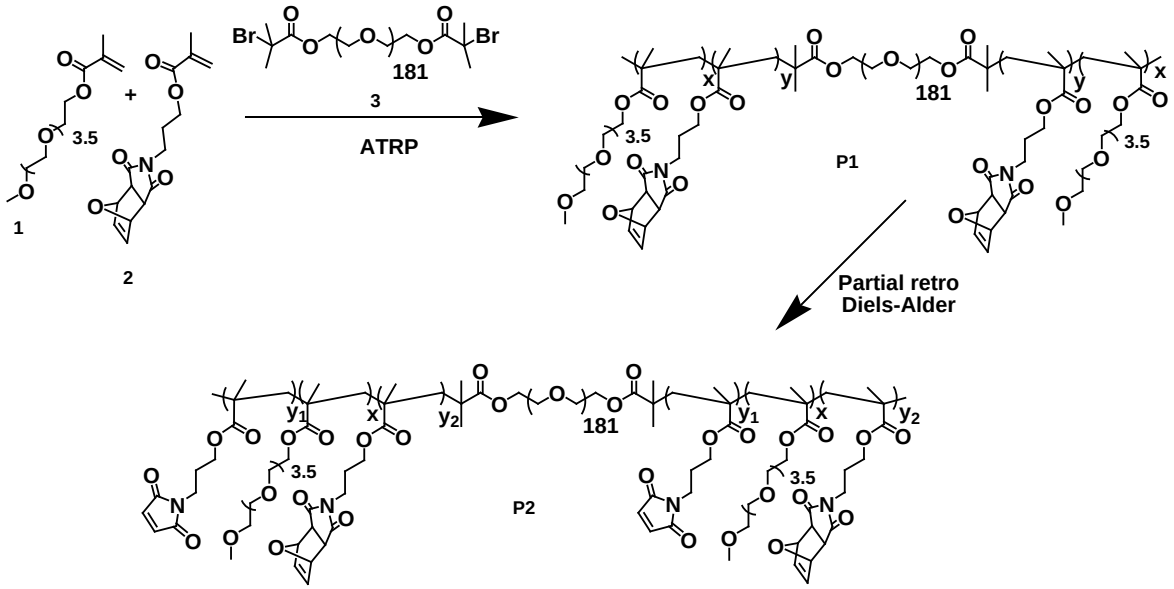

Figure 6.2. Overall reaction scheme for the synthesis of orthogonally reactive copolymer.

Retro Diels-Alder reaction of the copolymer P2 was investigated at 100° C in toluene to determine extent of cycloreversion with reaction time using ^{1}H-NMR spectroscopy. Figure 6.3 shows the evolution of the ^{1}H-NMR spectrum at t_0, 30 min, 1 h, 2 h, and 8 h.

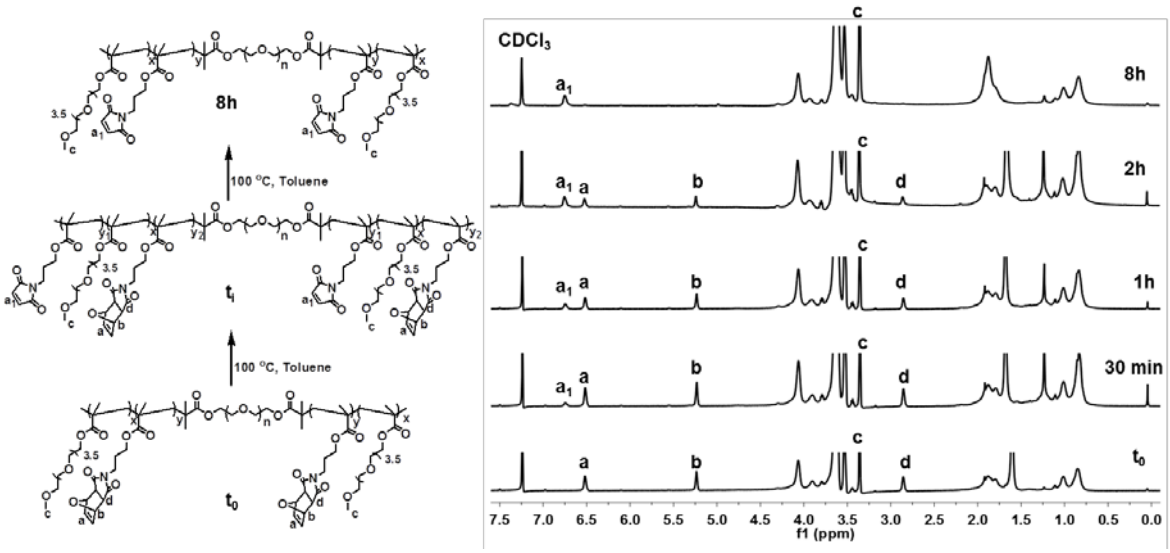

Figure 6.3. ^{1}H-NMR spectra (400 MHz, CDCI3) of furan-protected maleimide containing t_0, maleimide functionalized at different temperature intervals (t_i) after 30 min, 1 h, 2h partial retro Diels-Alder deprotection of the maleimide groups and completion of retro Diels-Alder.

Variation in functional group composition can be followed from Figure 1. In the ^{1}H-NMR spectrum of copolymer P1 before partial activation step (time $t_{o)}$, two types of vinylic protons are readily distinguishable at 6.51 and 5.23 ppm, originating from the bicylic moiety of the furan-maleimide cycloadduct. During the cycloreversion, appearance of a new proton resonance at 6.76 ppm and decrease of peak intensities of propton resonances at 6.51 and 5.23 ppm indicates the partial cycloreversion via the retro Diels-Alder reaction. By using the integrals of peaks from the vinylic protons a and b on bicyclic moiety and the proton a_1 on maleimide, ratio of protected and unmasked maleimide group can be calculated. It was observed that 18 % of the cycloadduct was converted to maleimide in 30 minutes. A conversion of 36 % and 56 % was observed in 60 min and 120 minutes respectively. After 8 hours, it was found that complete cycloreversion of all pendant side chains had taken place.

Interestingly, the slight change in molecular weight of the copolymer due to the loss of furan units was also witnessed in the GPC analyses of the copolymers (Figure 6.4). Additionaly in the FTIR spectra of the copolymers, the appearance and then an increase of the absorption band intensity at 696 cm^{-1} indicates the occurrence of retro Diels-Alder

reaction that results in the C=C-H stretching due the maleimide group that is produced through the cleavage of furan ring at 100° C. Similar observations using FTIR has been observed by others during the loss of furan group from the cycloadduct [167].

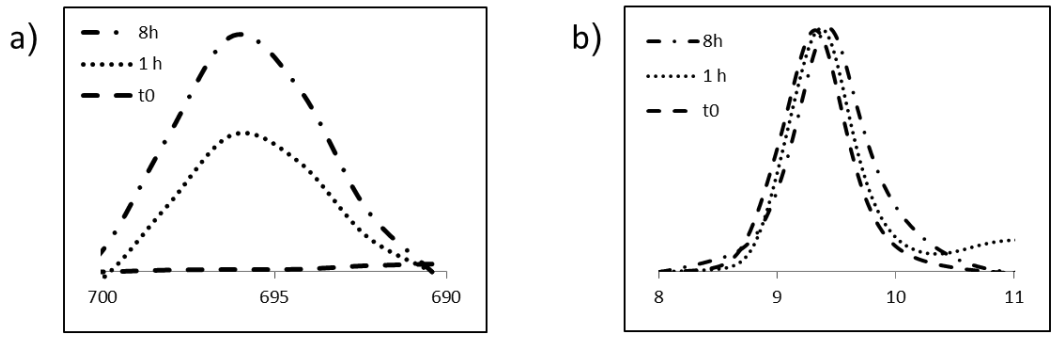

Figure 6.4. a) Enlarged FT-IR spectra of C=C-H stretching: P1 (t0) after 1 hour and 8 hours at 100 oC. b) GPC Spectra of copolymer P1 at before and after heating for 1 hour and 8 hour.

To show the orthogonal functionalization, we utilized the triblock copolymer P1 which is soluble in organic solvents and water, and can be analysed with conventional analysis techniques such as ^{1}H-NMR and GPC. Copolymer P2 was obtained by partial retro Diels-Alder reaction where 29 % of cycloadduct had reversed to maleimide functionality after 50 minutes via retro-DA reaction as inferred from ^{1}H-NMR spectrum (Figure 6.5). Then, copolymer P2 was functionalized with benzyl mercaptan via Michael-type conjugate addition to the maleimide units. Analysis of ^{1}H-NMR spectrum of thus obtained copolymer P3 shows the disappearance of the peak $\boldsymbol{a_1}$ at 6.76 ppm which belongs to vinylic protons on the maleimide and appearance of the new peak ***e*** between 7.32-7.14 ppm from aromatic proton resonances from the newly incorporated benzyl group (Figure 6.5). Then UV-initiated thiol-ene chemistry was utilized for functionalization of furan-protected maleimide-containing units by using thioglycerol as a model reactant, in the presence of 2,2-dimethoxy-2-phenylacetophenone (DMPA) as a photoinitiator under UV irradiation (λ_{ex} = 365 nm). Analysis of thus modified copolymer P4, showed the disappearance of the peak ***a*** at 6.51 ppm, and appearance of proton resonance ***h*** from CH_2-S in benzylmercaptan indicates successful thiol-ene addition. Furthermore, appearance of

new proton resonances **f, g** due to the hydrogens of –OH groups, and resonance **i** due from the proton adjacent to the sulphur atom (CH_2-S) proved successful addition of thioglycerol via radical mediated thiol-ene click reaction (Figure 6.5).

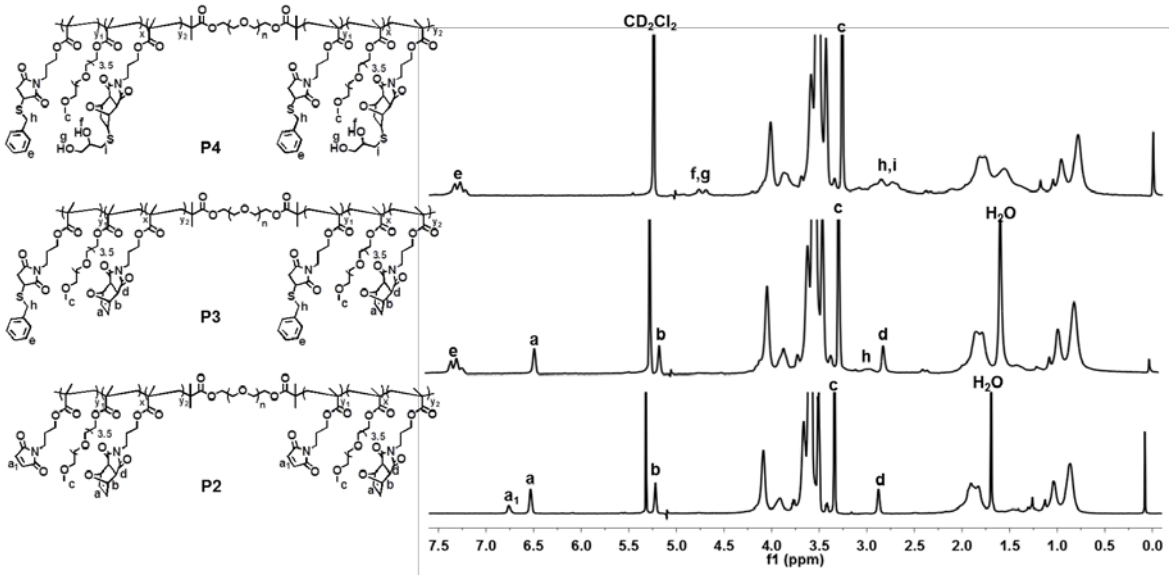

Figure 6.5. ^{1}H-NMR spectra (400 MHz, CD_2CI_2) of the product after partial retro Diels-Alder reaction (P2), the product after the Michael-Addition reaction of benzyl mercaptan to deprotected maleimide groups (P3), and the product after thiol-ene coupling with thioglycerol (P4).

6.3.2. Preparation of Patterned Hydrogels

The presented strategy was used for preparation of patterned surfaces and subsequent immobilization of ligands which were summarized in Figure 6.1 Copolymers containing furan-protected maleimides groups can be directly photo-patterned using thiol-containing crosslinkers. In this work, we used triblock copolymer P1, along with 2, 2′-(ethylenedioxy)diethanethiol as a crosslinker and DMPA as a photoinitiator to obtain hydrogel micro-patterns via photo-crosslinking. The mixture of the copolymer, DMPA and the crosslinker is spin coated onto a glass or silicon wafer modified with TMSA to promote surface adhesion of the hydrogel patterns. The spin cast film behaves like a negative resist. Exposure to UV irradiation though a photomask causes the exposed areas of the polymer film to become crosslinked (Figure 6.6). Therefore, the crosslinked part remains on the

surface wherever it is exposed and the patterns are developed by washing away the unreacted polymer in the masked areas with THF solution. Thus, the inverse image of the photomask is transferred to the substrate. Figure 6.6.a shows the optical image and Figure 6.6.b shows the SEM image of a typical hydrogel pattern obtained using this protocol. We were also able to produce hydrogel patterns using different ratio of alkene to thiol crosslinker. This allows preparation of hydrogels that contain excess of one of the reactive functional groups. For example, usage of excess thiol groups compared to available furan-protected maleimide units results in hydrogels containing excess thiol groups. These can be used as reactive groups for further functionalization. Most of the studies outlined here utilises less amount of thiol groups so that the hydrogel is abundant in masked maleimide group. This will result in generation of thiol-reactive maleimide containing hydrogels.

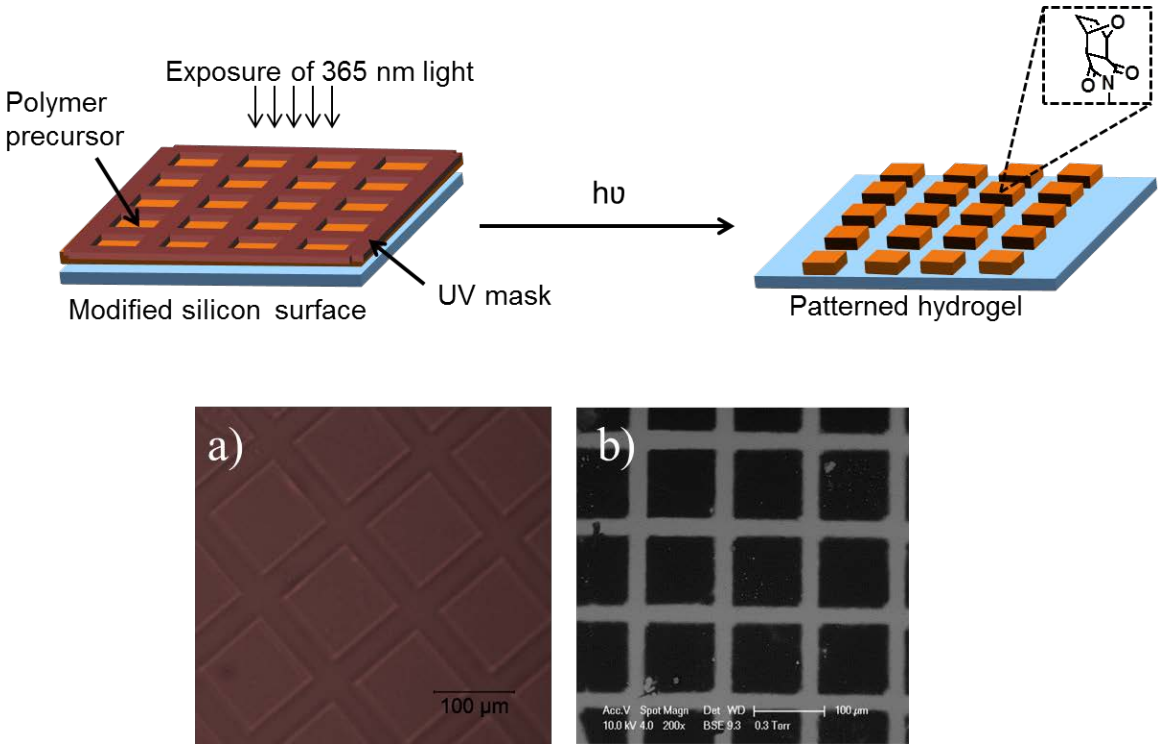

Figure 6.6. Schematic illustration of preparation of patterned hydrogel surface. (a) Optical microscopy image of patterned surface. (b) Scanning Electron Microscopy image for the patterned surface H1.

6.3.3. Functionalization of Reactive Hydrogel Micropatterns

6.3.3.1. Dye Immobilization onto hydrogel pattern. To develop a platform technology for thiol reactive hydrogel patterning, we deprotected the maleimide groups and created surfaces coated with reactive maleimide containing hydrogels by heating the surface at 100 ^{o}C for 30 min. In order to demonstrate successful functionalization of these hydrogels, dye and biomolecule immobilization experiments are performed on micropatterns formulated using a 3:1 stoichiometry of the maleimide:thiol functional groups during crosslinking. For dye immobilization experiments BODIPY-SH was used as a fluorescent probe as it is highly photostable. Fluorescence microscopy image of dye modified hydrogel pattern shows the expected bright green fluorescence (Figure 6.7a). The pattern possesses high degree of homogeneity and this proves that the hydrogels are quite robust and survive the thermal cycloreversion without film detachment from the surface. As a control experiment, surface containing hydrogel micropatterns that were not subjected to the retro Diels-Alder reaction were incubated in the dye containing solution. Fluorescence microscopy analysis of surfaces after washing with solvents did not reveal any fluorescence (Figure 6.7b). This is expected since no dye attachment is possible in absence of the maleimide groups.

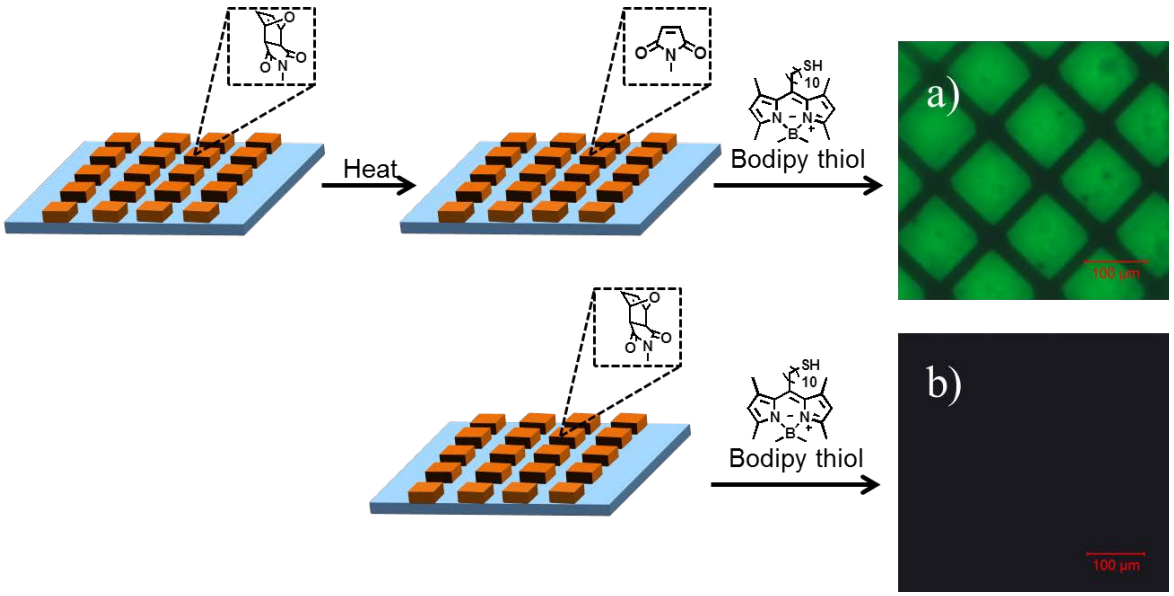

Figure 6.7. Fluorescence images of patterned PEG hydrogel (H2) (a) postfunctionalized by BODIPY-SH. (b) control: functionalization without heating.

6.3.3.2. Biomolecular Immobilization on Micro-patterned Hydrogels. We also envisioned that the maleimide surfaces can be modified with biotin units for biomolecular immobilization. Streptavidin has four binding sites for the high-affinity ligand biotin, and thus can be employed as an adaptor molecule between a biotinylated surface and other biotinylated molecules. For biomolecule attachment; biotin-SH was immobilized to the maleimide containing hydrogels via Michael addition. Then, streptavidin conjugated quantum dots (QD) were bound to biotinylated surface via non-covalent interactions. Investigation with fluorescence microscopy shows the streptavidin conjugated quantum dots were attached to the patterned surface (Figure 6.8). The high fluorescence of QDs is used to facilitate the investigation of interaction between the proteins and biotin ligand.

Biotin immobilization was also confirmed by examining the surfaces using XPS. The surface after attachment of biotin was shown to contain more nitrogen and carbon according to the XPS results. The immobilization of quantum dot conjugates via biotin-streptavidin interaction was confirmed from XPS spectra of Cd (3d), Zn (2p). Peaks at binding energy of Zn (2p) 1020 ev, Cd (3d 3/2) 410 eV, Cd (3d 5/2) 402.2 were clearly present (Figure 6.9). The survey spectra of different samples before and after immobilization of quantum dots clearly proves the attachment of streptavidin conjugated CdSe and ZnS quantum dots onto the surface (Figure 6.9). Additionally, to prove that conjugation of quantum dots was indeed via the specific biotin-streptavidin interaction, a control experiment was carried out. As a control experiment, non-biotinylated patterned hydrogel surfaces were treated with quantum dots. Upon analysis using fluorescence microscopy, a remarkable difference in fluorescence intensity between the control and biotinylated surface was observed. This shows the effective role played by the biotin ligand that was attached using the maleimide groups as functionalization units.

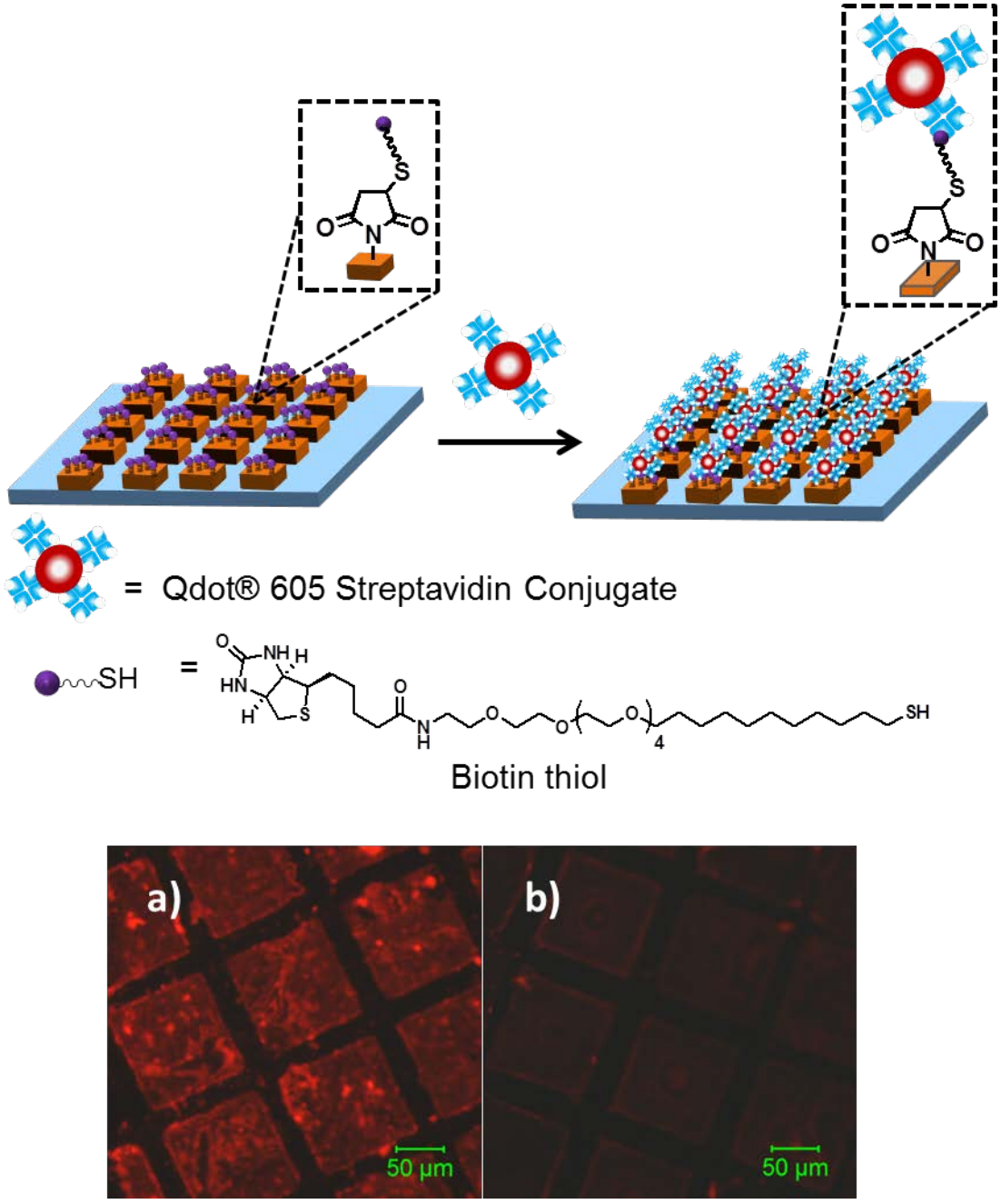

Figure 6.8. Conceptual scheme showing the attachment of streptavidin conjugate QDs to the biotinylated pattern (H3). (a) Fluorescence micrograph of a mixture of CdSe/ZnS QD-tagged streptavidin-biotin surface. (b) Control experiment: Fluorescence micrograph of a mixture of CdSe/ZnS QD-tagged streptavidin surface without biotinylation.

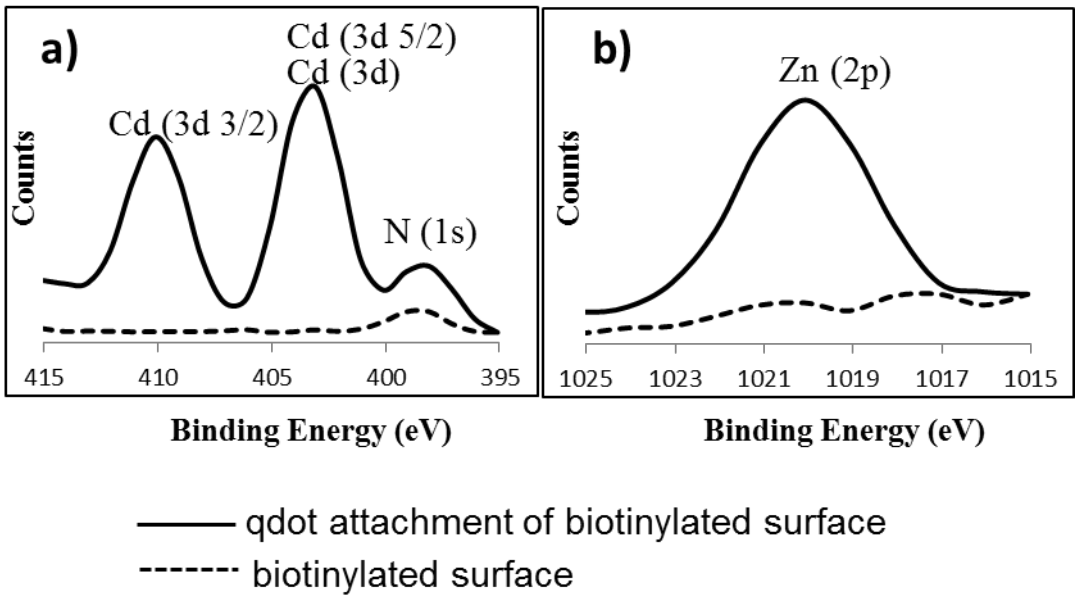

Figure 6.9. XPS Spectra of pattern H3 (a) Binding energy of Cd and N of biotinylated surface and after attachment of streptavidin conjugated QDS. (b) Binding energy of Zn of biotinylated surface and after attachment of streptavidin conjugated QDS.

6.4. Conclusion

Orthogonally functionalizable polymers were obtained from a single polymeric precursor using controlled deprotection of pendant furan-protected maleimide groups. A triblock copolymer and. The concept was further extended to fabricate micro-patterned hydrogel containing surfaces using the photochemical thiol-ene chemistry. UV crosslinking of furan protected maleimide groups on the copolymers using a dithiol based crosslinker was used to obtain gelation. Thereafter, residual furan-protected maleimide groups became available for further functionalization after their deprotection to thiol-reactive maleimide groups using the retro Diels-Alder reaction. These reactive hydrogel patterns were utilized for conjugation of dye molecules and biomolecular immobilizations. A fluorescent dye, BODIPY-SH was used as a model system to demonstrate effective attachment of dye onto hydrogels through Michael addition reaction. To demonstrate the protein immobilization, maleimide functional surfaces were first modified with biotin-SH. Then, the biotin groups were used for binding with streptavidin conjugated QDs. Overall, this approach provides a simple and powerful new strategy for the fabrication of micro-patterned reactive hydrogel arrays.

7. PATTERNED HYDROGELS VIA PHOTODIMERIZATION OF MALEIMIDE CONTAINING COPOLYMERS

7.1. Introduction

Photo-crosslinkable systems have been extensively investigated in fabrication of hydrogels due to the formation of densely crosslinked networks in a rapid fashion with spatial and temporal control. Crosslinking via photo-dimerization of pendant side chains along a polymeric backbone yields hydrogels with defined crosslinking junctions. Oftentimes, taking advantage of the reversible nature of the dimerization process, photo-responsive materials can be created. Among the various available photodimerizable groups, coumarins, cinnamic acids, anthracenes and maleimides are attractive candidates since they do not require additional photoinitiators. Photoinitiator-free systems are advantageous since both the photoinitiator and photoinitaitor-based side products can result in undesirable characteristics such as colour and odour in the final product. As explained in the introductory section, maleimides are attractive functional groups since they can not only introduce the desired crosslinking but also can be used as handles for subsequent functionalization of the material. Maleimides are known to give dimers containing a fused cyclobutane ring upon UV irradiation (Figure 7.1) [168-169]. In addition, residual maleimide groups can participate in both Diels-Alder and Michael-type addition reactions. Both of these reactions provide efficient handles to introduce various functional molecules into these materials.

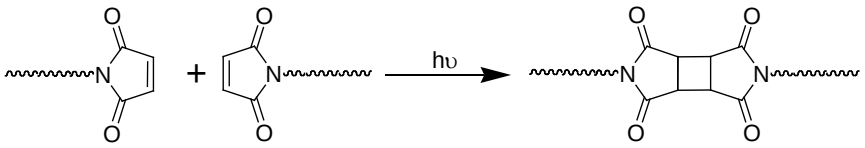

Figure 7.1. [2+2] photodimerization of maleimide groups.

As mentioned in Chapter 4, hydrogels are at the heart of many areas of research in biomaterial sciences such as tissue engineering since these materials can be tuned to exhibit properties similar to the natural materials like tissues [150]. Functionalization of these materials with biological cues is necessary to imitate the extracellular matrix. Patterning of polymeric scaffold materials is an emerging area since apart of applications

like biosensor arrays, cell growth, attachment and proliferation is affected by surface relief of these materials.

Herein, we utilized photo-dimerization of maleimide functional groups as a tool to develop novel PEG-based photoinitiator-free hydrogel systems (Figure 7.2). Maleimide containing ABA type triblock copolymers were synthesized and used as precursors for formation of functionalizable hydrogel. Thereafter, the gelation system was extended to design patterned hydrogel surfaces via photo-cycloaddition in thin films. Photolithography was used to obtain micro-patterned hydrogel structures on glass and Si/SiO_2 substrates. Functionalization of thus obtained reactive surfaces was studied to demonstrate their utility in biomolecular immobilization. Thiol and furan containing fluorescent dyes were used towards the derivatization of residual maleimide functional groups in the hydrogels via the Michael type conjugate addition and the Diels-Alder cycloaddition reaction respectively.

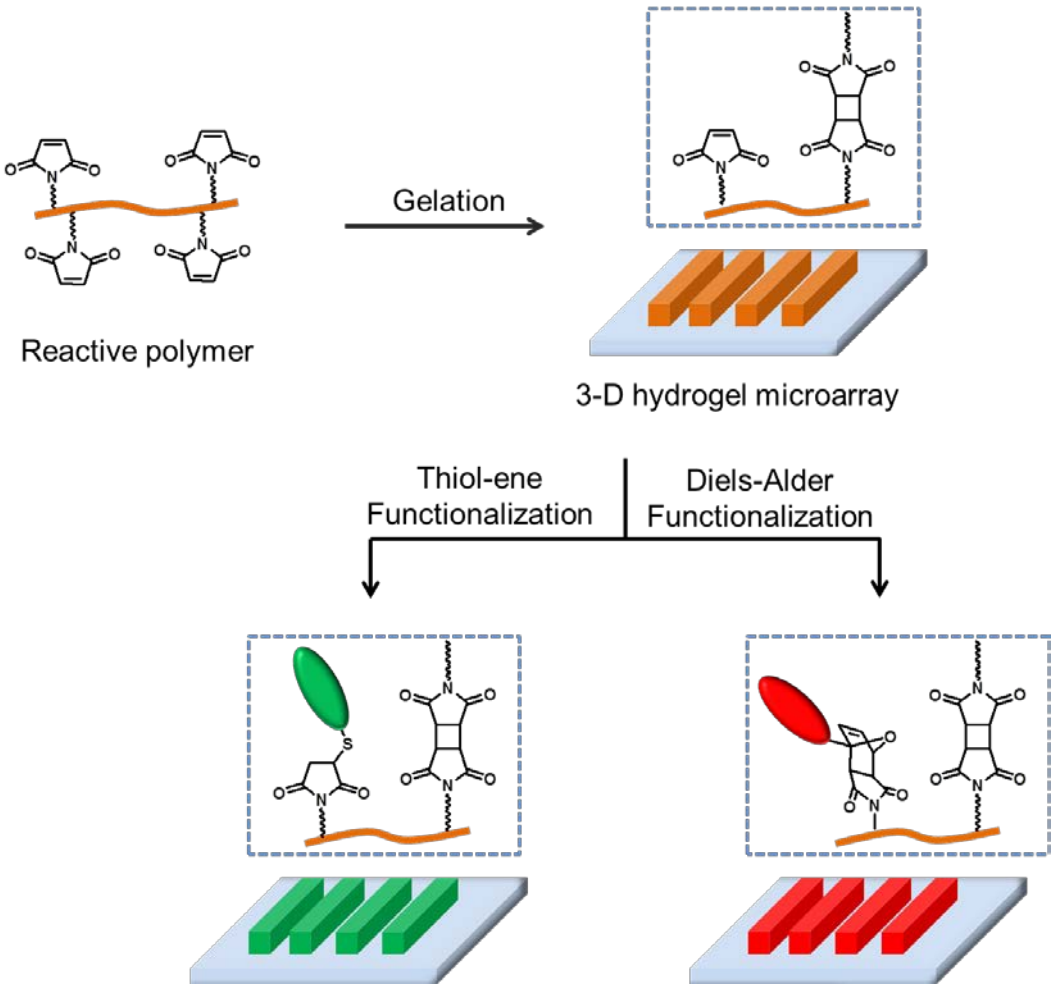

Figure 7.2. Schematic illustration of fabrication and functionalization of hydrogels.

7.2. Experimental

7.2.1 Materials

The furan protected maleimidyl methacrylate (FuMa-MA) monomer was synthesized according to a previous report [165]. Poly(ethylene glycol) methyl ether methacrylate (PEGMEMA, M_n = 300 Da) was purchased from Sigma Aldrich and purified by passing through the activated aluminum oxide column prior to use. Poly (ethylene glycol) (PEG, M_n = 8300 Da), was purchased from Fluka, 3-(trimethoxysilyl)propyl methacrylate (TMSMA), triethylamine (TEA), Copper(I)Bromide and 2,2'-Bipyridyl were obtained from Sigma Aldrich, 2-bromo-2-methylpropionyl bromide obtained from Acros and used as received. Whitesides Monothiol(Biotin-SH) was obtained from Nanoscience Instruments. Fluorescein conjugated ExtrAvidin (ExtrAvidin-TRITC) was obtained from Sigma and used as received. 4,4-Difluoro-1,3,5,7-tetramethyl-8-[(10-mercapto)]-4-bora-3a,4a-diaza-*s*-indacene (BODIPY-SH) and BODIPY-N_3 were synthesized according to literature procedures [166]. Anhydrous solvents such as dichloromethane (DCM), tetrahydrofuran (THF) and toluene were obtained from SciMatCo purification system and other solvents were dried over molecular sieves wherever necessary. Column chromatography was performed using silica gel 60 (43-60 nm, Merck). Thin layer chromatography was performed using silica gel plates (Kieselgel 60 F254, 0.2 mm, Merck). The plates were viewed under 254 nm UV lamp and/or developed by $KMnO_4$ stain. Blak-Ray® B-100 AP/R High Intensity 100 Watt/365 nm UV lamp was used for crosslinking processes.

7.2.2. Characterization

^{1}H-NMR spectra were recorded with a Varian Mercury VX 400 MHz spectrometer, and referenced to $CDCl_3$. The weight and number average molecular weights (M_w and M_n) as well as the polydispersity index (PDI) were determined by gel permeation chromatography (GPC) using a Shimadzu GPC furnished with a PSS-SDV (length/ID 8×300 mm, 10 mm particle size) mixed-C column. Polystyrene standards (1-150 kDa) were used for calibration. Tetrahydrofuran (THF) was used as eluent at a flow rate of 1 mL/min^{-1} at 30 ^{o}C. FT-IR spectra were recorded with a Thermo Fischer Scientific Inc. Nicolet 380 instrument (spectral range between 4000 and 450 cm^{-1}).

7.2.3. Synthesis of PEG ATRP Macroinitiator

A solution of HO-PEG-OH (M_n=8300 Da, 4.0 g, 0.502 mmol) was dissolved in toluene and dried azeotropically using toluene rotary evaporation, followed by drying under vacuum. The polymer HO-PEG-OH and triethylamine (0.15 mL, 1.06 mmol) was dissolved in anhydrous methylene chloride (30 mL) and the flask was in an ice-water bath. Then, 2-bromoisobutyryl bromide (0.62 mL, 5.02 mmol) was slowly added to the reaction mixture. The solution was warmed to room temperature and stirred for 24 h. The organic solvent was removed under reduced pressure. The crude product was dissolved in methylene chloride (250 mL) and washed with saturated $NaHCO_3$ solution (250 mL) three times. The combined organic layers were dried over anhydrous Na_2SO_4 and concentrated in vacuum. The crude product was dissolved in a minimum amount of methylene chloride and then precipitated in cold diethyl ether. The precipitate was recovered by simple filtration to yield the desired polymer as a white powder (yield = 85%). ^{1}H NMR (δ, ppm, $CDCl_3$) 4.32-4.29 (4H, m, -COO-*CH_2*-), 3.81-3.78 (4H, m, -COO-CH_2-*CH_2*-), 3.73-3.71 (4H, m, -COO-CH_2CH_2O-*CH_2*), 3.66-3.59(712H, br s, -CH_2CH_2O-), 3.45-3.43 (4H, m, -CH_2CH_2O-), 1.92 (12H, s, -CH_3-C-COO-).

7.2.4. Synthesis of ABA Triblock Copolymers (P1)

In a 10 mL flask, the PEG macroinitiator (Br−PEG−Br) [M_n=8300 Da] (0.100 g, 0.01 mmol), FuMa-MA monomer (0.100 g, 0.34 mmol) and PEGMEMA [M_n=300 Da] (0.052 g, 0.17 mmol) were dissolved in a mixture of MeOH (1.8 mL) and H_2O (0.2 mL). The flask was sealed with a rubber septum and thoroughly degassed under nitrogen purge. Polymerization was started after addition of a solution of 2, 2'-bipyridine (0.049 g, 0.31 mmol) and Cu(I)Br (0.022 g, 0.11 mmol) dissolved in MeOH (0.6 mL) and the polymerization was carried out at room temperature for 4 hours. After the polymerization, the reaction mixture was precipitated into cold diethyl ether (100 mL). The viscous liquid obtained after discarding the diethyl ether layer was diluted with DCM and passed over a column of basic alumina to remove the catalyst. After evaporating the organic solvent, the residue was dried under vacuum at room temperature (yield = 37%). ^{1}H NMR (δ, ppm, $CDCl_3$) 6.52 (s, 2H, CH=CH), 5.23 (s, 2H, CH bridgehead protons), 4.06 (br s, 2H, OCH_2), 3.92 (br s, 2H, OCH_2), 3.62-3.54 (712+14H, br s, -*CH_2CH_2*O-), 3.45-3.43 (4H,

m, -C*H*$_2$C*H*$_2$O-), 3.35 (br s, 3H, OC*H*$_3$), 2.84 (s, 2H,CH-CH, bridge protons), 1.92–0.82 (m, 6H+7H, -(C*H*$_3$)$_2$-C-COO-, NCH$_2$C*H*$_2$CH$_2$O, C*H*$_2$ and C*H*$_3$ along polymer.

7.2.5. Synthesis of ABA Triblock Copolymers (P2)

In a 10 mL flask, PEG macroinitiator (Br−PEG−Br) [M_n=8300 Da] (0.100 g, 0.01 mmol), FuMaMA monomer (0.150 g, 0.52 mmol) and PEGMEMA [M_n=300 Da] (0.155 g, 0.52 mmol) was dissolved in a mixture of MeOH (1.8 mL) and H_2O (0.3 mL). The flask was sealed with rubber septum and thoroughly degassed under nitrogen purge. Polymerization was started after addition of a solution of 2, 2'-bipyridyl (0.049 g, 0.31 mmol) and Cu(I)Br (0.022 g, 0.11 mmol) in MeOH (0.6 mL) and the polymerization was carried out at room temperature for 4 hours. After the polymerization, the reaction mixture precipitated into cold of diethyl ether (100 mL). The viscous liquid obtained after discarding the diethyl ether layer was diluted with DCM and passed over a column of basic alumina to remove the catalyst and then dried under vacuum at room temperature (yield = 47%). ^{1}H NMR (δ, ppm, $CDCl_3$) 6.52 (s, 2H, CH=CH), 5.23 (s, 2H, CH bridgehead protons), 4.06 (br s, 2H, OC*H*$_2$), 3.92 (br s, 2H, OC*H*$_2$), 3.62-3.54 (712+14H, br s, -*CH*$_2$*CH*$_2$O-), 3.45-3.43 (4H, m, -C*H*$_2$C*H*$_2$O-), 3.35 (br s, 3H, OC*H*$_3$), 2.84 (s, 2H,CH-CH, bridge protons), 1.92–0.82 (m, 6H+7H, -(C*H*$_3$)$_2$-C-COO-, NCH$_2$C*H*$_2$CH$_2$O, C*H*$_2$ and C*H*$_3$ along polymer.

7.2.6. Synthesis of ABA Triblock Copolymers (P3)

In a 10 mL flask, PEG macroinitiator (Br−PEG−Br) [M_n=8300 Da] (0.100 g, 0.01 mmol), FuMaMA monomer (0.075 g, 0.26 mmol), and PEGMEMA [M_n=300 Da] (0.231 g, 0.77 mmol), were dissolved in a mixture of MeOH (2.5 mL) and H_2O (0.2 mL). The flask was sealed with rubber septum and thoroughly degassed under nitrogen purge. Polymerization was started after addition of a solution of 2, 2'-bipyridyl (0.049 g, 0.31 mmol) and Cu(I)Br (0.022 g, 0.11 mmol) in MeOH (0.6 mL) and the polymerization was carried out at room temperature for 4 hours. After the polymerization, the reaction mixture was precipitated into cold diethyl ether (100 mL). The viscous liquid obtained after discarding the diethyl ether layer was diluted with DCM and passed over a column of basic alumina to remove the catalyst. After evaporating the organic solvent, the residue was

dried under vacuum at room temperature (yield = 32%) . ^{1}H NMR (δ, ppm, $CDCI_3$) 6.52 (s, 2H, CH=CH), 5.23 (s, 2H, CH bridgehead protons), 4.06 (br s, 2H, OCH_2), 3.92 (br s, 2H, OCH_2), 3.62-3.54 (712+14H, br s, -CH_2CH_2O-), 3.45-3.43 (4H, m, -CH_2CH_2O-), 3.35 (br s, 3H, OCH_3), 2.84 (s, 2H,CH-CH, bridge protons), 1.92–0.82 (m, 6H+7H, -(CH_3)$_2$-C-COO-, $NCH_2CH_2CH_2O$, CH_2 and CH_3 along polymer.

7.2.7. Deprotection of the ABA Triblock Copolymer P1 (P4)

Polymer P1 (0. 05 g) was dissolved in toluene (100 mL) and the solution was refluxed at 110 ^{o}C for 12 hours. Afterwards, solvent was concentrated under reduced pressure and the residue was dissolved in minimal amount of DCM and precipitated in diethyl ether. The resulting precipitate was filtered and dried under vacuum at room temperature. ^{1}H NMR (δ, ppm, $CDCl_3$) 6.73 (s, 2H, CH=CH), 4.06 (br s, 2H, OCH_2), 3.92 (br s, 2H, OCH_2), 3.62-3.54 (712+14H, br s, -CH_2CH_2O-), 3.45-3.43 (4H, m, -CH_2CH_2O-), 3.35 (br s, 3H, OCH_3), 2.84 (s, 2H,CH-CH, bridge protons), 1.92–0.82 (m, 6H+7H, -(CH_3)$_2$-C-COO-, $NCH_2CH_2CH_2O$, CH_2 and CH_3 along polymer.

7.2.8. Deprotection of the ABA Triblock Copolymer P2 (P5)

Polymer P2 (0. 05 g) was dissolved in toluene (100 mL) and the solution was refluxed at 110 ^{o}C for 12 hours. Afterwards, solvent was concentrated under reduced pressure and the residue was dissolved in minimum amount of DCM and precipitated in diethyl ether. The resulting precipitate was filtered and dried under vacuum at room temperature. ^{1}H NMR (δ, ppm, $CDCl_3$) 6.73 (s, 2H, CH=CH), 4.06 (br s, 2H, OCH_2), 3.92 (br s, 2H, OCH_2), 3.62-3.54 (712+14H, br s, -CH_2CH_2O-), 3.45-3.43 (4H, m, -CH_2CH_2O-), 3.35 (br s, 3H, OCH_3), 2.84 (s, 2H,CH-CH, bridge protons), 1.92–0.82 (m, 6H+7H, -(CH_3)$_2$-C-COO-, $NCH_2CH_2CH_2O$, CH_2 and CH_3 along polymer.

7.2.9. Deprotection of the ABA Triblock Copolymer P3 (P6)

Polymer P3 (0. 05 g) was dissolved in toluene (100 mL) and the polymer solution was refluxedat 110 ^{o}C for 12 hours. Afterwards, solvent was concentrated under reduced pressure and the residue was dissolved in minimum amount of DCM and precipitated in

diethyl ether. The resulting precipitate was filtered and dried under vacuum at room temperature. ^{1}H NMR (δ, ppm, $CDCl_3$) 6.73 (s, 2H, CH=CH), 4.06 (br s, 2H, OCH_2), 3.92 (br s, 2H, OCH_2), 3.62-3.54 (712+14H, br s, -CH_2CH_2O-), 3.45-3.43 (4H, m, -CH_2CH_2O-), 3.35 (br s, 3H, OCH_3), 2.84 (s, 2H,CH-CH, bridge protons), 1.92–0.82 (m, 6H+7H, -(CH_3)$_2$-C-COO-, $NCH_2CH_2CH_2O$, CH_2 and CH_3 along polymer.

7.2.10. General Synthesis of Bulk-Hydrogel via Photo-crosslinking

Bulk-hydrogels were prepared by UV-initiated photo-dimerization at ambient temperature. Unmasked maleimide functional group containing reactive triblock polymer (20 mg, 0.001 mmol) dissolved in a EtOH/ H_2O (70μL/10 μL) mixture was used as a hydrogel precursor. The synthesis of bulk-hydrogel was carried by irradiating the polymer mixture under UV-light (365 nm) for 30 min at room temperature. The photo-crosslinked bulk-hydrogels were washed with EtOH and H_2O respectively to remove unreacted polymers and then the hydrogel was freeze dried. As a control experiment, the polymeric precursor containing the masked maleimide groups as side chains was exposed to UV. No crosslinking or gelation occurred under the conditions that yield hydrogels when the maleimide containing copolymers are employed.

7.2.11. Modification of Glass Surface and Silicon Wafer Substrate with TMSMA

Glass surfaces and silicon wafers were treated with nonchromix acid solution (0.5 g / 20 mL nonchromix/H_2SO_4) for 1 hour to remove the native oxides, organic impurities and metallic contaminants, rinsed with deionized water, and then sonicated respectively in acetone and isopropyl alcohol and finally blown dry using nitrogen. TMSMA was used for modification of glass and silicon wafer to promote the covalent adhesion between the glass surface and the hydrogel. Clean surfaces were immersed in a solution of toluene containing TMSMA containing (1 wt % solution) under a nitrogen atmosphere. Immersed surfaces were sonicated for 1 hour and then left in the solution overnight. The modified wafers were washed several times in toluene and methanol and then dried under vacuum.

7.2.12. Preparation of Hydrogel Patterns

Micro-patterned hydrogel structures were successfully achieved using two approaches. Micro-molding in capillaries (MIMIC) technique was performed to obtain linear hydrogel microstructures and photo-patterning method was performed to obtain square patterns on solid substrates.

7.2.12.1. Micro Molding in Capillaries (MIMIC). For the MIMIC method, a polydimethylsiloxane (PDMS) stamp was used to obtain three-dimensional structured hydrogel pattern. The PDMS stamp with patterned structure obtained by using standard photolithography was carefully placed on the TMSMA modified surface. Polymer solution (10 wt % in EtOH/H_2O) was injected at the open end of channel of PDMS stamp and the channel was filled with polymer solution by capillary action. The surface was placed exposed to UV-light (365 nm) for 15 min. Thereafter, PDMS stamp was peeled off from the surface and hydrogel patterns on the surface were gently washed with THF to remove any unreacted material.

7.2.12.2. Photolithography. Selective photo patterning was performed through a photomask containing squares (100 x 100 micron). At first, the modified silicon wafer substrates are coated with polymer by spin coating using a 10 wt% polymer solution in a EtOH/H_2O system at 500 rpm for 10 s and 2000 rpm for 30 s. Thus obtained polymeric thin films were patterned by selective UV exposure through the photo mask, and crosslinked micr-patterns were washed with THF and dried under nitrogen.

7.2.12.3. Synthesis of BODIPY-Furan. NaH (488 mg, 12 mmol) was taken in a RBF with a stirbar and purged with N_2 for 10 minutes. 20 mL of anhydrous THF was added. Furfuryl alcohol (0.52 mL, 6 mmol) and propargyl bromide (1.55 mL, 18 mmol) was added. Reaction was stirred for 12 h. THF was evaporated and dissolved in 100 mL of DCM then washed with 20 mL of water 3 times. After filtration with hexane, 590 mg of furan alkyne was obtained. BODIPY-N_3 was synthesized according to literature procedure [19]. BODIPY-N_3 (45 mg, 0.104 mmol) and CuBr (2.24 mg, 0.0157 mmol) was taken into a reaction tube with a stirbar and 1 mL of THF was added. PMDETA (2.72 mg, 0.0157 mmol) and furan-alkyne (2-((prop-2-ynyloxy)methyl)furan) (21.29 mg, 0.157 mmol) was added and purged with N_2 stream for 10 mL. Second solution was added to first solution and reaction mixture was was stirred for 24 h at 40 ^oC. Then THF was evaporated and

product was dissolved in 50 mL of DCM and washed with 50 mL water 3 times. Column chromotography was performed bu using 15% ethyl acetate 85% hexane mixture (yield = 56%). ^{1}H-NMR (400 MHz, in $CDCl_3$) δ(ppm): 7.52 (s, 1H), 7.41 (q, 1H), 6.35 (m, 2H), 6.04 (s, 2H), 4.67 (d, 2H), 4.53 (s, 2H), 4.32 (t, 2H), 2.91 (m, 2H), 2.50 (s, 6H), 2.40 (s, 6H), 1.88 (m, 2H), 1.61 (m, 2H), 1.46 (m, 2H), 1.30 (br s, 10 H)

7.2.12.4. Functionalization of Patterned Hydrogel with BODIPYC10SH. The patterned hydrogel surfaces were incubated in a BODIPYC10SH (1mg/mL in THF) solution. After 18 hours, the surface containing thus modified hydrogel patterns was washed with THF to remove unbound dye molecules.

7.2.12.5. Functionalization of Patterned Hydrogel with Furan-BODIPY. Patterned surface was placed into a solution of Furan-BODIPY (1 mg/mL) THF solution for 30 min. Excess dye molecules were removed through washing with THF several times.

7.2.12.6. Biofunctionalization of Patterned Hydrogel. A solution of Biotin-SH in MeOH (1 mg/mL) was prepared and dropped onto a dried hydrogel pattern from polymer P5. After 45 min, the sample was washed with MeOH several times and dried under a gentle stream of nitrogen. A solution of ExtrAvidin (ExtrAvidin-TRITC (20 μL, 0.5 mM in H_2O) was dropped on the biotinylated patterned surface. The pattern was placed in dark for 45 min, and then gently rinsed with water to remove any physically adhering protein.

7.2.12.7. Control Experiment. As a control experiment a solution of ExtrAvidin (ExtrAvidin-TRITC (20 μL, 0.5 mM in H_2O) was dropped on patterned surface from polymer P5. The pattern was placed in dark for 45 min, and then gently rinsed with water to remove any physically adhering protein.

7.2.12.8. Swelling Studies of Bulk-Hydrogels. Prior to recording their swelling profiles, dried hydrogels were swollen in ultrapure water. Using a moist filter paper the excessive water on the sample surfaces was removed, and the weight of samples was measured periodically and replaced back into the same media. Swelling ratio was monitored until there was no further change in weight. The % water uptake was calculated using the following formula

% Water Uptake = 100 x $(W_{st}-W_{dt})/W_{dt}$

W_{st} and W_{dt} are the wet and dry weight of hydrogels at time t, respectively.

7.2.12.9. Scanning Electron Microscopy Analysis (SEM). Morphology of the bulk-hydrogels was investigated using a scanning electron microscopy (SEM), performed with a ESEM-FEG/EDAX Philips XL-30 (Philips, Eindhoven, The Netherlands) operating at 3 kV. Prior to analysis, the hydrogels were immersed in water for 2h at room temperature, frozen and lyophilized for 24 h.

7.2.12.10. Fluorescence Microscopy. Attachment of fluorescent dye molecules (BODIPY-SH) and fluorescently labelled enzyme (ExtrAvidin-TRITC) was determined using LD-A-Plan 10×/0.30 and 20x/0.30 objectives in a Zeiss Axio Observer inverted microscope (Zeiss Fluorescence Microscopy, Carl Zeiss Canada Ltd, Canada). Zeiss Filter set 38 (Excitation BP 470/40, Emission BP 525/50) was used for imaging of BODIPY-SH attached hydrogel surface. For visualization of fluorescently labelled enzyme (ExtrAvidin-TRITC), filter set 43 (Excitation BP 545/25, Emission BP 605/70) was used. Images were processed using Zeiss AxioVision software.

7.3. Results and Discussion

7.3.1. Synthesis and Characterization of Copolymers

Triblock copolymers (ABA type) comprising of hydrophobic furan-prtected maleimide-containing monomer (FuMa-MA) and hydrophilic PEG-based methacrylate (PEGMEMA) in their A blocks and a hydrophilic linear PEG segment as the middle block were synthesized using ATRP using a linear PEG-based macroinitiator (Figure 7.3). The macroinitiator was synthesized via end group modification of telechelic hydroxyl group containing linear PEG with 2-bromoisobutyryl bromide. Changing the feed ratio of the hydrophobic monomer FuMa-MA and the hydrophilic PEGMEMA monomer, a set of triblock copolymers were synthesized. Copper(I) bromide and 2, 2'-bipyridine in MeOH/H_2O solvent mixture was used as catalyst. A set of triblock polymers (P1–P3) were

obtained using the feed ratio of FuMa-MA:PEGMEMA 2:1, 1:1, and 1:3 with approximately same overall molecular weights. Table 7.1 provides a summary of different polymerization conditions that were examined along with the obtained results.

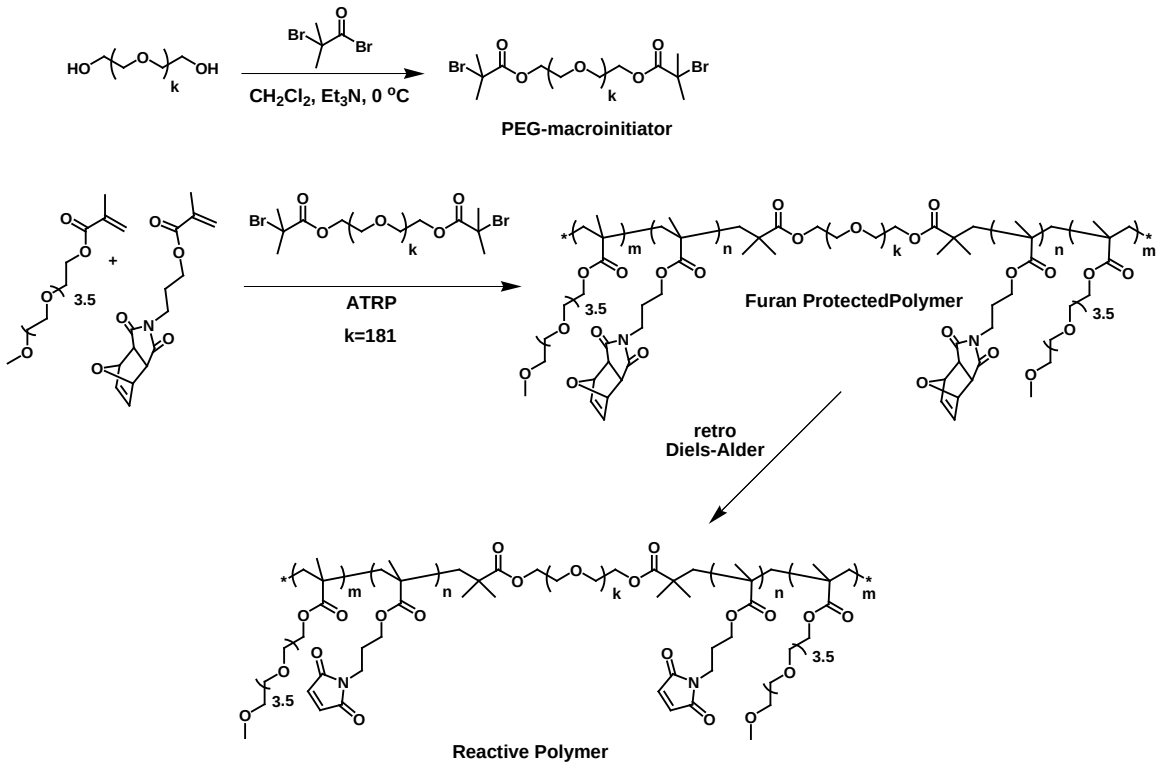

Figure 7.3. Synthesis of maleimide group containing ABA type triblock copolymers.

The chemical compositions of obtained copolymers were established using ^{1}HNMR spectroscopy. In the ^{1}HNMR spectra of the polymers, two types of vinylic protons are readily distinguishable at 6.52 and 5.23 originating from the bicyclic moiety of the cycloadduct (Figure 7.4). Comparsion of the integral ratio of peaks a or b belonging to the protons on the bicyclic unit to peak c belonging the terminal methoxy protons (-O-CH_3) on the PEGMEMA based side chain suggests that ratio of monomers incorporated in the final copolymer are similar to the feed. Polymers (P1-P3) were heated at 110 ^{o}C in anhydrous toluene for 12 hours to unmask the maleimide groups via the retro Diels-Alder reaction to yield reactive copolymers P4-P6. Complete cycloreversion of the cycloadduct to yield maleimide side chain containing polymers was achieved as inferred from ^{1}H NMR

analysis. During the cycloreversion, appearance of a new peak at 6.73 ppm and complete disappearance of peaks at 6.51 and 5.23 ppm revealed that the deprtection proceeds in a quantitative fashion (Figure 7.5). Furthermore, GPC analysis showed that there was no significant adverse effect of this thermal activation process on the molecular weight or its distribution of the copolymers (Figure 7.6). For instance, when polymer P2 (M_n =14600, M_w/M_n = 1.20) was subjected to the cycloreversion step for 12 h at 110 °C, maleimide functionalized triblock polymer P5 with similar characteristics (M_n = 14660, M_w/M_n = 1.28) was obtained.

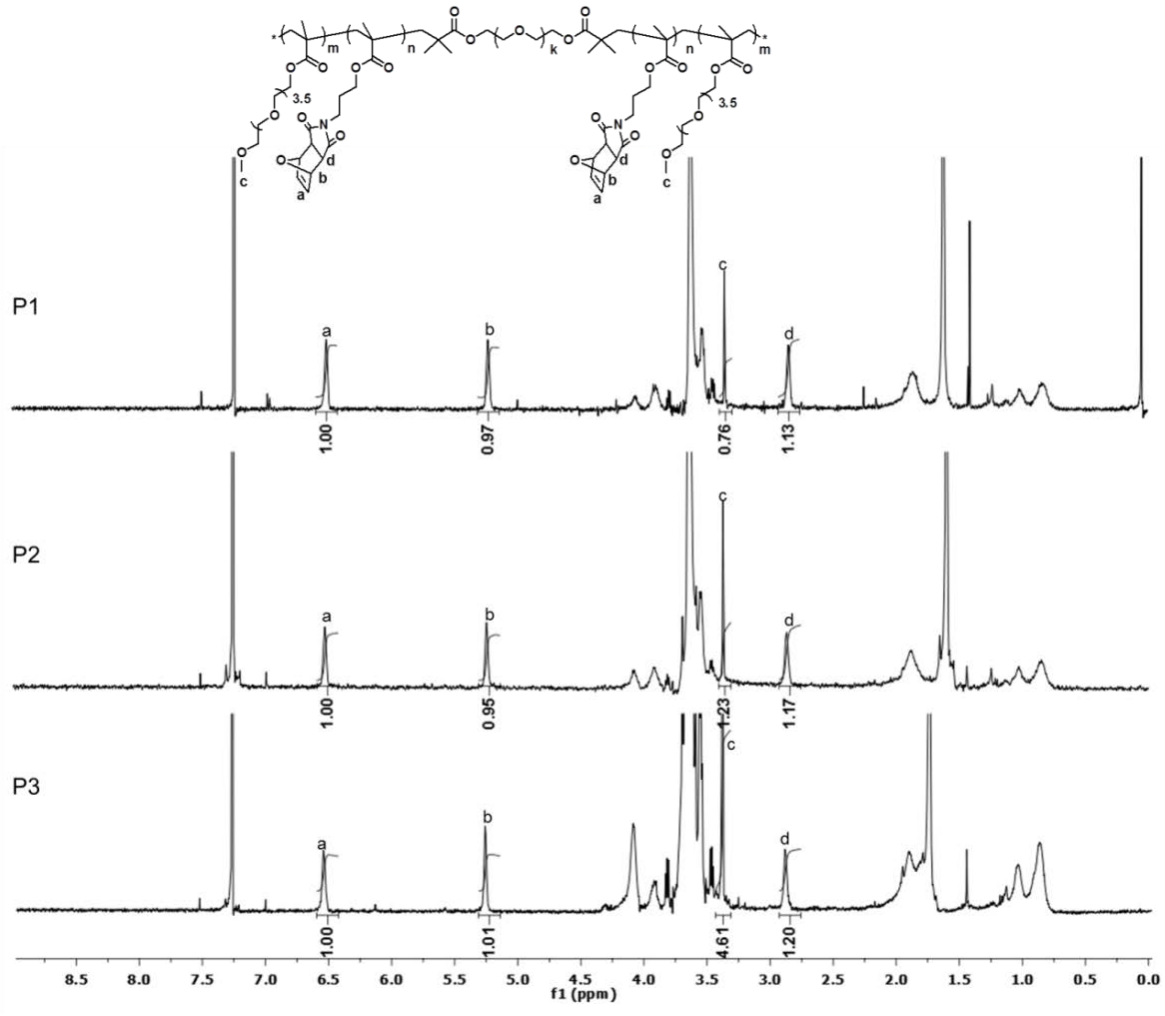

Figure 7.4. ^{1}H-NMR spectra of copolymers P1-P3.

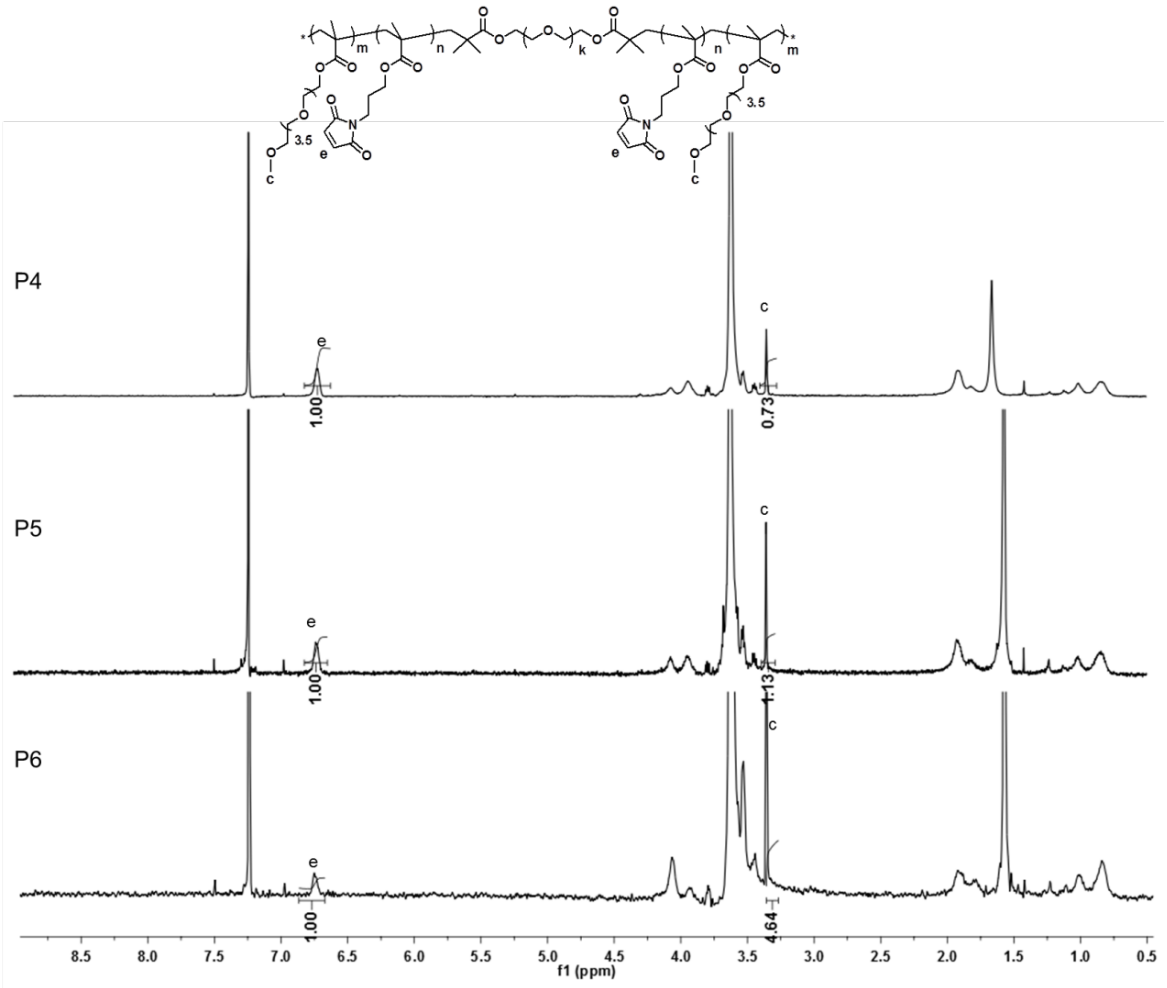

Figure 7.5. ^{1}H-NMR spectra of copolymers (P4-P6) obtained after the retro Diels-Alder reaction.

Table 7.1. Synthesis of ABA type triblock polymers and activated polymers via retro Diels Alder reaction.

Polymer	Feed ratio[b]	Obtained Ratio[c]	Mn (GPC)[d]	Mn (th)[e]	PDI[f]	Conversion (%)
	FuMa-MA : [PEGMEMA]	FuMa-MA : [PEGMEMA]				
P1	2.0:1.0	2.1 : 1.0	16175	6385	1.20	37
P2	1 .0:1.0	1.3 : 1.0	14600	8172	1.20	47
P3	1.0:3.0	1 .0 : 2.8	16310	24900	1.18	11
P4	2.0:1.0	2.1 : 1.0	14950	-	1.38	89
P5	1 .0:1.0	1.3 : 1.0	14660	-	1.28	92
P6	1.0:3.0	1 .0 : 2.8	21440	-	1.21	90

Initiator, PEG macroinitiator (M_n=8300 Da); catalyst: Copper(I) bromide/2, 2'bipyridyl; solvent: MeOH/H_2O, room temperature, 4h

[b] Feed ratio of monomers

[c] % Incorporation of monomers in the copolymer as determined by ^{1}H NMR.

[d] Estimated by SEC eluted with THF, using polystyrene calibrations.

[e] Theoretical molecular weight calculated according to: $Mn(th) = ([M]_0/[I]_0)x\ Conv.\ x\ (291.1n_i' + 300n_i'' + 8300n_i''')$ where 291.1, 300 and 8300 are the molecular weights of monomers and PEG macroinitiator respectively and n_i is the initial mol of monomers.

[f] Estimated by SEC eluted with THF, using polystyrene calibrations.

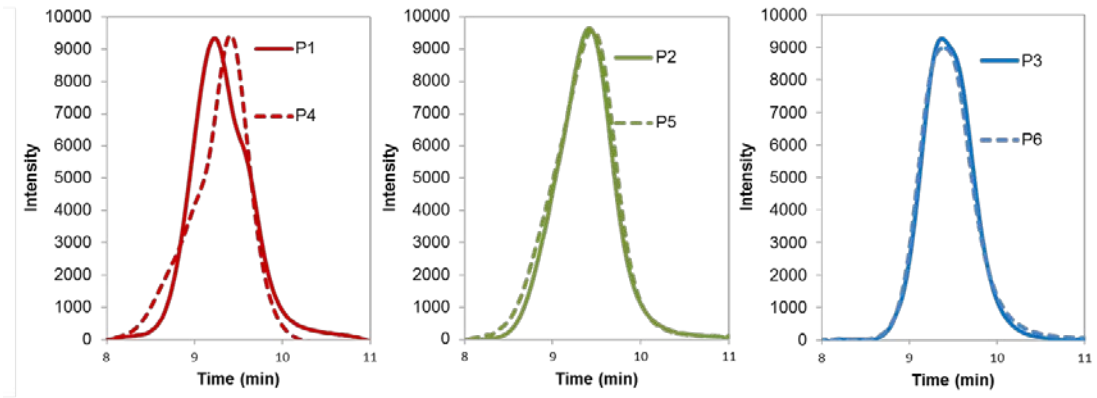

Figure 7.6. Gel Permeation Chromatographs for copolymers before and after retro Diels-Alder reaction.

7.3.2. Synthesis and Characterization of Bulk Hydrogels

Bulk hydrogels were prepared using these copolymers via photo-crosslinking in the absence of any additional photoinitiator at room temperature. Unmasked maleimide group containing reactive triblock copolymers were used as precursor to yield crosslinked hydrogel by irradiating under UV-light (365 nm) for 30 min at room temperature. As a control experiment, the polymer precursor before the activation step i.e. containing furan-protected maleimide groups were also exposed to UV irradiation under the same conditions to witness absence of any gelation.

The kinetics of hydrogel swelling was studied comparing the difference in swelling behaviour by considering the crosslinking density of bulk hydrogels with almost same molecular weight. All hydrogels quickly reached their equilibrium swelling within 30 minutes (Figure 7.7). Water uptake of hydrogel H1 (containing 2:1 ratio FuMa-MA: PEGMEMA) hydrogel was 810% after 25 min, whereas hydrogels H2 and H3 (H2, 1:1 FuMa-MA: PEGMEMA; H3, 1:3 FuMa-MA: PEGMEMA ratio) exhibited 500%, and 1675% water-uptake respectively in 25 min. One would expect that the water uptake will be dependent on the amount of crosslinking in the PEG hydrogel. We expect that as a consequence of the increased cross-linking density because of the higher number of maleimide groups in hydrogel H1, the water-uptake will be lower with respect to H2. However to our surprise, we observed a higher swelling for hydrogel H1 in comparison to H2. This was a reproducible trend that was found with many batches of hydrogels obtained under identical conditions. At this point, a clear explanation is not available for this observation. Moreover, as a result of the remarkably increased content of the hydrophilic monomer PEGMEMA, maximum water uptake was observed for hydrogel H3. Overall, all hydrogels exhibited good water uptake due to the presence of the long hydrophilic linear PEG chain (M_n=8000) unit in middle block.

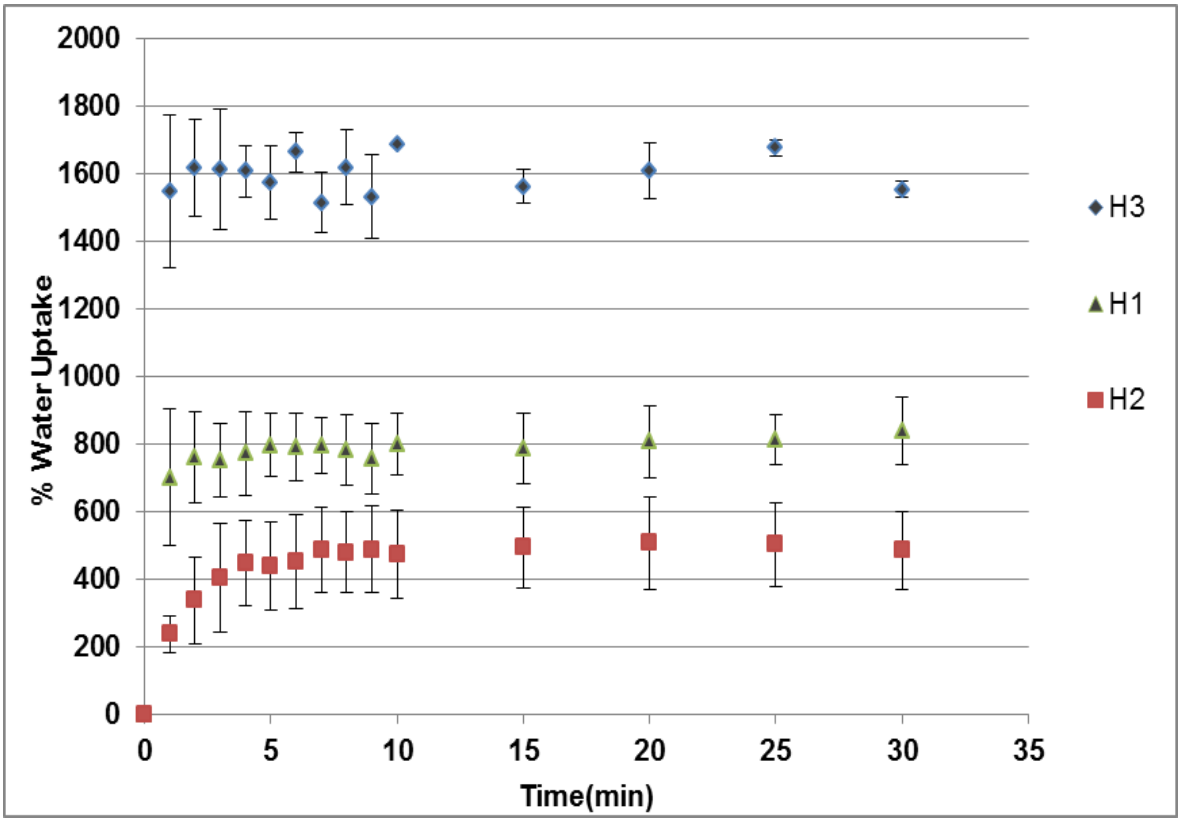

Figure 7.7. Water uptake measurements of hydrogels H1, H2 and H3.

To understand the structure of the hydrogels, morphological structures of the hydrogels were examined using a scanning electron microscopy (SEM). SEM analysis confirmed that triblock polymers form uniform structures after crosslinking. Figure 6.8 shows SEM microphotographs of freeze-dried bulk hydrogels containing different FuMa-MA/PEGMEMA ratios. While all structures were porous, the hydrogel H1 obtained using polymers containing the highest maleimide content shows the highest degree of crosslinking with lowest pore size (Figure 7.8).

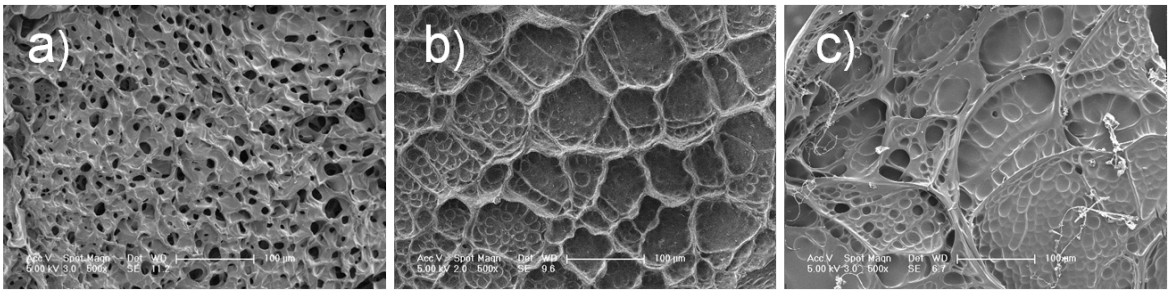

Figure 7.8. SEM microphotographs of bulk hydrogels a) H1 b) H2, c) H3.

7.3.3. Gelation Studies on Surfaces

7.3.3.1. Surface modification for good adhesion. Glass surface was modified with an acrylate containing organosilyl molecule which will enable adhesion of the hydrogel micropatterns onto the surface. For this purpose, glass substrate was coated with TMSMA under a nitrogen environment. Thus modified acrylate functional group containing surfaces were used as substrates for the hydrogel patterns.

7.3.3.2. Patterning via Micro Molding in Capillaries (MIMIC). PDMS surfaces containing well defined linear microchannels were attached onto the modified glass or silicon surfaces via gentle pressure and a mechanical adhesion was achieved between the PDMS and glass or silicon surfaces. Solutions containing the polymeric precursors (10 wt% in 10:1 EtOH/H_2O) were prepared from the maleimide containing copolymers P4-P6. Polymeric solutions were injected between the PDMS and glass surfaces to fill the microchannels. Upon exposure to UV irradiation for 15 minutes, patterned hydrogels were obtained via a [2+2] cycloaddition reaction between the maleimide groups. It can be envisioned that after the crosslinking reactions, some of the pendant maleimide groups will stay unreacted and this number of remaining maleimide groups will be proportional to the maleimide content of the corresponding copolymers. By using this approach, hydrogels with varying content of reactive maleimide groups can be fabricated (Figure 7.9).

7.3.3.3. Fabrication of Hydrogel Micro-patterns via Photolithograpy. A solution of copolymer P5 (10 wt% in EtOH/H_2O) was spin coated on modified silicon surfaces. A photomask was placed onto the polymer coated surfaces and the surfaces were subjected to UV irradiation for 5, 10 and 15 minutes at 365 nm (Figure 7.11). We expected that increasing the irradiation time will yield hydrogels with increasing crosslinking. For example, the number of residual maleimide groups in a hydrogel obtained via 15 minutes irradiation will be less compared to that in a hydrogel obtained with 5 minutes of irradiation.

7.3.4. Functionalization of Hydrogels Micro-patterns with Small Molecules

The successful functionalization of the maleimide groups on the patterned surface was confirmed via covalent immobilization of appropriately functionalized fluorescent dye molecules. As noted before, the amount of reactive maleimide groups on thus patterned hydrogels are predicted to be different depending on the maleimide ratio in the polymeric precursors or depending on the irradiation time. Hence the extent of functionalization via the attachment of dye molecules under similar conditions will provide an idea about the residual maleimide. We used two different dye molecules for the conjugation studies: a thiol containing dye, BODIPYC10SH; and a furan containing dye BODIPY-Furan. BODIPYC10SH was used for functionalization via thiol mediated Michael addition reaction whereas BODIPY-Furan was used for Diels Alder reaction mediated functionalization.

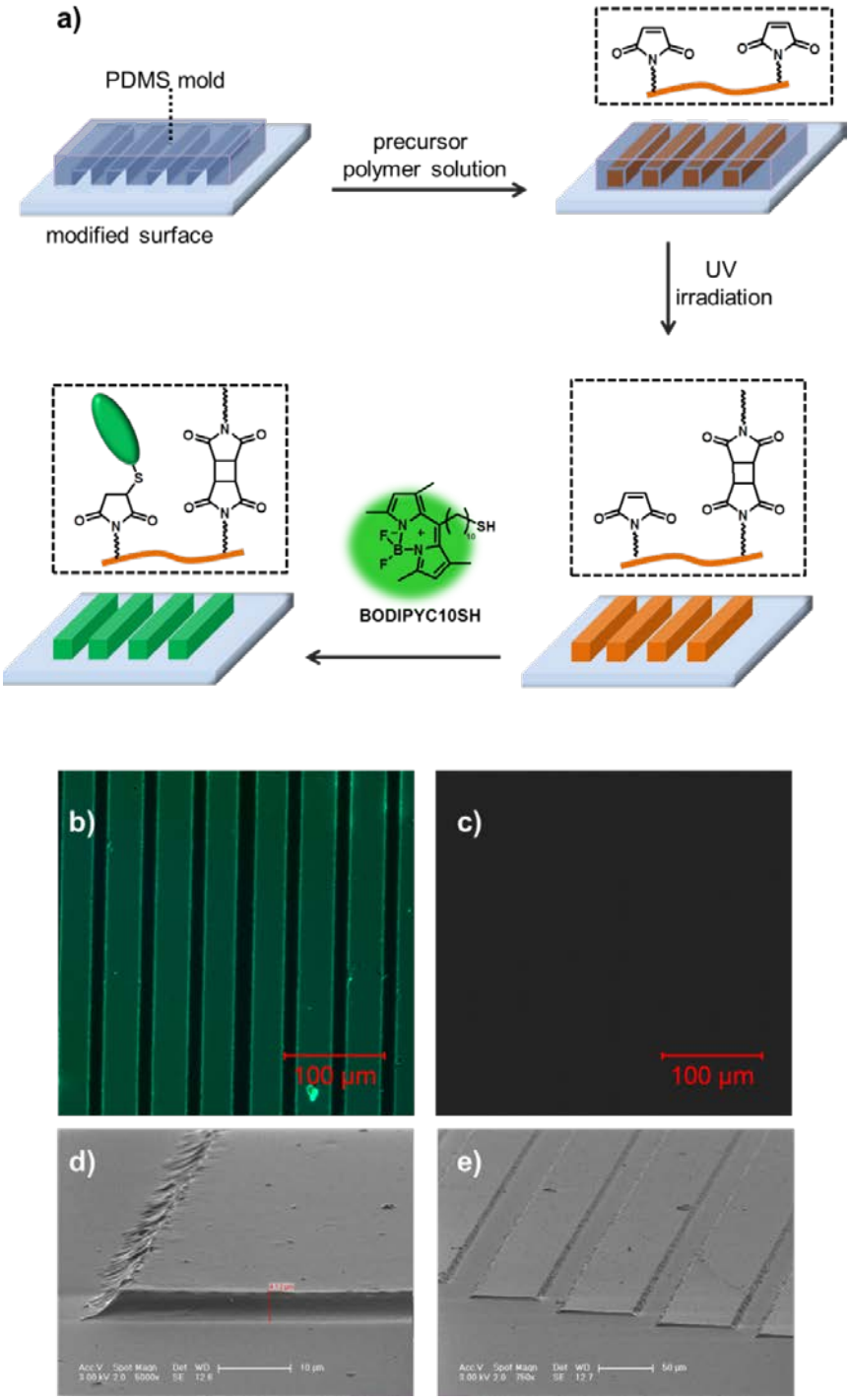

Figure 7.9. a) General scheme for patterning via MIMIC and functionalization of the patterned surface with BODIPYC10SH. b) Fluorescence microscopy image after BODIPYC10SH attachment to P2 at 500 ms and c) Fluorescence microscopy image before BODIPYC10SH attachment d) SEM image of patterned hydrogel surface at 5000 X magnification, e) SEM image of patterned hydrogel surface at 750 X magnification.

7.3.4.1 Synthesis and Functionalization of Hydrogels with Varying Maleimide group Content via Micromolding in Capillaries. Micropatterned surfaces were prepared from copolymers P4-P5 containing varying FuMa-MA/PEGMEMA ratios (2:1, 1:1 and 1:3 respectively) using the micromolding in capillaries technique. After the preparation of patterned hydrogel surfaces, derivatization of residual maleimide groups was achieved with a thiol containing dye, BODIPYC10SH. The successful covalent attachment of BODIPYC10SH to the surfaces was established using fluorescence microscopy (Figure 7.10). Furthermore, the extent of functionalization with the dye was found to be dependent on the amount of maleimide groups in the hydrogel precursors. For example, patterns obtained using copolymer P4 showed the highest fluorescence intensity since it has the highest maleimide content that enables the highest incorporation of dye molecules compared to the other hydrogels (Figure 7.10.a).

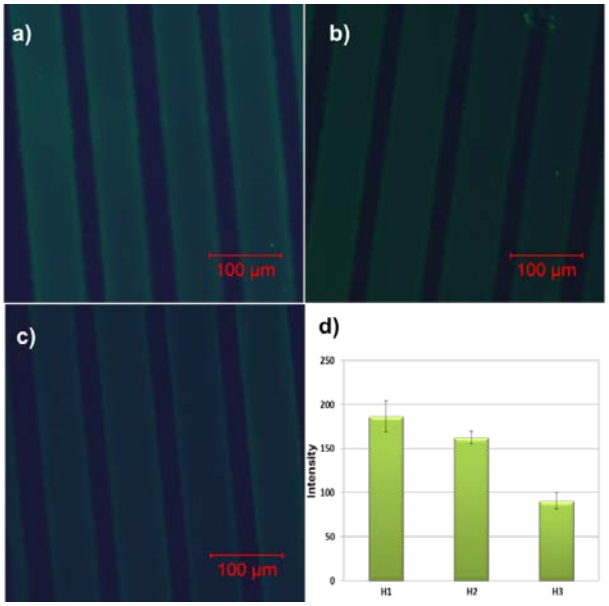

Figure 7.10. Fluorescence intensity of BODIPY-SH attached patterned hydrogel surface from different polymers a) patterned hydrogel using P4 polymer, b) patterned hydrogel using P5 polymer c) patterned hydrogel using P6 polymer, d) Relative fluorescence intensity of of the surface a, b and c.

7.3.4.2. Synthesis and Functionalization of Hydrogels via Photolithography. Copolymer P5 was used to fabricate a micro-patterned hydrogel through photolithography technique with the exposure of UV irradiation to induce the crosslinking. The duration of exposure to UV-irradiation was varied as 5, and 10 minutes with the goal of achieving different amounts of

crosslinking. It should be noted that increased amount of crosslinking will lead to a decrease in the amount of residual maleimide groups available for functionalization. All hydrogels were incubated with similar amount of the thiol-containing dye to obtain fluorescently labelled hydrogels (Figure7.11). The extent of dye attachment to hydrogel micro-patterns obtained using different UV-exposure was measured using fluorescence microscopy. As expected, it was observed that patterned hydrogel obtained with the shortest amount of exposure time showed the highest fluorescence intensity when compared to the other hydrogel. However, less exposure to UV irradiation reduced the efficiency of adhesion of the hydrogel micro-patterns onto the surfaces and they peeled off upon gentle agitation during the rinsing process (Figure 7.11.a).

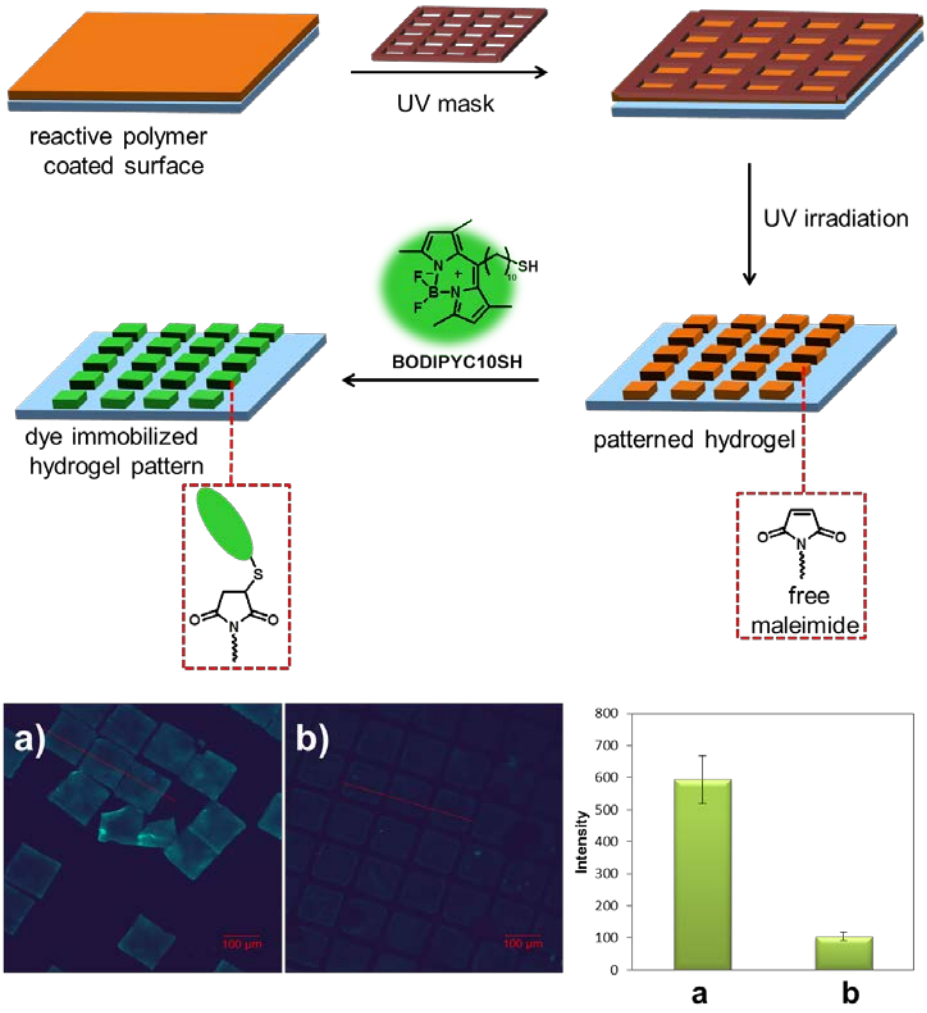

Figure 7.11. Patterning of P5 through photolithography and fluorescence microscope images of BODIPYC10SH immobilized patterns a) 5 min b) 10 min UV irradiation time.

7.3.4.3. Reversible Immobilization on the Micropatterned Hydrogels via the Diels-Alder/ retro Diels-Alder reactions. A micro-patterned hydrogel surface was prepared using copolymer P5 via photolithography, as described in the previous sections. Residual maleimide groups were derivatized with furan-containing BODIPY-based fluorescent dye using the Diels-Alder cycloaddition reaction. The effective attachment of the dye via cycloaddition between maleimide moiety and furan was clearly evident from the strong green fluorescence of the modified surface (Figure 7.12). To demonstrate the thermoreversibility of this functionalization via the retro Diels-Alder reaction, the surface containing dye-modified hydrogel patterns was heated in toluene at 110 ^{o}C. Loss of the fluorescence of the hydrogel micro-patterns suggests that the dye has effectively detached from the hydrogels (Figure 7.12.b). One can reattach the furan appended dye onto the renewed surface with similar efficiency as the initial functionalization by subjecting to a cycloaddition reaction.

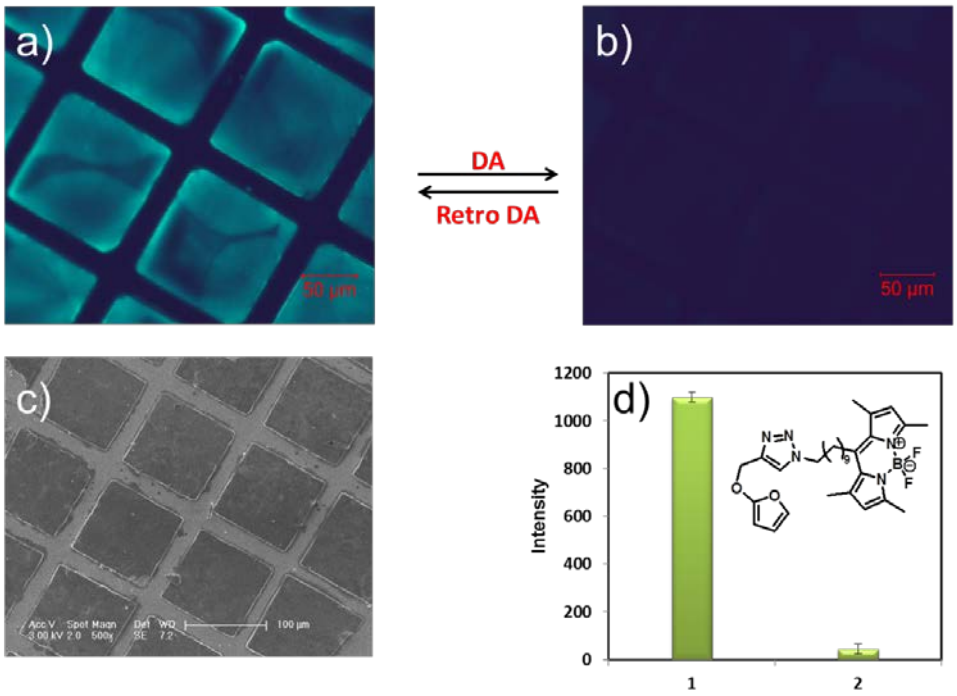

Figure 7.12. Attachment of furan containing dye molecule to the hydrogel pattern a) after dye attachment b) after removal of dye molecule c) SEM micrograph of the hydrogel pattern.d) Fluorescence intensity of the surface before and after attachment of the dye molecule.

7.3.5. Ligand-mediated Biomolecular Immobilization on Hydrogel Micro-patterns

The efficiency of biomolecular immobilization onto the patterned hydrogel surfaces was investigated. The protein Extravidin has four binding sites with very high affinity for the ligand biotin, and thus has been extensively employed as an adaptor molecule between a biotinylated surface and other biotinylated molecules. First, biotin-SH was conjugated to hydrogel micro-patterns obtained using copolymer P5 via the Michael addition reaction. Then, labelled Extravidin was bound to the biotinylated surface via non-covalent interactions. The bright red fluorescence in Figure 7.13.c proves the successful bioimmobilization of Extravidin onto the biotinylated hydrogels. As a control, we also performed the same experiment without biotinylation of the patterned hydrogel and no noticeable fluorescence was observed (Figure 7.13.d). It proves that Extravidin specifically binds to biotin ligands on the biotinylated hydrogel with minimal non-specific attachment.

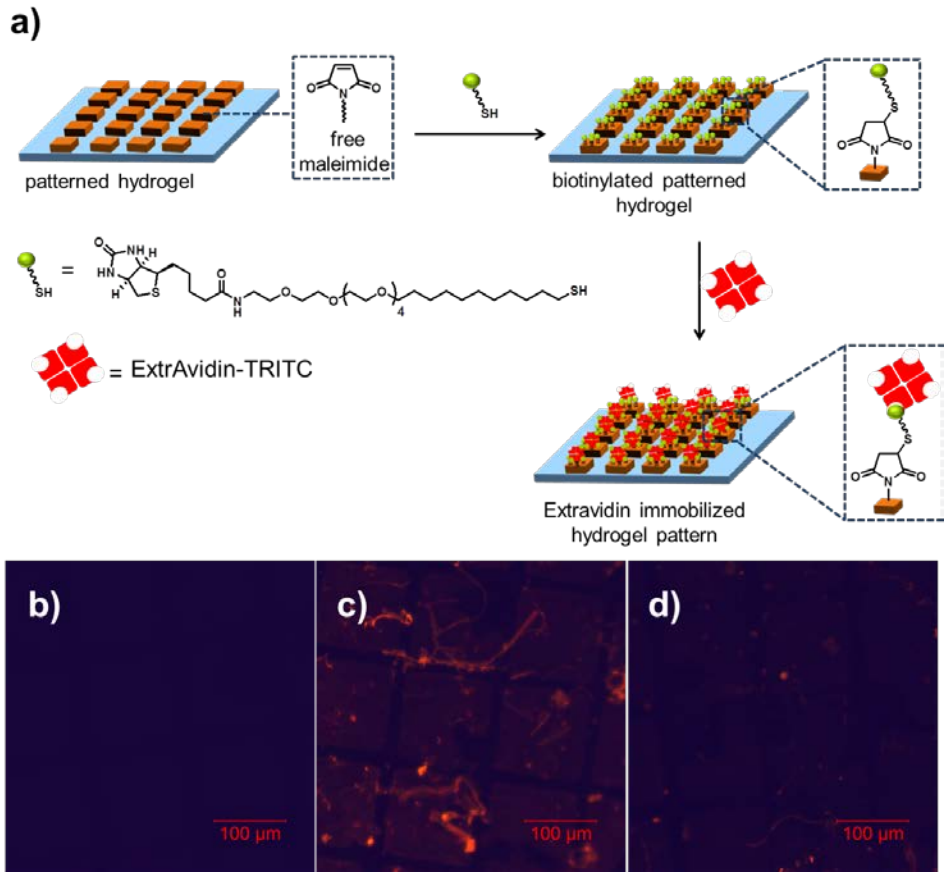

Figure 7.13. a) General schema for the immobilization of fluorescently labeled Extravidin to biotinylated surface. Fluorescence microscopy images of b) hydrogel pattern c) after attachment of ExtraAvidin to the biotinylated surface d) Control experiment: Extravidin immobilization without biotinylation.

7.4. Conclusion

ABA type triblock copolymers containing varying amounts of the maleimide functional group in the outer blocks were synthesized using a linear PEG macroinitiator as the middle block. Bulk and micro-patterned hydrogels utilizing these triblock copolymers were prepared under UV irradiation via a photoinitiator free photo-crosslinking of pendant maleimide groups. The effect of the composition of maleimide to PEG-based side chains on the water uptake capacity of bulk hydrogels was investigated. Scanning electron microscopy was used to study the morphology of the bulk hydrogels. SEM images revealed that the structure with higher porosity was observed for hydrogel with higher maleimide content. Different patterning strategies such as MIMIC and photolithography were employed to fabricate micro-patterned hydrogels. These patterned hydrogels were functionalized either *via* the Michael addition reaction using a thiol-containing dye or with the Diels-Alder cycloaddition through furan containing dye molecules. Additionally, tunability of the degree of functionalization of these hydrogels can be modified by either changing the amount of maleimide groups within the patterned hydrogels or changing the duration of UV irradiation. Overall, a single component gelation based strategy to obtain bulk and micro-patterned reactive functionalizable hydrogels was developed using the novel class of maleimide containing triblock copolymers.

8. CONCLUSIONS

In this dissertation we investigated the design of novel reactive polymeric materials for the application of in biomedical sciences. In particular, we developed synthetic strategies of fabricating novel functional polymers, multifunctional hydrogels and bio-functionalizable micro-patterned hydrogels on surfaces. These polymeric materials were designed to facilitate their efficient post-polymerization modification to conjugate molecules and/or or biomolecules of interest. For both the synthesis and functionalization of these polymeric materials combinations of various available “click” reactions were utilized. Proper combinations of functional group handles on these polymeric scaffolds provided orthogonal methods of their functionalization. Among the various ligation strategies, nucleophilic reactions between activated esters or carbonates, Huisgen-type 1,3-dipolar cycloaddition, thiol-epoxy chemistry, Diels-Alder reaction, [2+2] cycloaddition chemistry, radical thiol-ene reactions and Michael type thiol-maleimide coupling were the were employed as tools for synthesis and functionalization of these materials. Parallel utilization of various lithographic techniques during the fabrication of crosslinked polymeric systems allows the creation of functional micropatterns.

The first chapter of this dissertation provides general information about the current status of functionalizable polymeric materials obtained using reactive monomers and polymers. In addition, background information for the chemical ligation strategies and literature examples that are used in the design or functionalization of polymeric materials were briefly discussed.

The second chapter gives a general overwiew of the thesis. It describes in brief the goals of the research undertaken to culminate this thesis.

The third chapter described the synthesis of a novel amine-reactive carbonate monomer which was also used in the design of polymers with orthogonal reactivities. Since carbonate group plays an important role in drug delivery, carbonate containing orthogonally functionalizable polymers with hydrolyzable and non-hydrolyzable side chains was synthesized. Hydrolyzable or non-hydrolyzable characteristics were provides

one with the opportunity to attach both drug and targeting moiety at the same time for various biomedical applications. As a future work, fabrication of various drug delivery systems can be pursued utilizing the newly disclosed carbonate monomer.

The fourth chapter of the thesis describes the synthesis of reactive hydrogels and further modifications of them utilizing thiol-epoxy chemistry. Two different pathways were investigated to obtain hydrogels using the thiol-epoxy chemistry. First strategy involved the direct gelation of commercially available monomers or polymers via anionic thiol-epoxy reaction. Both PDMS and PEG based polymers were used for network formation to provide materials with enhanced mechanical properties while preserving the hydrophilic nature. After the gelation step, resulting secondary hydroxyl group was used as a reactive handle for functionalization. In the second strategy of this chapter we aimed to utilize thiol-epoxy chemistry for the post-modification of the hydrogels obtained using photo-crosslinking. So we synthesized copolymers containing both double bonds and epoxy groups in the side chains. In addition, side chains were incorporated with some diethylene glycol units which imparted thermo-responsiveness to these hydrogels.

Chapter five presented a strategy to design patterned hydrogel materials via non-covalent crosslinking and nanoimprint lithography. Nanoimprint lithography was used to create thiol-reactive sub-micron platforms that were stable via hydrophilic hydrophobic balance of the polymeric materials through non-covalent crosslinking. Balance between hydrophilic PEG and hydrophobic methyl methacrylate made the platforms stable and anti-biofouling property of PEG units prevented non-specific interactions to the patterned surfaces. These thiol-reactive patterned surfaces enabled successful immobilization of dyes, peptides and cells.

Chapter six outlines fabrication of hydrogels using thiol-ene crosslinking. Photolithography techniques were used in combination to obtain micropatterns. Furan-protected-maleimide based triblock copolymers were synthesized and functionalization of these polymers was done through partial activation of furan-protected maleimide chains. Residual furan-protected maleimide units after fabrication were activated to their thiol reactive form via retro Diels-Alder reaction and were used for various immobilization studies.

The last chapter of this dissertation addressed the synthesis of crosslinked polymeric materials without employing additional crosslinkers and photoinitiators. In that respect we focused on the dimerization of maleimide units in the side chains of triblock copolymers for the synthesis of both bulk hydrogels and patterned hydrogel surfaces. Also the remaining maleimide units after the crosslinking procedure are available for further functionalization. We used the remaining maleimide groups for conjugation studies via two different pathways: via the thiol mediated Michael reaction and the thermo-reversible Diels-Alder reaction.

In summary, various efficient coupling chemistries have been utilized to fabricate and functionalize multifunctional polymeric materials. The ease of their preparation and efficient functionalization makes them attractive candidates for several biomedical applications.

APPENDIX A: SPECTROSCOPY DATA

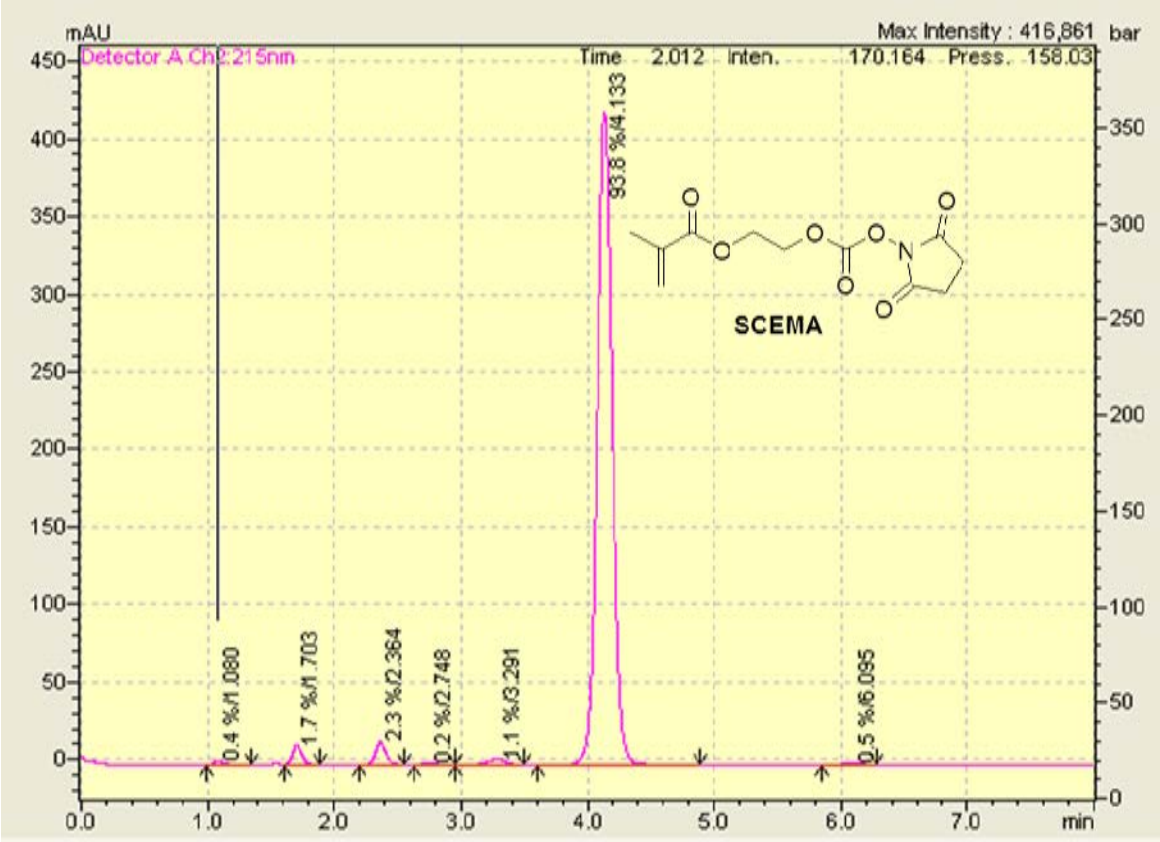

Figure A.1. HPLC spectrum of SCEMA (Chapter 3).

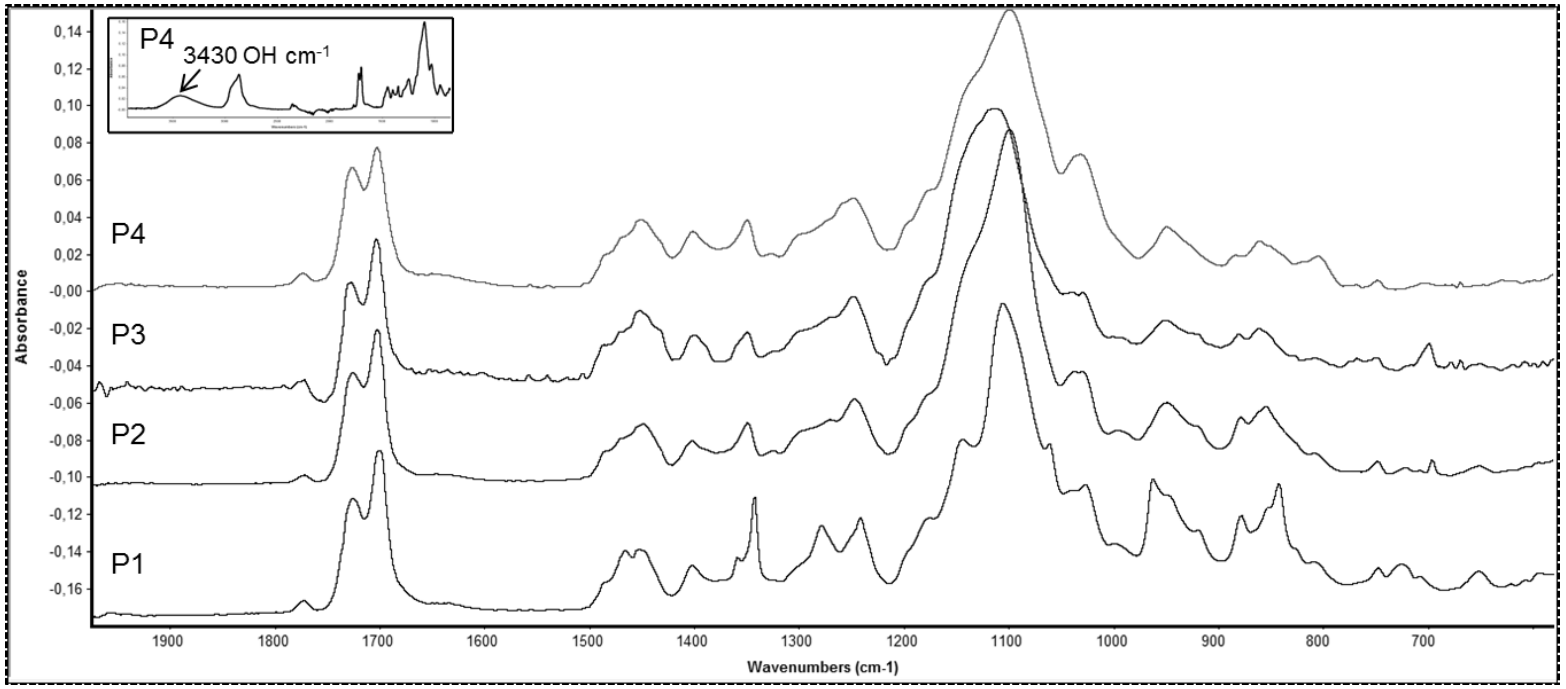

Figure A.2. FT-IR spectra of P1, P2, P3 and P4 (Chapter 6).

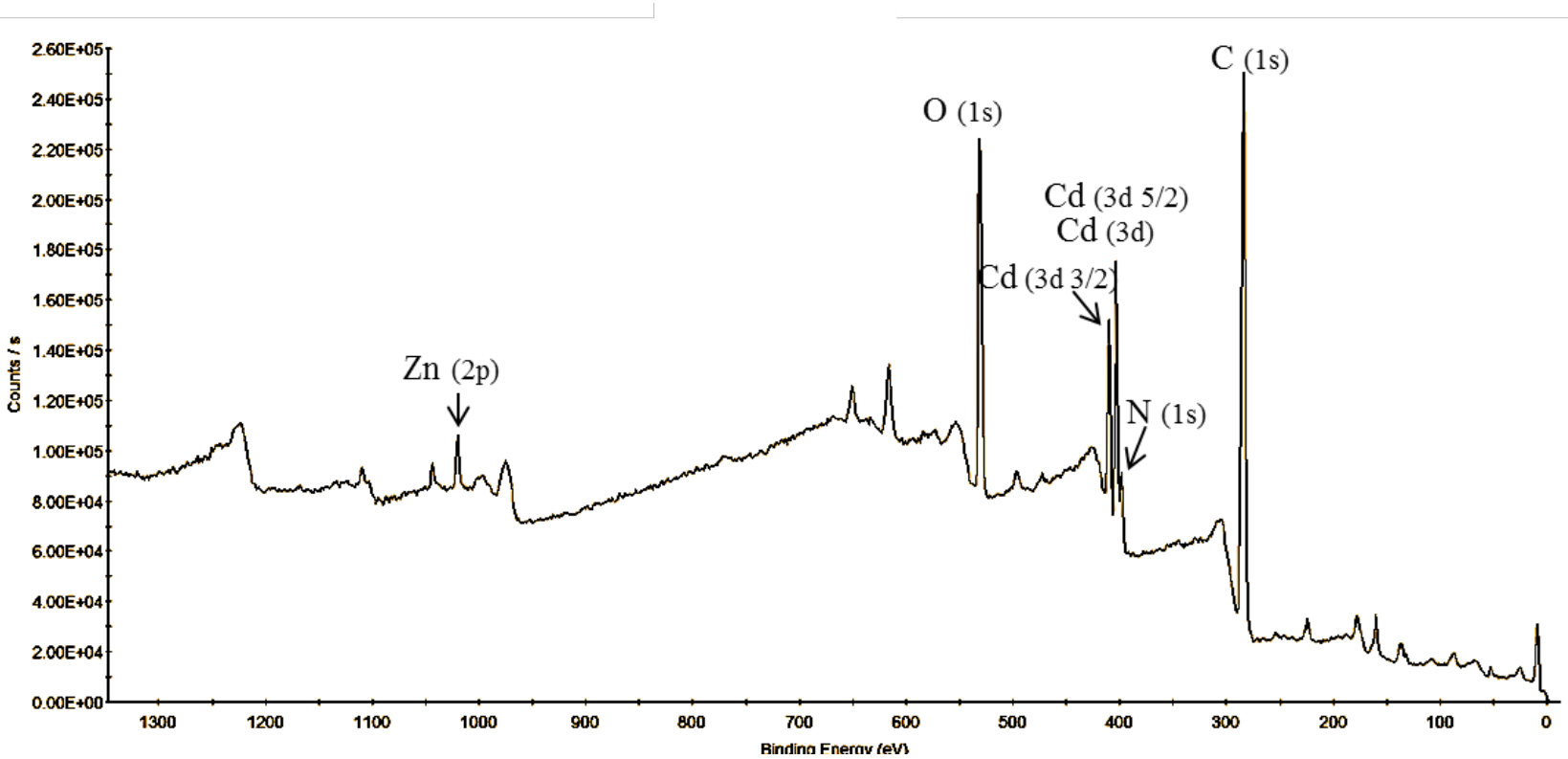

Figure A.3. XPS spectrum of pattern H3, after QD attachment to biotinylated surface (Chapter 6).

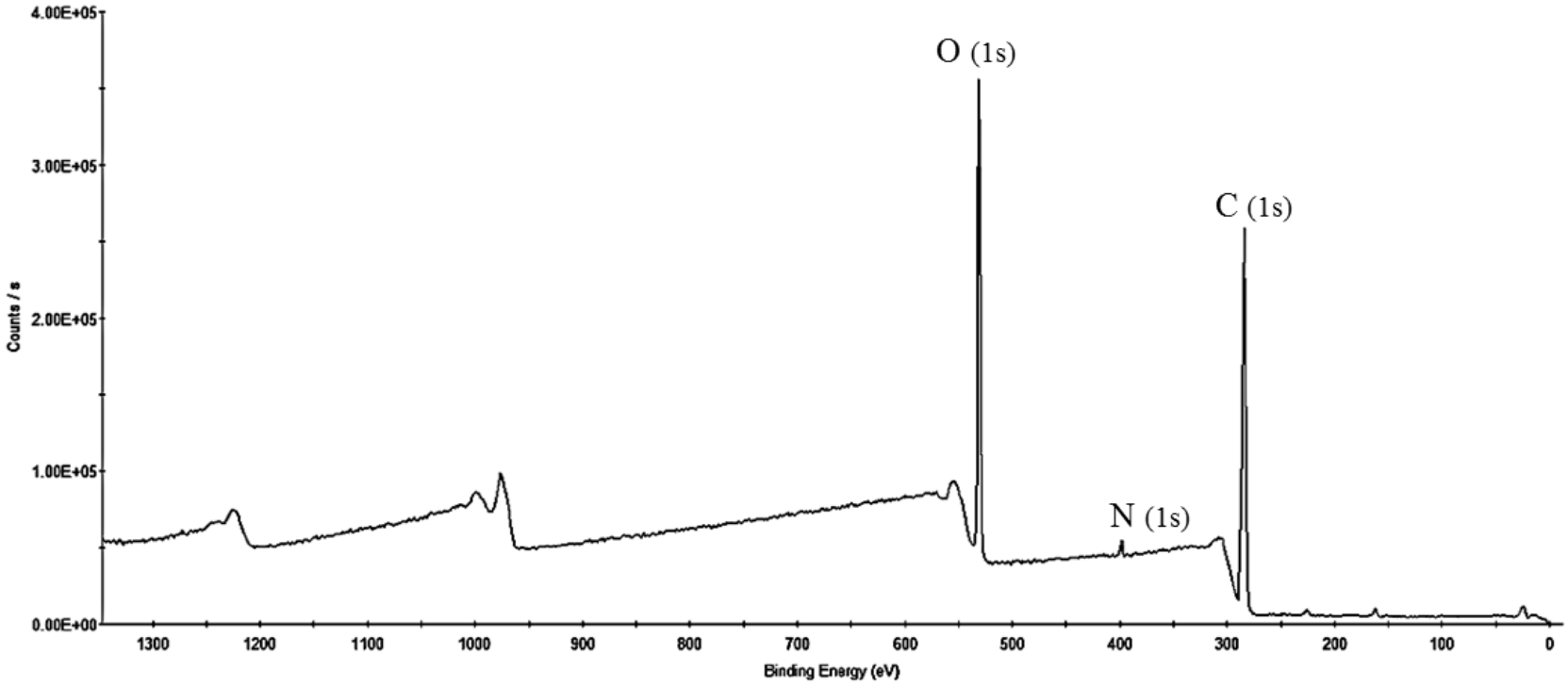

Figure A.4. XPS spectrum of pattern H3, after biotinylation (Chapter 6).

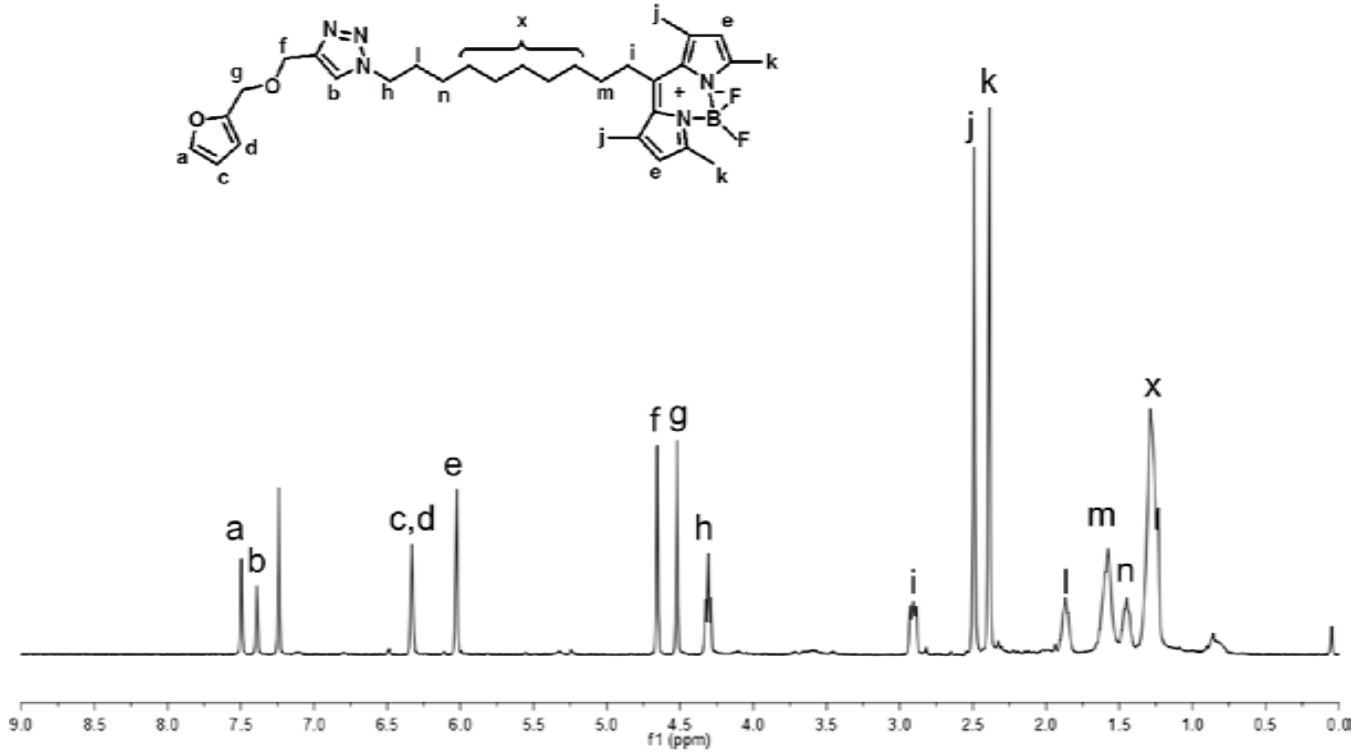

Figure A.5. H-NMR spectrum of BODIPY-Furan (Chapter 7).

REFERENCES

1. Theato, P., B. S. Sumerlin, R. K. O'Reilly, T. H. Epps, 3rd, "Stimuli Responsive Materials", *Chemical Society Reviews*, Vol. 42, pp. 7055-7056, 2013.

2. Tahir, M. N., M. Eberhardt, H. A. Therese, U. Kolb, P. Theato, W. E. Muller, H. C. Schroder, W. Tremel, "From Single Molecules to Nanoscopically Structured Functional Materials: Au Nanocrystal Growth on TiO_2 Nanowires Controlled by Surface-Bound Silicatein", *Angewandte Chemie International Edition*, Vol. 45, pp. 4803-4809, 2006.

3. Kessler, D., P. J. Roth, P. Theato, "Reactive Surface Coatings Based on Polysilsesquioxanes: Controlled Functionalization for Specific Protein Immobilization", *Langmuir*, Vol. 25, pp. 10068-10076, 2009.

4. Cheng, R., F. Meng, C. Deng, H. A. Klok, Z. Zhong, "Dual and Multi-Stimuli Responsive Polymeric Nanoparticles for Programmed Site-Specific Drug Delivery", *Biomaterials*, Vol. 34, pp. 3647-3657, 2013.

5. Perrier, S., S. P. Armes, X. S. Wang, F. Malet, D. M. Haddleton, "Copper(I)-Mediated Radical Polymerization of Methacrylates in Aqueous Solution", *Journal of Polymer Science Part a-Polymer Chemistry*, Vol. 39, pp. 1696-1707, 2001.

6. Levere, M. E., I. Willoughby, S. O'Donohue, A. de Cuendias, A. J. Grice, C. Fidge, C. R. Becer, D. M. Haddleton, "Assessment of Set-Lrp in Dmso Using Online Monitoring and Rapid Gpc", *Polymer Chemistry*, Vol. 1, pp. 1086-1094, 2010.

7. Rusu, E., E. Comanita, A. Airinei, G. Rusu, "Photosensitive Monomers and Polymers Derived from Glycidyl Cinnamate", *Iranian Polymer Journal*, Vol. 7, pp. 157-162, 1998.

8. Wiles, K. B., V. A. Bhanu, A. J. Pasquale, T. E. Long, J. E. McGrath, "Monomer Reactivity Ratios for Acrylonitrile-Methyl Acrylate Free-Radical Copolymerization", *Journal of Polymer Science Part a-Polymer Chemistry*, Vol. 42, pp. 2994-3001, 2004.

9. Beuermann, S., M. Buback, "Rate Coefficients of Free-Radical Polymerization Deduced from Pulsed Laser Experiments", *Progress in Polymer Science*, Vol. 27, pp. 191-254, 2002.

10. Buback, M., R. G. Gilbert, R. A. Hutchinson, B. Klumperman, F. D. Kuchta, B. G. Manders, K. F. Odriscoll, G. T. Russell, J. Schweer, "Critically Evaluated Rate

Coefficients for Free-Radical Polymerization .1. Propagation Rate Coefficient for Styrene", *Macromolecular Chemistry and Physics*, Vol. 196, pp. 3267-3280, 1995.

11. Beuermann, S., M. Buback, T. P. Davis, R. G. Gilbert, R. A. Hutchinson, O. F. Olaj, G. T. Russell, J. Schweer, A. M. vanHerk, "Critically Evaluated Rate Coefficients for Free-Radical Polymerization .2. Propagation Rate Coefficients for Methyl Methacrylate", *Macromolecular Chemistry and Physics*, Vol. 198, pp. 1545-1560, 1997.

12. Buback, M., A. Feldermann, C. Barner-Kowollik, I. Lacik, "Propagation Rate Coefficients of Acrylate-Methacrylate Free-Radical Bulk Copolymerizations", *Macromolecules*, Vol. 34, pp. 5439-5448, 2001.

13. Sreedhar, M., N. Satyanarayana, "Reactivity Ratios of the 3-Methoxy-4-(2-Hydroxy-3-Methacryloloxypropoxy)Benzaldehyde and Methyl-Methacrylate System from H-^{1}-NMR", *Polymer*, Vol. 35, pp. 3703-3705, 1994.

14. Mansfeld, U., C. Pietsch, R. Hoogenboom, C. R. Becer, U. S. Schubert, "Clickable Initiators, Monomers and Polymers in Controlled Radical Polymerizations – a Prospective Combination in Polymer Science", *Polymer Chemistry*, Vol. 1, p 1560, 2010.

15. Kolb, H. C., M. G. Finn, K. B. Sharpless, "Click Chemistry: Diverse Chemical Function from a Few Good Reactions", *Angewandte Chemie International Edition*, Vol. 40, pp. 2004-2021, 2001.

16. Evans, R. A., "The Rise of Azide-Alkyne 1,3-Dipolar 'Click' Cycloaddition and Its Application to Polymer Science and Surface Modification", *Australian Journal of Chemistry*, Vol. 60, pp. 384-395, 2007.

17. Killops, K. L., L. M. Campos, C. J. Hawker, "Robust, Efficient, and Orthogonal Synthesis of Dendrimers Via Thiol-Ene "Click" Chemistry", *Journal of the American Chemical Society*, Vol. 130, pp. 5062-5064, 2008.

18. DeForest, C. A., E. A. Sims, K. S. Anseth, "Peptide-Functionalized Click Hydrogels with Independently Tunable Mechanics and Chemical Functionality for 3d Cell Culture", *Chemistry of Materials*, Vol. 22, pp. 4783-4790, 2010.

19. Altin, H., I. Kosif, R. Sanyal, "Fabrication of "Clickable" Hydrogels Via Dendron-Polymer Conjugates", *Macromolecules*, Vol. 43, pp. 3801-3808, 2010.

20. Kim, Y. G., S. O. Ho, N. R. Gassman, Y. Korlann, E. V. Landorf, F. R. Collart, S. Weiss, "Efficient Site-Specific Labeling of Proteins Via Cysteines", *Bioconjugate Chemistry*, Vol. 19, pp. 786-791, 2008.

21. Heredia, K. L., H. D. Maynard, "Synthesis of Protein-Polymer Conjugates", *Organic & Biomolecular Chemistry*, Vol. 5, pp. 45-53, 2007.

22. Ho, H. T., F. Leroux, S. Pascual, V. Montembault, L. Fontaine, "Amine-Reactive Polymers Synthesized by Raft Polymerization Using an Azlactone Functional Trithiocarbonate Raft Agent", *Macromolecular Rapid Communications*, Vol. 33, pp. 1753-1758, 2012.

23. Batz, H. G., G. Franzmann, H. Ringsdorf, "Model Reactions for Synthesis of Pharmacologically Active Polymers by Way of Monomeric and Polymeric Reactive Esters", *Angewandte Chemie International Edition*, Vol. 11, pp. 1103-1104, 1972.

24. Ferruti, P., A. Fere, A. Bettelli, "High Polymers of Acrylic and Methacrylic Esters of N-Hydroxysuccinimide as Polyacrylamide and Polymethacrylamide Precursors", *Polymer*, Vol. 13, pp. 462-464, 1972.

25. Roth, P. J., F. D. Jochum, R. Zentel, P. Theato, "Synthesis of Hetero-Telechelic Alpha,Omega Bio-Functionalized Polymers", *Biomacromolecules*, Vol. 11, pp. 238-244, 2010.

26. Roth, P. J., M. Haase, T. Basche, P. Theato, R. Zentel, "Synthesis of Heterotelechelic Alpha,Omega Dye-Functionalized Polymer by the Raft Process and Energy Transfer between the End Groups", *Macromolecules*, Vol. 43, pp. 895-902, 2010.

27. Kessler, D., P. Theato, "Reactive Surface Coatings Based on Polysilsesquioxanes: Defined Adjustment of Surface Wettability", *Langmuir*, Vol. 25, pp. 14200-14206, 2009.

28. Kessler, D., P. J. Roth, P. Theato, "Reactive Surface Coatings Based on Polysilsesquioxanes: Controlled Functionalization for Specific Protein Immobilization", *Langmuir*, Vol. 25, pp. 10068-10076, 2009.

29. Wiss, K. T., O. D. Krishna, P. J. Roth, K. L. Kiick, P. Theato, "A Versatile Grafting-to Approach for the Bioconjugation of Polymers to Collagen-Like Peptides Using an Activated Ester Chain Transfer Agent", *Macromolecules*, Vol. 42, pp. 3860-3863, 2009.

30. Theato, P., J. U. Kim, J. C. Lee, "Controlled Radical Polymerization of Active Ester Monomers: Precursor Polymers for Highly Functionalized Materials", *Macromolecules*, Vol. 37, pp. 5475-5478, 2004.

31. Theato, P., "Synthesis of Well-Defined Polymeric Activated Esters", *Journal of Polymer Science Part a-Polymer Chemistry*, Vol. 46, pp. 6677-6687, 2008.

32. Savariar, E. N., S. Thayumanavan, "Controlled Polymerization of N-Isopropylacrylamide with an Activated Methacrylic Ester", *Journal of Polymer Science Part a-Polymer Chemistry*, Vol. 42, pp. 6340-6345, 2004.

33. Li, H. M., A. P. Bapat, M. Li, B. S. Sumerlin, "Protein Conjugation of Thermoresponsive Amine-Reactive Polymers Prepared by Raft", *Polymer Chemistry*, Vol. 2, pp. 323-327, 2011.

34. Bunte, C., O. Prucker, T. Konig, J. Ruhe, "Enzyme Containing Redox Polymer Networks for Biosensors or Biofuel Cells: A Photochemical Approach", *Langmuir*, Vol. 26, pp. 6019-6027, 2010.

35. Duwez, A. S., S. Cuenot, C. Jerome, S. Gabriel, R. Jerome, S. Rapino, F. Zerbetto, "Mechanochemistry: Targeted Delivery of Single Molecules", *Nature Nanotechnology*, Vol. 1, pp. 122-125, 2006.

36. Eberhardt, M., R. Mruk, R. Zentel, P. Theato, "Synthesis of Pentafluorophenyl(Meth)Acrylate Polymers: New Precursor Polymers for the Synthesis of Multifunctional Materials", *European Polymer Journal*, Vol. 41, pp. 1569-1575, 2005.

37. Morpurgo, M., E. A. Bayer, M. Wilchek, "N-Hydroxysuccinimide Carbonates and Carbamates Are Useful Reactive Reagents for Coupling Ligands to Lysines on Proteins", *Journal of Biochemical and Biophysical Methods*, Vol. 38, pp. 17-28, 1999.

38. Pessah, N., M. Reznik, M. Shamis, F. Yantiri, H. Xin, K. Bowdish, N. Shomron, G. Ast, D. Shabat, "Bioactivation of Carbamate-Based 20(S)-Camptothecin Prodrugs", *Bioorganic Medicinal & Chemistry*, Vol. 12, pp. 1859-1866, 2004.

39. Rokicki, G., "Aliphatic Cyclic Carbonates and Spiroorthocarbonates as Monomers", *Progress in Polymer Science*, Vol. 25, pp. 259-342, 2000.

40. Khandare, J., T. Minko, "Polymer-Drug Conjugates: Progress in Polymeric Prodrugs", *Progress in Polymer Science*, Vol. 31, pp. 359-397, 2006.

41. Simplicio, A. L., J. M. Clancy, J. F. Gilmer, "Prodrugs for Amines", *Molecules*, Vol. 13, pp. 519-547, 2008.

42. Diamanti, S., S. Arifuzzaman, A. Elsen, J. Genzer, R. A. Vaia, "Reactive Patterning Via Post-Functionalization of Polymer Brushes Utilizing Disuccinimidyl Carbonate Activation to Couple Primary Amines", *Polymer*, Vol. 49, pp. 3770-3779, 2008.

43. Lee, B. S., Y. S. Chi, K. B. Lee, Y. G. Kim, I. S. Choi, "Functionalization of Poly(Oligo(Ethylene Glycol)Methacrylate) Films on Gold and Si/Sio2 for Immobilization of Proteins and Cells: Spr and Qcm Studies", *Biomacromolecules*, Vol. 8, pp. 3922-3929, 2007.

44. Talbot, J. D. R., "The Kinetics of the Epoxy Amine Cure Reaction from a Solvation Perspective", *Journal of Polymer Science Part a-Polymer Chemistry*, Vol. 42, pp. 3579-3586, 2004.

45. Kang, T., R. J. Amir, A. Khan, K. Ohshimizu, J. N. Hunt, K. Sivanandan, M. I. Montanez, M. Malkoch, M. Ueda, C. J. Hawker, "Facile Access to Internally Functionalized Dendrimers through Efficient and Orthogonal Click Reactions", *Chemical Communications*, Vol. 46, pp. 1556-1558, 2010.

46. Hamid, Z. A. A., A. Blencowe, B. Ozcelik, J. A. Palmer, G. W. Stevens, K. M. Abberton, W. A. Morrison, A. J. Penington, G. G. Qiao, "Epoxy-Amine Synthesised Hydrogel Scaffolds for Soft-Tissue Engineering", *Biomaterials*, Vol. 31, pp. 6454-6467, 2010.

47. Roche, A. A., J. Bouchet, S. Bentadjine, "Formation of Epoxy-Diamine/Metal Interphases", *International Journal of Adhesion and Adhesives*, Vol. 22, pp. 431-441, 2002.

48. Qin, J. L., X. B. Jiang, L. Gao, Y. M. Chen, F. Xi, "Functional Polymeric Nanoobjects by Cross-Linking Bulk Self-Assemblies of Poly(Tert-Butyl Acrylate)-Block-Poly(Glycidyl Methacrylate)", *Macromolecules*, Vol. 43, pp. 8094-8100, 2010.

49. Yan, Y., D. J. Siegwart, "Scalable Synthesis and Derivation of Functional Polyesters Bearing Ene and Epoxide Side Chains", *Polymer Chemistry*, Vol. 5, p 1362-1371, 2014.

50. Decicco, C. P., J. L. Seng, K. E. Kennedy, M. B. Covington, P. K. Welch, E. C. Arner, R. L. Magolda, D. J. Nelson, "Amide Surrogates of Matrix Metalloproteinase Inhibitors: Urea and Sulfonamide Mimics", *Bioorganic & Medicinal Chemistry Letters*, Vol. 7, pp. 2331-2336, 1997.

51. Carnaroglio, D., K. Martina, G. Palmisano, A. Penoni, C. Domini, G. Cravotto, "One-Pot Sequential Synthesis of Isocyanates and Urea Derivatives Via a Microwave-Assisted Staudinger-Aza-Wittig Reaction", *Beilstein Journal of Organic Chemistry*, Vol. 9, pp. 2378-2386, 2013.

52. Duong, H. T. T., V. T. Huynh, P. de Souza, M. H. Stenzel, "Core-Cross-Linked Micelles Synthesized by Clicking Bifunctional Pt(Iv) Anticancer Drugs to Isocyanates", *Biomacromolecules*, Vol. 11, pp. 2290-2299, 2010.

53. Yilgor, E., I. Yilgor, "Hydrogen Bonding: A Critical Parameter in Designing Silicone Copolymers", *Polymer*, Vol. 42, pp. 7953-7959, 2001.

54. Takahara, A., J. Tashita, T. Kajiyama, M. Takayanagi, "Effect of Aggregation State of Hard Segment in Segmented Poly(Urethaneureas) on Their Fatigue Behavior after Interaction with Blood Components", *Journal of Biomedical Materials Research*, Vol. 19, pp. 13-34, 1985.

55. Hayashi, K., H. Takano, T. Matsuda, M. Umezu, "Mechanical Stability of Elastomeric Polymers for Blood Pump Applications", *Journal of Biomedical Materials Research*, Vol. 19, pp. 179-193, 1985.

56. Beck, J. B., K. L. Killops, T. Kang, K. Sivanandan, A. Bayles, M. E. Mackay, K. L. Wooley, C. J. Hawker, "Facile Preparation of Nanoparticles by Intramolecular Cross-Linking of Isocyanate Functionalized Copolymers", *Macromolecules*, Vol. 42, pp. 5629-5635, 2009.

57. Boyer, C., V. Bulmus, T. P. Davis, V. Ladmiral, J. Q. Liu, S. Perrier, "Bioapplications of Raft Polymerization", *Chemical Reviews*, Vol. 109, pp. 5402-5436, 2009.

58. Redeker, E. S., D. T. Ta, D. Cortens, B. Billen, W. Guedens, P. Adriaensens, "Protein Engineering for Directed Immobilization", *Bioconjugate Chemistry*, Vol. 24, pp. 1761-1777, 2013.

59. Hoyle, C. E., A. B. Lowe, C. N. Bowman, "Thiol-Click Chemistry: A Multifaceted Toolbox for Small Molecule and Polymer Synthesis", *Chemical Society Reviews*, Vol. 39, pp. 1355-1387, 2010.

60. Streitwieser, A., "Solvolytic Displacement Reactions at Saturated Carbon Atoms", *Chem Reviews*, Vol. 56, pp. 571-752, 1956.

61. Jian, Y., Y. He, Y. K. Sun, H. T. Yang, W. T. Yang, J. Nie, "Thiol-Epoxy/Thiol-Acrylate Hybrid Materials Synthesized by Photopolymerization", *Journal of Materials Chemistry C*, Vol. 1, pp. 4481-4489, 2013.

62. Brandle, A., A. Khan, "Thiol-Epoxy 'Click' Polymerization: Efficient Construction of Reactive and Functional Polymers", *Polymer Chemistry*, Vol. 3, pp. 3224-3227, 2012.

63. De, S., A. Khan, "Efficient Synthesis of Multifunctional Polymers Via Thiol-Epoxy "Click" Chemistry", *Chemical Communications*, Vol. 48, pp. 3130-3132, 2012.

64. Gadwal, I., A. Khan, "Protecting-Group-Free Synthesis of Chain-End Multifunctional Polymers by Combining Atrp with Thiol-Epoxy 'Click' Chemistry", *Polymer Chemistry*, Vol. 4, pp. 2440-2444, 2013.

65. Hoyle, C. E., C. N. Bowman, "Thiol-Ene Click Chemistry", *Angewandte Chemie International Edition*, Vol. 49, pp. 1540-1573, 2010.

66. Kade, M. J., D. J. Burke, C. J. Hawker, "The Power of Thiol-Ene Chemistry", *Journal of Polymer Science Part a-Polymer Chemistry*, Vol. 48, pp. 743-750, 2010.

67. Lowe, A. B., "Thiol-Ene "Click" Reactions and Recent Applications in Polymer and Materials Synthesis", *Polymer Chemistry*, Vol. 1, pp. 17-36, 2010.

68. Gupta, N., B. F. Lin, L. M. Campos, M. D. Dimitriou, S. T. Hikita, N. D. Treat, M. V. Tirrell, D. O. Clegg, E. J. Kramer, C. J. Hawker, "A Versatile Approach to High-Throughput Microarrays Using Thiol-Ene Chemistry (Vol 2, Pg 138, 2010)", *Nature Chemistry*, Vol. 4, pp. 424-424, 2012.

69. Sparks, B. J., E. F. T. Hoff, L. P. Hayes, D. L. Patton, "Mussel-Inspired Thiol-Ene Polymer Networks: Influencing Network Properties and Adhesion with Catechol Functionality", *Chemistry of Materials*, Vol. 24, pp. 3633-3642, 2012.

70. Goldmann, A. S., A. Walther, L. Nebhani, R. Joso, D. Ernst, K. Loos, C. Barner-Kowollik, L. Barner, A. H. E. Muller, "Surface Modification of Poly(Divinylbenzene) Microspheres Via Thiol-Ene Chemistry and Alkyne-Azide Click Reactions", *Macromolecules*, Vol. 42, pp. 3707-3714, 2009.

71. Bai, F., X. L. Yang, W. Q. Huang, "Synthesis of Narrow or Monodisperse Poly(Divinylbenzene) Microspheres by Distillation-Precipitation Polymerization", *Macromolecules*, Vol. 37, pp. 9746-9752, 2004.

72. Chatani, S., D. P. Nair, C. N. Bowman, "Relative Reactivity and Selectivity of Vinyl Sulfones and Acrylates Towards the Thiol-Michael Addition Reaction and Polymerization", *Polymer Chemistry*, Vol. 4, pp. 1048-1055, 2013.

73. Onbulak, S., S. Tempelaar, R. J. Pounder, O. Gok, R. Sanyal, A. P. Dove, A. Sanyal, "Synthesis and Functionalization of Thiol-Reactive Biodegradable Polymers", *Macromolecules*, Vol. 45, pp. 1715-1722, 2012.

74. Gu, W. F., G. J. Chen, M. H. Stenzel, "Synthesis of Glyco-Microspheres Via a Thiol-Ene Coupling Reaction", *Journal of Polymer Science Part a-Polymer Chemistry*, Vol. 47, pp. 5550-5556, 2009.

75. Yu, B., J. W. Chan, C. E. Hoyle, A. B. Lowe, "Sequential Thiol-Ene/Thiol-Ene and Thiol-Ene/Thiol-Yne Reactions as a Route to Well-Defined Mono and Bis End-Functionalized Poly(N-Isopropylacrylamide)", *Journal of Polymer Science Part a-Polymer Chemistry*, Vol. 47, pp. 3544-3557, 2009.

76. Sanyal, A., "Diels-Alder Cycloaddition-Cycloreversion: A Powerful Combo in Materials Design", *Macromolecular Chemistry and Physics*, Vol. 211, pp. 1417-1425, 2010.

77. Huisgen, R., "Centenary Lecture - 1,3-Dipolar Cycloadditions", *Proceedings of the Chemical Society of London*, pp. 357-369, 1961.

78. Kolb, H. C., M. G. Finn, K. B. Sharpless, "Click Chemistry: Diverse Chemical Function from a Few Good Reactions", *Angewandte Chemie-International Edition*, Vol. 40, pp. 2004-2021, 2001.

79. Rostovtsev, V. V., L. G. Green, V. V. Fokin, K. B. Sharpless, "A Stepwise Huisgen Cycloaddition Process: Copper(I)-Catalyzed Regioselective "Ligation" of Azides and Terminal Alkynes", *Angewandte Chemie-International Edition*, Vol. 41, pp. 2596-2599, 2002.

80. Baskin, J. M., J. A. Prescher, S. T. Laughlin, N. J. Agard, P. V. Chang, I. A. Miller, A. Lo, J. A. Codelli, C. R. Bertozzi, "Copper-Free Click Chemistry for Dynamic in Vivo Imaging", *Proceedings of the National Academy of Sciences of the United States of America*, Vol. 104, pp. 16793-16797, 2007.

81. Polaske, N. W., D. V. McGrath, J. R. McElhanon, "Thermally Reversible Dendronized Linear Ab Step-Polymers Via "Click" Chemistry", *Macromolecules*, Vol. 44, pp. 3203-3210, 2011.

82. Kose, M. M., S. Onbulak, I. I. Yilmaz, A. Sanyal, "Orthogonally "Clickable" Biodegradable Dendrons", *Macromolecules*, Vol. 44, pp. 2707-2714, 2011.

83. Robb, M. J., L. A. Connal, B. F. Lee, N. A. Lynd, C. J. Hawker, "Functional Block Copolymer Nanoparticles: Toward the Next Generation of Delivery Vehicles", *Polymer Chemistry*, Vol. 3, pp. 1618-1628, 2012.

84. Tasdelen, M. A., "Diels-Alder "Click" Reactions: Recent Applications in Polymer and Material Science", *Polymer Chemistry*, Vol. 2, pp. 2133-2145, 2011.

85. Durmaz, H., A. Sanyal, G. Hizal, U. Tunca, "Double Click Reaction Strategies for Polymer Conjugation and Post-Functionalization of Polymers", *Polymer Chemistry*, Vol. 3, pp. 825-835, 2012.

86. Hizal, G., U. Tunca, A. Sanyal, "Discrete Macromolecular Constructs Via the Diels-Alder "Click" Reaction", *Journal of Polymer Science Part a-Polymer Chemistry*, Vol. 49, pp. 4103-4120, 2011.

87. Brocksom, T. J., J. Nakamura, M. L. Ferreira, U. Brocksom, "The Diels-Alder Reaction: An Update", *Journal of the Brazilian Chemical Society*, Vol. 12, pp. 597-622, 2001.

88. Omurtag, P. S., U. S. Gunay, A. Dag, H. Durmaz, G. Hizal, U. Tunca, "Diels-Alder Click Reaction for the Preparation of Polycarbonate Block Copolymers", *Journal of Polymer Science Part a-Polymer Chemistry*, Vol. 51, pp. 2252-2259, 2013.

89. Kose, M. M., G. Yesilbag, A. Sanyal, "Segment Block Dendrimers Via Diels-Alder Cycloaddition", *Organic Letters*, Vol. 10, pp. 2353-2356, 2008.

90. Owen, S. C., S. A. Fisher, R. Y. Tam, C. M. Nimmo, M. S. Shoichet, "Hyaluronic Acid Click Hydrogels Emulate the Extracellular Matrix", *Langmuir*, Vol. 29, pp. 7393-7400, 2013.

91. Gevrek, T. N., R. N. Ozdeslik, G. S. Sahin, G. Yesilbag, S. Mutlu, A. Sanyal, "Functionalization of Reactive Polymeric Coatings Via Diels-Alder Reaction Using Microcontact Printing", *Macromolecular Chemistry and Physics*, Vol. 213, pp. 166-172, 2012.

92. Tonga, M., N. Cengiz, M. M. Kose, T. Dede, A. Sanyal, "Dendronized Polymers Via Diels-Alder "Click" Reaction", *Journal of Polymer Science Part a-Polymer Chemistry*, Vol. 48, pp. 410-416, 2010.

93. Seiffert, S., W. Oppermann, K. Saalwaechter, "Hydrogel Formation by Photocrosslinking of Dimethylmaleimide Functionalized Polyacrylamide", *Polymer*, Vol. 48, pp. 5599-5611, 2007.

94. Schmeling, N., K. Hunger, G. Engler, B. Breiten, P. Rolling, A. Mixa, C. Staudt, K. Kleinermanns, "Photo-Crosslinking of Poly[Ethene-Stat-(Methacrylic Acid)] Functionalised with Maleimide Side Groups", *Polymer International*, Vol. 58, pp. 720-727, 2009.

95. Tonga, M., G. Y. Tonga, G. Seber, O. Gok, A. Sanyal, "Dendronized Polystyrene Via Orthogonal Double-Click Reactions", *Journal of Polymer Science Part a-Polymer Chemistry*, Vol. 51, pp. 5029-5037, 2013.

96. Yilmaz, I. I., M. Arslan, A. Sanyal, "Design and Synthesis of Novel "Orthogonally" Functionalizable Maleimide-Based Styrenic Copolymers", *Macromolecular Rapid Communications*, Vol. 33, pp. 856-862, 2012.

97. Yang, S. K., M. Weck, "Covalent and Orthogonal Multi-Functionalization of Terpolymers", *Soft Matter*, Vol. 5, pp. 582-585, 2009.

98. Dag, A., H. Sahin, H. Durmaz, G. Hizal, U. Tunca, "Block-Brush Copolymers Via Romp and Sequential Double Click Reaction Strategy", *Journal of Polymer Science Part a-Polymer Chemistry*, Vol. 49, pp. 886-892, 2011.

99. Dag, A., H. Durmaz, E. Demir, G. Hizal, U. Tunca, "Heterograft Copolymers Via Double Click Reactions Using One-Pot Technique", *Journal of Polymer Science Part a-Polymer Chemistry*, Vol. 46, pp. 6969-6977, 2008.

100. D'Souza, A. J. M., E. M. Topp, "Release from Polymeric Prodrugs: Linkages and Their Degradation", *Journal of Pharmaceutical Sciences*, Vol. 93, pp. 1962-1979, 2004.

101. Zovko, M., B. Zorc, P. Novak, P. Tepes, B. Cetina-Cizmek, M. Horvat, "Macromolecular Prodrugs Xi. Synthesis and Characterization of Polymer-Estradiol Conjugate", *International Journal of Pharmaceutics*, Vol. 285, pp. 35-41, 2004.

102. Gac-Breton, S., J. Coudane, M. Boustta, M. Vert, "Norfloxacin-Poly(L-Lysine Citramide Imide) Conjugates and Structure-Dependence of the Drug Release", *Journal of Drug Targeting*, Vol. 12, pp. 297-307, 2004.

103. Li, X. L., N. W. Adams, D. B. Bennett, J. Feijen, S. W. Kim, "Synthesis of Poly(Hydroxypropylglutamine-Prazosin Carbamate) and Release Studies", *Pharmaceutical Research*, Vol. 8, pp. 527-530, 1991.

104. Zhao, H., K. Yang, A. Martinez, A. Basu, R. Chintala, H. C. Liu, A. Janjua, M. L. Wang, D. Filpula, "Linear and Branched Bicin Linkers for Releasable Pegylation of Macromolecules: Controlled Release in Vivo and in Vitro from Mono- and Multi-Pegylated Proteins", *Bioconjugate Chemistry*, Vol. 17, pp. 341-351, 2006.

105. Digilio, G., L. Barbero, C. Bracco, D. Corpillo, P. Esposito, G. Piquet, S. Traversa, S. Aime, "Nmr Structure of Two Novel Polyethylene Glycol Conjugates of the Human

Growth Hormone-Releasing Factor, Hgrf(1-29)-Nh2", *Journal of the American Chemical Society*, Vol. 125, pp. 3458-3470, 2003.

106. Greenwald, R. B., H. Zhao, J. Xia, D. C. Wu, S. Nervi, S. F. Stinson, E. Majerova, C. Bramhall, D. W. Zaharevitz, "Poly(Ethylene Glycol) Prodrugs of the Cdk Inhibitor, Alsterpaullone (Nsc 705701): Synthesis and Pharmacokinetic Studies", *Bioconjugate Chemistry*, Vol. 15, pp. 1076-1083, 2004.

107. Greenwald, R. B., Y. H. Choe, J. McGuire, C. D. Conover, "Effective Drug Delivery by Pegylated Drug Conjugates", *Advanced Drug Delivery Reviews*, Vol. 55, pp. 217-250, 2003.

108. Yoo, H. S., J. E. Oh, K. H. Lee, T. G. Park, "Biodegradable Nanoparticles Containing Doxorubicin-Plga Conjugate for Sustained Release", *Pharmaceutical Research*, Vol. 16, pp. 1114-1118, 1999.

109. Saari, W. S., J. E. Schwering, P. A. Lyle, S. J. Smith, E. L. Engelhardt, "Cyclization-Activated Prodrugs. Basic Esters of 5-Bromo-2'-Deoxyuridine", *Journal of Medicinal Chemistry*, Vol. 33, pp. 2590-2595, 1990.

110. Saari, W. S., J. E. Schwering, P. A. Lyle, S. J. Smith, E. L. Engelhardt, "Cyclization-Activated Prodrugs. Basic Carbamates of 4-Hydroxyanisole", *Journal of Medicinal Chemistry*, Vol. 33, pp. 97-101, 1990.

111. Ballatore, C., E. Hyde, R. F. Deiches, V. M. Lee, J. Q. Trojanowski, D. Huryn, A. B. Smith, 3rd, "Paclitaxel C-10 Carbamates: Potential Candidates for the Treatment of Neurodegenerative Tauopathies", *Bioorganic Medicinal Chemistry Letters*, Vol. 17, pp. 3642-3646, 2007.

112. Sproat, B. S., D. M. Brown, "A New Linkage for Solid Phase Synthesis of Oligodeoxyribonucleotides", *Nucleic Acids Research*, Vol. 13, pp. 2979-2987, 1985.

113. Tan, B. H., H. Hussain, Y. Liu, C. B. He, T. P. Davis, "Synthesis and Self-Assembly of Brush-Type Poly[Poly(Ethylene Glycol)Methyl Ether Methacrylate]-Block-Poly(Pentafluorostyrene) Amphiphilic Diblock Copolymers in Aqueous Solution", *Langmuir*, Vol. 26, pp. 2361-2368, 2010.

114. Stachowiak, T. B., D. A. Mair, T. G. Holden, L. J. Lee, F. Svec, J. M. J. Frechet, "Hydrophilic Surface Modification of Cyclic Olefin Copolymer Microfluidic Chips Using Sequential Photografting", *Journal of Separation Science*, Vol. 30, pp. 1088-1093, 2007.

115. Guanti, G., S. Perrozzi, R. Riva, "O-Protecting Groups as Long-Range Stereocontrolling Elements in the Addition of Acetylides to 4-Substituted Quinolines", *Tetrahedron-Asymmetry*, Vol. 13, pp. 2703-2726, 2002.

116. Monge, S., D. M. Haddleton, "Synthesis of Precursors of Poly(Acryl Amides) by Copper Mediated Living Radical Polymerization in Dmso", *European Polymer Journal*, Vol. 40, pp. 37-45, 2004.

117. Sumerlin, B. S., N. V. Tsarevsky, G. Louche, R. Y. Lee, K. Matyjaszewski, "Highly Efficient "Click" Functionalization of Poly(3-Azidopropyl Methacrylate) Prepared by Atrp", *Macromolecules*, Vol. 38, pp. 7540-7545, 2005.

118. DeForest, C. A., K. S. Anseth, "Advances in Bioactive Hydrogels to Probe and Direct Cell Fate", *Annual Review of Chemical and Biomolecular Engineering*, Vol. 3, pp. 421-444, 2012.

119. Slaughter, B. V., S. S. Khurshid, O. Z. Fisher, A. Khademhosseini, N. A. Peppas, "Hydrogels in Regenerative Medicine", *Advanced Materials*, Vol. 21, pp. 3307-3329, 2009.

120. Lin, C. C., K. S. Anseth, "Peg Hydrogels for the Controlled Release of Biomolecules in Regenerative Medicine", *Pharmaceutical Research*, Vol. 26, pp. 631-643, 2009.

121. Drury, J. L., D. J. Mooney, "Hydrogels for Tissue Engineering: Scaffold Design Variables and Applications", *Biomaterials*, Vol. 24, pp. 4337-4351, 2003.

122. Azagarsamy, M. A., K. S. Anseth, "Bioorthogonal Click Chemistry: An Indispensable Tool to Create Multifaceted Cell Culture Scaffolds", *Acs Macro Letters*, Vol. 2, pp. 5-9, 2013.

123. Nimmo, C. M., M. S. Shoichet, "Regenerative Biomaterials That "Click": Simple, Aqueous-Based Protocols for Hydrogel Synthesis, Surface Immobilization, and 3d Patterning", *Bioconjugate Chemistry*, Vol. 22, pp. 2199-209, 2011.

124. DeForest, C. A., K. S. Anseth, "Photoreversible Patterning of Biomolecules within Click-Based Hydrogels", *Angewandte Chemie International Edition*, Vol. 51, pp. 1816-1819, 2012.

125. Malkoch, M., R. Vestberg, N. Gupta, L. Mespouille, P. Dubois, A. F. Mason, J. L. Hedrick, Q. Liao, C. W. Frank, K. Kingsbury, C. J. Hawker, "Synthesis of Well-Defined Hydrogel Networks Using Click Chemistry", *Chemical Communications*, pp. 2774-2776, 2006.

126. Gupta, N., B. F. Lin, L. M. Campos, M. D. Dimitriou, S. T. Hikita, N. D. Treat, M. V. Tirrell, D. O. Clegg, E. J. Kramer, C. J. Hawker, "A Versatile Approach to High-Throughput Microarrays Using Thiol-Ene Chemistry", *Nature Chemistry*, Vol. 2, pp. 138-145, 2010.

127. DeForest, C. A., B. D. Polizzotti, K. S. Anseth, "Sequential Click Reactions for Synthesizing and Patterning Three-Dimensional Cell Microenvironments", *Nature Materials*, Vol. 8, pp. 659-664, 2009.

128. Subramani, C., N. Cengiz, K. Saha, T. N. Gevrek, X. Yu, Y. Jeong, A. Bajaj, A. Sanyal, V. M. Rotello, "Direct Fabrication of Functional and Biofunctional Nanostructures through Reactive Imprinting", *Advanced Materials*, Vol. 23, pp. 3165-3169, 2011.

129. Oberg, K., Y. Hed, I. Joelsson Rahmn, J. Kelly, P. Lowenhielm, M. Malkoch, "Dual-Purpose Peg Scaffolds for the Preparation of Soft and Biofunctional Hydrogels: The Convergence between Cuaac and Thiol-Ene Reactions", *Chemical Communications*, Vol. 49, pp. 6938-6940, 2013.

130. Yigit, S., R. Sanyal, A. Sanyal, "Fabrication and Functionalization of Hydrogels through "Click" Chemistry", *Chemistry-An Asian Journal*, Vol. 6, pp. 2648-2659, 2011.

131. Matyjaszewski, K., "Atom Transfer Radical Polymerization (Atrp): Current Status and Future Perspectives", *Macromolecules*, Vol. 45, pp. 4015-4039, 2012.

132. Parker, R. E., N. S. Isaacs, "Mechanisms of Epoxide Reactions", *Chemical Reviews*, Vol. 59, pp. 737-799, 1959.

133. Hamid, Z. A., A. Blencowe, B. Ozcelik, J. A. Palmer, G. W. Stevens, K. M. Abberton, W. A. Morrison, A. J. Penington, G. G. Qiao, "Epoxy-Amine Synthesised Hydrogel Scaffolds for Soft-Tissue Engineering", *Biomaterials*, Vol. 31, pp. 6454-6467, 2010.

134. De, S., C. Stelzer, A. Khan, "A General Synthetic Strategy to Prepare Poly(Ethylene Glycol)-Based Multifunctional Copolymers", *Polymer Chemistry*, Vol. 3, pp. 2342-2345, 2012.

135. Carioscia, J. A., J. W. Stansbury, C. N. Bowman, "Evaluation and Control of Thiol-Ene/Thiol-Epoxy Hybrid Networks", *Polymer*, Vol. 48, pp. 1526-1532, 2007.

136. Li, S. P., J. Han, C. Gao, "High-Density and Hetero-Functional Group Engineering of Segmented Hyperbranched Polymers Via Click Chemistry", *Polymer Chemistry*, Vol. 4, pp. 1774-1787, 2013.

137. Zalipsky, S., J. M. Harris, "Introduction to Chemistry and Biological Applications of Poly(Ethylene Glycol)", *Poly(Ethylene Glycol)*, Vol. 680, pp. 1-13, 1997.

138. Davis, F. F., "Commentary - the Origin of Pegnology", *Advanced Drug Delivery Reviews*, Vol. 54, pp. 457-458, 2002.

139. Cui, J., M. A. Lackey, A. E. Madkour, E. M. Saffer, D. M. Griffin, S. R. Bhatia, A. J. Crosby, G. N. Tew, "Synthetically Simple, Highly Resilient Hydrogels", *Biomacromolecules*, Vol. 13, pp. 584-588, 2012.

140. Erbil, C., E. Kazancioglu, N. Uyanik, "Synthesis, Characterization and Thermoreversible Behaviours of Poly(Dimethyl Siloxane)/Poly(N-Isopropyl Acrylamide) Semi-Interpenetrating Networks", *European Polymer Journal*, Vol. 40, pp. 1145-1154, 2004.

141. Hou, Y., C. A. Schoener, K. R. Regan, D. Munoz-Pinto, M. S. Hahn, M. A. Grunlan, "Photo-Cross-Linked Pdmsstar-Peg Hydrogels: Synthesis, Characterization, and Potential Application for Tissue Engineering Scaffolds", *Biomacromolecules*, Vol. 11, pp. 648-656, 2010.

142. Bailey, B. M., R. Fei, D. Munoz-Pinto, M. S. Hahn, M. A. Grunlan, "Pdms(Star)-Peg Hydrogels Prepared Via Solvent-Induced Phase Separation (Sips) and Their Potential Utility as Tissue Engineering Scaffolds", *Acta Biomaterialia*, Vol. 8, pp. 4324-4333, 2012.

143. Munoz-Pinto, D. J., R. E. McMahon, M. A. Kanzelberger, A. C. Jimenez-Vergara, M. A. Grunlan, M. S. Hahn, "Inorganic-Organic Hybrid Scaffolds for Osteochondral Regeneration", *Journal of Biomedical Materials Research Part A*, Vol. 94, pp. 112-121, 2010.

144. Wu, J. A., Q. Ge, P. T. Mather, "Peg-Poss Multiblock Polyurethanes: Synthesis, Characterization, and Hydrogel Formation", *Macromolecules*, Vol. 43, pp. 7637-7649, 2010.

145. Albanese, D., D. Landini, M. Penso, "Tetrabutylammonium Fluoride - a Powerful Catalyst for the Regioselective Opening of Epoxides with Thiols", *Synthesis-Stuttgart*, pp. 34-36, 1994.

146. Konno, H., E. Toshiro, N. Hinoda, "An Epoxide Ring-Opening Reaction Via Hypervalent Silicate Intermediate: Synthesis of Statine", *Synthesis-Stuttgart*, pp. 2161-2164, 2003.

147. Bryant, S. J., K. S. Anseth, D. A. Lee, D. L. Bader, "Crosslinking Density Influences the Morphology of Chondrocytes Photoencapsulated in Peg Hydrogels During the Application of Compressive Strain", *Journal of Orthopaedic Research*, Vol. 22, pp. 1143-1149, 2004.

148. Discher, D. E., D. J. Mooney, P. W. Zandstra, "Growth Factors, Matrices, and Forces Combine and Control Stem Cells", *Science*, Vol. 324, pp. 1673-1677, 2009.

149. Munoz-Bonilla, A., M. Fernandez-Garcia, D. M. Haddleton, "Synthesis and Aqueous Solution Properties of Stimuli-Responsive Triblock Copolymers", *Soft Matter*, Vol. 3, pp. 725-731, 2007.

150. Turunen, S., A. M. Haaparanta, R. Aanismaa, M. Kellomaki, "Chemical and Topographical Patterning of Hydrogels for Neural Cell Guidance in Vitro", *Journal of Tissue Engineering and Regenerative Medicine*, Vol. 7, pp. 253-270, 2013.

151. Alsina, B., F. Giraldez, C. Pujades, "Patterning and Cell Fate in Ear Development", *International Journal of Developmental Biology*, Vol. 53, pp. 1503-1513, 2009.

152. Kane, R. S., S. Takayama, E. Ostuni, D. E. Ingber, G. M. Whitesides, "Patterning Proteins and Cells Using Soft Lithography", *Biomaterials*, Vol. 20, pp. 2363-2376, 1999.

153. Persano, L., A. Camposeo, D. Pisignano, "Integrated Bottom-up and Top-Down Soft Lithographies and Microfabrication Approaches to Multifunctional Polymers", *Journal of Materials Chemistry C*, Vol. 1, pp. 7663-7680, 2013.

154. Tseng, A. A., A. Notargiacomo, "Nanoscale Fabrication by Nonconventional Approaches", *Journal of Nanoscience & Nanotechnology*, Vol. 5, pp. 683-702, 2005.

155. Biswas, A., I. S. Bayer, A. S. Biris, T. Wang, E. Dervishi, F. Faupel, "Advances in Top-Down and Bottom-up Surface Nanofabrication: Techniques, Applications & Future Prospects", *Advances in Colloid and Interface Science*, Vol. 170, pp. 2-27, 2012.

156. Minne, S. C., P. Flueckiger, H. T. Soh, C. F. Quate, "Atomic-Force Microscope Lithography Using Amorphous-Silicon as a Resist and Advances in Parallel Operation", *Journal of Vacuum Science & Technology B*, Vol. 13, pp. 1380-1385, 1995.

157. Gates, B. D., Q. B. Xu, M. Stewart, D. Ryan, C. G. Willson, G. M. Whitesides, "New Approaches to Nanofabrication: Molding, Printing, and Other Techniques", *Chemical Reviews*, Vol. 105, pp. 1171-1196, 2005.

158. Guo, L. J., "Nanoimprint Lithography: Methods and Material Requirements", *Advanced Materials*, Vol. 19, pp. 495-513, 2007.

159. Nikkhah, M., F. Edalat, S. Manoucheri, A. Khademhosseini, "Engineering Microscale Topographies to Control the Cell-Substrate Interface", *Biomaterials*, Vol. 33, pp. 5230-5246, 2012.

160. Song, W., H. X. Lu, N. Kawazoe, G. P. Chen, "Adipogenic Differentiation of Individual Mesenchymal Stem Cell on Different Geometric Micropatterns", *Langmuir*, Vol. 27, pp. 6155-6162, 2011.

161. Bae, H., A. F. Ahari, H. Shin, J. W. Nichol, C. B. Hutson, M. Masaeli, S. H. Kim, H. Aubin, S. Yamanlar, A. Khademhosseini, "Cell-Laden Microengineered Pullulan Methacrylate Hydrogels Promote Cell Proliferation and 3d Cluster Formation", *Soft Matter*, Vol. 7, pp. 1903-1911, 2011.

162. Rothschild, M., "Projection Optical Lithography", *Materials Today*, Vol. 8, pp. 18-24, 2005.

163. Yang, S. P., C. Y. Yang, T. M. Lee, T. S. Lui, "Effects of Calcium-Phosphate Topography on Osteoblast Mechanobiology Determined Using a Cytodetacher", *Materials Science & Engineering C-Materials for Biological Applications*, Vol. 32, pp. 254-262, 2012.

164. Revzin, A., R. G. Tompkins, M. Toner, "Surface Engineering with Poly(Ethylene Glycol) Photolithography to Create High-Density Cell Arrays on Glass", *Langmuir*, Vol. 19, pp. 9855-9862, 2003.

165. Dispinar, T., R. Sanyal, A. Sanyal, "A Diels-Alder/Retro Diels-Alder Strategy to Synthesize Polymers Bearing Maleimide Side Chains", *Journal of Polymer Science Part a-Polymer Chemistry*, Vol. 45, pp. 4545-4551, 2007.

166. Shepherd, J. L., A. Kell, E. Chung, C. W. Sinclar, M. S. Workentin, D. Bizzotto, "Selective Reductive Desorption of a Sam-Coated Gold Electrode Revealed Using Fluorescence Microscopy", *Journal of the American Chemical Society*, Vol. 126, pp. 8329-8335, 2004.

167. Decker, C., C. Bianchi, S. Jonsson, "Light-Induced Crosslinking Polymerization of a Novel N-Substituted Bis-Maleimide Monomer", *Polymer*, Vol. 45, pp. 5803-5811, 2004.

168. Hoyle, C. E., S. C. Clark, K. Viswanathan, S. Jonsson, "Laser Flash Photolysis of Bismaleimides", *Photochemical & Photobiological Sciences*, Vol. 2, pp. 1074-1079, 2003.

169. Schryver, J. P. F. C. D., "Photochemistry of Nonconjugated Bichromophoric Systems. Intramolecular Photocycloaddition of N,N□-Alkylenedimaleimides in Solution", *Journal of the American Chemical Society*, Vol. 95, p 9.